Virginia Water Resources Research Center **Bulletin 179**
Virginia Polytechnic Institute and State University

A Model of Nitrate Leaching From Agricultural Systems In Virginia's Northern Neck

Terrence G. Johnson, John C. Parker

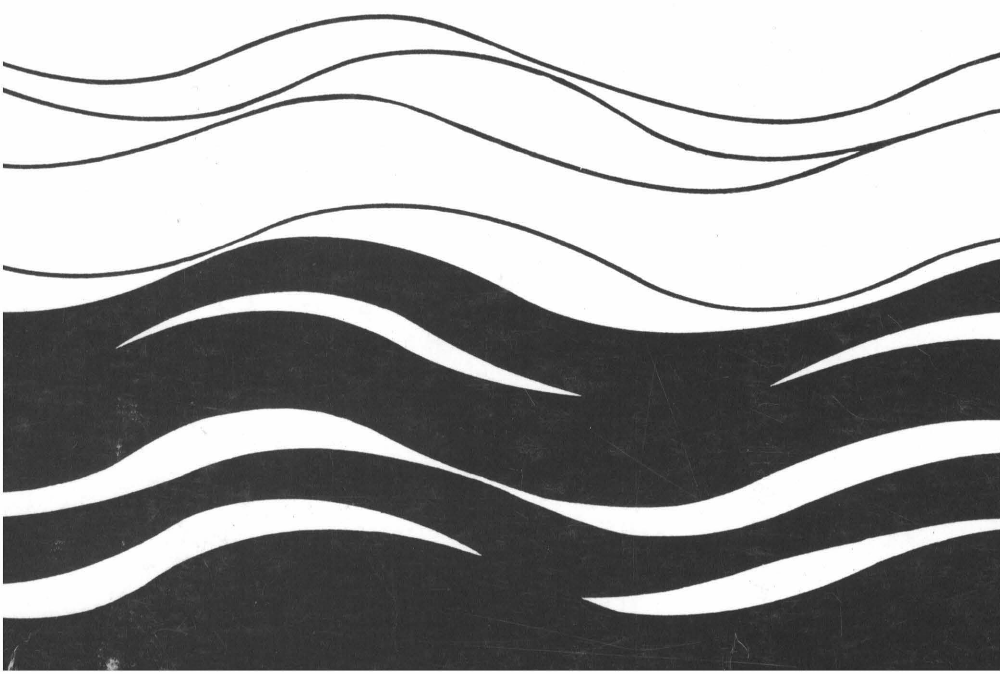

Bulletin 179
June 1993

A Model of Nitrate Leaching From Agricultural Systems In Virginia's Northern Neck

Terrence G. Johnson
John C. Parker

Department of Crop and Soil Environmental Sciences
Virginia Polytechnic Institute and State University

VPI-VWRRC-BULL 179
3C

Virginia Water Resources Research Center
Virginia Polytechnic Institute and State University
Blacksburg • 1993

Table of Contents

List of Tables

List of Figures

Acknowledgements

Thanks to W.T. Price, Velva Groover, Mark Stolt, D.C. Martens, B. Cannel, and Richard Cooke for their help and support.

The members of the Project Advisory Committee: Scott Alexander and Burt Tuxford, Virginia Water Control Board; Dennis Lynch, U.S. Geological Survey; Patti Lynn and Sarah Pugh, Virginia Department of Agriculture and Consumer Services; Chuck Landers, U.S. Department of Agriculture Soil Conservation Service; Ray Reneau, Department of Crop and Soil Environmental Sciences, Virginia Tech; and Theo Dillaha, Department of Agricultural Engineering, Virginia Tech, deserve special credit and thanks for providing suggestions and comments during this five-year research project. The successful completion of this investigation and the relevance of the Virginia Water Resources Research Center's total research program can be partially attributed to the guidance and participation of these knowledgeable and interested members of this committee.

Diana L. Weigmann
Interim Director

Abstract

A model (VT-CROPS) was developed to simulate the long-term effects of nitrogen (N) leaching to groundwater in the Northern Neck region of Virginia and, ultimately, to the Chesapeake Bay. VT-CROPS simulates N fate and transport in a soil-plant-atmosphere continuum in a vertical slice between two crop rows, enabling consideration of nonuniform fertilizer placement and root growth patterns. VT-CROPS models atmospheric, soil, and crop subsystems. Atmospheric conditions (rainfall, temperature, solar radiation) may be entered directly by the user or generated by using a stochastic climatic generator. The soil subsystem simulates runoff, infiltration, drainage and soil-water redistribution, N immobilization, nitrification, mineralization, denitrification, and advective N transport. The crop subsystem simulates plant N uptake, and vegetative and reproductive growth in response to soil and climatic factors, explicitly for maize or wheat. VT-CROPS simulates soybean in a crop rotation, empirically accounting for leaf area and root growth. The model is capable of simulating long-term cropping sequences under minimum and conventional tillage practices for continuous maize or for rotations involving maize, wheat, soybean, and fallow.

Critical internal model parameters were calibrated through comparison of output to field data. The sensitivity of output to input variables was determined. Model output is most sensitive to the climatic variables. Model-predicted crop performance variables—grain and total dry matter yields and N content—and soil N content were compared with available field data from two sites over a three-year period for maize. Data from six sites over a one-year period were tested for wheat. Predictions for maize and total N content were fairly accurate, with a tendency to greater error in dry years. Predictions for wheat were somewhat less accurate, but incomplete field data precluded determining the source of discrepancies.

Long-term model predictions, for two-year crop rotations with minimum and conventional tillage, were evaluated by comparing performance variables with literature values. Appropriate responses were obtained for N transformation processes. Mass conservation for soil water and N were good. Maize performance variables were within the range of literature values, and were higher under minimum till. Wheat yields and N contents were somewhat higher than values reported in the literature. Nitrogen load is correlated to drainage and water use over the short run, and to rainfall and drainage over longer periods. Minimum tillage did not increase N load to groundwater. Over a year, nitrogen load was periodic, with most leaching taking place from January through April. More than

50% of the N load over a rotation was lost during an extended fallow period that followed soybeans. Nitrogen load increased with fertilizer rates; however, the N leaching fraction was optimal at rates of 150-200 kg/ha.

The model was applied to the Virginia counties of Richmond, Westmoreland, Lancaster, King George, and Northumberland to assess the potential for long-term N leaching to groundwater. Soil surveys indicated that 34 soil map units occurred within 123,000 hectares of cultivated land. To reduce the number of simulations, principal component analysis and cluster analysis were used to subdivide the cultivated area into 10 land units based on different soil properties. Historical climatic data from the area were used to calibrate the stochastic climatic generator.

Analyses were performed to determine long-term crop performance and N loads to groundwater and surface waters in the study area over a 26-year period (13 rotations). Two management systems were applied to the land units. The first management system consisted of a rotation of minimum-tilled maize, conventionally tilled wheat, minimum-tilled soybeans, and a fallow period. The second management system had a similar cropping sequence, but all crops were conventionally tilled. In both cases, fertilizer was applied at a rate of 150 kg-N/ha/crop. With the exception of two land units, mean yield, water use, and N uptake over the simulation were fairly uniform among the land units. Runoff and drainage were highly variable between land units and over time within units. Mineralization, denitrification, and N load were highly variable both between land units and over time. Nitrogen load ranged from 66 to 131 kg/ha/rotation between land units.

Long-term average N loads and N concentrations from the cultivated area and from the total area of the study region were estimated. For this analysis, it was assumed that 80% of the cultivated area was under minimum till and 20% under conventional tillage. An area-weighted average of 5.4 million kg-N/ha/year, or 29% of total N applied, is discharged to groundwater, with an average drainage concentration of 9.9 mg/l. The average N concentration from the study area (including uncultivated areas) to groundwater is estimated at 5.1 mg/l. Average N concentration to the Chesapeake Bay from all sources, after dilution with runoff, is 4.5 mg/l, which is lower than the drinking water standard for nitrate N of 10 mg/l.

The possibility of using sewage sludge as a replacement for, or in consort with, N fertilizer was investigated for a typical land unit, under a conventionally tilled maize-wheat-soybean-fallow rotation. Simulations were conducted with 100%, 50%, and 0% sludge (CN ratio of 12). With fertilizer N augmenting the sludge, the total N input (250 kg/ha) was the same for each treatment. Mean yields were similar for 50% and 0% sludge, but lowered by 10% and 16%, respectively, for maize and wheat with 100% sludge. Discrepancies in yields were attributed to the fact that mineralization rates of sludge are not high enough to supply the crop N requirement during periods of peak uptake. Nitrate leaching was reduced by 41% and 25% with 100% and 50% sludge applications, respectively.

1 Introduction

The importance of groundwater as a natural resource to the United States cannot be overemphasized. Over 50% of all inhabitants, and over 90% of rural inhabitants, depend on groundwater for drinking water (Anderson, 1987; Canter et al., 1987). It is estimated that groundwater supplies 25% of the fresh water used in the United States (Fletcher, 1991). Therefore, public concerns over possible deterioration of groundwater quality from nitrogen (N) contamination are justified. Originating primarily from diffuse sources, N is classified as a nonpoint-source pollutant. The problem of groundwater contamination increased with the advent of the green revolution of the 1950s, which resulted in the development of high-yielding crop cultivars with high fertilizer requirements. Consequently, N fertilizer application rates in the United States increased from 2.7 million tons in 1960 to 10.5 million tons in 1985 (Anderson, 1987). Of the N fertilizer, 43% is applied to maize and 14% is applied to wheat. In addition to chemical fertilizer, an estimated 70% of the 1.1 billion tons of animal manure produced annually provides approximately 8% of the N required for crop production (Anderson, 1987).

Typical plant uptake of N fertilizer is about 50% of the amount applied (Hallberg, 1987). However, only 30-35% or less is typically removed in grain (Gerwig et al., 1979; Blackmer, 1984). After one year of fertilizer application, Blackmer found that 60-65% of fertilizer N was lost to processes other than grain harvest. Hallberg summarized experiments in which the amount of N leached in tile effluent was monitored, and concluded that approximately 50% of the applied N was lost in drainage. This does not include N leached below tiles under unsaturated conditions.

Nitrate (NO_3^-) and ammonium (NH_4^+) ions are the two mineral forms of N that are most common in soils. Both are natural products of the N cycle and are available for plant uptake. Upon mineralization of organic matter, NH_4^+ is produced. Under normal temperature conditions, NH_4^+ does not persist in soils in appreciable quantities, as it rapidly converts to NO_3^--N by the process of nitrification. Nitrate not taken up by plants may be immobilized by microbes or converted to gaseous species by denitrification. However, denitrification is generally significant only when soil moisture is near saturation. Nitrate remaining in the soil can be lost as runoff or as drainage. Due to its negative charge, which excludes it from cation exchange sites, leaching of NO_3^--N readily occurs. Once NO_3^--N is leached beyond the root zone, attenuation by biological processes is much slower.

High NO_3^--N in drinking water is known to cause methemoglobinemia in infants—a condition caused by NO_3^--N oxidizing hemoglobin, reducing its capability to transport oxygen (Keeney, 1983). Infants under 3-6 months are particularly susceptible because the enzyme system that reduces methemoglobin is not well developed (Keeney and Follett, 1991). High methemoglobin levels can result in brain damage or even death—of the number of reported methemoglobinemia cases, 7-8% resulted in death (USEPA, 1985). The National Health Service Standard for NO_3^--N in drinking water, 10 mg/l, is believed to protect infants adequately against methemoglobinemia.

Agricultural practices in the United States cause widespread groundwater pollution. Twenty-nine states have identified nonpoint discharges from agriculture to groundwater as major concerns (Anderson, 1987). Francis et al. (1982) reported that 2.7% of U.S. drinking water supplies for 22 million rural families exceeded the maximum legal limit for NO_3^--N. In a 1984 nation-wide survey by the United States Geological Survey (USGS), in which 124,000 wells were sampled, 6% had NO_3^--N above the legal limit, and over 20% had more than 3 mg/l (Madison and Brunett, 1985). The picture looks even gloomier in certain localities. Fletcher (1991), reporting on the finding of the South Dakota Department of Water and Natural Resources (1984), stated that, of wells tested in the Big Sioux aquifer, 25% exceeded the legal limit for NO_3^--N in drinking water. From 1960 to 1985, groundwater NO_3^--N in the Big Spring watershed in northern Iowa, where land use is dominated by agricultural production, increased from less than 10 mg/l to more than 45 mg/l (Hallberg, 1987).

In addition to the problem of groundwater contamination, N contamination of surface waters is a problem. In Virginia, attention has been focused on declining water quality in the Chesapeake Bay caused by N and phosphorus (P) pollution (USEPA, 1983a). These nutrients are essential to plant growth and are important to aquatic ecosystem diversity; however, in excess, they cause algal blooms with subsequent increases in turbidity and decreased dissolved oxygen levels. The majority of the P pollution in the bay originates from point sources, mainly sewage plants. Point sources are relatively easy to control by reducing loads at the source. On the other hand, nitrogen loading to the bay originates primarily from nonpoint sources, mainly agricultural runoff and drainage. The USEPA (1983a) estimates that an average of 67% of the N entering the bay originates from cropland. Nonpoint sources are diffuse and function primarily during rainfall events as runoff or interflow from drainage, so they are stochastic and transient in nature (Bailey and Swank, 1983).

Due to the diffuse and transient nature of N transport and transformation processes, and the need to maintain high levels of agricultural production, controlling nonpoint sources of N is difficult. Management strategies aimed at reducing the N loading to the Chesapeake Bay have stressed conservation tillage. Though conservation tillage is usually effective in reducing runoff from cropland, increases in drainage flux ultimately could increase the leaching of N to groundwater. In addition to degrading groundwater quality, the discharge of groundwater to surface water bodies may provide a major source of contamination to streams that feed the bay.

To protect Virginia's water resources, it is necessary to establish the long-term effects of current agricultural management practices on groundwater quality and to evaluate alternative practices. Therefore, quantitative assessment of NO_3^--N leaching from soils is essential. Nitrogen contamination resulting from agricultural activities is due to a combination of complex, interacting factors controlled by agricultural management practices and watershed and climatic characteristics. These conditions necessitate a systems approach to study the transport and transformation of N in an agri-environmental context. The most cost-effective means of determining cause and effect relationships, extending the utility of limited and costly field data, and identifying optimal control technologies is through the use of simulation models (Bailey and Swank, 1983).

A number of available models simulate specific portions of the N cycle in an agricultural context (e.g., see review by Vachaud et al., 1990). Models range from simple empirical models to sophisticated mechanistic models that simulate water flow, N transport and fate, and physiology for various crops. No model, however, is available that evaluates long-term N leaching behavior of cropping systems involving rotations of maize, wheat, soybeans, and fallow, which are common in the Northern Neck of Virginia. This project was initiated under funding from the Virginia Water Resources Research Center to develop a model to study the problem of N contamination of groundwater and surface water associated with agricultural practices in the Northern Neck. The specific objectives of this research were to:

- develop a mechanistic model capable of predicting N leaching and crop yields from two-year rotations involving maize, wheat, soybean, and fallow under minimum and conventional tillage;

- validate the model using available field data; and

- determine the short- and long-term effects of management strategies and climatic factors on NO_3^--N leaching to groundwater.

To accomplish these objectives, the model VT-CROPS was developed. VT-CROPS is a soil-plant-atmosphere continuum model that simulates temporally variable climatic behavior and yield responses and N fate and transport for cropping rotations involving maize, wheat, soybeans, and fallow. Crop rotation refers to the successive growing of different crops on the same piece of land, as opposed to continuous cropping (National Research Council, 1989). System processes accounted for by the model include: runoff, infiltration, evaporation, soil water flow, N immobilization, nitrification, N mineralization, denitrification, N plant uptake, advective N transport, and vegetative and reproductive growth in response to soil and climatic conditions.

VT-CROPS was based on several previously developed models. Water and N transport and transformations and maize phenology are based on the model VT-MAIZE (Newkirk et al., 1987a,b), to which a number of modifications were made to make it workable and to improve its accuracy. VT-MAIZE is based on the RHIZOS portion of the cotton simulation model, GOSSYM (Baker et al., 1983), to model flow, N reactions, and root growth in a two-dimensional soil subsystem, and the model CERES-Maize (Jones and Kiniry, 1986), which models maize growth and N uptake. VT-CROPS uses a modified version of CERES-Wheat (Ritchie and Otter, 1984) to simulate wheat growth and N use. Stochastic climatic processes are modeled using an adaptation of the program WGEN (Richardson and Wright, 1984).

VT-CROPS models maize and wheat growth from germination through all their phenological stages to maturity. Soybeans are modeled implicitly. Soybean phenology is not modeled, but soil and atmospheric subsystems are simulated for a fixed period (95 days), at the end of which yields are calculated based on the ratio of actual to potential evapotranspiration. Soybean root distributions are modeled by expressions developed from the work of Mitchell and Russell (1971), and leaf area index over time is calculated from expressions developed from the work of Jolliff and Cox (1986). For fallow periods, only the soil and atmospheric subsystems are simulated. VT-CROPS assumes that soybean takes up N passively in the convection stream and fixes the remainder to meet its requirements, while the soil supplies the N requirement of maize and wheat.

VT-CROPS is capable of simulating two cropping sequences:

A. Maize - wheat - soybeans - fallow (in a two-year rotation)

B. Maize - fallow (in a one-year rotation)

Planting dates for maize and wheat are fixed on Julian day 131 and 288, respectively, of the first year of a rotation. The start of fallow periods and the planting of soybeans are not fixed, but depend on the maturity dates of maize and wheat. For cropping sequence A, a fallow period lies between the maturity of maize and day 288 of year 1, and an extended fallow period following the soybean crop to the end of the rotation. There is also a two-week fallow period between the end of the wheat crop and the beginning of the soybean growth. For cropping sequence B, following the maize crop, a fallow period ends the year. Single or multiple rotations can be simulated for a specified time period using generated climatic data to evaluate long-term system behavior. Various management options may be simulated, including minimum or conventional tillage and N source type, amount, depth, and timing of application.

This text reports results of model validation investigations for biomass production and grain yield, N uptake and partitioning, and soil N content and distribution at the end of the season for the maize and wheat portions of the model based on available field data. Also reported are the results of the model's application to predict N loading to groundwater under common management practices in the Virginia counties of Richmond, Westmoreland, Northumberland, Lancaster, and King George. Sludge application as an N source also is evaluated.

Throughout this text, *evapotranspiration* means the sum of soil evaporation and plant transpiration, and is used interchangeably with *crop water use* or *water use*.

2 Literature Review

2.1 Modeling Approaches to Vadose Zone Transport

Mathematical models used to predict chemical transport and transformations in the vadose zone belong to the general class of models referred to as *leaching models* (Wagenet et al., 1990). Leaching models vary widely in their conceptual approach and degree of complexity. Depending on its intended use, a leaching model can be classified as either *research-* or *management-oriented* (Addiscot and Wagenet, 1985; Wagenet et al., 1990). A research-oriented model is intended to contribute to the understanding and interactions of system processes, or to test assumptions regarding the system. On the other hand, management-oriented models are used in a decision-making framework, and usually pay less attention to the fundamentals of system functioning (Vachaud et al., 1990).

Many approaches may be used to broadly classify mathematical models based on the conceptual approach employed. Such classifications may hinge on the parameterization used, as lumped or distributed parameter models (Novotony and Chester, 1981); the role time plays, as either stochastic or dynamic (Woolhiser and Brakenside, 1982); or the recognition of random variations in model parameters, as either stochastic or deterministic (Addiscot and Wagenet, 1985). The approach of Addiscot and Wagenet is most pertinent to leaching models, and will be used here.

Deterministic models treat model parameters as being free from random variations (Woolhiser and Brakenside, 1982); hence, their outcome is unique. Stochastic models recognize the uncertainty in input parameters and outcomes and account for it (Addiscot and Wagenet, 1985).

2.1.1 Deterministic Models

Deterministic models can be subdivided further, depending on how much of the system fundamentals they incorporate. Mechanistic deterministic models are those that incorporate fundamental mechanisms governing system behavior, e.g., the advective-dispersive-reactive transport (ADR) equation. On the other hand, those that simplify system processes with no claim to the fundamentals are referred to as *functional* (Addiscot and Wagenet, 1985). Mechanistic models and research models are usually analogous, as are functional and management models.

2.1.1.1 Mechanistic Deterministic Models. This group of models predict solute migration through *advective, dispersive,* and *reactive* processes. Advection refers to the transport of solute with the mean soil-water flow. Dispersion, accurately referred to as *hydrodynamic dispersion* (Bear 1972, Bear and Verruijt, 1987), accounts for the aggregate effect of transport by molecular diffusion and mechanical dispersion. Mechanical dispersion is a macroscopic factor accounting for transport due to velocity variations at the pore scale, unaccounted for by the mean velocity. Reactions describe the aggregate effects of sources and sinks on aqueous transport, examples of which are interphase mass transfer and chemical/microbial transformations.

Water Flow: Accurate predictions of solute migration in the unsaturated zone is predicated on accurate determination of aqueous fluxes and water content distributions. Water content distribution, in a transient system, commonly is determined by solving Richard's equation, derived by substituting the Darcy flux equation into the conservation of mass equation. Written for the arbitrary dimensions, Richard's equation is

$$\frac{\partial \theta}{\partial t} = \frac{\partial}{\partial x_i}\left[K(\theta)\,\frac{\partial h}{\partial x_i} + K(\theta)\,\frac{\partial z}{\partial x_i}\right] + R(x_i,t) \tag{1}$$

where θ is soil water content; $K(\theta)$ is the soil hydraulic conductivity function $(LT^{-1})_1$, which, for unsaturated flow, is a nonlinear function of water content; h is soil water pressure potential (L); x_i is the dimension (L); t is time (T); and $R(x_i,t)$ is the source/sink term, which, for unsaturated flow, represents root water uptake. The Einstein summation notation is implied in equation 1.

Note, even though the vadose zone, in pristine environments, is a two-fluid phase system of water and air, only the water phase equation is solved. This is made possible through Richard's assumption, which states that gas pressures are essentially constant. Other assumptions inherent in equation 1 are the rigidity of the porous media and the incompressibility of water and porous media (Bear, 1972). Equation 1 has two independent variables, h and θ; therefore, another equation is necessary to obtain a unique solution. Provision of the other equation is made possible by the definition of soil water capacity $C(h)$ (L^{-1}); the slope of the soil water characteristic curve at any given θ (Hillel, 1971)

$$C(h) = \frac{d\theta}{dh} \tag{2}$$

The soil water capacity function, which is typically bell shaped, is zero for a saturated soil until the air entry pressure is exceeded during drainage. Thereafter, $C(\theta)$ increases to a maximum and then decreases, approaching zero at a residual saturation where large changes in h produce small changes in θ. Use of equation 2 and application of the Chain Rule of calculus to either the spatial or temporal derivative in equation 1 results in two solvable forms of equation 1. The most commonly used form resulting from an expansion of the temporal derivative, known as the *potential* or *capacity* form of Richard's equation (Selim and Iskander, 1981; and Jury et al., 1991), is

$$C(h)\,\frac{\partial h}{\partial t} = \frac{\partial}{\partial x_i}\left[K(h)\,\frac{\partial h}{\partial x_i} + K(h)\,\frac{\partial z}{\partial x_i}\right] + R(x_i,t) \tag{3}$$

Equation 3 must be solved numerically because it is nonlinear in h. The hydraulic or piezometric head gradient, $(\partial(h+z)/\partial x_i)$, is the driving force of water flow. This potential form is preferred, since it is applicable to layered soils due the continuity of hydraulic potential. The solution of equation 3, subject to appropriate initial and boundary conditions, yields the distribution of water pressure over the domain. Commonly encountered boundary conditions for water flow are of two types: the first type, or Dirichlet boundary condition, specifies the primary variable or hydraulic head; the second type, or Neumann boundary condition, specifies the gradient in the primary variable, in this case the flux. For more information on flow boundary conditions, refer to Bear and Veruijt (1987). From the water pressure distribution, the water content, θ, and water flux, q (LT^{-1}), can be calculated.

Equation 3 assumes that the relationship between h and θ is unique. In general, hysteresis exists in the h and θ functions, which makes them unique for monotonic wetting or drying only. For any given h, the water content of a soil is higher for drainage than it is for imbibition. Hence, $C(h)$ and $K(h)$ are not single-valued functions. Hysteresis results from the trapping of nonwetting fluids upon water imbibition, the ink-bottle effect in pores, and differences in the liquid contact between an advancing and a receding front in soil pores (Corey, 1986; Bear and Verruijt, 1987; Jury et al., 1991). Most models, however, disregard hysteresis in simulating water flow. In certain instances, the effects of hysteresis may be substantial (Russo et al., 1989; Lenhard et al., 1992).

A less-used form of Richard's equation may be obtained by chaining out the spatial derivative in equation 1 and making use of equation 2. This results in the so-called *water content* or *diffusivity* form of Richard's equation (Jury et al., 1991)

$$\frac{\partial \theta}{\partial t} = \frac{\partial}{\partial x_i}\left[D(\theta)\frac{\partial \theta}{\partial x_i} + K(\theta)\frac{\partial z}{\partial x_i}\right] + R(x_i,t) \tag{4}$$

With the exception of the gravity term, equation 4 is mathematically similar to the molecular diffusion and the heat conduction equations. The *soil water diffusivity* function, $D(\theta)$ (L^2T^{-1}), is defined as

$$D(\theta) = \frac{K(\theta)}{C(\theta)} \tag{5}$$

Among the advantages to the use of equation 4 are that $D(\theta)$ is less nonlinear than $K(\theta)$, and $K(\theta)$ is less hysteretic than $K(h)$. These advantages, however, are outweighed by the fact that equation 4 holds for homogeneous soils only. Hence, very few models use equation 4 (e.g., Shaffer, 1985). It is used mainly to study horizontal infiltration in soils, where it reduces to a form mathematically identical to the heat conduction equation, which has analytical solutions readily available (e.g., Carslaw and Jaeger, 1959).

The gradient in water content ($\partial\theta/\partial x_i$) is not the true driving force of water flow, and is only continuous in homogeneous systems. In heterogeneous media, the water content gradient is infinite, and $D(\theta)$ is undefined at the boundary of layers, due to discontinuity in θ, and causes problems in equation 4.

Solution of either form of the flow equation requires specification of the $K(h)$ and $\theta(h)$ functions. Modeling approaches for the hydraulic functions range from table look-up with interpolation (Wagenet and Hutson, 1987) to the use of analytic expressions (Kalurachchi and Parker, 1990). A number of analytic expressions of soil hydraulic functions have been developed in recent times (Brooks and Corey, 1966; Mualem, 1976; van Genuchten, 1980). The van Genuchten model, probably the most widely used model, is discussed in section 3.

Solute Transport: Given the distribution of water content and water flux, the distribution of an aqueous nonvolatile species can be determined by solution of the ADR, which may be written as

$$\frac{\partial \rho s}{\partial t} + \frac{\partial \theta c}{\partial t} = \frac{\partial}{\partial x_i}\left[\theta D_h \frac{\partial c}{\partial x_i}\right] - \frac{\partial (qc)}{\partial x_i} + \gamma \tag{6}$$

where ρ is soil bulk density (ML^{-3}); s is the solid phase concentration (MM^{-1}); c is the aqueous phase concentration (ML^{-3}); D_h is the dispersion coefficient (L^2T^{-1}); and γ is the aggregate effect of source/sink terms other than solid phase partitioning ($ML^{-3}T^{-1}$).
The dispersion coefficient is

$$D_h = D + \tau D_d \tag{7}$$

where D is the mechanical dispersion coefficient (L^2T^{-1}); τ is a tortuosity factor that accounts for the effect of water configuration in the pores; and D_d is the aqueous molecular diffusion coefficient (L^2T^{-1}). The assumption in equation 7 is that the dispersive flux can be described by an equation analogous to the Fickian diffusive flux equation. Typically, D has been observed to be directly proportional to pore water velocity, V (LT^{-1}) (Bear, 1972), and is calculated as

$$D = \alpha V \tag{8}$$

where $V = q/\theta$ and the proportionality constant and α is the dispersivity (L), which is highly scale-dependent (Gelhar et al., 1985).

Equation 6 cannot be solved uniquely because it has two unknowns. Another equation is needed to overcome this problem. This other equation, describing aqueous-solid phase interactions, is supplied by the adsorption isotherm. An aqueous-solid adsorption isotherm expresses the relationship between the quantity of a substance adsorbed on the solid phase and that in the aqueous phase, under isothermal conditions (Bear, 1987). The linear equilibrium Freundlich isotherm, most commonly used to model sorption in porous media (Vachaud et al., 1990), is

$$s = K_d c \tag{9}$$

where K_d is the equilibrium partition coefficient.

By using the chain rule on the second temporal derivative in equation 6, making use of equation 9, using the fact that, for incompressible media, ρ is time invariant in expanding the first time derivative, expanding the second spatial derivative in equation 6 and making use of the continuity of water flow, the transport equation may be expressed as

$$R\frac{\partial c}{\partial t} = \frac{1\partial}{\theta\partial x_i}\left[\theta D_h\frac{\partial c}{\partial x_i}\right] - \frac{q}{\theta}\frac{\partial c}{\partial x_i} + \frac{\gamma}{\theta} \tag{10}$$

where R is the retardation factor for solute by the solid phase, defined as

$$R = 1 + \frac{\rho K_d}{\theta} \tag{11}$$

Equation 10 is the most common form of the single-specie transport equation solved for the unsaturated zone.

The literature contains examples of the use of nonequilibrium models to describe solid-liquid sorption-desorption (e.g., van Genuchten et al., 1974); however, superior results to equilibrium models were obtained only at high pore water velocities (Vachaud et al., 1990).

To determine the migration of chemical species in the vadose zone, the transport equation is solved, subject to appropriate initial and boundary conditions, subsequent to the flow equation. The commonly encountered boundary conditions for solute transport are of two types: type-I, where the primary variable, C, is specified; and type-III, or Cauchy (Bear, 1987), for flux boundary conditions, since it involves both C and its gradient.

As stated earlier, the flow equation is nonlinear. In addition, typical field situations have complex boundaries and/or boundary conditions for both flow and transport. Hence, they are not amenable to analytical solutions.

Numerical Models: Solution of the flow and transport equations for various unsaturated field situations is fairly commonplace. Examples are: predicting phosphorus removal from soils during land treatment of wastewater (e.g., Ryden et al., 1981); N removal and behavior during land application of wastewater (e.g., Selim and Iskander, 1981); flow and transport of organic substances (e.g., Kalurachchi and Parker, 1990) with mobile-immobile liquid (e.g., Brusseau, 1992); crop growth (e.g., Nimah and Hanks, 1973); and N leaching (Newkirk et al., 1987a,b).

Traditionally, these equations are solved numerically using the finite difference approach (e.g., Addiscot and Wagenet, 1985) or the finite element method (Kalurachchi and Parker, 1990). The finite elements method has the advantage because it is more flexible with respect to the geometry of the problems that can be handled.

2.1.1.2 Deterministic Functional Models. This group of models simplifies the treatment of transport processes. Addiscott and Wagenet (1985) subdivided this group into capacity and layer models.

Capacity models use soil water field capacity, rather than pore water velocity, to determine the travel distance of a solute front in response to an infiltration event. Capacity models are driven by events such as rainfall or irrigation (Addiscott and Wagenet, 1985). Addiscott and Wagenet reported the successful application of a capacity model to predict field chloride concentrations (De Smedt and Wierenga, 1978). Chichester and Smith (1978) were less successful in predicting field lysimeter NO_3^- movement. Capacity models cannot account for solute residues in the profile at the beginning of a simulation and cannot simulate heterogeneous media (Addiscott and Wagenet, 1985).

Layer or compartmental models divide the soil into horizontal layers, and perform mass balances on individual layers (Addiscott and Wagenet, 1985). Layer models are capacity models applied differentially over the soil domain to overcome the heterogeneity problem encountered with capacity models. Typically, for water flow, they use the *tipping-bucket* concept, where incoming water adds to the water content of a cell, and, after allowing for mixing (treating a layer as completely stirred), water in excess of field capacity drains to the adjoining layer. Mass flux of solute to the adjoining layer is the product of drainage and solute concentration of the current layer. The same concept is applied to water removal. Layer models have been applied to field situations with limited success (Addiscott and Wagenet, 1985).

2.1.2 Stochastic Models

Stochastic models assume that soil properties are spatially variable, and claim to account for this variability. Addiscott and Wagenet (1985) recognized two classes of stochastic models: one that superimposes spatial variability on existing mechanistic models, and one that does not take transport mechanisms into account, but focuses on the variability of solute transfer itself.

2.1.2.1 Stochastic-Mechanistic Models. This approach uses randomly generated input parameters to drive the flow and transport equations for a number of realizations. Conceptually, the soil is treated as a number of homogeneous tubes with different hydraulic properties (Addiscott and Wagenet, 1985; Vachaud et al., 1990). Scaling theory then is applied to the flow and transport equations, resulting in the parameters $K(h)$, $D(h)$, v, and R_d being treated as random stochastic processes, defined by probability density functions (Vachaud et al., 1990). Samples from these distributions, using Monte Carlo techniques, have been used to drive solutions to the flow and transport equations. Model results are a distribution of the state variables that can be characterized and their moments determined. This approach was used successfully to simulate solute (chloride) concentrations in bare fields (Bresler et al., 1979). However, when applied to cropped areas to predict NO_3^- concentration, results were not as good (Wagenet and Rao, 1983). From this, it was concluded that the presence of crop roots reduced the effect of spatially variable hydraulic properties (Wagenet and Rao, 1983).

Nonlinearities in Richard's equation makes it unattractive for use in stochastic-mechanistic models. Solution of nonlinear differential equations requires an iterative numerical procedure, which may not converge. Superimposed on this, the mechanistic model must be solved repeatedly to generate sufficient realizations to adequately characterize densities of state variables. This often makes the procedure computationally tedious and unattractive.

2.1.2.2 Nonmechanistic Stochastic Models. An assumption of the ADR equation is that dispersion has an equivalent effect on solute mixing as diffusion. For this to be the case, the solute must be detained in the porous media long enough for mixing to occur (Jury et al., 1991). If the solute detention time is not long enough, then the ADR equation is unable to describe solute migration with a constant dispersion coefficient (Gelhar and Axness, 1983). Jury et al. (1991) stated that, on large, structured field soils, the ADR requires longer times to be valid than in small, uniformly packed laboratory columns. It was with these inadequacies in mind that Jury (1982) proposed a transfer function model for solute transport. This approach attempts to measure solute distribution over some travel distance as

$$P_L(I_0) = \int_0^{I_0} f_L(I)dI \tag{12}$$

where P_L is cumulative distribution function for solute arrival at a distance L, and $f_L(I)$ is the probability density function summarizing the probability that surface solute fluxes will arrive at L as the surface flux increases from I to $I + dI$.

By taking solution samples over the field, the parameters of $f_L(I)$, generally taken to be lognormal (Bigger and Nielson, 1976), are determined. One drawback of the method is that it can be used only to make predictions at a distance L (Jury and Roth, 1990). Jury (1982) used this approach to accurately describe solute concentrations in the field. However, we have yet to determine the accuracy with which the method predicts fluxes as well as its applicability to heterogeneous soils (Addiscott and Wagenet, 1985).

2.2 Water Flow in the Soil-Plant-Atmosphere Continuum

2.2.1 Continuum Approach to Water Flow

Conceptually, the flow of water from the soil, through the plant, and to the atmosphere, can be thought of as occurring in a Soil-Plant-Atmosphere Continuum (SPAC) (Hillel, 1980). The flow includes movement from the soil to the roots, absorption by the roots, flow through the roots to the xylem in the stem, flow from the xylem to the leaves, evaporation from the leaves, and vapor transport away from the leaves (Kramer, 1983).

Water flow through the SPAC follows classical potential flow theory; that is, water flows from regions of high to low potential. Consequently, the flow of water is analogous to the flow of energy through a series of variable resistors, and can be described using the mathematical analogy of Ohm's law. The flow of water in any section (i) of the SPAC may be described by

$$q_i = \frac{\Delta\psi_i}{R_i} \tag{13}$$

where q_i is the flux density of water; $\Delta\psi_i$ is the potential drop; and R_i is the resistance. This resistance not only varies from one section to the next, but, in each section, it varies temporally due to changes in plant physiological conditions, soil water status, and atmospheric conditions (Kramer, 1983). In cases where the atmospheric evaporative demand is being met, the flow of water through the continuum approaches steady state conditions, and equation 13 becomes

$$q_i = q = \frac{\Delta\psi_i}{R_i} \tag{14}$$

where q is the steady state flux density through the continuum. The potential difference between the soil and the atmosphere is on the order of hundreds of bars, with the greatest potential drop occurring in the transfer of water between the plant leaves and the atmosphere (Hillel, 1980).

Water flow from the soil to plant roots is described by Darcy's law as

$$q_s = K(\theta)\frac{\Delta\psi_s}{\Delta x} \tag{15}$$

where $\Delta\psi_s/\Delta x$ is the potential gradient over distance x; and $K(\theta)$ is the hydraulic conductivity. The analogy with the flow of electricity can be preserved by defining hydraulic resistance, R_s, as $R_s = \Delta x/K$. Thus, equation 15 becomes

$$q_i = \frac{\Delta\psi_s}{R_s} \tag{16}$$

where ψ is the sum of the gravitational, water pressure, and solute potentials of the soil water. R_s is dependent on $K(\theta)$, which is, in turn, directly proportional to the soil pressure potential. From this relationship between $K(\theta)$ and R_s, it can be inferred that R_s is inversely proportional to the soil water pressure potential. Other factors affecting R_s are rooting density and depth. It is obvious that R_s varies with soil moisture status and with plant development. Similar relationships can be developed for other parts of the SPAC.

The stomatal resistance, which controls the transfer of water from the plant leaves, is particularly variable. In cases where the plant cannot supply the evaporative demand of the atmosphere, the stomatal resistance becomes infinitely great, resulting in a low flux of water from the plant (Kramer, 1983).

2.2.2 Approaches to Modeling Root Water Uptake

Root water uptake is a significant component in the water budget equation in the crop root zone, and accounts for the reaction term, $R(z,t)$, previously alluded to. Principally, there are two approaches to modeling water uptake by roots: microscopic and macroscopic (Selim and Iskander, 1981; Moltz, 1981). The microscopic approach considers water flow to an individual root, assumed to be cylindrical and of infinite length, which reduces the problem to one of radial flow. A description of water flow to roots is provided by a solution to Richard's equation in radial coordinates subject to boundary conditions at the root surface and at some radius of influence.

The macroscopic approach uses semi-empirical equations, and computes water uptake rate, S (T^{-1}), over a differential element of the root zone, ignoring the individual root. The rate of uptake in each element depends on the length of the root, the hydraulic properties of the soil, and the soil moisture status (Selim and Iskander, 1981; Moltz, 1981). Moltz summarizes the most commonly used of these macroscopic equations. Probably the most used of these equations is that of Moltz and Remson (1970), which is

$$S(z,t) = \frac{TL(z)\ D(\theta)}{\int_{o}^{d} L(z)D(\theta)dz} \tag{17}$$

where T (LT^{-1}) is the transpiration rate; L (L^{-2}) is the root length density over a volume element; and $D(\theta)$ is the soil water diffusivity as previously defined.

2.3 Nutrient Supply to Roots

2.3.1 Overview of Supply Mechanisms

The soil is the natural medium in which plants grow. A plant's root absorbs water and nutrients necessary for the successful growth of the crop. For these nutrients to be taken up by the roots, they must be supplied to them. There are three mechanisms by which nutrients are supplied to plant roots: interception, mass flow, and diffusion.

Root interception refers to nutrients encountered by roots as they grow. These nutrients are readily available for plant uptake, and need not be transported to the root surfaces. Generally, the amount of nutrients supplied to the plant by this process is small, typically less than 1% of the available plant nutrients (Barber, 1984). Factors affecting interception include root volume, root diameter, and mechanical impedance to root growth (Barber, 1984). The greater the volume of plant roots, the greater the interfacial contact between the soil and roots. For a given volume of roots, the smaller the diameter, the greater the root surface area-soil interface. Anything that mechanically impedes root growth, such as dense soils, will restrict interception.

Mass flow refers to supply of nutrients to the roots by the convective stream of water. The amount of nutrients supplied to roots by mass flow is the product of the plant water uptake and the concentration of nutrients in the soil water. The relative importance of mass flow as a supply mechanism varies with climate, crop, and the nutrient in question. For maize, more than 75% of the N, but less than 3% of the P, needed is supplied by mass flow (Barber, 1984). The amount of nutrients supplied to roots by mass flow can be calculated as

$$J_m = q_w C_n \tag{18}$$

where J_m is the mass flux of nutrients to the roots, C_n is the mean nutrient concentration in soil solution, and q_w is the Darcy velocity. Hence, the nutrient flux to the roots by mass flow is affected by the rate of water uptake, which depends on the crop growth stage, plant species, climate, and soil moisture availability. If the concentration of nutrients in the soil solution is low, then the nutrient flux to roots will be low, even though the water flux may be high.

With continued uptake of nutrients supplied by interception and mass flow, there is a reduction in the concentration of nutrients at the soil root interface. This creates a chemical potential gradient normal to the root surface, resulting in the diffusion of nutrients toward the roots. Diffusion results from the random motion of ions and molecules known as Brownian motion. Where a concentration gradient is present, the net movement is away from the area of high concentration. Since the continued adsorption of nutrients by roots prevents the attainment of equilibrium, diffusion is ongoing. The path over which diffusion takes place ranges from 0.1 to 15 mm (Barber, 1984). Fick's first law gives the diffusive flux (J_d) of nutrients as

$$J_d = -D_e \frac{dC}{dn} \tag{19}$$

where D_e is the effective diffusion coefficient; and dC/dn is the concentration gradient perpendicular to the root surface. The effective diffusion coefficient (Nye and Tinker, 1977) may be calculated as

$$D_e = D\theta\tau \frac{dC}{dS} \tag{20}$$

where D is diffusion coefficient in water; θ is water content; τ is the tortuosity factor and dC/dS the reciprocal of the buffer power of the ion in question. Nutrients that are purely adsorbed will have a smaller dC/dS value. Fertilizer additions can cause an increase in dC/dS and larger D_e. The tortuosity increases with bulk density up to 1.3 g/cm^3. With the reduced pore space, there is increased continuity in the aqueous phase (Barber, 1984). D is given by the Stokes-Einstein equation as

$$D = \frac{K_b\, T}{6\pi \gamma_i\, \mu} \tag{21}$$

where K_b is the Boltzman constant, T is absolute temperature, γ_i is the ionic radius (L), and μ is the viscosity of water.

2.3.2 Approaches to Modeling Nutrient Uptake

The two approaches for modeling nutrient uptake by roots are the same as for water uptake—microscopic and macroscopic (Selim and Iskander, 1981; Moltz, 1981).

The microscopic approach considers nutrient fluxes to individual roots, and involves a solution to the transport equation in radial coordinates, as with water flow (e.g., Claassen and Barber, 1976).

Nutrient fluxes to roots sometimes can be described using Michaelis--Menton kinetics (Nye and Marriot, 1969). The macroscopic approach uses this, where nutrient uptake rate, J_n (MT^{-1}) is calculated as (Selim and Iskander, 1981)

$$J_n = \frac{V_{max} C L}{k_m + C} \tag{22}$$

where V_{max} ($ML^{-1}T^{-1}$) is the maximum nutrient uptake rate per unit length of root, C (ML^{-3}) is the concentration of nutrient, L is the root length density, and k_m (ML^{-3}) is the half-saturation constant.

2.4 Modeling Nitrogen Transformation in Soils

2.4.1 Overview of Processes

Nitrogen species in the biosphere exist in a dynamic equilibrium in which they are constantly being transformed through a series of complicated biochemical pathways known as the N cycle. The N transformation processes recognized are (1) immobilization or assimilation of inorganic forms of N by plants and microorganisms; (2) mineralization, the conversion of organic nitrogenous forms to NH_4^+; (3) nitrification, the oxidation of NH_4^+ to NO_3^-; (4) denitrification, the reduction of NO_3^- to N_2O and N_2; and (5) fixation of molecular N by microorganisms to NH_4^+ and organic forms (Keeney, 1981).

Section 2.3 discussed plant uptake; in this section, only microbial immobilization is discussed. Also, fixation is not dealt with, as it is not considered explicitly in this study. In addition, because of the equilibrium between organic and mineral forms of N, it is convenient to discuss mineralization and immobilization together.

2.4.2 Mineralization-Immobilization

A dynamic equilibrium exists between organic and inorganic forms of N in soils. The equilibrium level of mineral N is determined by the net effect of two opposing processes—mineralization and immobilization.

Crop residues in soils are used by microorganisms as a source of energy to fuel their metabolic activities. These organic materials are broken down enzymatically, and organic forms of N are mineralized during the process, some of which are incorporated in the microbial tissue. The net amount of N mineralized depends on the C-N ratio of the organic material. Materials with a high C-N ratio initially have a net immobilization (negative mineralization); those with a low C-N ratio usually have net mineralization. For crop residue with N content greater than 1.5-2.0% and C-N ratio less than 30:1, net mineralization is usually the norm (Schepers and Mosier, 1991). With continued decomposition, the C-N of the residue approaches that of the native soil humus, i.e., 10:1, and becomes indistinguishable from it. At this point, the residue is referred to as stable, with low mineralization rates.

Mineralization rate is affected by type of substrate, temperature, soil moisture, and aeration. In temperate-zone soils, annual mineralization rates range from 2-4% of the 1000-5000 kg/ha of organic N (Keeney, 1981).

Modeling approaches to mineralization-immobilization generally recognize soil organic matter to consist of two fractions: the slowly mineralized humus or stable organic matter fraction, and the readily mineralized, freshly added organic matter, such as crop residue or manure. Modeling approaches range from simple first-order expressions with different rate constants for the different fractions (e.g., Mehran and Tanji, 1974; Frissel and van Veen, 1981; Shaffer et al., 1991), to more complex analyses that explicitly account for biomass growth using Monod kinetics (e.g., Frissel and van Veen, 1981). In either case, rate constants are affected by environmental factors.

2.4.3 Nitrification

Nitrification refers to the microbially mediated oxidation of the product of mineralization (NH_4^+) that ultimately produces stable NO_3^-. A number of unstable intermediaries have been recognized in the oxidation of NH_4^+ to NO_3^-. However, the two main reactions recognized are the partial oxidation of NH_4^+ to nitrite (NO_2^-) by the bacteria *Nitrosomonas* and the oxidation of NO_2^- to NO_3^- by the bacteria *Nitrobacter* (Keeney, 1981). Nitrite has a very short half life in soils under normal circumstances, and is rapidly converted to NO_3^-. Nitrifiers are efficient, and, during the warm months, soil NH_4^+ is rapidly oxidized to NO_3^-. Factors affecting nitrification rate include temperature, moisture, and pH. Optimal nitrification rates are observed at neutral to slightly alkaline pH values (Focht and Verstraete, 1977).

The simplest approach to modeling nitrification uses a first-order reaction, with a rate constant that may depend on environmental factors such as temperature, water content, etc. (e.g., Shaffer et al., 1991; Mehran and Tanji, 1974). A more realistic approach uses the Michaelis-Menton equation. This approach recognizes a limiting nitrification rate at high substrate (NH_4^+) concentrations. More sophisticated approaches (e.g., Leggett and Iskander, 1981) model the oxidation of NH_4^+ to NO_2^- and of NO_2^- to NO_3^- with explicit consideration for the growth rates of oxidizers, and for possible nonlinear effects and interactions of environmental factors such as pH and temperature.

2.4.4 Denitrification

Denitrification is the process by which facultative aerobes use NO_3^- as their terminal electron acceptor under reducing conditions. The main products of denitrification are nitrous oxide (N_2O) and molecular N (N_2); however, under acidic conditions, nitric oxide (NO) may be liberated (Ryden, 1981). The primary factor promoting denitrification is the absence of oxygen, although complete anaerobiosis is not necessary since denitrification can proceed in micranoxic zones in close proximity to aerobic ones (Keeney, 1981). Other factors affecting denitrification are the amount of available carbon (C), type of organic matter, pH, and temperature. Optimal denitrification rates occur at neutral to slightly alkaline pH values (Focht and Verstraete, 1977).

Depending on the system of interest, denitrification may or may not be a desirable process. For cropping systems, it is undesirable, since it removes plant available N. However, for land renovation of wastewater, denitrification usually is promoted.

Rates of denitrification observed in the field depend on the NO_3^- concentration, the organic matter type, and the prevailing soil conditions. For irrigated vegetables in California, denitrification rates of 0.7-2.0 kg ha^{-1} day^{-1} following a rainfall or irrigation event were observed, compared to background levels of 0.1-0.2 kg ha^{-1} day^{-1} (Ryden and Lund, 1980). For manured, uncropped soil, rates as high as 70 kg ha^{-1} day^{-1} have been measured (Rolston et al., 1978).

From experimental studies, the order of denitrification has been estimated to be zero- to first-order reaction. The simplest modeling approach accounts for denitrification as a first-order process (e.g., Mehran and Tanji, 1974; Tanji and Gupta, 1978). The low concentration ranges of NO_3^- often found in soils justifies this approach. Probably a more accurate approach models denitrification as the product of two simultaneous Michaelis-Menton equations, the substrates being NO_3^- and C (Bowman and Focht, 1974). In all cases, the rate constants are modified by environmental factors.

2.5 Simulation Models for Nitrate Leaching in the Soil-Plant-Atmosphere Continuum

A number of simulation models are available that simulate N transport and transformation in the vadose zone. However, only a few of these explicitly account for actively growing crops. In this section, some of the more popular N leaching models that simulate root uptake of water and N and provide some estimate of crop productivity are reviewed. Special attention is paid to model attributes and weaknesses of relevance to this study. Finally, the justifications for a new model are addressed.

2.5.1 NLEAP

Nitrate Leaching and Economic Analysis Package (NLEAP) (Shaffer et al., 1991) is a user-oriented, noncrop-specific, one-dimensional, deterministic-capacity model for the estimation of NO_3^- leaching, crop performance, and economic impact of different crop management systems. The model can function in two modes: a screening mode and a detailed mode.

In the screening mode, computations are performed on a yearly basis using empirical relations and simple mass balances for water and N. In this mode, the annual NO_3^- leaching risk potential is the output, which can be determined for different crop management practices and climatic data. This mode is intended to identify potential N leaching problems and to determine whether detailed analyses are required. No economic summary is provided in this mode.

In the detailed mode, model computations are performed either over monthly intervals or on an event basis (rainfall, irrigation, tillage, etc.). Processes accounted for include N transformations (mineralization, immobilization, volatilization, denitrification, and N uptake), evapotranspiration, water flow, and N transport. The model also determines the risks of N leached from the root zone and aquifer contamination. For a detailed simulation, the soil is divided into two zones: an active zone (30.5 cm depth) and an inactive zone (the rest of the soil). Nitrogen transformation and plant root processes are confined to the active zone.

The model's incorporation of economic analysis and risks analysis is unique; however, the model's treatment of basic system processes severely limits its utility. In its most detailed mode, system processes are updated only following an event. In any event, the capacity-driven water flow and transport does not allow for redistribution of moisture at water contents below field capacity. Although this method of analysis can reasonably account for percolation following a rainfall or irrigation event, it cannot account for moisture redistribution following evapotranspiration. The model does not account for water fluxes from a water table, which may be substantial in the presence of shallow water tables. The model accounts for two soil zones, based entirely on the amount of biological activity. No allowance is made for physical soil layering. The model is incapable of long-term simulations of cropping systems involving rotations.

2.5.2 CREAMS

Chemicals Runoff and Erosion from Agricultural Management Systems (CREAMS) (Knisel, 1980) is a field-scale deterministic-capacity model that simulates surface and subsurface pollutant loading from different agricultural management systems. CREAMS, by design, is a continuous simulation model, but can be executed in an event-oriented mode. It estimates runoff, sediment load, nutrient load (N and P), and pesticide load in runoff and leachate.

CREAMS consist of four submodels: the hydrology submodel simulates runoff, infiltration, redistribution, and evapotranspiration; the erosion submodel estimates sediment load; the nutrient submodel simulates plant uptake of N, N and P in runoff and sediment, N in drainage, and N transformations; and the pesticide submodel simulates pesticide runoff to soil and partitioning among the different phases.

CREAMS' treatment of surface processes is particularly good, so it is an excellent model for evaluating runoff and soil erosion. However, its treatment of the subsurface is crude. Flow and transport are considered in only one dimension, and are dependent only on the field capacity of the soil. This does not allow for the redistribution of moisture at moisture contents below field capacity. Water flow is unidirectional from soil surface to bottom; i.e., the model cannot simulate water flow from a shallow water table. Nutrient uptake takes place over the entire root zone, with no regard for variations in root depth as the crop matures.

2.5.3 CERES-Maize

CERES-Maize (Jones and Kiniry, 1986) is a one-dimensional, research-level, continuous-simulation model of maize growth and development in the soil-plant-atmosphere continuum for different management systems. It estimates runoff, infiltration, moisture redistribution, N immobilization including plant uptake, nitrification, mineralization, denitrification, soil temperature, and maize vegetative and reproductive growth in response to soil and climatic factors. Moisture redistribution following infiltration is modeled using a tipping-bucket approach, using field capacity as the upper limit of soil moisture availability. Moisture fluxes following evapotranspiration are determined using the diffusivity form of the Darcy flux equation. Convective transport of N is considered.

The model is rigorous in its treatment of maize physiological processes in relation to soil and atmospheric factors. However, the model is one-dimensional, does not simulate conservation tillage, and is incapable of performing long-term multicrop simulations.

2.5.4 NTRM

Nitrogen Tillage Residue Management (NTRM) (Shaffer, 1985) is a field-scale, one-dimensional, deterministic model that continuously simulates soil erosion and maize production under different management practices, in both the short and the long term. Processes simulated include water and heat flow, solute transport (NH_4^+, NO_3^-, Ca^{2+}, Mg^{2+}, Na^+, HCO_3^-, CO_3^{2-}, SO_4^{2-}, and urea), chemical equilibria (dissolution-precipitation, ion exchange, dissociation, and ion pairing), N transformations (mineralization, immobilization, nitrification, denitrification, urea hydrolysis, N fixation, crop uptake), and plant growth and tillage management.

The model is detailed in its treatment of system processes, with physically based treatment of water flow and chemical transport. NTRM is unique among leaching crop productivity models in its treatment of salt transport and chemical equilibria. Such attributes would be useful in evaluating crop productivity in saline environments. Water flow is determined by a solution to the water content form of Richard's equation, which makes it applicable to physically homogeneous systems only. Additionally, the model does not simulate multicrop continuous systems.

2.5.5 Rationale for New Model

As previously stated, the dominant cropping system of the Northern Neck involves a two-year rotation of maize, wheat, soybeans, and fallow. Therefore, it would be prudent to continuously simulate these crops sequentially over long time periods to realistically simulate N leaching from this area. The major shortcoming of the available crop growth N-leaching models investigated, of relevance to this study, is their inability to perform long-term continuous simulation involving multicrop sequences that include fallow periods.

A feature of the management of high N-use crops is that they are planted in rows. The existence of an inter-row makes the distribution of roots, water content, and nutrients decidedly two-dimensional. Since horizontal gradients exist, water flow and nutrient transport will be two-dimensional also. Given this reality, it would be appropriate to model a two-dimensional vertical slice between two rows, rather than the vertical dimensions only. Available crop growth N-leaching models are exclusively one-dimensional.

3 Description of VT-CROPS

3.1 Overview

VT-CROPS models three interacting subsystems: the atmospheric subsystem, the soil subsystem, and the crop subsystem. Figure 1 depicts the general subsystem interaction.

Although the climatic subsystem is not modeled explicitly, its interactions with the other subsystems are considered explicitly. The climatic subsystem supplies daily solar radiation, maximum and minimum temperature, and rainfall amounts to the soil and crop subsystems. Climatic data either is input directly or is generated stochastically by a weather generator.

The crop subsystem simulates the growth and development of maize, wheat, and soybeans. It accumulates and partitions dry matter and N among the different plant components, and advances the plant through its phenological growth stages. The crop subsystem interacts with the climatic and soil subsystems. The climatic subsystem determines transpirational demand and the development and growth of the crop. Air temperature is the stimulus for advancing the plant through its phenological growth stages, and solar radiation is the stimulus for carbohydrate (CHO) production. Low levels of moisture and N in the soil impair the plant's ability to produce CHO.

The soil subsystem routes rainfall to runoff or infiltration, computes soil moisture changes and drainage, and models soil N movement and transformations in the soil. Water and N are passed to the crop, depending on amounts and distributions in the soil, evaporative demand, root distribution, and crop growth as mediated by the climatic and crop subsystem models.

3.1.1 Detailed Subroutine Flow

Figure 2 shows the order in which subroutines are called during program execution.

Through the subroutine READ, VT-CROPS first reads the input data specified by the user through a series of input data files (Appendix 1). VT-CROPS then echoes this data, using subroutine WRTINT, to a series of output files. Model variables then are initialized through subroutines PROGRI, SINPUT, and NINPUT. PROGRI primarily initializes crop parameters, SINPUT initializes soil variables other than N simulation variables, and NINPUT initializes N variables. If synthetic climatic data are to be used, two years of data are generated by subroutine WGEN; if not, historical data are read from an input file specified by the user.

The soil subsystem is simulated daily for all crop and fallow periods. Subroutine SOIL controls the soil subsystem, thereby controlling all subroutines that simulate soil processes and events. If fertilizer is to be added on a given day, FRTLIZ is called. If irrigation is being simulated, IRRIG is called when irrigation water needs to be applied. SNOW is called only during wheat growth or extended fallow to determine snow fall or melt, depending on the temperature and precipitation status of the day. If rainfall, snow melt, and/or irrigation is greater than zero, GRAFLO is called. GRAFLO determines surface runoff, infiltration, and the initial percolation of moisture. TSOLT is called daily to update the temperature of cells. The N transformation subroutines are called if N is being simulated. TMNIM simulates the mineralization-immobilization of organic-N, TNITF determines the nitrification of NH_4^+ to NO_3^-, and TDNIT simulates the denitrification of NO_3^-. SOIL then calls PET2, which determines potential and actual evapotranspiration. N uptake is determined by UPTAK2. CAPFL2 redistributes soil moisture and N, following crop uptake and evaporation.

SOIL then passes control back to the main program, where, if the crop is maize or wheat, phenology is simulated. Nine phenological growth stages are simulated: stages 7-9 represent presowing to germination, and stages 1-6 are periods of active growth (i.e., emergence to maturity). The passage from one growth stage to the next is predicated on the accumulation of a specified number of degree days. Subroutine PHENOL determines the crops phenological advancement based on the accumulation of heat units; if wheat is being simulated, COLD determines possible adverse effects of low temperatures on growth. If the required number of degree days for a given crop growth stage is accumulated, the current growth stage ends, and PHASEW is called for wheat and PHASEI is called for maize. These subroutines initialize the parameters for the current stage and call subroutines WRITE and ENDSTG to produce crop parameters for the previous stage. If the crop is actively growing (i.e., growth stage less than 7), subroutine GROSUW is called for wheat, or GROSUB for maize, to determine CHO assimilation and partitioning. If the CHO partitioned to the roots is greater than 0, control then passes to RUTGRO, which determines the daily root growth based on the net CHO partitioned to the roots. If nitrogen is being simulated, subroutines NFACT2 and NPART2 are called—NFACT2 determines nitrogen factors affecting crop productivity, and NPART2 partitions N uptake to the different plant parts.

If maize or wheat is not being simulated, it is either soybean or fallow. If it is soybean, MAIN calls RUTGRO to determine daily root growth.

Control then passes back to the main program, which increments the date if the crop is not mature, and repeats the above sequence. If, at any time during a simulation, the weather data are exhausted, more data are generated if synthetic data are being used; if not, execution is halted. Maturity dates for maize and wheat are determined by the accumulation of degree days; maturity date of soybean and end of fallow periods are determined a priori. If date is equal to the maturity date, HARVST is called and crop-yield parameters are determined and written to output files. If a next crop is being simulated and there are climatic data, the next crop is determined and simulation begins; if another crop is to be simulated but climatic data are needed, data are generated if synthetic data is being used; otherwise, the program terminates. After the last crop in a sequence of rotations is simulated, the program terminates.

3.2 Atmospheric Subsystem

Atmospheric parameters that drive the soil and crop subsystems are daily rainfall, daily solar radiation, and maximum and minimum daily temperature. If historical data are available, these may be entered directly. Otherwise, a stochastic weather generator algorithm is employed. A time-series model described by Richardson and Wright (1984) is used to simulate climatic variables. An autoregressive time-series analysis is used for rainfall with varying monthly statistical distributions. Maximum and minimum temperatures on wet and dry days and solar radiation are assumed to follow mean sinusoidal trends. Variations about the mean are normal, with seasonally varying coefficients of variation. Procedures for calibration of the stochastic weather model from historical data have been discussed by Richardson and Wright (1984). When VT-CROPS is executed in a stochastic mode, daily weather data are generated automatically and passed to the crop and soil subsystem models.

3.2.1 Weather Generator Submodel

The climatic weather generator simulates maximum temperature, minimum temperature, solar radiation, and precipitation over a specified time interval. The approach used maintains the temporal and autocorrelation structure of weather variables. Daily temperature and solar radiation generated are affected by the occurrence of rainfall. Precipitation is generated independently, then the magnitude of minimum and maximum temperature and solar radiation depends on the wet or dry status of the day.

3.2.1.1 Precipitation. Precipitation is generated using a Markov chain-gamma model. Wet or dry days are generated using a first-order Markov chain; i.e., the occurrence of rainfall on the current day is conditioned only on the wet or dry status of the previous day. In the event of a wet day, the amount of rainfall is generated using a two-parameter gamma distribution.

The user must enter the probability of a wet day followed by a wet day, P_{ww}, and that of a wet day followed by a dry day, P_{wd}. From these probabilities, the transition probabilities of a dry day following a wet day, P_{dw}, and that of a dry day following a dry day, P_{dd}, are fully defined as

$$P_{dw} = 1 - P_{ww} \tag{23)a$$

$$P_{dd} = 1 - P_{wd} \tag{23)b$$

It is customary to generate probabilities by sampling from a uniform distribution on the interval 0 and 1. A uniform distribution is sampled daily. In the event that the previous day was wet and the sampled number is less than or equal to P_{ww}, then the current day precipitates also; otherwise it is a dry day.

The conditional probabilities P_{ww} and P_{wd} and, thus, P_{dw} and P_{dd}, vary temporally at any given location (Richardson and Wright, 1984). This temporal variation is preserved by allowing the conditional probabilities to vary each month.

Given that it rains on the current day, the amount of precipitation is determined using a two-parameter gamma distribution. The two-parameter gamma distribution is attractive for generating rainfall because of the few parameters to be determined, and the fact that small magnitude outcomes have high frequencies and only non-negative outcomes are possible. Richardson (1982) found the gamma distribution to give better results for rainfall than other similar types of distributions. The probability density function of a two-parameter gamma function is given by

$$f(p) = \frac{p^{\alpha-1} e^{-\frac{p}{\beta}}}{\beta^{\alpha}\Gamma(\alpha)}, \quad p,\ \alpha,\ \beta > 0 \tag{24}$$

where $f(p)$ is the density function of p; α and β are shape and scale parameters, respectively; and $\Gamma(\alpha)$ is the gamma function of α. The relationship between α and β and population moments is given by Law and Kelton (1991) as

$$\beta = \frac{\sigma^2}{\mu} \tag{25a}$$

$$\alpha = \left(\frac{\mu}{\sigma}\right)^2 \tag{25b}$$

where μ is the population mean and σ^2 is the variance.

Rainfall amount is calculated by first determining the cumulative probability, $F(p)$, by sampling from a uniform distribution on the interval 0 and 1. From the inverse probability of $F(p)$, the amount of rainfall is determined. The cumulative density function of the gamma distribution is not of a closed form; therefore, its inverse is not easily found. However, algorithms are available through which this can be accomplished (e.g., Law and Kelton, 1991).

Not unlike the conditional probabilities, α and β are allowed to vary monthly for each location.

3.2.1.2 Temperature and Solar Radiation. Maximum temperature (T_{max}), minimum temperature (T_{min}), and solar radiation (r) are generated using a weekly stationary generating process of Matalas (1967), as

$$x_i(j) = Ax_{i-1}(j) + B\epsilon_i(j) \tag{26}$$

where x_i and $x_{i-1}(j)$ are 3x1 column vectors whose elements are the standardized, normally-distributed values of T_{max}, T_{min}, and r for day i and i-1 respectively; ϵ_i is a 3x1 column vector of normally distributed residuals; and A and B are 3x3 matrices with elements so defined as to preserve the serial and cross correlation among the variables. Actual mathematical definition can be found in Richardson and Wright (1984). The unstandardized variates are contained in the column vector t_i, calculated as

$$t_i(j) = m_i(j)\left(x_i(j)\ w_i(j) + 1\right) \tag{27}$$

where $m_i(j)$ is a column vector of estimates of rainfall dependent, mean of variables; and $w_i(j)$ is a column vector containing rainfall dependent, coefficient of variations. The variables $m_i(j)$ and $w_i(j)$ are allowed to vary as a simple harmonic, using the cosine function as

$$u_i = \bar{u} + C^A \cos\left(0.0172(i - t)\right) \tag{28}$$

where u_i is the mean value of $m_i(j)$ or $w_i(j)$ on day i, $\bar{u}$ is the mean of the harmonic, C^A is the amplitude, and t is the position of the harmonic. The variables $\bar{u}$, C^A, and t must be evaluated from actual data for wet and dry days separately.

3.3 Soil Subsystem

3.3.1 Overview

The soil domain is represented as a two-dimensional vertical slice between crop rows as in the RHIZOS portion of the cotton model GOSSYM (Baker et al., 1983). The inter-row spacing and the profile depth specified by the user are partitioned to form a matrix of equal-sized cells or grids (figure 3). Soil layers may be defined that represent soil profile horizons of different properties (figure 4). Soil water retention characteristics for each layer are defined in terms of the parametric model of van Genuchten (1980).

The soil subsystem model consists of three submodels: the soil temperature submodel, the nitrogen submodel, and the water submodel. A conceptual diagram of the soil subsystem is shown in figure 5.

3.3.2 Tillage Management

Tillage effects on soil properties are determined during the initialization of model parameters prior to crop simulation in subroutine NINPUT, and, as such, do not fall in any of the soil submodels mentioned.

3.3.2.1 Effects of Tillage. *Minimum tillage* refers to any combination of tillage and crop management system that leaves 30% or more of the soil surface covered by crop residue to reduce runoff (Mannering et al., 1987). In the literature, the term often is used interchangeably with *conservation tillage*, *reduced tillage*, and *low tillage*. In addition to reducing runoff, minimum tillage also may reduce land preparation time, labor and fuel, and machinery cost (Throckmorton, 1986). Disadvantages of minimum tillage include increased use of herbicides and pesticides for weed and pest control.

In 1985, it was estimated that approximately one-third of all cropland in the United States was under some form of conservation tillage (Conservation Tillage Information Center, 1982-85). The U.S. Department of

Agriculture Office of Planning (1975) estimates that, by the year 2010, 95% of all cropland in the nation will be under minimum tillage.

3.3.2.2 Modeling Tillage. VT-CROPS simulates the fraction of soil surface coverage from crop residue under minimum tillage. Under conventional tillage, no surface coverage is assumed. The fraction of the soil covered under minimum till is calculated following the approach of van Doren and Allmoras (1978) as

$$\Delta CS_m = 1 - \exp(-1.68x10^{-4}\frac{W_d}{\rho^s}d) \tag{29}$$

where ΔCS_m is a fraction of soil surface covered by mulch, W_d is dry weight of residue (metric tons ha^{-1}), ρ^s is the specific dry density of residue (g cm^{-3}), and d is the diameter of cylindrical residue pieces in meters. The effective soil albedo is adjusted according to the approach suggested by van Doren and Allmoras (1978) as

$$\chi_{ef} = \chi_s + \Delta CS_m(\chi_r - \chi_s) \tag{30}$$

where χ_{ef} is the effective soil albedo, and χ_r and χ_s are the reflectance coefficients for soil and residue, respectively.

In addition to soil albedo, the infiltration of rainfall is directly increased under minimum tillage. Increases in infiltration rates are effected by selecting appropriate runoff curve numbers reflecting tillage practice. Mannering et al. (1987) reported that, of the factors most critical to erosion control, surface coverage from seedbed preparation to canopy establishment is the most important. Changes in the surface water balance will, in turn, affect other processes such as leaching, thermal diffusivity, moisture availability, evapotranspiration, and N transformations.

3.3.3 Soil Temperature Submodel

Soil temperature is important as a control for root growth and nitrogen transformation rates. A one-dimensional analytical model for heat transfer is programmed in subroutine TSOLT, following the approach used in the EPIC model (Williams and Renard, 1985). The temperature submodel first converts the calendar day of year (t) to a radian fraction of one year (R_f), and converts solar radiation from Langleys/day (ξ_L) to mega-Joule/day (ξ_M) as

$$R_f = 0.0172(t - 200) \tag{31}$$

$$\xi_M = 0.04184\ \xi_L \tag{32}$$

The surface albedo (χ) is updated as

$$\chi = \chi_{ef} \qquad \zeta \geq 6 \tag{33a}$$

$$\chi = 0.23 - (0.23 - \chi_{ef}) \exp(-0.75 LAI) \quad \zeta < 6 \tag{33b}$$

and the mean daily air temperature (T_{mn}) is computed as

$$T_{mn} = \frac{T_{max} + T_{min}}{2} \tag{34}$$

where χ_{ef} is the soil albedo; LAI is the leaf area index of the crop, the ratio of total leaf area to ground surface covered; ζ is the crop growth stage; T_{max} is the maximum daily temperature; and T_{min} is the minimum temperature. Daily surface temperature is determined as

$$T_t^0 = (1 - \chi)A + \chi T_{t-1}^0 \tag{35}$$

where

$$A = \left\{ T_{mn} \left[1.0 - \frac{\xi}{3.35 \times 10^7} \right] + T_{max} \frac{\xi}{800} \right\} \tag{36}$$

and T_{t-1}^0 is the previous day's surface temperature. The most recent 5-day running average surface temperature (T_5) is determined as

$$T_5 = 0.20 \sum_{d=1}^{5} T_d^0 \tag{37}$$

The surface temperature effect on the damping depth (F_{dp}) is calculated as

$$F_{dp} = T_s - \left[T + \delta_t \times \frac{\cos(R_f)}{2.0} \right] \tag{38}$$

where $\bar{T}$ is the average annual ambient air temperature (°C), δ_t is the annual amplitude of mean monthly air temperature (°C), and R_f is the day of the year as a radian fraction of one year.

TSOLT calculates a scaling factor (S_f), which is used in the determination of the damping depth for soil temperature

$$S_f = \frac{\Sigma_\theta}{(0.356 - 0.144\ \bar{\rho})\ Z} \tag{39}$$

where Σ_θ is the total soil water in the profile in mm, Z is the total depth of the soil profile in mm, and $\bar{\rho}$ is the average bulk density of the soil profile in gm cm^{-3}.

The maximum damping depth (Dp_{max}) in mm as a function of the average soil bulk density for each soil layer is calculated as

$$Dp_{max} = 1000 + \frac{2500\ \bar{\rho}}{\bar{\rho} + 686\ \exp(-5.63\ \bar{\rho})} \tag{40}$$

The actual damping depth (Dp) is calculated as

$$Dp = F\ Dp_{max} \tag{41)a}$$

where

$$F = \exp\left\{ \left(\log_{10} \frac{500}{Dp_{max}} \right) \left(\frac{1-\theta}{1+\theta} \right)^2 \right\} \tag{41)b}$$

where θ is the moisture content at that depth.

The temperature at each depth (T_d) is updated as

$$T_d = T + \left\{ \frac{\delta_t}{2} \cos(R_f) + F_{dp} \right\} \exp\left[\frac{-Z_d}{Dp} \right] \tag{42}$$

where Z_d is the depth in mm.

3.3.4 Soil Water Submodel

3.3.4.1 Water Flow Equation. Water flow and water content distribution in a two-dimensional isotropic nonhomogeneous domain is determined in subroutine CAPFL2, using the Darcy flux equation

$$q_i = K(\theta)\,\frac{\partial H}{\partial x_i} \qquad i = 1,2 \tag{43}$$

and the continuity of mass equation

$$\frac{\partial \theta}{\partial t} = -\frac{\partial q_i}{\partial x_i} \tag{44}$$

where q_i is the water flux (cm day^{-1}) in the i-th direction, x or y; θ is moisture content; t is time (day); $K(\theta)$ is the soil hydraulic conductivity function (cm day^{-1}); H is the water hydraulic head (cm), the sum of pressure and gravitational heads; and x_i is the horizontal or vertical coordinate (cm).

Using the water content distribution from the previous time step, equation 43 is used to estimate water fluxes due to capillary flow between centers of adjacent cells using explicit finite difference of the form

$$q_i^{t+\Delta t} = \overline{K}\,(\theta)\,\frac{\left(H_{i-\Delta i}^{t} - H_i^{t}\right)}{\Delta i} \tag{45}$$

where t is the previous time, Δt is the time increment; and Δi is the spatial increment in the x or y directions.

The water contents are subsequently updated using an explicit block-centered backward finite difference approximation of equation 44 as

$$\theta^{t+\Delta t} = \frac{\left(q_i^{t+\Delta t} - q_{i-\Delta i}^{t+\Delta t}\right)}{\Delta i}\,\Delta t + \theta^{t} \tag{46}$$

Note: For equations 43-46, the Einstein summation convention is implied.

Water content, pressure head, and conductivity are described by van Genuchten's (1980) parametric model as

$$K(\theta) = K_s \, \theta^{\frac{1}{2}} \left(1.0 - (1.0 - \theta^{\frac{1}{m}})^m\right)^2 \tag{47a}$$

$$\theta = (\theta_s - \theta_r) \left(1.0 + (\alpha|h|)^n \right) + \theta_r \tag{47b}$$

where θ_s is the saturated water content, θ_r is the residual water content, α (cm^{-1}) and n are pore-size distribution parameters, and $m = 1 - 1/n$.

Initial and Boundary Conditions: At $t = 0$, the initial distribution of moisture (θ_0) is specified by the user as

$$\theta(y) = \theta_0(y) \quad at \ z = 0 \tag{48}$$

The initial soil moisture content is allowed to vary vertically in each layer.

The surface boundary is stipulated as a flux boundary condition. The flux can be controlled by rain, irrigation, or surface evaporation, and is given by

$$q(t) = K(\theta) \left[\frac{\partial h}{\partial z} + 1 \right] \quad at \ z = 0 \tag{49}$$

The bottom boundary can be stipulated as follows:

- If the soil profile extends to great depth, the profile is treated as a semi-infinite medium, and a unit hydraulic gradient boundary condition is imposed at the bottom as

$$\frac{\partial h}{\partial z} = 0 \quad at \ z = d \tag{50}$$

- If the water table is encountered at some depth d, the boundary condition is one of constant head

$$h = 0 \quad at \ z = d \tag{51}$$

On the vertical sides, the boundary condition is zero flux

$$\frac{\partial h}{\partial x} = 0 \quad at \ x = 0 \ and \ x = l \tag{52}$$

where l is the mid-row spacing of the crop. In a multi-layer profile, the boundary conditions at the interfaces are such that there is continuity of soil water potential (figure 4).

Capillary flow is defined as that occurring below field capacity. Gravity flow at higher water contents is modeled using a simple tipping-bucket approach that distributes water in excess of field capacity to lower layers as soon as they become full. Field capacity is defined operationally as the water content at h = -100 cm. Mass balance error at the end of each time increment is partitioned equally to the cells, provided the moisture limits of a cell are not violated. The harmonic mean of the hydraulic conductivities between two adjacent cells in horizontal and vertical directions is used in all calculations.

3.3.4.2 Soil Evapotranspiration. Evaporation is applied as an outward flux at the soil surface. Evaporative demand is partitioned to the uncovered areas first. If demand is not met, then covered areas supply the remainder. Water is taken up by the root system to meet the transpirational demand computed in the crop module. Transpirational demand is partitioned to each cell containing roots, based on a root uptake factor. Uptake factors over the domain sum to unity, and are based proportionately on the soil water diffusivity and the root weight and age in each cell. Cell moisture content is reduced to reflect transpirational demand or available soil moisture, whichever is less. In the event that soil is unable to supply optimal crop moisture needs, plant water stress factors are calculated, and growth is reduced accordingly.

3.3.4.3 Soil Water Runoff and Infiltration. Following a rainfall or irrigation event, the amount of water that infiltrates the soil or runs off is determined in the subroutine GRAFLO.

The amount of runoff is calculated using the SCS curve number technique (SCS, 1972). GRAFLO first selects the appropriate runoff curve number (CN_r) depending on soil surface coverage that crop leaf area affords as

$$CN_r = CNF_r \qquad LAI/2.5 < 0.33 \tag{53)a}$$

$$CN_r = CN2_r \qquad 0.33 \le LAI/2.5 < 0.69 \tag{53)b}$$

$$CN_r = 2\ CN2_r - CNF_r \qquad 0.69 < LAI/2.5 \tag{53c}$$

where *LAI* is leaf area index, CNF_r and $CN2_r$ are fallow and average curve numbers, respectively, and 2.5 is the maximum *LAI*. Following the approach of Kinsel (1980), the curve number affecting runoff (CNI_r) is calculated

$$CNI_r = -16.91 + 1.248 CN_r - 0.01379 CN_r^2 - 0.0001172\ CN_r^3 \tag{54}$$

The amount of water on the soil surface (*S*) is calculated as

$$S = 254.0 \left[\frac{100}{CNI_r - 1.0} \right] \left(1 - F_\theta \right) \tag{55}$$

where F_θ is the soil moisture factor affecting runoff, which is calculated as

$$F_\theta = \sum_{l=1}^{NL} W_l \left[\frac{\overline{\theta}^l - \theta_L^l}{\theta_s^l - \theta_L^l} \right] \tag{56}$$

where $\overline{\theta}^l$ is the average water content of layer *l*, θ^l is the saturated moisture content of the layer, θ_L^l is the lower limit of available moisture; *NL* is the number of layers, and W_l is a runoff weighting factor calculated as

$$W_l = \exp(- b\ Z_{l-1}) - \exp(- b\ Z_l) \qquad \sum_{l=1}^{NL} W_l \leq 0.995 \tag{57a}$$

$$W_l = 0.0 \qquad \sum_{l=1}^{NL} W_l > 0.995 \tag{57b}$$

where Z_l is the depth of the layer *l*, and *b* is an internally defined constant.

GRAFLO then calculates the amount of runoff (*Q*) using the SCS equation (SCS, 1972)
where *P* is the rainfall amount for the day.

$$Q = \frac{(P - 0.2\, S)^2}{P + 0.8\, S} \tag{58}$$

The amount of infiltration (I_i) is calculated as

$$I_i = P - Q \tag{59}$$

The amount of water infiltrating the soil is divided evenly among all surface cells. The amount of water entering a cell above the drained upper limit is passed to the cell below. As a cell drains to its drained upper limit, N is leached to the lower cell by the process of advection.

3.3.5 Nitrogen Transport Submodel

3.3.5.1 Transport Equation. The processes contributing to N transport in soils are advection, molecular diffusion, and mechanical dispersion. VT-CROPS explicitly considers only advection. Keeney (1983) pointed out that, considering the complexity and uncertainty in modeling N transformations, and the fact that numerical dispersion will tend to compensate for ignoring dispersive transport, such a simplification is adequate. With this simplification, the transport equation, with the implied Einstein summation, has the form

$$\frac{\partial(\theta_i c_n)}{\partial t} = - \frac{\partial q_i c_n}{\partial x_i} \tag{60}$$

where c_n is the concentration of NO_3^-, and q_i is the Darcy flux in the x_i direction. Equation 60 is solved by a block-centered explicit finite difference scheme using a time step of one day.

Initial and Boundary Conditions: The initial distribution of NO_3^- is specified as

$$c_n(z) = c_n^0(z) \ at\ t = 0 \tag{61}$$

where (c_n^0) is the initial concentration of NO_3^-, which is allowed to vary vertically in the soil profile.

The surface boundary condition before or after fertilizer application is a zero flux condition given by

$$c_{in} = 0 \; at \; z = 0 \tag{62}$$

where c_{in} is the influent concentration at the surface. At the lower boundary when the Darcy flux is downward, a flux boundary condition is imposed for transport with the effluent flux equal to the product of concentration and Darcy velocity. However, when flow is upward, the transport boundary condition is specified as zero flux, thus preventing the entry of NO_3^- through the lower boundary into the root zone.

The user specifies the mode, amount, source type, number of applications, and timing of fertilizer applications. Fertilizer may be applied superficially, incorporated, or banded into the soil. Plant uptake is treated as an internal sink.

3.3.6 Nitrogen Transformations

The processes of N mineralization, immobilization, nitrification, and denitrification take place in the N submodel, while N advection and uptake take place in the water submodel. Figure 6 is a block diagram of N transformations and transport processes accounted for by VT-CROPS. The N submodel assumes that NH_4^+ is strongly adsorbed and, hence, is not subjected to aqueous phase convection. Conversely, it assumes the NO_3^- species is found exclusively in the soil solution and is susceptible to leaching. Crop plants can use both NH_4^+ and NO_3^- sources of N. However, since maize is grown when soil NH_4^+ contents are low due to high soil temperatures, only NO_3^--N is used by maize. Wheat is capable of using both N species.

3.3.6.1 Nitrogen Mineralization and Immobilization. The release of NH_4^+-N from organic sources due to mineralization is calculated in the subroutine TMNIM. Two approaches are available for simulating N mineralization and immobilization—method I is indigenous to VT-CROPS; method II was inherited from VT-MAIZE and modified.

Method I: An alternate mineralization approach was deemed necessary since the original method did not model sludge mineralization effectively, and only modeled net mineralization, even when high C-N ratio organic material was added to the soil. When high C-N ratio organic material is added to a soil, net immobilization of mineral N sources is the initial result.

Like the original procedure, this method identifies two sources of organic matter—a stable fraction comprised of soil humus, and a fresh fraction comprised of crop residue, sludge, and other foreign organic sources. The stable organic matter, comprising a relatively large pool, is unreactive; hence, its rate of oxidation is much slower than the fresh organic matter pool. The stable organic fraction is assumed to have a constant C-N ratio of 10; that of fresh organic matter is determined initially by the N content of incorporated organic matter, and is updated as oxidation proceeds. The oxidation of both organic fractions is modeled as a first-order rate process.

Given its low C-N ratio, the oxidation of stable organic matter is assumed to always result in net mineralization. The amount of stable organic N mineralized, $\Delta N_c^{m,h}$ (mg cm^{-3}), is calculated from the first-order rate equation as

$$\Delta N_c^{m,h} = f_f^1 \, K_c^{m,h} \, N_c^h \, \Delta t \tag{63}$$

where $K_c^{m,h}$ (day^{-1}) is the optimal first-order rate constant for humus mineralization, reduced by soil water and temperature stress factors; f_f^1 is a user input factor for modifying $K_c^{m,h}$; N_c^h is the cell stable organic matter N content (mg cm^{-3}); and Δt is the time increment (day).

The evaluation of the optimal first-order rate constant deserves special attention. As pointed out by Keeney (1981), 2-4% of stable organic N is mineralized annually. As a first-order estimate, it is assumed that 3% of stable organic N is mineralized. Therefore, $K_c^{m,h}$ can be estimated as

$$K_c^{m,h} = \frac{-\ ln(0.97)}{365} = 8.345 \times 10^{-5} \ day^{-1} \tag{64}$$

In the case of fresh organic matter, the oxidation of carbon in a cell ($\Delta C_c^{c,f}$) is modeled as a first-order process using

$$\Delta C_c^{c,f} = f_f^2 \, K_c^{c,f} \, C_c^f \, \Delta t \tag{65}$$

where f_f^2 is a correction factor entered by the user; $K_c^{c,f}$ is the optimal first-order carbon oxidation rate constant, modified multiplicatively by cell temperature (F_T) and soil water deficit factors (F_θ^1); and C_c^f is the fresh organic carbon content of a cell, assumed to be 40% of the fresh organic matter in the cell, the carbon fraction of a basic structural unit of CHO.

A first estimate of $K_c^{c,f}$ can be made as follows: The USEPA (1983b) reported that 40% and 60% of the organic N in sludge was mineralized one and two years after soil incorporation, respectively. If it is assumed that 60% of the organic carbon is oxidized after two years, then

$$K_c^{c,f} = F_f \frac{-ln(0.40)}{730.0} \tag{66}$$

can estimate $K_c^{c,f}$, where F_f is a calibration factor, the value of which is determined for site-specific conditions.

The fresh organic matter mineralized in a cell ($\Delta N_c^{m,f}$) is calculated as

$$\Delta N_c^{m,f} = \Delta C_c^{c,f}\left(30.0 - CN_c\right)F_N \tag{67}$$

where CN_c is the cell C-N ratio, and F_N is a mineral N availability factor, which has a value of 1 for immobilization. Note that C-N ratios less than 30 result in mineralization; i.e., production of NH_4^+ from organic sources; and C-N ratios greater than 30 result in immobilization (negative mineralization); i.e., production of fresh organic N from mineral N.

The amount of mineralization that takes place in a cell is limited to a fraction (MN_{max}) of the fresh organic N in a cell per day. Ten percent of fresh organic N mineralized is immediately immobilized in the stable organic fraction.

The amount of N immobilization that takes place in a cell is constrained by the sum of available NH_4^+-N and NO_3^--N in a cell. Available NH_4^+-N is immobilized first, and NO_3^--N accounts for the difference. Available mineral N species is the amount in excess of 1 mg gm^{-1}.

VT-CROPS then updates the mineral N, organic N, and organic matter pools.

This method is considered superior to the original since (1) it allows for the modeling of net immobilization when high C-N ratio organic materials are incorporated in the soil, and (2) it allows for carbon oxidation in fresh organic matter. With method II, only nitrogen mineralization is modeled, so the ratio of fresh organic matter always increases; with method I, the ratio can, more realistically, go either way.

Method II: Nitrogen mineralization and immobilization are modeled using a modified PAPRAN approach (Seligman and van Keulen, 1981). With this approach, the immobilization that is modeled refers to a fraction of the N mineralized over a time increment, so net mineralization is always the result, regardless of the C-N ratio of the organic matter. Two sources of organic matter are recognized: (1) fresh organic matter and (2) stable or humic organic matter, modeled as first-order processes with different rates of mineralization (Newkirk et al., 1987a).

The optimal rate constant for the mineralization of fresh organic matter ($K_c^{m,f}$) is determined daily in each cell, based on the ratio of fresh organic N remaining (N_c^f) to the initial amount contained in the cell ($N_c^{f,0}$). Depending on the fraction of $N_c^{f,0}$ remaining, the predominant type of CHO being mineralized and, hence, $K_c^{m,f}$ is determined. Three types of CHO are identified in fresh organic matter—simple CHO, cellulose, and lignin—with $K_c^{m,f}$ of 0.8, 0.05, and 0.0095 day^{-1}, respectively (Newkirk et al., 1987a). The optimal rate constant for mineralization of fresh organic matter is modified multiplicatively by soil temperature (F_T), mineral N (F_N), and the first of two moisture (F_θ^1) deficit factors. The optimal rate constant for the mineralization of humus ($K_c^{m,h}$) is set at 1.12×10^{-4} day^{-1}, which the user has the option to modify, and is reduced multiplicatively by F_T, F_N, F_θ, and a cell C-N ratio factor (F_{CN}). TMNIM calculates the N mineralized from fresh organic matter in a cell, $\Delta N_c^{m,f}$, (mg cm^3) and humus, $\Delta N_c^{m,h}$, (mg cm^3) as

$$\Delta N_c^{m,f} = K_c^{m,f} \; N_c^f \Delta t \tag{68)a}$$

$$\Delta N_c^{m,h} = f_f^1 K_c^{m,h} \; N_c^h \Delta t \tag{68)b}$$

where f_f^1 is a factor entered by the user that modifies the mineralization rate of humus; N_c^f (mg cm^3) and N_c^h (mg cm^3) are the amounts of fresh organic N and stable organic N in a cell, respectively; and Δt is the time increment. Two percent of $\Delta N_c^{m,f}$ is assumed to be immobilized by soil microbes, and is returned to N_c^f. TMNIM then updates the organic fractions and ammonium-nitrate fractions. The stable organic matter ($\Delta OM_c^{m,h}$) and $\Delta N_c^{m,h}$ are updated, assuming that 20% of the fresh organic matter mineralized is converted to humus, and that 4% of the humic fraction is N.

3.3.6.2 Ammonium Nitrification. The maximum rate of nitrification, i.e., the conversion of NH_4^+-N to NO_3^--N, is determined using classical single substrate Michaelis-Menton kinetics. The rate is modified if temperature or moisture is limiting (Newkirk et al., 1987a). Nitrification calculations are performed in the subroutine TNITF, which first updates the soil water deficit and soil temperature factors affecting nitrification in a cell.

The amount of nitrification, ΔN_{nh4}, that takes place in a cell over a time increment is calculated as

$$\Delta N_{nh4} = V_{nh4}^{max} \left[\frac{N_{nh4}}{K_{nh4} + N_{nh4}} \right] \Delta t \tag{69}$$

where V_{nh4}^{max} is the maximum rate of NH_4^+-N nitrified (mg cm^{-3} day^{-1}); V_{nh4}^{max} is the optimum rate, V_{nh4}^{op}, (0.4/Z mg cm^{-3} day^{-1}) reduced by the more limiting of temperature (F_T) stress or the first moisture deficit (F_θ^1) factor as

$$V_{nh4}^{max} = \min \left(F_\theta^1, F_T \right) V_{nh4}^{op} \tag{70}$$

K_{nh4} is the Michaelis-Menton half-saturation constant (mg cm^{-3}), reduced from the optimum of 0.9/Z mg cm^{-3} as with V_{nh4}^{max}; N_{nh4} is the NH_4^+-N content of a cell (mg cm^{-3}); and Z is the vertical extent of the domain (cm).

The NH_4^+-N and NO_3^--N content of the cell are subsequently updated.

In VT-MAIZE, only V_{nh4}^{op} was affected by the stress factors; this is unreasonable, since a reduction in V_{nh4}^{op} also will result in a reduction in K_{nh4} by definition.

3.3.6.3 Denitrification. Denitrification, as determined in the subroutine TDNIT, takes place only when the cell moisture content exceeds the drained upper limit, and when the cell NO_3^--N content exceeds 1 mg cm^{-3}. The equation of Bowman and Focht (1974), who described denitrification kinetics using a dual substrate Michaelis-Menton model, is used to model denitrification as

$$\Delta N_{def} = \frac{V_{max}\, C_n\, C_c\, \Delta t}{(C_n + K_n)(C_c + K_c)} \tag{71}$$

where ΔN_{def} is the amount of denitrification (mg cm^{-1}) over a time increment Δt; V_{max} is the maximum denitrification rate reduced from the optimum of 0.15 mg cm^{-3} day^{-1} by the more limiting of the second moisture stress factor, F_θ^2 or F_T; C_c is the carbon content of a cell (mg cm^{-3}); and K_n and K_c are the corresponding Michaelis-Menton constants, reduced from their optimum values of 0.17 and 0.50 mg cm^{-3} (Bowman and Focht, 1974) by the more limiting of F_θ^2 or F_T.

Not unlike nitrification, V_{max} was the only parameter in equation 69 affected by the stress factors in VT-MAIZE.

3.3.6.4 Nitrogen Transformation Stress Factors.

Carbon Nitrogen Ratio Factor (F_{CN}): This factor allows for an increase in the humus mineralization rate constant in method II if the C-N ratio of the cell is less than 25, or decreases the rate constant if the C-N ratio is greater than 25. The C-N ratio factor is calculated as

$$F_{CN} = \exp\left\{ - 0.693 \left[\frac{C{:}N_c - 25}{25} \right] \right\} \tag{72}$$

where $C{:}N_c$ is the C-N ratio of the cell including inorganic N.

Temperature Stress Factor (F_T): The temperature stress factor allows for an approximate doubling of the rate of processes for every 10° C increase in temperature up to 30° C, and a halving of the rate for every 10° C increase thereafter. In the calculation of F_T, use is made of the Arrenhius equation of the form

$$FT = 1.680x10^{9} \exp\left\{ \frac{-13}{1.99x10^{-3} \left(\mathrm{T} + 273 \right)} \right\} \tag{73)a}$$

where

$$\mathrm{T} = T \qquad T \leq 30 \tag{73)b}$$

$$\mathrm{T} = 60 - T \qquad T > 30 \tag{73)c}$$

where T is the cell temperature in degrees Celsius, and 273 changes degrees Celsius to Kelvin.

Mineral N Availability Factor (F_N): This factor is used in the mineralization of fresh organic N. It allows for higher mineralization rates at shallow depths (≤ 50 cm) when the inorganic N content of the soil is below some threshold, or a decrease in the mineralization rate if the inorganic N content is above this value. The mineral N availability factor is calculated as

$$F_N = \frac{\Omega_N}{N_T} \qquad d_c \leq 50 \tag{74)a}$$

$$F_N = 0.05 \qquad d_c > 50 \tag{74)b}$$

where d_c is the cell depth (cm); Ω_N is the cell threshold N content (mg cm^{-3}), a constant to be calibrated; and N_T is the available inorganic N content of a cell (mg cm^{-3}). The upper limit of F_N is 2.0.

Soil Moisture Stress Factors: Two soil moisture availability factors affecting N transformation are defined. The first, F_θ^1, affects mineralization and nitrification; the second, F_θ^2, affects denitrification. The soil moisture availability factor affecting mineralization and nitrification is calculated as

$$F_\theta^1 = \frac{\theta_s - \theta}{\theta_s - \theta_r} \qquad \theta_r \le \theta \le \theta_s \tag{75}$$

where θ is the cell moisture content, θ_s is the saturated moisture content of the cell, and θ_r is the cell residual moisture content.

The soil moisture availability factor affecting denitrification allows for increase denitrification rate if cell moisture content is above the drained upper limit, and is calculated as

$$F_\theta^2 = \frac{\theta_s - \theta}{\theta_s - \theta_u} \qquad \theta_u \le \theta \le \theta_s \tag{76}$$

where θ_u is the drained upper limit of available moisture, or field capacity, operationally defined as the water content at negative 100 cm water pressure.

3.4 Crop Subsystem

Water and N uptake, as well as dry matter and grain yield by maize and wheat, are modeled based on the CERES-Maize (Jones and Kiniry, 1986) and CERES-Wheat (Ritchie and Otter, 1984) programs. The crops are modeled through various growth stages controlled by degree-day accumulation and varietal characteristics. Root growth is simulated based on the RHIZOS portion of the cotton simulation model GOSSYM (Baker et al., 1983).

The following sections briefly outline the crop modeling procedures used. Where modifications to the original models were made, such changes are detailed.

3.4.1 Phenologic Development of Maize and Wheat

VT-CROPS models maize and wheat development through nine phenologic growth stages. The stages, in chronological order, are defined as: stage 7, presowing; 8, sowing to germination; 9, germination to emergence; 1, emergence to end of juvenile stage; 2, end of juvenile stage to tassel initiation; 3, tassel initiation to end of leaf growth and silking; 4, silking to beginning of grain fill; 5, effective grain filling; 6, end of grain filling to physiological maturity (Newkirk et al., 1987a).

Growth stage 7 is optional, and is simulated only if a model run begins before the crop planting date. Stage 8 begins on the crop planting date. Advancement to stage 9 is dependent on the value of the soil water deficit factor in the cell. The deficit factor is calculated as the sum of 65% of the available moisture of the cell in which the seed was planted, plus 35% of the available moisture of the cell below. If the soil water deficit factor exceeds 0.02, then germination is initiated. If, within 40 or 90 days for maize and wheat, respectively, germination is not initiated, then crop failure results. Advancement through stages 1-6 depends on the accumulated daily thermal time exceeding a certain threshold in each stage. The threshold thermal time parameters are entered by the user, and are stage and variety dependent. Each day, the incremental thermal time is determined as the excess of mean atmospheric temperature over some base temperature, modified for extremes in temperature. Daily values of thermal time are not allowed to be negative. The base temperature varies with the crop and its stage of development.

3.4.2 Carbohydrate Assimilation

Daily CHO production is determined in subroutine GROSUB for maize, and subroutine GROSUW for wheat. Potential CHO (ΔC_p) is determined as a function of photosynthetically active solar radiation (PAR)—assumed to be 2.1% of solar radiation—and leaf area index (LAI) (Newkirk et al., 1987a), as

$$\Delta C_p = \frac{k\ PAR^n}{D_{pl}} \left(1 - \exp\left(- KN\ LAI \right) \right) \tag{77}$$

where k, n, and KN are constants with values to be determined during model calibration. Actual CHO (ΔC) then is calculated as the product of C, and the minimum of atmospheric temperature (T^1_{def}) stress factor, the first of two soil moisture deficit factors (Θ^1_{def}) or the second of two N deficit (N^1_{def}) factors (Newkirk et al., 1987a), as

$$\Delta C = \Delta C_p \min \left(T^1_{def}, \Theta^1_{def}, N^2_{def} \right) \tag{78}$$

3.4.3 Carbohydrate Partitioning

The fractionation of daily CHO to the different plant parts varies with crop and crop growth stage.

Stage 1: The daily CHO produced (ΔCHO_p) is partitioned between leaves, stem, and roots in wheat and maize, with the leaves having priority. The daily leaf growth (ΔCHO_l) is calculated as a function of the ratio of accumulated thermal time to the growth stage thermal time threshold. Leaf growth is modified by Θ^2_{def} for maize, and the most limiting of Θ^2_{def}, N^2_{def}, and T^1_{def} for wheat. Root and stem growth (ΔCHO_{ex}) is calculated from the CHO excess after leaf growth as

$$\Delta CHO_{ex} = \Delta CHO_p - \Delta CHO_l \qquad \Delta CHO_l \le \left(1 - f^1_m \right) \Delta CHO_p \tag{79a}$$

$$\Delta CHO_{ex} = f^1_m \, \Delta CHO_p \qquad \Delta CHO_l > \left(1 - f^1_m \right) \Delta CHO_p \tag{79b}$$

where f^1_m is the minimum fraction of CHO that can be partitioned to the roots and stem, the value of f^1_m for maize and wheat to be calibrated. If the fraction of CHO partitioned to the roots and stem is less than f_m, the difference is made up for by reducing seed reserve and/or CHO fraction to leaves. The excess CHO after leaf growth (ΔCHO_{ex}) is partitioned between the roots and stem as

$$\Delta CHO_r = f^1_r \, \Delta CHO_{ex} \tag{80a}$$

$$\Delta CHO_s = \left(1 - f^1_r \right) \Delta CHO_{ex} \tag{80b}$$

where ΔCHO_r and ΔCHO_s are the amount of ΔCHO_p sent to the roots and stems, respectively, and f^1_r is the fraction of ΔCHO_{ex} that goes to the roots in stage 1.

Stage 2: For maize, carbohydrate is partitioned to the stem, roots, and leaves as in stage one, f^2_m and f^2_r being the fractions replacing f^1_m and f^1_r in equations 79 and 80. For wheat, CHO is partitioned to the stem, leaves, and roots, with the roots and stem having priority. The amount of CHO partitioned to the stem and roots is calculated as

$$\Delta CHO_s = \left(k_l + k_3 \nabla_2 \right) f_{ex} \Delta CHO_p \tag{81)a}$$

$$\Delta CHO_r = \left(1 - f_{ex} \right) \Delta CHO_p \tag{81)b}$$

where k_l and k_3 are constants to be calibrated, ∇_2 is the ratio of accumulated thermal to the thermal time threshold for stage 2, and f_{ex} is the fraction of ΔCHO_p not partitioned to the roots, calculated as

$$f_{ex} = k_1 + k_2 \min \left(\Theta^2_{def}, N^2_{def} \right) \tag{82}$$

where k_1 and k_2 are constants to be calibrated. After partitioning to the stem and roots, the excess CHO goes to the leaves.

Stage 3: For maize, CHO is partitioned to the stem, leaves, and roots, with the leaves and stem having priority. The fraction of CHO partitioned to the leaves depends on the leaf area increase, which depends on the number of leaves; that which goes to the stem is based on the plant leaf weight and the number of leaves, and that partitioned to the roots is the difference, providing it is not less than 10% of CHO (Newkirk et al., 1987a).

For wheat, CHO is partitioned between the roots, leaves, and stem, with the roots having priority. The amount of CHO partitioned to the roots is calculated using equations 81 and 82, with the constants being stage dependent. Carbohydrate partitioned to the stem calculates from the equation as

$$\Delta CHO_s = f_{ex} \Delta CHO_p \tag{83}$$

Stage 4: For maize, CHO is partitioned to the ears, stems, and roots, with the ears and stems having priority. Carbohydrate partitioned to the stem and ear is calculated as

$$\Delta CHO_e = k_4 \Delta_h \Theta^2_{def} \tag{84)a}$$

$$\Delta CHO_s = k_6 \Delta CHO_e \tag{84)b}$$

where Δ_h is the incremental thermal time units, and k_4 and k_6 are constants to be calibrated. The excess of CHO not partitioned to the ear and stem is sent to the roots, provided that its fraction of CHO_p is not less than some lower limit, f_{low}.

For wheat, CHO produced during stage 4 is partitioned to the roots and stem using equations 81 and 82, with stage-dependent constants to be determined.

Stage 5: For maize, carbohydrate is partitioned to the grains, stem, and roots, with priority given to the grains. Daily grain CHO is calculated as a function of daily grain fill rate and the number of grains per plant, reduced by N^1_{def}. The daily grain fill rate is calculated as a function of atmospheric temperature and the maximum grain fill rate, a crop genetic parameter entered by the user. If crop grain fill rate is less than 0.1 for two consecutive days, then the crop matures due to slow grain fill (Newkirk et al., 1987a). The amount CHO partitioned to the stem and the roots is calculated from excess after grain fill (ΔCHO_{ex}) as

$$\Delta CHO_r = f_r^5 \, \Delta CHO_{ex} \tag{85)a}$$

$$\Delta CHO_s = \left(1 - f_r^5 \right) \Delta CHO_{ex} \tag{85)b}$$

where f_r^5 is the fraction of excess that goes to the root.

VT-MAIZE has no provision for controlling the stover-grain ratio. In consequence, depending on the prevailing conditions, unrealistic ratios may be obtained. Typical values for stover-grain ratios range from 0.54 to 1.79 with a mean of 1.0 (Triplett and Mannering, 1978). VT-CROPS ensures that the stover-grain ratio stays within the range of 0.8-1.20. If this ratio is greater than 1.2, no less than 80% of the CHO goes to grain. Conversely, if it is less than 0.8, then 80% of the CHO goes to the stem.

The partitioning of CHO in wheat in stage 5 is similar to the partitioning for maize. Stover-grain ratio in wheat typically ranges from 0.49 to 2.24 (Triplett and Mannering, 1978). VT-CROPS ensures that the stover-grain ratio for wheat stays within the range of 0.6-2.0, a feature that was lacking in the parent model.

3.4.4 Root Growth and Distribution

Root growth in VT-CROPS originates from the left and right sides of the modeled domain, in the cells in which the seed was planted, and proceeds horizontally toward the center and vertically with time. Root growth in VT-CROPS is modeled using a modified form of the RHIZOS portion of the cotton simulation model GOSSYM. By this conceptualization, roots are divided into three age classes: class 1 roots are up to 3 days old, class 2 roots are 4-12 days old, and class 3 roots are more than 12 days old. The daily root growth of a cell is calculated as a function of the cell root growth potential and the incremental CHO partitioned to the roots. The cell root growth potential is determined as the sum of 100% of class 1 roots, 50% of class 2 roots, and 20% of class 3 roots, by weight. The cell root growth potential is reduced by the most limiting of soil temperature, moisture, and N stress factors. The soil temperature stress factor is the same as that affecting N transformations. It is assumed that soil moisture limits growth when the available soil moisture is less than 25% of cell available moisture capacity; therefore, the soil moisture stress factor affecting cell root growth is calculated as 75% of the ratio of available soil moisture to available soil moisture capacity. The soil N stress factor affecting root growth (N^r_{def}), with a zero lower bound, is calculated as (Newkirk et al., 1987a)

$$N^r_{def} = 1.0 - 1.17 \exp\left(0.015\Theta_n \right) \tag{86}$$

where Θ_n is the cell mineral N content in gm N gm^{-1} soil. The daily root growth of a cell is calculated as

$$\Delta R_c = \frac{\Delta C_r \Phi^r_c}{\sum\limits_{1=1}^{N} \Phi^r_i} \tag{87}$$

where ΔR_c is the daily root growth of a cell; ΔC_r is the daily CHO partitioned to the modeled surface area; and the remainder is a weighting factor that distributes the root CHO as a function of the ratio of cell root growth potential (Φ^r_c) to the total root growth potential summed over all cells containing roots (N).

The CHO partitioned to the modeled soil surface (ΔC_r) is determined from the CHO partitioned to the root per plant (ΔCHO_r). This process was necessary since the soil surface area modeled corresponded to that occupied by a plant only under fortuitous circumstances—ΔC_r was estimated as

$$\Delta C_r = f_d \, \Delta CHO_r \tag{88}$$

where f_d is a correction factor that accounts for the disparity between the soil area modeled and that occupied by a plant based on planting density. VT-MAIZE calculated f_d as

$$f_d = \frac{\rho^p V_c}{(ROWS)\ (RZNC)\ (RZV)} \tag{89}$$

where ρ^p is the crop planting density (plants m^{-2}), V_c is the cell volume, *ROWS* is the crop row density (rows of crop m^{-2} area), *RZNC* is the number of cells in the root zone containing roots, and *RZV* is the specific root zone volume (cm^3 m^{-1}-length). In addition to not being able to rationalize equation 89, VT-MAIZE gave erroneous results, underestimating ΔC_r. It is worth mentioning that the same f_d was used in converting soil N uptake to plant N uptake per plant, in which case it grossly overestimated N uptake, resulting in huge N mass balance errors. VT-CROPS calculates f_d as

$$f_d = \frac{N_K \, \Delta x \, \rho^p}{10^4} \tag{90}$$

where N_K is the number of columns in the soil matrix, and Δx is the cell width (cm); $N_K \Delta x$ is the modeled area, i.e., inter-row spacing times unit width; and 10^4 converts area from cm^2 to m^2.

If, in any cell, the root length is less than the cell's dimensions, then ΔR_c goes in that cell. However, if the root length is greater than the cell dimensions, then ΔR_c is partitioned to the current cell, the cell below, and the cell toward the center of the domain; i.e., the roots are allowed to grow out of the current cell. The cell growth is distributed to the cells based on the water capillary potential of the cell (ψ^i) and the cell geotropism factor (GF^i). The cell geotropism factor allows for more vertical than lateral root growth; it is 1 for the current cell and the cell toward the center, and 10 for the cell below. In the event that no cells exist toward the center or below the current cell, then their respective GF^i is set to zero. The amount of ΔR_c partitioned to a cell (ΔR_c^i) is calculated as

$$\Delta R_c^i = \frac{\Delta R_c \; GF^i/\psi^i}{\sum_{i=1}^{3} GF^i/\psi^i} \tag{91}$$

i = current cell, cell to center, cell below

This approach for distributing roots within the domain has two interrelated problems: (1) the specific root volume, i.e., the volume of roots per volume of soil, was high, greater than 4% at shallow depths; and (2) the crop rooting depth was shallow, less then 30 cm for both maize and wheat. Gross under-predictions of rooting depth can have severe ramifications for plant N and water uptake and subsequent N leaching and drainage. Root specific volume is seldom greater than 1% in the top 15-20 cm of the root zone for maize (Barber, 1984), and decreases with depth; it is also known that the effective rooting depth of maize can be in excess of 150 cm (Barber, 1984; Triplett and Mannering, 1978), and that for wheat in excess of 50 cm (Triplett and Mannering, 1978). VT-CROPS ensures deeper root penetration by controlling the root specific volume. VT-CROPS divides the soil domain into three zones for maize and two for wheat, providing the soil depth is not limiting. The specific root volume is not allowed to exceed a prescribed maximum (RV_{max}) in each zone, providing a maximum rooting depth of at least 150 cm and 50 cm for maize and wheat, respectively, for deep soils. Zone 1 goes down to 20 cm depth with RV_{max} of 0.8% and 0.4% for maize and wheat, respectively; zone 2 goes from 20-50 cm with a RV_{max} 0.4% and 0.2% for maize and wheat, respectively; and zone 3 goes down to 150 cm for maize with an RV_{max} of 0.1%. In the event RV_{max} is exceeded, excess root mass is distributed as with equation 87, setting the current cell geotropism factor to zero.

Root length for calculating uptake of water and N and determining cell growth is calculated assuming roots are cylindrical with a gravimetric water content of 87.5%, a density of 1 gm cm^{-3}, and a mean diameter of 0.03 cm and 0.02 cm for maize and wheat, respectively. VT-MAIZE used 26.5% for root moisture; however, VT-CROPS corrected this to reflect the more realistic value of 92-93% reported by Mengel and Kirby (1979).

3.4.5 Crop Growth Stress Factors

3.4.5.1 Atmospheric Temperature Stress Factors. There are two atmospheric temperature stress factors affecting CHO production and partitioning, both of which vary on the interval (0,1). The first factor that affects CHO production is calculated assuming optimum CHO production at 26° C as (Newkirk et al., 1987a)

$$T^1_{def} = 1 - 0.0025\,(0.25T_{min} + 0.75T_{max} - 26.0)^2 \tag{92}$$

For wheat, T_{def} is set to zero for temperatures lower than -3.0° C.

The second factor that affects leaf expansion in wheat is calculated as

$$T^2_{def} = 1.2 - 0.0042\,\frac{(T_{min} + T_{max})^2}{4} \tag{93}$$

3.4.5.2 Soil N Deficit Factors. Two soil N deficit factors are used in VT-CROPS, N^1_{de} and N^2_{def}. Soil N deficit factor 1 is calculated as (Newkirk et al., 1987a)

$$N^1_{def} = \frac{\Delta N_a}{f_{ne}\Delta C} \tag{94}$$

where ΔN_a is plant N uptake over a time step, and f_{ne} is optimal plant N content. The value of f_{ne} varies with the crop and growth stage. During vegetative growth, f_{ne} is taken as the optimal stover N content (f^s_{ne}) and the optimal N content of grain (f^g_{ne}) during reproductive growth. Parent models (VT-MAIZE and CERES-wheat) used

$$f^s_{ne} = 0.04 \tag{95)a}$$

$$f^g_{ne} = \frac{GPC}{6.25} \tag{95)b}$$

where *GPC* is the optimal grain protein content, taken as 11.25% and 15% for maize and wheat, respectively, and 6.25 is the ratio of protein to N in amino acids. An optimal stover N content of 4% translates into an optimal protein content of 25%, which is far too high for stover and could not be justified from the literature. This resulted in low values of N deficit factors when soil N was limiting, and unreasonably low crop yields or unreasonably high stover N content when soil N was adequate. A more realistic value of 1% was used for f^s_{ne} in VT-CROPS for both maize and wheat.

The second N deficit (N^2_{def}) factor is calculated from the first as
where k_n is a constant to be determined during model calibration.

$$N_{def}^2 = N_{def}^1 \qquad N_{def}^1 > \frac{1}{k_n} \tag{96a}$$

$$N_{def}^2 = k_n N_{def}^1 \qquad N_{def}^1 \leq \frac{1}{k_n} \tag{96b}$$

3.4.5.3 Soil Moisture Deficit Factors. Two moisture deficit factors affect crop growth. The first (Θ_{def}^1) is calculated as the ratio of actual to potential evapotranspiration; the second (Θ_{def}^2) is calculated as

$$\Theta_{def}^2 = k_\theta \, \Theta_{def}^1 \tag{97}$$

where k_θ is a constant to be calibrated. Carbohydrate production is modified by Θ_{def}^1, and leaf area expansion is affected by Θ_{def}^2.

3.4.6 Modeling Soybean

VT-CROPS does not model the phenology of soybean; it models only soybean's interaction with the soil and atmosphere subsystem. Thus, soil temperature, evapotranspiration, and N transformations, flow, and transport are explicitly simulated during this period. Unlike maize and wheat, where the accumulation of thermal time controls the maturity of the crop, soybean is modeled for a specified period of time (120 days), after which, yields of grain stover and roots are estimated.

3.4.6.1 Soybean Water Use. VT-CROPS calculates potential evaporation based on the approach of Ritchie (1972), which computes potential evapotranspiration as a function of the leaf area index (LAI) of the crop. Estimates of LAI over time for soybean were calculated as

$$LAI = \exp\left(- 2.33 + 0.005\delta t \right) \tag{98a}$$

$$LAI = 20.65 - 0.16\delta t) \tag{98b}$$

where δt is the number of days since the simulation of soybean began. Equation 98 was developed by regressing data of Cox and Jolliff (1986) on soybean LAI over time. Leaf area index was observed to increase exponentially over time to a maximum; thereafter, it decreased more or less linearly. Equations 98a and 98b explain 95% and 96%, respectively, of the observed variation (r^2) in LAI. The daily LAI is used to determine the potential evapotranspiration, which is partitioned between soil potential, soil evaporation, and transpiration following the method of Ritchie, is outlined elsewhere in this document.

Soybean Root Water Uptake: To model temporal and spatial variations in water uptake, an expression was needed to describe soybean root growth over time. An expression developed from a simple regression analysis on the data of Mitchell and Russell (1971) was used to model soybean root extension. The resulting equation, with an r^2 of 0.92, is

$$RD_{soy} = 1.54\delta t \tag{99}$$

where RD_{soy} is the rooting depth of soybeans. Horizontal extension was approximated by assuming soybean roots grow three times as fast laterally as they do vertically, until roots have grown into all columns. Mitchell and Russell (1971) found greater than 90% of soybean roots in the top 20 cm of the root zone, so VT-CROPS assumes the water uptake potential due to root length density of soybean to be 10 times as great in the top 20 cm of the soil root zone as compared to cells below. The cell water uptake potential (Γ_w^i) is calculated as the product of the cell water uptake potential due to root length density and the soil water diffusivity of the cell. The cell root water uptake (R_c) is calculated as

$$R_c = \frac{\Gamma_w^i \, PT}{\sum_{i=1}^{m} \Gamma_w^i} \tag{100}$$

where PT is the potential transpiration rate (cm^3 day^{-1}) and m is the number of cells containing roots. Note that R_c is constrained by the available soil moisture in a cell.

3.4.6.2 Soybean Nitrogen Uptake. Fageria (1991) reported that efficient N fixation can result in over 80% of crop N in soybean; however, under field conditions, N fixation normally accounts for 25-75% of crop N. Schepers and Mosier (1991) stated that, in the southeastern United States, soybean fixes 72-217 kg ha^{-1}. VT-CROPS models N uptake by soybean passively; i.e., N uptake is the product of cell water uptake and NO_3^- concentration, summed over all cells containing roots. At the end of soybean simulation, when the yields of the different plant parts are calculated, it is assumed that their N content is optimal, as a minimum. If the passive N uptake was less than the optimum, then the difference was assumed to be fixed. If passive uptake was greater than optimal levels, then super-optimal N levels are allowed.

Soybean Yields: At the end of the simulation period, soybean grain yield (Y_s^g) is estimated according to Doorenbos and Kassam (1979) as

$$Y_s^g = Y_s^{max} \left[1 - \beta \left[1 - \frac{ET_A}{ET_P} \right] \right] \tag{101}$$

where Y_s^{max} is the soybean grain yield when optimally supplied with water (maximum yield will vary with variety and climatic conditions—a value of 5500 kg ha (Shibles et al., 1975) is used here); β is a crop yield response factor to moisture stress, with a value of one for sensitive crops—a value of 0.85 is used here (Doorenbos and Kassam, 1979); ET_A and ET_P are actual and potential evapotranspiration, respectively.

In the simulation of soybean, the plant parts of primary importance are the roots and the straw, which are returned to the soil and influence N transformation and subsequent transport processes. Harvest index (HI), the fraction of above-ground biomass that ends up in grain, commonly ranges from 30 to 40% for soybean (Fageria et al., 1991); VT-CROPS uses an HI of 0.35 to estimate straw yield (Y_s^s) from the definition of HI as

$$Y_s^s = y_s^g \left[\frac{1}{HI} - 1 \right] \tag{102}$$

Mitchell and Russell (1971) found the mass of soybean roots to vary from 1.52 to 5.94 gm plant, for a mean of 4.4 gm plant, for eight varieties at maturity under field conditions in Iowa at a planting density of 38,000 plants ha^{-1}. Using a root mass of 5 gm plant at that planting density gives a root mass maximum of 1900 kg ha^{-1}; VT-CROPS uses this to calculate root mass, Y_s^r, (kg ha^{-1}) as

$$Y_s^r = \frac{Y_s^g}{Y_s^{max}} 1900 \tag{103}$$

3.4.6.3 Nitrogen Content of Soybean Plant Parts. Nitrogen content of the different plant parts is calculated assuming their N contents are optimal as a minimum. Optimal N contents were taken to be 6.5% for grain and 0.85% for straw and roots (Meisinger and Randall, 1991). If the sum of optimal N is less than N uptake, then the deficit is assumed to be fixed and the N contents are optimal. In the rare event that optimal N yield is less than N uptake the difference is distributed to the different plant parts, and N yield of the different parts is estimated as

$$Y_n^i = Y_{nop}^i + \frac{\left[Y_n^p - \sum_{j=i}^{3} Y_{nop}^j \right] Y_{nop}^i}{\sum_{j=i}^{3} Y_{nop}^j} \tag{104}$$

j = *grain, stover, root*

where Y_n^i is N yield of the i^{th} plant part, Y_{nop}^i is the optimal N yield of the i^{th} plant, and Y_n^p is the root uptake of N.

3.4.7 Evapotranspiration

VT-CROPS models evapotranspiration following the approach of Ritchie (1972), an approach inherited from VT-MAIZE. With this approach, potential evapotranspiration (PET) is calculated to reflect the evaporative demand of the atmosphere as a function of incoming solar radiation, soil albedo, and atmospheric temperature. The potential soil evaporation and plant uptake is determined as a function of LAI and a two-stage drying process for soil evaporation, provided the PET is not exceeded (Ritchie, 1972).

Actual soil evaporation is modeled by lowering the soil moisture in the surface layer to reflect the potential evaporative demand. For an actively growing crop, moisture is extracted from the unshaded area first; if the demand is not satisfied from the unshaded area, then the remainder may be supplied by the shaded areas. Soil water evaporation cannot lower the moisture content of a cell below the lower limit of available moisture of that cell.

The potential transpiration is partitioned to each cell containing roots according to the equation of Moltz and Remson (1970), modified for two dimensions. The potential transpiration rate per cell is calculated as

$$T_c^p = TP_p^p \; f_c^t \; \Delta z \Delta x \tag{105}$$

where T_c^p is the cell transpiration potential (cm^3 day^{-1}); T_p^p is the plant transpiration potential rate (cm^3 day^{-1}), calculated as the transpiration rate (cm^3 cm^{-2} day^{-1}) times the area being modeled; and f_c^t (cm^{-2}) is the cell transpiration weighting factor. The cell transpiration weighting factor is defined as

$$f_c^t = \frac{A_c(x,z)D(h)}{\int_0^L \int_0^W A(x,z)D(h)dzdx} \tag{106}$$

where $A(x,z)$ is the root length density factor, $D(h)$ is the soil water diffusivity of the cell, and L and W are the vertical and horizontal extent. VT-CROPS estimates f_c^t over discrete units as

$$f_c^t = \frac{A_c(x,z)D(h)}{\sum_{j=i}^{m} \sum_{i=1}^{n} A(x,z)D(h)\Delta z \Delta x} \tag{107}$$

where m is the number of rows containing roots, and n is the number of columns in the matrix.

Water is removed from the cell to satisfy T_c^p, provided the cell moisture content is not lowered below the lower limit of available moisture.

3.4.8 Nitrogen Uptake

Passive and active N uptake are modeled for maize and wheat. Passive uptake is the uptake of NO_3^--N in the transpiration stream (Newkirk et al., 1987a). With passive uptake, NO_3^--N is taken into the plant by the advection of soil water to the roots. If the plant is undernourished with N, then, in addition, active N uptake as described by a first-order single substrate Michaelis-Menton kinetic model, following the approach of Barber (1984), is allowed as

$$U^n = U_{max}^n \left[\frac{C_n - [Cn]_{min}}{K_m + C_n - [Cn]_{min}} \right] \delta R_l \tag{108}$$

where U^n is net influx of N (μmoles per day); U_{max}^n is the maximum influx rate (μmoles per day cm^{-1} root); C_n is the NO_3^--N concentration, (μmoles cm^{-3}); $[Cn]_{min}$ is the threshold NO_3^--N concentration below which N uptake ceases (taken as 0.004 and 0.003 μmoles cm^{-3} for maize and wheat, respectively); K_m (μmoles cm^{-3}) is the Michaelis-Menton half-saturation constant for N uptake; and δR_l is the cell root length (cm).

From the work of Barber (1976), the following regression equation was developed relating U_{max}^n to the age of maize, Δt_{mz}, (Newkirk et al., 1987a)

$$U^n_{max} = f_{up} \exp\left(-\ 0.7392\ -\ 0.0869\ \Delta t_{mz}\right) \tag{109}$$

where f_{up} is a calibration factor that may vary with crop, stage of growth, and nutritional status. In the case of wheat, $U^n_{max} = f_{up}0.0864$ μ moles cm^{-1} day^{-1}. Both NH_4^+ and NO_3^- are taken up actively by wheat.

3.4.9 Partitioning of N Uptake

The plant N uptake is partitioned to the different plant parts depending on the N demand of the plant part and on the growth stage of the crop. N uptake is partitioned to root and stover during growth stages 1-4, and to grain, root, and stover during stage 5.

The N demand is computed as the difference between some optimal N level and the actual N level. Only positive demands are defined. During growth stages 1-4, the optimal N uptake is taken as 1% of dry weight (as opposed to 4% in VT-MAIZE). The N uptake is distributed according to the ratio of the plant part N demand in relation to the total demand of the plant (note that VT-CROPS allows for the accumulation of N above the optimal). If no demands exist, then uptake is distributed according to the mass fraction of the plant parts.

During growth stage 5, the grain has priority over the roots and stover for N uptake. Nitrogen is partitioned to the grain to satisfy its demand first, and any excess is partitioned to the roots and stover according to their mass fractions. Optimal grain N content is calculated based on a 11.28% and 15% protein content for maize and wheat, respectively. Optimal N contents are lowered based on the most limiting of atmospheric temperature (T_{def}) and soil N (N^1_{def}) stress factors. In the event grain N demand is not met, VT-CROPS is able to translocate N above optimal levels from stem and roots to the grain to meet its demand. Previously, the 4% optimal N content used in stages 1-4 in VT-MAIZE resulted in stover and root N contents that were much higher than for grain—an untenable scenario. Nitrogen is translocated from the roots only after the reserve of the stem is used.

3.5 Sequencing Model Runs and the Passing of Variables

At crop maturity, the subroutine HARVST is called. HARVST computes crop yield of grain, stover, and root, and their N contents, based on plant dry matter accumulation and N uptake. Grain yields are reported at 15.5%, 13.5%, and 10% moisture for maize, wheat, and soybeans, respectively.

Soil variables on moisture, mineral N, organic matter, and organic N content, root and stover yield, and root and stover N are temporarily stored for use in a subsequent rotation.

Following each crop, a fallow period ensues. At the beginning of a fallow period, the crop roots and root N from the previous crop are incorporated into the fresh organic matter and fresh organic N of the cell in which they were accumulated. At the end of a fallow period, 80% of the above-ground residue and N from the previous crop are incorporated into the soil. The residue is incorporated to some user-specified depth if conventional tillage is practiced, or within the surface layer if minimum tillage is practiced.

The inter-row spacing modeled for wheat is half that of maize and soybean, but the cell dimensions are the same. Therefore, the domain modeled for wheat is half that for other crops, including fallow periods; this can be done because of the physical symmetry of the modeled domain. At the beginning of the fallow period subsequent to wheat, the soil variables from the previous run are mirrored onto the other half of the domain. Conservation of mass is ensured at each stage.

3.6 Model Input and Output

VT-CROPS was developed to run on an IBM mainframe under the VM-CMS operating system. Since it is programmed with standard FORTRAN 77, it may be easily ported to run on other computers, including 386- or 486-based PCs. Multiple simulations can be accomplished during program execution, provided there is available disk space. There are 16 possible input files—the actual number of files created depends on various user-specified options. Input files define the cropping sequence, soil properties, and initial conditions of the system to be modeled according to IBSNAT (IBSNAT, 1985) specifications. Examples of input data files and instructions for model execution are given in Appendix A.

Simulation results are provided by the model in six output files:

- The yield listing file provides information on the system modeled to ensure that the intended simulation was performed. It also provides the crop water balance at the end of each growth stage, and yields at the end of the each growing season.

- The crop listing contains crop parameters during the growing season.

- The water listing gives information on plant water balance characteristics as they accumulate over the season.

- The nitrogen listing furnishes the final distribution of N with depth for each crop within a sequence.

- The leaching listing contains information on plant uptake of N and water, amount of NO_3^--N and water leached, surface runoff, and soil water balance over time.

- The error listing contains warnings and error messages generated.

4 Model Calibration and Sensitivity Analysis

4.1 Model Calibration

The model VT-CROPS contains a number of internally fixed parameters that cannot be modified at runtime, and whose values often are taken from the literature directly, or indirectly obtained from surrogate data. Often, literature values are intelligent guesses or are evaluated under ideal conditions, atypical of normal field conditions. Therefore, literature values are, at best, order of magnitude estimates. Through model calibration, improved estimates of model parameters can be obtained.

Model calibration was undertaken to determine the appropriate values for internal model parameters. Calibration was accomplished by trial and error; i.e., by varying parameter values and comparing model output with observed data until the difference between observed and predicted results were within prescribed tolerance limits. The model was calibrated for the variables deemed important for N leaching, namely, grain yield, stover, grain-N, stover-N, and soil N content at the end of the growing season for the maize and wheat crops.

Maize data were obtained from two field sites in Virginia: the Blacksburg experimental station in Montgomery County for 1986-1988, and the Nomini Creek basin in Westmoreland County for 1986 and 1988 (Menelik, 1990). At the Blacksburg site, the soil is a Groseclose silt loam (typic Hapludult, clayey, mixed, mesic); at Nomini Creek the soil is a Suffolk sandy loam (typic Hapludult, coarse loamy, mixed, thermic). These two sites collectively received eight experimental treatments each year, involving four fertilization rates (0, 75, 150, and 225 kg-N ha^{-1}), and two tillage systems—minimum and conventional tillage. Of a total of 40 maize experiments, 2 were used in the calibration exercise; the remainder were used for model validation. The treatments used for calibration were Blacksburg 1988 conventional till and Nomini Creek 1986 minimum till, both with no N fertilizer added. The zero N fertilizer treatments were chosen because they should allow effective calibration of N deficit factors and N uptake parameters under conditions of N stress. The soil at Nomini Creek has poor moisture retention capacity (table 3); this, coupled with the relatively low rainfall of 1986, should enable effective calibration of maize moisture deficit factors under drought conditions.

Field data for wheat were available for the 1988-89 growing season from six sites around Virginia; at each site, there were two treatments—0 and 150 kg-N ha^{-1} (Alley and Scharf, 1989). One of these sites, located on the Brandon Plantation in Prince Georges County, with no fertilizer N applied, was used for model calibration. All the others were used for model validation. The soil type at Brandon Plantation is Pamunky loam (ultic Hapludalf, fine loamy, mixed, thermic). The zero N treatment was selected for wheat for the same reason as maize.

Rainfall data collected at the sites were used in all simulations. Solar radiation and temperature were taken from the nearest monitoring station. Soil properties and initial conditions were estimated from laboratory measurements. Table 1 shows the crop varieties and management practices simulated during model calibration, and tables 2-4 show the soil properties modeled at the respective sites.

The final values of internal model parameters determined during this exercise are given in table 5 (the parameters are defined in section 3). Table 6 shows the observed and predicted results at the end of calibration. Calibration was more comprehensive for maize than for wheat, as the wheat data were incomplete with no information on stover yield nor N content. Consequently, calibration of N and CHO partitioning between grain and stover for wheat was done so as to ensure that rational grain-stover yield and N ratios were obtained.

Soil mineral N distribution was not calibrated, but final results are given in figure 7.

4.2 Sensitivity Analysis

4.2.1 Overview

In any modeling exercise, the performance of state variables and their relationship to model parameters and system processes should be characterized. This can be facilitated by a sensitivity analysis.

A sensitivity analysis was performed to give some perspective on the performance of the physical system and to determine the relative importance of input parameters and system processes. In addition, a sensitivity analysis also aids model verification, as anomalous sensitivities could indicate model errors. Young et al. (1971) used sensitivity analysis to rank model variables. If parameter variances are known, sensitivity analysis can be extended (error analysis) to provide estimates of the variances of state variables (Dawdy et al., 1972; Coleman and De Coursey, 1976). This was not attempted in this study.

The scenario modeled involved a two-year rotation of maize, wheat, soybean, and fallow; all crops conventionally tilled with 150 kg-N ha^{-1} applied to maize and wheat. Simulations were run for two rotations, and sensitivities calculated from the results of the second rotation, thereby reducing the impact of model initial conditions. Simulations were conducted on a hypothetical soil with properties intermediate between sand and loam, with a water table located 1.5 m below the surface. The properties of the hypothetical soil are given in table 7.

The sensitivity of a state variable to a variation in a model parameter may be defined as the change in the state variable per unit change in the parameter; i.e., the partial derivative of the state variable with respect to the parameter. In this study, a relative sensitivity, defined as the percentage change in a state variable per 1% change in a parameter, was determined. Relative sensitivities were determined for a number of crop and soil state variables to the parameters or variables of interest (tables 8-11). Each parameter was perturbed by +10% of its base case value, and partial derivatives estimated, using a forward difference procedure, as

$$\Pi_i \equiv \frac{\partial(V/V(\bar{p}_i))}{\partial(p_i/\bar{p}_i)} \doteq \frac{V(\bar{p}_i + \Delta\bar{p}_i) - V(\bar{p}_i)}{\Delta\bar{p}_i} \cdot \frac{\bar{p}_i}{V(\bar{p}_i)} \tag{110}$$

where Π_i is a vector of sensitivities corresponding to parameter i perturbed and all others at their base case value; $V(\bar{p}_i)$ is a vector of state variable response corresponding to parameter vector $\bar{p}_i$, in which all parameters, including parameter i, are at their base case value; $V(\bar{p}_i + \Delta\bar{p}_i)$ is a vector of state variable response corresponding to a parameter vector in which parameter i is perturbed, and all others are at their base case value; and $\Delta\bar{p}_i$ is the perturbation in parameter i, taken to be 10% of the base case value.

Relative sensitivity is dimensionless, and allows comparison between different state variables. Relative sensitivities of the model to the climatic variables and model input parameters were calculated (tables 8-11). The climatic variables are the forcing functions of the model. Often, a complete climatic data set is unavailable at a site to be modeled, in which event data from the nearest monitoring station is used; it is useful, therefore, to know the magnitude of the error that could be incurred under such circumstances. Contingent on how sensitive state variables are to specific model parameters, intelligent guesses may suffice, or accurate determinations may be necessary.

4.2.2 Results of the Sensitivity Analysis

4.2.2.1 Relative Sensitivity of Crop Variables. Tables 8-10 summarize the result of the sensitivity analysis of the crop state variables. Negative sensitivities indicate a reduction in state variable response with an increase in parameter value.

Of the three crops simulated, soybean is the least sensitive to parameter perturbations, with identical sensitivities for all state variables (table 10). This is not an unexpected response because of the relatively simple implicit approach used in the modeling of soybean. Only the evapotranspiration of soybean is modeled; hence, crop state variables will be sensitive only to climatic variables and model parameters that affect evapotranspiration.

Wheat is the most sensitive of the crops, with positive sensitivities for all state variables and almost identical sensitivities for stover yield and stover N (table 9). The sensitivity of wheat is due in part to its extended growth period (often more than 240 days), as opposed to maize and soybean (often less than 120 days).

For maize, stover yield and N are more sensitive than grain yield and N (table 8). The greater sensitivity of stover can be explained by the approach used to partition CHO and N, in which priority is given to the grain over stover, and the possibility for translocation of CHO and N from stover to grain if daily productions are sub-optimal.

4.2.2.2 Sensitivity to Climatic Variables. Interestingly, the crop state variables are insensitive to increases in rainfall—increasing the amount of rain does not necessarily increase the amount of water that is available for crop growth, since, at water contents above field capacity, a soil is going to drain to its field capacity in any event. Crop yields will be more dependent on the distribution and frequency of rainfall than on the amount. On the other hand, soil variables other than water use and denitrification are all sensitive to rainfall (table 11).

Maize grain yield and N uptake responded negatively to increasing the solar radiation, even though total CHO and stover production increased. At a glance, this might appear to be an anomaly, because, as modeled, potential CHO increases linearly with solar radiation. However, upon close examination, it is evident that, in addition, soil water deficits increase with solar radiation, particularly during grain fill. VT-CROPS calculates potential evapotranspiration as a function of daily solar radiation and maximum temperature. Soil water deficit factors are proportional to the ratio of actual to potential evapotranspiration. Soil water deficits will be greater in the latter stages of maize growth (i.e., grain fill) when moisture demands are great and soil moisture reserves have been depleted.

Wheat state variables all responded positively to increases in solar radiation. This, of course, is because potential CHO production increases linearly with solar radiation, and wheat is grown in the cooler months when soil water deficits are not likely to be a major factor in limiting yield. With the exception of runoff and mineralization, the soil state variables are sensitive to solar radiation, with only water use responding positively. Due to the effect of solar radiation on CHO production, water use was more sensitive to solar radiation than any of the other variables or input parameters investigated.

Maize responded negatively to increases in maximum temperature, while the converse is true for wheat; maize is grown in the warmer months and wheat in the cooler months, and, as modeled, temperatures above 26° C produce negative responses on CHO production. All the soil N state variables are sensitive to increases in maximum temperatures, all with negative responses. The responses of mineralization and denitrification are due to the effect of temperature stress factors on these processes; that of N leached is due to the combined effect of reduced drainage and increased crop N uptake.

Wheat responded positively to increases in minimum temperature, due to being grown in the cooler months. Maize grain responded positively, but stover responded negatively, mainly because maize is grown in the warmer months, and grain has priority over stover for N and CHO, and because of the possible N and CHO translocation from stover. Of the soil variables, only denitrification and N leached were sensitive to increases in minimum temperature.

4.2.2.3 Sensitivity to Input Parameters. Maize and soybean are insensitive to the model parameters investigated. On the other hand, wheat, particularly grain N, is sensitive to soil hydraulic parameters, planting depth, planting density, soil albedo, and organic N mineralization rates (table 11). Interestingly, the wheat state variables are more sensitive to the humus N mineralization rate than to the mineralization rate of fresh organic N. This is because the fresh organic N content of the soil at peak wheat N uptake is typically low; consequently, humus N mineralization is a more significant process than fresh organic N mineralization over this time window.

Runoff, being a surface phenomenon, is insensitive to all the model input parameters investigated. Drainage and water use are insensitive to most of the input parameters, showing only slight sensitivity to the hydraulic parameters, saturated water content, and *α*. Nitrogen leached is sensitive to planting density, water retention parameter *n*, and soil albedo, showing negative responses in all cases. Nitrogen mineralization is sensitive to water table depth and, understandably, fresh organic matter mineralization rate, showing positive responses. Increasing the water table depth increases the zone over which mineralization and crop uptake occur; increasing N uptake increases the soil mineral N deficit factor, which further promotes mineralization. The relative insensitivity of mineralization to humus N mineralization rate over extended time periods is because humus mineralization is of second-order importance to fresh organic N mineralization. Denitrification is sensitive only to soil water retention parameter *n*.

4.3 Summary

A model calibration exercise was undertaken to determine appropriate values for critical model parameters. Calibration was done by trial and error, and the results of this exercise were reported.

A sensitivity analysis was performed to determine which variables need to be determined with most accuracy, and to aid in model verification. Generally, most of the sensitivities obtained could be explained by the mechanistic modeling approach used to model particular processes. Sensitivities did not attain inordinate values that would indicate major programming errors.

Of the crops simulated, wheat is the most sensitive to climatic variables. Crop and soil state variables are, in general, more sensitive to the climatic variables than the input parameters. The crops are most sensitive to the climatic variables (solar radiation and maximum and minimum temperature), the input parameters (plant density and soil albedo), and the hydraulic parameters (saturated hydraulic conductivity, saturated water content, depth to water table, and *n*). The soil state variables are most sensitive to the climatic variables, soil hydraulic parameters, soil albedo, and planting density. Nitrogen leaching is most sensitive to climatic variables (rainfall, solar radiation, and maximum temperature) and input parameters (*n*, soil albedo, and planting density).

5 Model Validation

Model validation is the process of determining that a conceptual model is an accurate representation of the real system (Law and Kelton, 1991). Verification is accomplished by ensuring that the simulation program performs as intended, which involves checking that the conceptual model has been translated correctly into the computer program, i.e., code debugging. Validation is the process that indicates how well the model represents reality. A simulation model is said to be credible when the model and its output are accepted as valid (Carson, 1986).

Law and Kelton (1991) stated that model validation should be performed on those output variables that are important in decision making. In this analysis, validation was performed on grain yield, biomass, grain and total N uptake, and soil N at the end of a growing season. In any N leaching management system, the primary decision-making variables are grain yield and N flux to groundwater. Grain yield is important, since the adoption of any management strategy is incumbent on its relative economic advantage; the importance of N flux to groundwater is obvious. Since data were not available on N leaching, it was necessary to validate the variables that determine the amount of N leaching, namely, residual soil N and N uptake. Over the long term, N content and the amount of crop residue returned to the soil also will influence N leaching.

5.1 Graphical and Tabular Analysis

Even though statistical goodness-of-fit techniques may lend objectivity to the validation procedure, the importance of graphical techniques, though subjective, should not be overlooked (Green and Stephenson, 1986). Under certain circumstances, graphical representations may be even more valuable than statistical methods, since the information they impart is more practical and can give insight into model malfunctioning. Loague and Green (1991) mentioned four types of graphical displays that can be used: (1) profile comparison between observed and predicted quantities, (2) comparison of medians and ranges of integrated values of predicted and observed data, (3) paired comparison between observed and predicted integrated values, and (4) comparison of cumulative distribution functions for integrated values. In this analysis, types 1 and 3 are used.

Model validation analyses were performed to test the model's capability of predicting maize and wheat biomass and grain yields, soil N content, and soil N distribution at the end of the growing season. Data were provided by Dr. Ray Reneau, Dr. Mark Alley, and others for various sites in Virginia.

5.1.1 Results for Maize

Maize data were available for two field sites from the Blacksburg experimental station in Montgomery County for 1986-1988, and the Nomini Creek drainage basin of Westmoreland County for 1986 and 1988.

The soil type at the Blacksburg experimental station is Groseclose silt loam (typic Hapludult, clayey, mixed mesic). Groseclose soil is a well-drained, gently sloping (2-7% slope) soil occurring on ridgetops (Menelik, 1990). At Nomini Creek, the soil type is Suffolk sandy loam (typic Hapludult, coarse-loamy, siliceous, thermic), a deep, well-drained, flat (0-2% slope) soil located on ridgetops in the coastal plain area of Virginia (Menelik, 1990).

The cultural and fertilizer management practices used in the maize validation experiments are shown in tables 12 and 13, respectively. Eight maize treatments were applied, involving 0, 75, 150, and 225 kg/ha N, each applied for minimum and conventional tillage. Data on 40 experiments were available between the two sites, of which 38 were used in this exercise (2 were used in model calibration previously).

Soil hydraulic properties were estimated from laboratory measurements, supplemented where necessary by estimates based on field descriptions. Rainfall data were available for the sites; data for the remaining weather variables were obtained from the closest station. Observed stover and grain N content data from the Blacksburg site were used to calibrate N uptake factors and grain-stover partitioning relations in the maize model.

5.1.1.1 Crop Yield Variables. Data were available on grain and stover yield, N uptake and partitioning between grain and stover, and soil N content and distribution at the end of the season. Tables 14-21 summarize the result of the validation exercises for grain and biomass yield and N uptake. Model performance varied with site.

Good correspondence occurred between measured and predicted crop parameters at the Blacksburg site (tables 14-17), except for 1987 under conventional tillage, where the model underestimated grain yield and N content considerably (tables 14 and 16).

There was good correspondence between measured and predicted crop parameters at the Nomini Creek site for 1986 (tables 18-21). For 1988, the model performed poorly in predicting biomass, grain yield, and grain N content; however, total N uptake for the same year was predicted with good accuracy (tables 18-21).

As a criterion for comparing model performance at the two sites, correlation coefficients (*r*) were computed; table 22 summarizes the *r* between the measured and predicted variables for the two sites. It should be noted that the correlation coefficient is biased against the site with the largest residuals; yields, soil N, and, consequently, residuals were higher at the Blacksburg site. That notwithstanding, overall, the model performed better at the Blacksburg site (with *r* ranging from 0.36 to 0.70). At Nomini Creek, the model performed poorly for grain and grain N; however, model biomass N and soil N were highly correlated with those observed. Assuming that the poor model performance at Nomini Creek is due to model inadequacies and not to inaccurate site properties, an explanation for this may be sought. The soil texture at the Nomini Creek site is sandy with poor moisture retention. Under these circumstances, possible inadequacies in the calculation of the effect of moisture deficits on yield may have been accentuated.

5.1.1.2 Soil N Distribution and Content. Figures 8 and 9 show measured and predicted soil N distributions at the end of the growing season for 75 and 150 kg/ha under minimum and conventional till at Nomini Creek 1986 and Blacksburg 1988, respectively. Here again, there was a good correspondence between measured and predicted soil N distribution; however, model results tended to over-predict the peak N concentration. In most cases, the model underestimated the depth of peak N concentration. This inability to predict the spatial distribution of N with greater precision may be partly due to neglecting dispersion. The N distribution for the treatments simulated at both sites are tabulated in Appendix B.

The model's ability to predict total N content at the end of the season was satisfactory (figures 10-14), except for Nomini Creek 1988 under conventional tillage (figure 11b), where the model overestimated soil N content. Generally, the correspondence between measured and predicted soil N content improved as the amount of N fertilizer applied increased.

5.1.2 Results for Wheat

Tables 13 and 23 show the fertilizer and cultural practices simulated for wheat validation experiments. The soil taxonomic classifications for the sites are given in tables 24 and 25. Wheat data were available for

1988-89 from six sites across Virginia, with two fertilizer application rates at each site (tables 24 and 25). Of a total of 12 experiments, 11 were used for validation; the other one was used in model calibration previously. Conventional tillage was used at all wheat sites. Soil hydraulic properties for the sites were estimated from laboratory core measurements. Rainfall data was available at each site; however, solar radiation and maximum and minimum temperature were taken from nearby stations. Limited or no data was available on total N uptake, N partitioning, or stover yield, and only some sites had grain yield or grain N data (tables 24 and 25).

Tables 24 and 25 show results of the wheat validation analyses for grain yield and N uptake. There is good correspondence between the measured and predicted grain yield. Predicted grain N contents agreed fairly well with measured values when no fertilizer was applied at sites where grain N data were available (table 24). However, agreement was poor when fertilizer was applied, with the model over-predicting grain N content (table 25). The poor grain N response observed when fertilizer was applied was due to lodging in the field, which is not accounted for by the model. Lodging is a condition where luxuriant vegetative crop growth occurs under conditions of high soil N; as a result, the crop becomes susceptible to toppling.

Figure 15 shows measured and predicted N distributions approximately 24 weeks into the growing season at the Randolph and VCIA sites. The agreement between measured and predicted results was satisfactory at Randolph for both treatments. Agreement was acceptable for VCIA when no N was applied, but less agreeable when fertilizer was applied. Discrepancies between measured and predicted results may be due in part to the fact that the model disregards dispersive transport.

The model's inability to predict N distributions accurately does not affect its ability to predict total N in the profile, as demonstrated in figure 16. Here again, model performance was better when no N was applied to wheat.

5.2 Statistical Evaluation of Results

To determine whether a simulation model is validated, it must be established that model results closely resemble those from the system it intends to mimic. Statistical procedures offer an objective means by which the closeness between model and system output can be determined. It is of interest to note that statistical procedures are not purely objective, since the choice of a method and level of significance are subjective, in addition to any other biases inherent in the method. Hence, the conclusion reached will be biased by these (Green and Stephenson, 1986). Statistical validation involves determining that some objective function satisfies a null hypothesis. Objective functions for validating a model include sum of squared residuals (Green and Stephenson, 1986; James and Burgess, 1982), sum of absolute error (Green and Stephenson, 1986), relative error (Green and Stephenson, 1986; James and Burgess, 1982; Thomann, 1982), root mean square error (Green and Stephenson, 1986; Thomann, 1982), and mean deviation (Green and Stephenson, 1986). The sum of squared residuals by way of regression analysis, and the mean deviation by way of a paired-t confidence interval are the objective functions used in this study.

In statistical analyses, the significance level ($1-\alpha$) must be selected. Associated with the choice of α are type-I and type-II errors. A type-I error is committed when a good model is rejected; a type-II error is committed when a bad model is accepted. Type-I errors may be regarded as the modeler's risk, and type-II errors as the user's risk (Loague and Green, 1991); that is, the modeler may prefer to use a small α, but the user wants a large α. In this study, an α level of 0.05 is used.

5.2.1 Regression Analysis

Thomann (1982) discussed objective statistical criteria for determining whether a model has been validated adequately. The regression analysis method was used to determine whether the model had been adequately validated by fitting the following model to each response variable.

$$x_i = a' + b' c_i + \epsilon_i \tag{111}$$

where x_i is the observed response, c_i is the predicted response, a' is the intercept, b' is the slope, and ϵ_i is the error.

The assumptions inherent in fitting equation 111 are: (1) the independent variable is a nonrandom variable measured without error; (2) the dependent variable is a random variable with ϵ_is that are identically and normally distributed with expectation zero and constant variance (i.e., *iid* $N\{0,\sigma^2\}$) (Haan, 1977). If all these assumptions are met, the least square estimators can be proven to be maximum likelihood estimators (Haan, 1977).

Ideally, a fit of equation 111 should yield a straight line through the origin of slope 1. To determine whether the model has been validated, the following null hypothesis must be satisfied

$$H_o\colon a' = 0 \text{ and } b' = 1 \tag{112}$$

The test statistic with a two-tailed student t distribution with 2.5% significance in either tail and n-2 degrees of freedom for slope and intercept, respectively, is

$$t = \frac{|\,1 - b\,|}{S_b} \qquad \text{(113)a}$$

$$t = \frac{a}{S_a} \qquad \text{(113)b}$$

where t is the test statistic, b is the estimate of $b/$, a is the estimate of $a/$, and S_a and S_b are estimates of the standard deviation of intercept and slope, respectively, estimated as (Walpole and Myers, 1989)

$$S_b = \left[\frac{S^2}{\sum_{i=1}^{n} (c_i - \bar{c})^2} \right]^{\frac{1}{2}} \qquad \text{(114)a}$$

$$S_a = \left[\frac{S^2 \sum_{i=1}^{n} c_i}{n \sum_{i=1}^{n} (c_i - \bar{c})^2} \right]^{\frac{1}{2}} \qquad \text{(114)b}$$

where $\bar{c}$ is the expected value of the response variable, n is the number of observations, and S^2 is an unbiased estimate of statistical model variance. The regression model variance was estimated as (Walpole and Myers, 1989)

$$S^2 = \frac{\sum_{i=1}^{n} (x_i - a - bc_i)^2}{n - 2} \tag{115}$$

The response variables analyzed were biomass and grain yield, total crop and grain N uptake, and soil N content. The data for maize and wheat were pooled and analyzed over the entire spatial and temporal profile for grain yield and soil N content. Data were not available for wheat biomass and total N uptake, and grain N data were incomplete and were excluded from the analysis. The fraction of observed results that is explained by the model and the correlation coefficient (r) was calculated by standard statistical procedures (Walpole and Myers, 1989). An estimate of VT-CROPS model variance (S_m^2) is given by (Thomann, 1982)

$$S_m^2 = \frac{\sum_{i=1}^{n} (x_i - c_i)^2}{n} \tag{116}$$

Confidence intervals were calculated for the regression line (CI_l) and for the estimated points (CI_p) as

$$CI_l^k = a' + b' c_i^k \pm S \left[\frac{1}{n} + \frac{c_i^{k2}}{\sum_{i=1}^{n} (c_i - \bar{c})^2} \right] t_n - 2, 1 - \alpha/2 \tag{117)a}$$

$$CI_p^k = a' + b' c_i^k \pm S \left[1 + \frac{1}{n} + \frac{c_i^{k2}}{\sum_{i=1}^{n} (c_i - \bar{c})^2} \right] t_n - 2, 1 - \alpha/2 \tag{117)b}$$

where CI_l^k and CI_p^k are the confidence interval on the regression line and points, respectively, at independent variable c_i^k.

Figures 17-19 show the fitted regression equation and the data points. Best fits were obtained for soil N content (r = 0.83), total N uptake (r = 0.76) and grain N content (r = 0.72). Of the variables investigated, these are the most pertinent to N leaching.

Table 26 summarizes the result of the regression analysis and t test that was done on the model variables. Grain yield, grain N content, and soil N content predictions were validated by this analysis. Biomass N uptake was not validated, even though it had the second highest correlation coefficient.

5.2.2 Examination of Regression Assumptions

The assumption of nonrandomness and absence of error in the independent variable was adhered to, as the VT-CROPS model output was used in this capacity.

That the mean of the ϵ_is equals zero is not just an assumption, but a guarantee by the least squares estimator (Haan, 1977).

The normality of residuals and the constancy of variance may be evaluated by an examination of the residuals.

The constancy of variance was evaluated by making a residual plot. In the interest of brevity, a composite of residuals plot was made. To accomplish this, standardized residuals were plotted against normalized independent variables. Given a mean of zero, residuals for each variable (R_i) were standardized as

$$r_i = \frac{R_i}{S_R} \tag{118}$$

where r_i is a standardized residual ($\bar{r} = 0$, $S_r = 1$) and S_R is an estimate of the standard deviation of the residuals. Independent variables were normalized between zero and one as

$$N_i = \frac{c_i}{c_{max}} \tag{119}$$

where c_{max} is the maximum VT-CROPS output for a given variable. Figure 20 shows the residual plot that results; the randomness of the residuals is evident. There seems to be a slight tendency toward increasing residuals with independent variable, but not enough to warrant further attention.

The Kolmogorov-Smirnov (K-S) test was used to ascertain the normality of the residuals. The program VTFIT (Cooke and Mostaghimi, 1992) was used to fit normal distribution to the variable residuals individually and compositely. A K-S statistic was calculated as (Law and Kelton, 1991)

$$KS = \left[\sqrt{n} - 0.01 + \frac{0.85}{\sqrt{n}} \right] D_n \tag{120}$$

where D_n is the maximum vertical distance between observed and fitted distributions. The null hypothesis on the K-S statistic is that the residuals are normally distributed. For computed K-S greater than a critical value, at some a priori level (0.05), the null hypothesis is rejected. Table 27 summarizes the result of this analysis. The p-values of the K-S statistics of the residuals for the variables are all less than 0.95; hence, the null hypothesis cannot be rejected. The p-value for the composite residuals is also given. Therefore, the assumption of the normality of the residuals has been verified. Figure 21 shows the observed frequency plot and fitted distribution for the composite residuals. A composite plot is perfectly valid, since the groups of residuals are all from the same distribution with identical parameters; i.e., mean zero and a standard deviation of one.

5.2.3 Paired-t Confidence Interval Method

A shortcoming of a least squares regression analysis is that it regresses toward the expectation of the dependent variable; i.e., it estimates with the highest confidence around the mean (see figures 17-19), and the confidence in its estimates decreases with increasing distance from the mean in either direction. Therefore, for data with high CVs, the reliability of estimates, particularly those far from the mean, is suspect. The data for the variables used in this analysis have CVs ranging from 28% to 62% (table 26). As an alternative, a statistically more robust method of evaluating the validity of the model is constructing paired-t confidence intervals (Law and Kelton, 1991). This approach reduces a two-variable problem, measured and predicted, to one variable by examining the residuals between them. The method is attested to be more robust since skewness in the data may be attenuated by computing residuals (Law and Kelton, 1991). For each pair of observed and predicted data, the difference (Z_i) was calculated as

$$Z_i = x_i - C_i \qquad i = 1,2...n \tag{121}$$

where n is the number of observations. The only assumption required by the test is that the Z_is are independent and identically distributed with the expectation $E(Z_i) = \mu$. For a valid model, μ should be zero. The objective of this analysis was to construct a confidence interval at some a priori level of confidence. If it contains zero, the model variable is said to be validated. An estimate of μ is given by

$$\bar{Z}(n) = \frac{\sum_{i=1}^{n} Z_i}{n} \tag{122}$$

An unbiased estimate of the variance of $\bar{Z}(n)$ is given by

$$S_{\bar{z}}^2 = \frac{\sum_{i=1}^{n} (Z_i - \bar{Z}(n))^2}{n(n-1)} \tag{123}$$

For sufficiently large n (by the central limit theorem), an approximate two-tailed paired-t confidence interval on $\bar{Z}(n)$ with precision 1-α is given by

$$Z(n) \pm t_{n-1,\,1-\alpha/2}\, S_{\bar{z}} \tag{124}$$

Paired-t confidence intervals at α = 0.05 were determined for soil N, biomass yield, grain yield, total N uptake, and grain N. The results of this analysis are presented in table 28. All variables were validated except grain yield, which also had the lowest correlation coefficient. Biomass and total N uptake were not validated by regression analyses, but were validated by the paired-t confidence interval.

5.3 Summary of Validation Exercise

Validation analyses were performed to determine the model accuracy in predicting observed biomass and grain yield, biomass and grain N content, and soil N distribution and content for maize and wheat. For maize, data were available for a period of three years at three sites; for wheat, data were available for 1988 at six sites.

The model predicted total soil N content at the end of crop growing periods fairly accurately; soil N distribution with depth was not predicted with the same accuracy. The latter result is likely due to a great extent to spatial variability in soil properties, which was not accurately known. Total soil N, on the other hand, is an integral measure over the entire soil profile and, as such, is less sensitive to soil variability. Nitrogen leaching, which is of primary importance to groundwater contamination, is closely linked to total soil N content. Maize yield and N uptake were predicted by the model fairly accurately; wheat yield and N uptake were predicted less accurately. This may reflect a need to refine the N uptake and grain-leaf-root partitioning relations in the model, and to account for the effects of lodging and other factors.

Possible deficiencies that may affect model predictions include:

- The model disregards dispersive transport, which may result in an underprediction of the peak N concentration in the soil profile.

- Crop lodging, which may result in poor performance of wheat under fertilized field conditions, is not accounted for by the model.

Two statistical procedures were used to objectively determine the model variables that were validated: regression analysis and the paired-t confidence interval. Regression model assumptions were verified; however, inherent weakness in the method limits the interpretive value of the results. There is no way of explicitly verifying the assumption of the normality of mean residuals in the paired-t confidence interval method, except that the central limit theorem guarantees this. Grain nitrogen and soil N content at the end of the season were validated by both methods. Grain yield was validated by regression analysis, but not by paired-t confidence interval. Biomass and total N uptake were validated by the paired-t confidence method, but not by regression analyses.

For maize, data were available on 40 experiments from 2 sites, spanning 3 years. For wheat, 12 data sets were available from 6 sites for 1 growing season. To improve the model's credibility, it is recommended that additional validation be done on complete data sets for both crops. Maize and wheat crop behavior were investigated independently in this study; however, the objective of the model is to perform long-term simulations of cropping systems in which there is interdependence between crops due to continuity in time. Therefore, validation of the model for entire crop rotations would lend greater credibility to model results. Pertinent variables to N leaching that were not validated directly include net mineralization, denitrification, drainage, and some measure of N leaching itself.

The most pertinent variable to N leaching over the short run is soil N content. However, over the longer term, total N uptake and grain N content are also important. The difference between total N uptake and grain N content is usually returned to the soil as crop residue. This indicates that more work needs to be done on the model to refine crop performance variables. It is worth mentioning that, due to the lack of data, N flux from the root zone was not investigated in this analysis, only N content and distribution. This could lead to problems in N leaching predictions, since soil water content and solute concentration are not necessarily good indicators of fluxes through the root zone (Addiscott and Wagenet, 1985). While it is evident that additional validation would be advantageous, it should be kept in mind that "there is no such thing as completely valid model" (Law and Kelton, 1991).

6 Evaluation of Long-Term Model Predictions

6.1 Overview

Model runs for the validation analyses in section 5 were of short duration—generally 8 months or less. In addition, due to the lack of pertinent data, N leaching was not validated. In this section, long-term model performance will be investigated by looking at output to varying levels of input and management. Nitrate leaching and its relationship to other variables will be explicitly evaluated. Model runs were performed for 26-year periods involving 13 2-year crop rotations of maize-wheat--soybean-fallow for 2 management systems: (1) conventional tillage applied to all crops, and (2) minimum-tilled maize and soybean with conventionally tilled wheat.

Simulations were carried out for a hypothetical sandy loam to sandy soil with three profile horizons to a depth of 150 cm (table 7). A water table was assumed to be present at 150 cm. Tables 21 and 22 show the crop management practices simulated. An average soil surface runoff curve number of 81 was used for conventional tillage, and 85 for minimum tillage; mean annual atmospheric temperature was assumed to be 12.2° C; amplitude in annual temperature was assumed to be 28.2° C; and a soil albedo of 0.13 was used.

6.2 Atmospheric Submodel Calibration

The atmospheric subsystem is one of the three subsystems modeled by VT-CROPS, and provides daily rainfall, solar radiation, rainfall, and maximum and minimum temperatures to the soil and crop subsystem models. These data may be generated by a stochastic weather generator algorithm in the program. Use of the climatic generator requires calibration to obtain the submodel climatic parameters pertinent to the area for which it is to be applied. Our interest in this project was to assess N leaching from soils in the Northern Neck area of Virginia, so calibration was undertaken based on suitable observed weather data.

Richardson and Wright (1984) recommend that a minimum of 20 years of data be used for calibration. Long-term daily rainfall and maximum and minimum temperature data were available from the Hydrologic Information Storage and Retrieval System (HISARS) for the Northern Neck. Long-term daily solar radiation data for the area were not available. Five years of available solar radiation data from Warsaw, Virginia, were used for calibration of radiation model parameters.

Calibration and validation procedures described by Richardson and Wright (1984) were used to fit statistical parameters to the measured records and to verify generated climatic data against observed data. Figure 22 illustrates the simulated daily averages of maximum and minimum temperature, solar radiation, and annual rainfall over a 25-year period using the calibrated weather generator.

6.3 Model Evaluation

6.3.1 Evaluation of Mineralization Routine

Because mineralization (immobilization) is a major source (sink) of N to the soil system, the performance of the N mineralization routine warrants special attention. This was accomplished through a series of simulations involving the incorporation of varying amounts of organic material with varying C-N ratio, and varying initial soil mineral N content. Simulations were run for periods of two years, during which, no fertilizer was added and the N dynamics were observed. In all cases, cropping system 1 was used. The soil described previously was used with a stable organic N content of 6040 kg ha^{-1}, which corresponds to a humus content of over 150 tons ha^{-1}; the C-N ratio of humus was assumed to be 10.

The first scenario investigated involved the incorporation of 15 tons ha^{-1} of organic material with a C-N ratio of 12, which amounts to 500 kg-N ha^{-1}, with no incorporation of the residues of the crops being grown. Figure 23 shows the N dynamics that resulted over two years.

Due to its low C-N ratio, mineralization of the organic material was initiated immediately. As organic N was mineralized, the fresh organic N content of the soil was reduced correspondingly; hence, the fresh organic N curve mirrors the mineralized N curve since there was no residue incorporation. During the first 100 days, when mineralization of fresh organic N was high, there was an increase in the soil humus N content (net immobilization in the stable fraction). Although humus was being mineralized, its rate of mineralization was slow relative to that of fresh organic N; in addition, the model assumes that 10% of the fresh organic N mineralized is immobilized immediately into humus N; hence, there was net immobilization by the stable organic fraction during this period. For the remainder of the simulation period, the soil humus N content was fairly constant; i.e., mineralization of humus approximately equaled immobilization of fresh organic N mineralized—a realistic outcome.

During the period of maize growth, root uptake reduced the amount of mineralized N that was retained by the soil. When maize N uptake was at its peak (days 40-90), all of the N mineralized was taken up by the crop; note also that the N mineralization rate peaked during this period, due to a soil mineral N availability factor that provided an impulse for accelerated mineralization rates under mineral N poor conditions. During the fallow period that followed maize, all the N that was mineralized effected a corresponding increase in soil mineral N content.

Initially, during wheat growth, the soil N attained an equilibrium N content as the wheat crop was dormant, N leaching was low, and the cooler temperatures reduced mineralization rates. However, later, the soil N content was reduced—first, due to N leaching during the high leaching months of December-February, and, second, due to crop N uptake. As the soil mineral N content was reduced below its equilibrium content, the mineralization rate increased. During the peak N uptake period (days 330-390), the soil N content remained at a low, even though the mineralization rate was at its highest for the period.

Throughout the soybean growing period, N mineralization persisted at low rates, due to fresh organic N and C-N ratio becoming limiting, even though soil N content was low. Eighty percent of the 500 kg ha^{-1} incorporated was mineralized over the two-year period.

The second scenario was similar to the first, but was more realistic, in that crop residues were incorporated in the soil. Figure 24 shows the N dynamics that resulted; note the delayed residue incorporation till at the beginning of the subsequent crop—a model feature. The fresh organic N content of the soil after one year was 250 kg ha^{-1} and 185 kg ha^{-1} after two years; i.e., 50% and 63% of the initial 500 kg ha^{-1} was mineralized after one and two years, respectively; the USEPA (1983b) estimates that approximately 40% and 60% of applied organic material will be mineralized after one and two years, respectively. Figure 25 shows the C-N ratio of fresh organic material and the fresh organic matter content over the simulation period. As mineralization proceeded, the C-N ratio increased toward its equilibrium value of 30; at this value, there was no net mineralization or immobilization, but organic matter was still being oxidized, which lowers the C-N ratio. At equilibrium, the C-N ratio appears constant, but it fluctuated somewhat around this value. Note also the increases in the C-N ratio of the soil fresh organic matter as the high C-N ratio crop residues are mixed in.

The third scenario was similar to the second, except that there was an additional incorporation of 7.5 tons ha^{-1} of organic material with a C-N ratio of 12 on day 330, around the initiation of peak N uptake by wheat. Note the second organic N incorporation (figure 26) and the almost instantaneous mineral N release, not all of which was taken up by the wheat crop.

The fourth scenario involved the incorporation of 15 tons ha^{-1} of an organic material with a high C-N ratio of 50, which translates into an 120 kg ha^{-1} organic N, into a soil with a low initial mineral N content of 50 kg ha^{-1}. Under these conditions (figure 27a), net immobilization (negative mineralization) resulted initially. However, the amount of immobilization (5 kg ha^{-1}) is limited by the availability of mineral N. As the oxidation of fresh organic matter advances, and the C-N ratio reduces to less than 30, net mineralization results. Note also the small but negative slope of humus N line (i.e., net mineralization from the stable fraction) because of the low N content of fresh organic material.

The final scenario was similar to the fourth, except that the soil N content was initially high (190 kg-N ha^{-1}). In this case, the amount of immobilization is not limited by the soil inorganic N content, and 67 kg ha^{-1} of N is immobilized within the first 15 days (figure 27b). In the first 100 days, there were two distinct periods of reduction in the soil inorganic N; first, there was a steep decrease due to N immobilization, followed by a more gradual reduction due to N uptake. There was a slight depletion in stable organic N, but, because more N was immobilized, the rate of depletion is less than in the previous case. Figure 28 shows the approach of the C-N ratio of stable organic N towards equilibrium.

6.3.2 Changes in Soil Inorganic Nitrogen with Time

Figure 29 shows the simulated soil inorganic N profile for each month during the third year of a 26-year simulation. The first month of sampling (figure 29a) represents the soil N profile on day 129, two days prior to planting and fertilizing the maize crop. An increase in soil N content is observed one month after fertilizer application. As time progressed and N was lost, primarily by plant uptake, the soil N content gradually decreased (figure 29a). Increasing depth to the peak N concentration reflects percolation of moisture through the soil system with time. Split application of N to wheat, with 20% added in month 7, is reflected with an increase in N content at shallow depths (figure 29b). The remaining 80% was added in month 13 (not shown). Further increases in soil N content (months 8-10) are due to organic N mineralization—during this period, the wheat crop is dormant; hence, there is little N uptake. By month 11, due to convection of soil water, peak soil N had migrated to a greater depth. By month 12, the soil N content had dissipated due to leaching and/or crop uptake.

6.3.3 Nitrogen Balance Relations

Mineral N sources to the soil system include fertilizer N and mineralization of organic matter. The sinks for mineral N are crop uptake, N leaching, and denitrification. For these simulations, fertilizer input was constant at 150 kg-N ha^{-1} per crop (table 31). Figures 30 and 31 show N mineralization, denitrification, crop N uptake, and N leached by rotation for the management systems simulated with rainfall amount superimposed; table 31 summarizes the means and coefficients of variation (CVs) for the N sources and sinks. Nitrogen source/sink components varied over relatively narrow ranges, with coefficients of variation ranging from 8% for N mineralization to 15% for denitrification.

Mineralization and N leached are strongly dependent on rainfall amounts (figures 30a and 31b). Denitrification is weakly dependent on rainfall amount (figure 30b), and N uptake is fairly independent of rainfall amount (figure 31a).

There was little difference between N transformation variables for the two management systems. Mean mineralization and crop N uptake were slightly higher for conventional till; N leached and denitrification was slightly higher for minimum till.

Mineralization rates ranged from 37-70 kg ha^{-1} $year^{-1}$ with a mean of 57 kg ha^{-1} $year^{-1}$ for conventional till, and from 38-68 kg ha^{-1} $year^{-1}$ with a mean of 56 kg ha^{-1} $year^{-1}$ for minimum till. These differences do not appear to be physically significant. Estimates of mineralization rates in the literature are scarce and uncertain; Schepers and Mosier (1991) estimated mineralization rates in field soils with 1% organic matter to range from 45 to 90 kg ha^{-1}. Data in the literature on comparative mineralization rates in conventional and minimum tilled systems are even more scarce, but the consensus of opinion is that mineralization is greater under conventionally tilled systems (Free, 1970; Moschler et al., 1972; Stanford et al., 1973). The rationale given for higher mineralization under conventional tillage is an improved oxidative condition due to a lower moisture content. However, mineralization rates are expected to increase from dry to moist soil moisture conditions and to decrease again under waterlogged conditions (Keeney, 1983). Therefore, the advantage of one tillage system over another, with respect to mineralization rates, is highly soil and climate dependent.

Gilliam and Hoyt (1987), in a survey of available literature, concluded that denitrification rates are generally higher under minimum tillage due to higher soil moisture. The mean annual denitrification rate was 10.7 kg ha^{-1} (range 9.3-15.4) for minimum till and 10.8 (range 8.5-16.6) for conventional till. The impact of management systems on denitrification is expected to be small, given the coarse texture of the soil. Simulations on a finer-textured soil, with higher moisture retention capacity, may show a tillage effect on denitrification. Information is scarce on denitrification rates, but Groffman (1985) found rates less than 10.0 kg/ha/year under both minimum and conventional tilled systems in Georgia soils. Meisinger and Randall (1991), summarizing the finding of a number of researchers, reported denitrification rates ranging from 4 to 25 kg ha^{-1} $year^{-1}$ in moderately drained soils.

There is a wide disparity in the literature on the effect of tillage practices on N leaching. It ranges from increased N leaching under minimum tillage (Thomas et al., 1973; Tyler and Thomas, 1979), to no difference between tillage systems (Kitur et al., 1984), to increased N leaching under conventional tillage (Kanwar et al., 1985). The consensus is that the amount of N leached for a given tillage system is highly climate-dependent. In the simulations conducted, there was no advantage for one tillage system over the other (table 31) even though drainage was higher for conventional till. The low water-holding capacity of the soil investigated may have influenced the results.

Figure 32 summarizes the mineral N mass balance by rotations over an extended simulation period. The percentage error in soil mineral N (ΔM_N) is calculated as

$$\Delta M_N = \frac{N_{in} - N_{out}}{N_{in}} \times 100 \qquad (125)$$

where ΔM_N is the percentage of mineral N input that is unaccounted for; N_{in} is the total mineral N input over a rotation, i.e., the sum of N fertilizer and N mineralized; and N_{out} is the total mineral N output, i.e., the sum of crop N uptake, N leached, denitrification, and increases in soil mineral N content over the period. The net change in mineral N fluctuated around zero and ranged from -3.9 to 7.2% for conventional till, and -4.0 to 5.7% for minimum till. Over the 26-year simulation period, the percentage of N input that is unaccounted for is 1.7% for conventional till and 0.7% for minimum till, which indicates that mass balance errors in the model are small.

6.3.4 Water Balance Relations

Figure 33 shows the potential and actual evapotranspiration and its components, soil evaporation, and crop transpiration for the crops over typical growing seasons.

Potential evapotranspiration is independent of the crop development, and depends only on the prevailing climatic conditions. Evapotranspiration, on the other hand, depends not only on the stage of development of the crop and the climatic conditions, but also on the ability of the soil to supply needed moisture. This difference is reflected in differences between potential and actual evapotranspiration curves. Soil evaporation is dependent on the climatic conditions, the soil water status in the upper reaches of the soil, and the crop development stage. Crop transpiration increases to a maximum with leaf area, and decreases thereafter.

Note the differences in the skew in the curves for the different crops; this is related to the climatic condition under which particular crops are grown. The maize curve is the most symmetric, due to maize being grown when temperatures and solar radiation are high; the wheat curves have a left skew, and the soybean a right skew, because the warmest and brightest months are toward the end of the wheat crop and the beginning of the soybean crop.

Table 32 summarizes the water balance components per rotation for the two management systems simulated. The source of moisture into the system is rainfall, and the sinks are evapotranspiration, drainage, and runoff. Figure 34 shows a typical crop water budget by month over a rotation. There is an absence of drainage during peak water uptake. During these periods, water use is frequently greater than rainfall, and soil moisture reserve accounts for the difference. Differences between rainfall and drainage following peak uptake reflect the replenishment of depleted moisture reserve.

Runoff was higher for the conventional tillage scenario and, consequently, drainage was lower. Runoff ranged from 41 to 108 mm yr^{-1} with a mean of 65 mm yr^{-1} for conventional till, and from 26 to 79 mm yr^{-1} with a mean of 43 mm yr^{-1} for minimum till. On average, runoff was 34% lower for conventional till. Glen and Angle (1987) found 27% less runoff from no-till corn than from conventionally tilled corn in the Chesapeake Bay watershed. Also, Gilliam and Hoyt (1987) summarized results from tillage experiments, and found runoff to be reduced 9-109% by reduced tillage practices. The net of water influx and efflux to the soil, which represents the change in water storage, was small over each two-year rotation (table 32).

Figure 35 shows the hydrologic budget by rotation for the two management systems simulated. Drainage and runoff are highly sensitive to rainfall amounts, but water use (ET) is not. Table 34 shows that runoff was consistently higher for conventional till, and underscores its positive correlation with rainfall amount.

6.3.5 Plant Partitioning of Dry Matter Production and Nitrogen

Tables 33-35 show the partitioning of dry matter and N between the different plant parts for maize, wheat, and soybean, respectively, over the 26-year simulations for each management scenario.

6.3.5.1 Maize Results. Total above-ground biomass production was higher for minimum tillage than for conventional tillage, ranging from 9434 to 13,495 kg ha^{-1} for conventional tillage, and from 9,239 to 13,265 kg ha^{-1} for minimum tillage. Typical literature values ranged from 9,300 to 17,000 kg ha^{-1} (Triplett and Mannering, 1978).

Root mass ranged from 1,116 to 2,733 kg ha^{-1} (mean 1746) for conventional till, and from 1,084 to 2,444 kg ha^{-1} (mean 1668) for minimum till. Typical literature values for maize root mass range from 1,300 to 2,500 kg ha^{-1} (Triplett and Mannering, 1978).

Maize yields varied over a fairly narrow range from 5,352 to 6,825 kg ha^{-1} for conventional till, and from 4,808 to 7,002 kg ha^{-1} for minimum till. Mean maize yield was slightly higher under minimum tillage—6,021 kg ha^{-1}—as opposed to 5,890 kg ha^{-1} for conventional till. The grain harvest index ranged from 47 to 63%; typical literature values range from 35 to 65% (Triplett and Mannering, 1978).

Total N uptake ranged from 135 to 182 kg ha^{-1} for conventional till, and from 128 to 178 kg ha^{-1} for minimum till. The grain N harvest index ranged from 62 to 75% with a mean of 68%; typical literature values range from 61 to 78% with a mean of 70% (Schepers and Mosier, 1991). Tillage practice has only a slight effect on grain N content—under conventional till, grain N content ranged from 1.34 to 1.69% with a mean of 1.58%; under minimum till grain N content ranged from 1.32 to 1.79% with a mean of 1.60%. Typical literature values range from 1.35 to 1.75% with a mean of 1.55% (Meisinger and Randall, 1991). Mean stover N content ranged from 0.74 to 1.27% with a mean of 0.96%—somewhat high compared to literature values, which typically range from

0.6 to 1.0% (Schepers and Mosier, 1991). An average of 62.8% of the applied N was harvested, which compares favorably with a national average of 64.5% (Bock and Hergert, 1991).

6.3.5.2 Wheat Results. Under both management systems, wheat was grown under conventional tillage. Hence, there were only slight differences between N uptake and crop yield results for the management systems evaluated. Differences observed may be attributed to residual effects of different tillage management practices applied to the preceding maize crop.

Predicted total above-ground dry matter production ranged from 7,852 to 9,826 kg ha^{-1} with a mean of 8,614 kg ha^{-1}, which compares favorably with literature values, which range from 6,900 to 8,400 kg ha^{-1} with a mean of 8,000 kg ha^{-1} (Triplett and Mannering, 1978). Predicted wheat root production was high, ranging from 1,521 to 3,381 kg ha^{-1} with a mean of 2,340 kg ha^{-1}, compared to literature values ranging from 970 to 1,300 kg ha^{-1} with a mean of 1,000 kg ha^{-1} (Triplett and Mannering, 1978). Wheat yields varied from 3,125 to 5,718 kg ha^{-1} over the 13 rotations, with a mean of 3,577 kg ha^{-1}. The grain harvest index ranged from 37 to 66%, which compares well with the observed spectrum of 31-65% (Triplett and Mannering, 1978). The grain N harvest index ranged from 55 to 77% with a mean of 64%; observed values are much higher, ranging from 74 to 86% with a mean of 80% (Schepers and Mosier, 1991).

6.3.5.3 Soybean Results. Variations in soybean CHO and N partitioning reflect the availability of soil moisture. Due to the simple approach used to distribute CHO and N, soybean yield ratios are constant.

6.4 Nitrogen Leaching and Its Relations with Hydrologic Variables

6.4.1 Short-Term Variations in Nitrogen Leaching

To evaluate short-term fluctuations in N leaching, monthly N losses over a two-year crop rotation were investigated for the 150 kg-N ha^{-1} $crop^{-1}$ fertilizer application treatments with both tillage systems. To overcome effects of initial conditions, the second rotation in the 13-rotation sequence was used in this analysis. The monthly N flux was plotted against residual soil N and the hydrologic variables, rainfall, crop water use, and drainage.

6.4.1.1 Nitrogen Leaching and Residual Soil N. Figures 36a and 36b show the short-term temporal fluctuations in N flux and mineral soil N content for the two tillage treatments. Mineral soil N is lagged by one month, since the N leached by the end of the current month would be influenced by the soil N content at the end of the previous month, rather than that of the current month. In general, N losses increased with an increase in soil N, but the overall results were more pronouncedly influenced by the hydrologic variables. In fact, the correlation coefficient (r) between N load and residual N was only 0.15 (table 36).

As a result of fertilizer additions for maize, a steep increase in soil N occurred in month 2 (June of year 1). The effect of adding 20% of wheat N (30 kg/ha) is observed in month 7. Addition of 80% of the wheat fertilizer (120 kg/ha) in month 13 (May of year 2) for wheat also is seen, even though an actively growing crop had removed a considerable amount. Even though the mineral soil N was lagged one month, there is an additional two-month lag between periods of high soil N and high N leaching (or between low soil N and low leaching). This is due to the travel time for N to move through the soil profile.

There was a gradual increase in mineral soil N during months 16-21 (July-February of year 2). This period corresponds to soybean crop and fallow, when there is little or no N uptake. The gradual increase in soil N is due to net mineralization over immobilization. Persistent leaching of N follows this period and appears critical in any leaching management system.

More N is leached in the second year of the rotation, during months January-April, than the first, since the second year involves an extended fallow with no N uptake, whereas wheat in the first year provides a sink for some soil N and soil water. During the winter months, evapotranspiration and N uptake are low; hence, more N and water are available for leaching and drainage, respectively.

6.4.1.2 Nitrogen Leaching and Water Balance Components. Figure 37a shows the monthly variations in N flux, rainfall, and water use for management 1. A similar pattern was observed for management 2. The N flux patterns tend to be qualitatively similar to that for rainfall (r = 0.15) (table 36), although large rainfall amounts do not necessarily result in large N loads. The highest period of N leaching occurred near the end of the rotation (months 21-24), which does not correspond to the highest rainfall period.

Fluctuations in N flux versus crop water use and rainfall are depicted in figure 37a. Crop water also is highly related to the N leaching patterns (r = 0.44) over the short run. High N leaching consistently corresponds with low water use, and vice versa. During the period of extensive fallow (months 19-24), water use was at its lowest, while N leaching was at its highest. During the period of rapid growth for maize and wheat (months 13 and 12-14, respectively), water use was at its highest, while N fluxes were at their lowest. Nitrogen leaching is closely related to water use in the short term, because water use not only affects the drainage flux, but also the mineral N concentration in the soil. During periods of rapid crop growth, evapotranspiration and N uptake rates are high, resulting in low drainage fluxes as well as low concentrations of N in drainage water.

Drainage patterns were more strongly related to N load than rainfall (figure 37b), with an *r* of 0.58 (table 36). However, the highest drainage flux did not result in the highest N flux. Drainage patterns were similar for both management scenarios. The relationship between N load and drainage is obvious, since drainage is the vehicle by which N is transported from a soil.

6.4.1.3 Summary of Short-Term Nitrogen Leaching Response. Figure 38 summarizes the N leaching pattern over a rotation for the two tillage systems investigated. High N fluxes occurred during the main leaching period (January-April) of the second year, when water use was low and residual soil N was high. During the first of these periods, a crop of winter wheat offered some protection from leaching. Thus, provided the maize crop was successful, the residual N and the resulting N fluxes will be considerably lower in year 1 than for the corresponding period in year 2. However, during the long fallow period in year 2, water use was at its lowest, and organic matter mineralization increased the soil N content, leading to high N fluxes. For the conventional and minimum tillage systems, 55% and 60%, respectively, of the total N load was leached during January-April of the second year. To reduce N leaching, the period of extended fallow in year 2 should be avoided by the use of a cover crop that will immobilize available N and increase water use.

6.4.2 Long-Term Nitrate Fluxes to Groundwater

This section evaluates the long-term relationship between tillage practices and water balance variables and N leaching patterns, using the 150 kg-N ha^{-1} per crop simulation. N loads to groundwater per rotation were evaluated over the 13-rotation sequence. Data were evaluated by rotation rather than by year, since crop and management practices differed from the first year of a rotation to the second, making temporal trends difficult to discern.

Figure 39a shows N fluxes versus drainage by rotation. Drainage loss was consistently higher for minimum tillage than conventional tillage, although the differences were small. In the long term, N loads were directly proportional to drainage for both management systems, with an *r* of 0.53 (table 36). Rainfall amount, as alluded to earlier (figure 31b), is correlated well with N load (r = 0.55) (table 36).

There was little variation in crop water use between rotations (figure 39b). Hence, no trend could be identified between N flux and water-use pattern (r = 0.05). If rainfall was low during periods of peak consumption, the soil system compensated by using its moisture reserves. The depleted moisture reserve is subsequently replenished over the fall and winter months, when water use is low. Over the long term, drainage is more sensitive to rainfall than to water-use patterns. Consequently, the distinct short-term relationship observed between water-use patterns and N fluxes is absent over longer periods.

6.5 Evaluation of Model Response to Varying Input

6.5.1 Overview

To evaluate the effects of different management practices on model performance, sensitivity analyses were performed in which the varying amounts of fertilizer were applied to both management systems, and the means of performance variables reported. Fertilizer amounts ranged from 0 to 400 kg ha^{-1} for both maize and wheat crops. For wheat, 20% of the N was applied at planting; the remaining 80% was applied on Julian day 100 of the following year during peak uptake.

6.5.2 Grain Yield and Nitrogen Uptake

6.5.2.1 Maize Yield and Nitrogen Uptake. Figure 40a shows the maize grain yield response to varying levels of fertilizer N. Under both tillage systems, mean yields increased with fertilizer level and plateaued at a N application rate of 200 kg ha-*1*. Simulated means of yield ranged from 3,840 kg ha^{-1} for no N added to 6,850 kg ha^{-1} for 400 kg-N ha^{-1}—an 80% increase. Differences in maize yields for conventional tillage (system 1) and minimum tillage (system 2) were small.

Mean N uptake for maize ranged from an average of 17 kg ha^{-1} for no added N to 185 kg ha^{-1} for 400 kg-N ha^{-1}. Figure 40b shows the sensitivity of N uptake to varying levels of N for the different management scenarios simulated.

6.5.2.2 Wheat Yield and Nitrogen Uptake. Mean wheat yields ranged from 976 kg ha^{-1} for no added N to 5,928 kg ha^{-1} for 400 kg-N ha^{-1}. Yields increased roughly with fertilizer application, and were still increasing at 400 kg-N ha^{-1}, even though the rate of increase had slowed considerably (figure 41a). Mean wheat N uptake varied from 43 kg ha^{-1} to 198 kg ha^{-1} for applications of 0-400 kg-N ha^{-1}. Nitrogen uptake responded somewhat linearly to increasing levels of fertilizer (figure 41b) up to 150 kg-N ha^{-1}.

6.5.3 Runoff, Water Use, and Drainage

Average annual runoff at a given fertilizer application rate was higher for conventional tillage (64-67 mm yr^{-1}) than for minimum tillage (42-47 mm yr^{-1}). Runoff amounts decreased slightly as fertilizer rates increased up to 100 kg-N ha^{-1}, and became constant thereafter (figure 42a). The reduction in runoff with fertilizer amount may be attributed to higher surface cover, due to increased leaf area as the fertilizer rates increases.

Figure 42b shows the average crop water use for the management practices simulated. Values represent averages per year over all crops for the 26-year simulation. Average annual water use varied over a narrow range from 454 to 491 mm. Crop water use increased with fertilizer rate up to 100 kg-N ha^{-1} per crop; thereafter, water use remained constant, even though yields increased. Differences between management scenarios were small.

The sensitivity of drainage (figure 43) was opposite that of water use. Greater drainage occurred for minimum till than for conventional tillage, although differences were small compared to total water use. Since evapotranspiration and drainage are the two principal sinks for rainfall, it is expected that drainage fluxes will decrease as evapotranspiration increases.

6.5.4 Nitrogen Leaching

The average N leached per year ranged from 17 kg ha^{-1} for no applied N to 206 kg ha^{-1} for 400 kg-N ha^{-1} per crop (figure 44a). Leaching was similar for both tillage systems. For higher N application rates, the conventional tillage system attained slightly higher N loads.

Mean leachate concentration was operationally defined as the quotient of mean annual N flux and mean annual water drainage flux. Curves for the two tillage systems were similar to figure 44a, with mean N leachate concentrations ranging from 3.3-42.4 mg/l for fertilizer rates of 0-400 kg-N ha^{-1} $crop^{-1}$.

The N leaching fraction was operationally defined as the ratio of N flux to groundwater to fertilizer application rate. Note that, for N leached, no distinction is made between fertilizer and mineralized N. Figure 44b shows the N leaching fraction as a function of fertilizer levels. The leaching fraction is high at the lowest fertilizer rates, diminishes markedly for fertilizer rates up to 100 kg-N ha^{-1}, stays constant at 150 kg-N ha^{-1}, and increases somewhat linearly thereafter. At low fertilizer rates, more N mineralization occurs as organic N is mobilized to satisfy the deficit in mineral N. Some of this mineralized organic N is leached, resulting in a high N leaching fraction. In addition, under conditions of low soil N, the crop rooting system is not optimally developed to take advantage of N present deeper in the profile. For higher N fertilizer rates, N-use efficiency initially increases until some optimal level of crop development is reached (ca. 150 kg-N ha^{-1}). Thereafter, further increases in fertilizer N are used with diminishing efficiency by the crops. At fertilizer rates less than 200 kg-N ha^{-1} per crop, N leaching fractions were similar for both tillage systems. At higher fertilizer rates, N leaching fractions were slightly higher for the conventional tillage system.

6.6 Summary of Model Performance

Simulations were performed to evaluate the long-term performance of N and water mass balances and crop yield variables for the purposes of model verification. Model verification was done in three stages: (1) model output was verified against reported values; (2) N leaching and its relationship to hydrologic variables was investigated; and (3) the sensitivity of model output to varying fertilizer amounts and management was evaluated.

The soil mineralization routine was evaluated extensively, and appropriate responses were obtained in all cases. The soil mineral N profile behaved rationally over time, with appropriate response to fertilizer additions. The amount of N transformed by different mechanisms was generally consistent with values reported in the literature. Errors in soil mineral N over a rotation fluctuated around a mean near zero, indicating good mass conservation in the solution. Likewise, mass balance errors in the water flow solution were observed to be very small. Dry matter production, grain and root production, and N uptake were higher for maize grown under minimum tillage than for conventional tillage. Ranges of maize-yield performance variables were within values reported in the literature. Differences between wheat yield parameters for the different management scenarios were small. Mean dry-matter production, grain and root production, and N uptake were generally higher than values reported in the literature.

Over the short run, N load was strongly related to drainage and water use. Over the long term, N load was more strongly related to rainfall and drainage. The N leaching pattern over a rotation was decidedly periodic. More than 50% of the N load was leached over the extended fallow period that followed soybean.

Crop yields and hydrologic variables responded appropriately to increases in fertilizer rates. Nitrogen flux to groundwater increased with fertilizer rates. However, N leaching fraction was quadratic in its response, with the N leaching fraction being optimal at about 150-200 kg-N ha^{-1}.

7 Site Selection and Model Application

This section illustrates some applications of the model. Crop performance and N load under existing management from the Northern Neck are evaluated over the long term. In addition, the use of sewage sludge as an alternative N source is evaluated. This section is divided into three subsections: 7.1 deals with definition of the study area and subdivision of soils into land units; 7.2 evaluates crop performance and N leaching and its effect on regional groundwater quality from the land units; and 7.3 investigates the use of sludge as a replacement for, or in consort with, mineral fertilizer.

7.1 Study Area Selection and Division of Soils

7.1.1 Study Area Description

The Northern Neck region of Virginia is bounded to the north by the Potomac River, to the south by the Rappahannock River, to the east by the Chesapeake Bay, and to the west by the fall line. This area was selected for study due to: (1) its high agricultural productivity, (2) its proximity to the bay and potential for directly affecting water quality of the bay, and (3) its well-defined hydrologic boundaries. The counties studied include Richmond, Westmoreland, Lancaster, King George, and Northumberland.

Data on the properties and areal extent of various soil types were obtained from soil survey reports, which indicated a total of 67 soil series within the study area, 34 of which were suitable for cultivation. The study area encompassed approximately 252,000 hectares, with 118,000 hectares of crop land. To minimize the number of VT-CROPS simulations required to characterize N leaching characteristics from cropped land in the study area, we wanted to determine whether the 34 soil series could be grouped into a smaller number of land units having similar hydrologic and other properties pertinent to crop production. Specific parameters of relevance that are available from soil survey reports include slope, soil organic matter content, depth to water table, depth of solum, number of soil layers, hydrologic group, pH, permeability, water-holding capacity, and soil texture.

A methodology involving the use of cluster analysis and principal components analysis was used to define land units; a description of the methodology follows.

7.1.2 Cluster Analysis

Cluster analysis refers to a number of methods that use multivariate data to assign individuals to groups that are more or less homogeneous and distinct from other groups (Davis, 1986). A number of clustering methods are available; the most common are hierarchical, partitioning, and overlapping (Seber, 1984).

Hierarchical clustering is the most popular of the methods, wherein small clusters are successively grouped into larger clusters, forming a tree of clusters. Hierarchical clustering can proceed from the bottom up, starting with n groups of one individual per group, or by agglomerative methods that iteratively fuse like members into clusters, ultimately ending with one cluster of n individuals. Alternatively, one may start with a single group of n individuals and, via divisive methods, end up with n groups of one individual per group (Seber, 1984). Whatever the approach, the resulting tree of clusters is usually graphically represented by a dendrogram. The bottom-up hierarchical clustering method was used in this analysis.

7.1.2.1 Similarity Measure. Hierarchical clustering starts with n individuals on which p measurements have been made per individual to form an nxp matrix. To agglomerate like individuals, some measures of similarity or resemblance must be computed between individuals. A number of methods are available for computing similarity matrices between individuals, including: Euclidian distance, sum of absolute difference, maximum difference, Mahalanobis distance, correlation coefficient, sine coefficient, and cosine coefficient (Romesburg, 1984). Most similarity measures are sensitive to the units of measurement of the variables. To overcome this problem, variables usually are standardized by dividing by the range or the standard deviation. Seber (1984) points out that standardizing variables creates the problem of increasing within-cluster variance and decreasing between-cluster variance, making clusters less distinct. Also, by standardizing data using the variance, the significance of variables with small variances is increased. This may be a desired feature if high variability is primarily due to data uncertainty.

Another problem encountered with multivariate data is that variables are often correlated. Therefore, some of the information found in one variable also is contained in some of the other p-1 variables. This could lead to unreliable estimates of similarity measures by some methods. The Mahalanobis distance (Δ), one of the methods used, overcomes problems associated with correlated variables and standardization (Seber, 1984). It is calculated as

$$\Delta(x_{ik}, x_{jk}) = \left((x_{ik} - x_{jk})^T S^{-1}(x_{ik} - x_{jk})\right)^{\frac{1}{2}} \tag{126a}$$

where

$$S = \sum_i (x_{ik} - \overline{x_k})(x_{ik} - \overline{x_k})^T / n-1 \tag{126b}$$

in which S^{-1} is the inverse of the covariance matrix (S), x_{ik} and x_{jk} are the kth observations on the ith and jth individuals, respectively, and $\overline{x}_k$ is the mean of the kth variable. The Mahalanobis distance is invariant to a linear transformation of the form

$$y_i = Ax_i + b \tag{127}$$

providing matrix A is nonsingular. Standardizing data by its mean and variance or scaling with the range are examples of such transformations.

7.1.2.2 Agglomerative Methods. Agglomerative methods begin with an nxn matrix of similarities and n groups with one individual per group. It begins by fusing the two nearest individuals into one cluster, leaving $n-2$ clusters with one individual each. The two most similar individuals of the $n-1$ remaining clusters are joined, and the procedure is repeated n times to give one cluster of n individuals. A number of methods have been proposed for defining the similarities of the most recent cluster to those already present; those most widely used are: single linkage (or nearest neighbor), complete linkage (or maximum distance), median distance, incremental sums of square (or Ward's method), and group average. Seber (1984) discusses the merits and demerits of each method.

7.1.3 Principal Component Analysis

Whenever multivariate data are collected on a group of individuals, the variables are often correlated. When this occurs, some of the information contained in one variable also is contained in some of the other $p-1$ variables. Principal component analysis transforms these variables into p uncorrelated variables called principal components. The principal components are a linear combination of the original variables such that (Haan, 1977)

$$Z = X A \tag{128}$$

where X is an nxp matrix of n observations on p variables, Z is an nxp matrix of uncorrelated scores, and A is a pxp transformation matrix comprised of p eigenvectors or principal component vectors of length p. Each eigenvector, a_i, corresponds to an eigenvalue (λ_i) such that

$$(S\ \lambda_i\ I)a_i = 0 \tag{129}$$

where S is the covariance matrix and I is the identity matrix. For a nontrivial solution to equation 129, we must have

$$|S - \lambda_i I| = 0 \tag{130}$$

For the special case of a 2x2 matrix, equation 130 becomes

$$(S_{11}-\lambda_1)(S_{22}-\lambda_2) - S_{21}S_{12} = 0 \tag{131}$$

Equation 131 is a quadratic and has two solutions. For symmetric matrices such as the covariance matrix, real $\lambda_i S$ are guaranteed (Davis, 1985). Having solved for the λ_i, the a_i are determined by solving equation 129.

Given that p variates are correlated, it may be desirable to explain the variance of X with q less than p orthogonal components. Therefore, Z is constructed so that z_i explains the maximum variance left unexplained by the first i-1 components. Hence, in the solution of equation 130, λ_1 is the largest characteristic root, λ_2 the next, and so on. It is also possible that pq-transformed variables may not contribute to the variance, i.e., having λ_i ($i > q$) approximately zero. By definition,

$$Var(z_i) = \lambda_i \tag{132}$$

Hence, given that the first principal component is the largest root, it explains most of the variance, followed by the second, etc. Another useful property is that the sum of λ_i is equal to the total variance of the variables (V), i.e.,

$$D_\lambda = trace(S) = V \tag{133}$$

where

$$D_\lambda = \sum_{i=1}^{p} \lambda_i \tag{134}$$

The fraction of the total variance (f_i) explained by the ith principal component is

$$f_i = \lambda_i / V \tag{135}$$

7.1.4 Analytic Method

Data on the 34 soil series (table 39) used in this study were obtained from county soil survey reports. The variables used were: number of soil horizons, pH, bulk density, water-holding capacity, permeability, depth to water table, organic matter content, slope, and hydrologic group. All data used were quantitative. Qualitative data, such as soil textural class, were excluded; however, texture is reflected in quantitative variables such as water-holding capacity and permeability. For pH, bulk density, and water-holding capacity, the weighted average of the horizon values was used, with the weight corresponding to the horizon thickness. The minimum value of the horizon values was used as the series value for permeability. The value of the surface horizon organic matter content was used. Soil hydrologic classes, usually represented by alphabetic characters, were replaced by numbers, with a = 1, b = 2, etc.

IMSL (1987) subroutines for cluster and principal component analysis were employed for the analyses. They are:

- CORVC - calculates variance-covariance matrix on data
- MVIND - performs a Chi-square test for significant correlation on the covariance matrix
- PRINC - performs principal component analysis on the data
- CDIST - computes a matrix of similarity between the rows or columns of a matrix for a specified similarity measure
- CLINK - performs a hierarchical clustering of the individuals using the similarity matrix produced by CDIST (the user specifies the clustering method to be used)

7.1.5 Results

Each variable was standardized by its mean and standard deviation during the analysis, and the covariance matrix was determined (table 37). The Chi-square test was used to determine whether there were significant correlations among the variables. A Chi-square score of 64.9 with 36 degrees of freedom was obtained with a P-value of 0.002, indicating significant correlations among the variables.

Table 38 summarizes the cluster analysis methods that were used for the soils data. There are no statistical methods available for comparing the results of different cluster analysis methods (Davis, 1986). Typically, the method that gives the highest cophenetic correlation is selected, as this indicates less distortion in data in constructing the dendrogram. In this analysis, the groups produced by the combination of absolute cosine and Ward's methods were selected (table 37). Even though these methods gave an inferior cophenetic correlation compared to the other methods, they gave better-sized groups. Other methods produced many single-membered groups, and few groups with many members.

Table 40 summarizes the land units (soil groups) and their properties. Values for saturated hydraulic conductivity and water-retention parameters (θ_s, θ_r, α, n) for each class were obtained from Carsel and Parrish (1988), who tabulated statistics of hydraulic properties for the 12 USDA textual classes. Bulk density values were estimated assuming a particle density of 2.65 g/cm^3. All other properties were obtained from soil survey reports. Weighted averages over reported ranges were taken where appropriate. Land units that did not have a water table within 150 cm were treated as semi-infinite; otherwise, the depth to water table was specified.

7.2 Agricultural Production and Water Quality

Long-term nitrogen loads to groundwater and surface waters from agricultural practices in the Northern Neck under current management conditions are investigated in this section. For each land unit, simulations were performed for two-year rotations of maize, wheat, soybeans, and fallow for two tillage systems: (1) conventional tillage for all crops, and (2) minimum till for maize and soybeans, and conventional till for wheat. All simulations were run for 26 years (13 rotations) for each land unit. Crop cultural and fertilizer practices simulated are similar to those in tables 29 and 30. Fertilizer application rates of 150 kg N ha^{-1} per crop were used for both maize and wheat. For maize, 100% of the N was applied at planting; for wheat, 20% of the N was applied at planting, and the remaining 80% was applied on Julian day 100 of the following year.

The long-term productivity and nitrogen leaching for individual land units are evaluated in this section. Also, the behavior of the regional watershed as a whole is investigated in terms of groundwater and surface water quality.

7.2.1 Mean Crop Yields and Nitrogen Uptake

Average maize yields ranged from 5,016 to 6,000 kg ha^{-1} (table 41). Mean maize yields were similar for all land units—around 5500-6000 kg ha^{-1}, except for units 4 and 9, which yielded around 5000 kg ha^{-1}. Differences in yields between tillage practices appear physically insignificant. Average N uptake (table 41) followed a similar pattern to grain yield, with land units 4 and 9 set apart with lower N uptake.

The average wheat yield for the land units ranged from approximately 3,013 to 3,740 kg^{-1} ha^{-1} (table 41). Not unlike maize, land units 4 and 9 stood apart with lower yields. In all cases, wheat was grown under conventional tillage; therefore, there was little variation between yields under the different management systems. Wheat N uptake (table 41) followed the same pattern as yields.

Incidentally, though the crop responses to land units 4 and 9 are similar, they are different in their modeled properties. Land unit 4 is clay loam to sandy loam soil, which has a shallow rooting zone due to a water table at 30 cm (table 39); land unit 9 is modeled as a deep, excessively drained sandy soil, so it retains moisture poorly.

7.2.2 Soil Water and Nitrogen Dynamics

Total water use, drainage, runoff, denitrification, mineralization, and N loads were determined for the land units and tillage systems simulated (Appendix C, tables 1-10). Averages of each variable over the simulation period are discussed here. Means and coefficients of variation (CVs) of the variables are given in tables 42 and 43.

7.2.2.1 Mean Land Unit Responses of Hydrologic Variables Over Time. Predicted runoff was sensitive to the hydrologic properties of the land units (table 42). Average runoff ranged from 10 mm $rotation^{-1}$ for soil unit 9 under minimum till to 363 mm $rotation^{-1}$ for soil unit 4 under conventional till. Land unit 4, with a shallow water table and poor hydrologic characteristics, predictably had the highest runoff. Units with an inherently high runoff potential (2, 3, 4, 5, 7) had the highest runoff, and vice versa. Runoff was highly variable over time, as reflected by the high CVs, ranging from 19 to 66%. Runoff was consistently higher under management system 1 (conventional till) than under management system 2 (minimum till). Runoff for management system 2 had a higher CV for all land units.

Average water use ranged from 838 to 1,113 mm rotation^{-1} (table 41). Water use was predictably highest for land units with the highest crop yields (1, 2, 5, 6, 10). Land units 4 and 9 had the lowest water use and, correspondingly, the lowest yield. Soil unit 9 is a deep, excessively drained soil, and soil unit 4 has a rooting restriction due to a shallow water table. Of the variables investigated, crop water use showed the least variation over time, with CVs ranging from 3 to 8%. In general, differences in predicted water use between the tillage management systems were insignificant.

Differences in average drainage varied widely for land units, ranging from 661 to 1,240 mm rotation^{-1} (table 42). Land unit 9, with low crop yields and excessively drained moisture status, had the highest drainage; drainage was not as high with unit 4 because of high runoff. Land units 1, 2, and 5, with high available moisture retention, high crop water uptake, and high runoff, showed low drainage losses. Drainage from all land units was higher for minimum till than for conventional till. This is due largely to reduced runoff under minimum-till conditions. CVs for drainage ranged from 15 to 24%. Like runoff, the least variability in drainage was found in those land units with the highest drainage.

7.2.2.2 Nitrogen Dynamics and the Land Units. Average N mineralization rates ranged from 57 to 214 kg ha^{-1} rotation^{-1} (table 43). In general, the land units with the least drainage (1, 2, 5)—the highest moisture retention—had the highest mineralization rates. Even though unit 4 may have had the highest mineralization rate per unit of soil volume due to its high water content, the presence of a shallow water table severely reduced the soil volume over which total mineralization is integrated. Land unit 9, with its excessively drained condition, had the lowest N mineralization rate. Coefficients of variation for mineralization ranged from 10 to 50%, with the highest CVs belonging to land units with the lowest mineralization rates. Differences in mineralization rates between management systems were small—no pattern was discernible.

Average denitrification rates ranged from 11 to 89 kg ha^{-1} rotation^{-1}. Like mineralization, the land units with the lowest drainage (1, 2, 5) had the highest denitrification. CVs ranged from 11 to 27%, with the higher CVs for land units with the lowest denitrification rates. Differences between tillage systems appear insignificant.

Average N flux ranged from 66 to 131 kg ha^{-1} rotation^{-1} (table 43). Land unit 4 had the highest N flux due to high drainage, low crop N uptake, a short residence time, and reasonably high mineralization rates. Land unit 9 had the highest drainage flux and second lowest N uptake, but had the lowest N flux to groundwater. As a result of the poor soil moisture status, the contribution of mineralization to the inorganic N pool of unit 9 was small. The CVs of N flux ranged from 11 to 41%. The highest CV was observed for land unit 1, which also had the second highest mean N flux. Differences in N flux due tillage practices are small. Figure 45 shows the leaching percentage for each land unit, defined as the ratio of mean N flux to fertilizer application rate multiplied by 100. Leaching percentages for the land units ranged from 22 to 43%, for a mean of 33%.

7.2.3 Long-Term Effects of Cropping Systems on Water Quality

Drainage, runoff, and N loads from the preceding analysis were used to estimate long-term temporally and areally averaged groundwater N concentrations in the Northern Neck, and average flux concentrations entering the Chesapeake Bay. Time-averaged fluxes from each land unit were used. Averaging over the entire areal domain was performed considering the areas associated with various land units. The mean concentration of N in drainage water from land unit i ($\bar{C}_{di}$) is estimated as

$$\overline{C_{di}} = \frac{\overline{N_i}}{\overline{V_i}} \tag{136}$$

where $\bar{N}_i$ is the time-averaged N mass per rotation leached from land unit i (kg), and $\bar{V}_i$ is the time-averaged water drainage volume per rotation from land unit i (m^3). Note that 10 is the number of cultivated land units.

Time-averaged drainage volumes from land units in the study area are computed as

$$\overline{V_i} = \left(f_1\, \overline{v_{1i}} + f_2\, \overline{v_{2i}}\right) A_1 \tag{137}$$

where $\bar{v}_{1i}$ and $\bar{v}_{2i}$ are the time-averaged drainage fluxes for land unit i (m per rotation) under tillage system 1 or 2, respectively; f_1 and f_2 are the land fractions of tillage systems 1 and 2; and A_i is the total area of land unit i. For each land unit, 20% was estimated to be conventionally tilled, and 80% to be minimum tilled (i.e., $f_1 = 0.2$ and $f_2 = 0.8$), which approximates the current practices in the area.

The time-averaged N mass in leachate per rotation from the land units is computed as

$$\overline{N}_i = \left(f_1\,\overline{n_{1i}} + f_2\,\overline{n_{2i}}\right) A_i \tag{138}$$

where $\bar{n}_{1i}$ and $\bar{n}_{2i}$ are the time-averaged N fluxes for land unit i (kg per m^2 per rotation) under tillage system 1 and 2, respectively, and other variables are as previously defined.

The mean concentration of N in drainage water from the entire cultivated area ($\bar{C}_d$) was estimated as

$$\overline{C}_d = \frac{\sum_{i=1}^{10} \overline{N}_i}{\sum_{i=1}^{10} \overline{V}_i} \tag{139}$$

where 10 is the number of cultivated land units.

Since water drainage also occurs from nonagricultural land, $\bar{C}_d$ will overestimate the regional N concentration in groundwater. Assuming zero N leaching from uncultivated land, which is mostly forested, the long-term average groundwater N concentration ($\bar{C}_g$) from agricultural sources in the study area, after dilution from drainage from uncultivated areas, may be estimated as

$$\overline{C}_g = \frac{\sum_{i=1}^{10} \overline{N}_i}{v_n A_n + \sum_{i=1}^{10} \overline{V}_i} \tag{140}$$

where v_n is the drainage flux (m/rotation) from uncultivated land and A_n is the area of uncultivated land. Annual drainage from uncultivated land was estimated as the mean annual rainfall minus evapotranspiration. Water use from nonagricultural areas was estimated from the relationship of Turc (USDA SCS, 1972), which relates evapotranspiration (E) from a watershed to rainfall and temperature as

$$E = \frac{P}{\left[0.9 + \left(\frac{P}{I_t}\right)^2\right]^{\frac{1}{2}}} \tag{141}$$

where P is the annual precipitation and I_t is an air temperature factor estimated as

$$I_t = 300 + 25\ T + 0.05\ T^3 \tag{142}$$

where T is the mean air temperature (°C), estimated as the average of the long-term minimum and maximum daily temperatures from the weather generator, yielding $T = 14.6°$ C. Table 44 shows the breakdown of estimates of water use and drainage by rotation from the uncropped area.

Water entering the Chesapeake Bay from the Northern Neck watershed comes from direct surface runoff as well as groundwater discharges. The long-term average concentration of water entering the bay, therefore, will be a flux-weighted average of surface water and groundwater. Assuming N contamination occurs primarily from groundwater, the average N concentration ($\overline{C}_s$) of water from the study area that enters the bay from combined groundwater and surface water sources was estimated as

$$\overline{C}_s = \frac{\sum_{i=1}^{10} \overline{N}_i}{v_n A_n + \sum_{i=1}^{10} (\overline{V}_i + \overline{R}_i)} \tag{143}$$

where $\overline{R}_i$ is the time-averaged runoff volume per rotation from land unit i (m^3) computed from the predicted time-averaged runoff per area for each land unit in a manner exactly analogous to equation 137.

Table 45 summarizes the runoff, drainage, N loads, and concentrations from each land unit. Land unit 7 had the highest N drainage concentration due its low drainage and high N flux, and unit 9 the lowest. On average, 5.4 million kg ha^{-1} $year^{-1}$ N (or 29% of mineral N input) is discharged to groundwater. Average drainage concentration from the land units ranged from 5.4 to 21.1 mg l^{-1}, with an area weighted mean of 9.9 mg l^{-1} from 123,000 ha of cultivated land.

Contributions of drainage and runoff from agricultural and nonagricultural land in the study area and the corresponding N concentrations are given in table 46. The results indicate an average concentration of N in groundwater in the entire study area (cultivated and uncultivated land) of 5.1 mg l^{-1}, and an average concentration in all waters entering the bay from the Northern Neck after dilution with runoff of 4.5 mg l^{-1}.

Nitrate-N concentrations were determined on groundwater samples from 204 monitoring wells at Nomini Creek, a subwatershed of the Northern Neck basin (Mostaghimi et al. 1990). Concentrations ranged from 0.02 to 16.9 mg l, with a mean of 5.1 mg l and a CV of 73%. Observed and predicted upper limit and mean are almost identical. It may be assumed the lower measured limit is background level; in this study a zero background level is implied.

7.2.4 Summary of Agricultural Production and Water Quality

Twenty-six-year simulations were performed on the land units to evaluate long-term crop performance, N load to groundwater, and its effect on water quality. Simulations were performed for two management systems: in system 1, all crops were conventionally tilled; system 2 had minimum-tilled maize and soybeans and conventionally tilled wheat. All simulations used the same time series of climatic data.

Mean grain yields over the study area were 5660 and 3442 kg ha^{-1} rotation for maize and wheat, respectively. There was little variability in mean yields between the land units. This is because the same time series of climatic data were used for all land units, and, as established in the sensitivity analysis, crop yield variables are most sensitive to the climatic variables. In addition, the method of obtaining the properties for the land units averages over the properties of soil types, thereby reducing the variability between units. Despite the lack of variability in yield, yields appear significantly lower in land unit 1, which is very shallow, and land unit 9, which is deep but excessively drained.

Mean N uptakes over the land units were 132 and 154 kg ha^{-1} $rotation^{-1}$ for maize and wheat, respectively, and followed a pattern similar to yield.

The hydrologic variable responses were consistent with the modeled properties of the land units and crop performances. Mean crop water use, like yield, was slightly variable; however, drainage and water use were highly variable.

Mineralization and denitrification were correlated because of their dependence on soil moisture availability. Land units with superior moisture retention had the highest mineralization and denitrification rates.

Average N fluxes ranged from 66 to 132 kg ha^{-1} $rotation^{-1}$, with an arithmetic mean of 100 kg ha^{-1} $rotation^{-1}$, or 33% of the total mineral N input. Crop N uptake was not necessarily a good indicator of N leaching potential—land unit 9 had the second lowest N uptake and the lowest N load, due to the paltry contributions of organic N mineralization to the mineral N pool.

Runoff, drainage, and N loads from the cropped areas were used to estimate temporally and areally averaged groundwater N concentrations in the Northern Neck. Estimates of nonagricultural water use were determined from the relationship of Turc (SCS, 1972). On an areally weighted basis, 29% of the mineral N input to the study area is leached. Average concentration of drainage from the study area is estimated at 5.1 mg l^{-1}; after dilution with runoff estimate fell to 4.5 mg l^{-1}. Agreement with measured values within the watershed was excellent.

7.3 Modeling Sewage Sludge Application as a Nitrogen Source

Municipal sewage sludge is the residue from municipal wastewater treatment. The advent of stricter regulations governing the discharge of sewage into surface waters has led to increased interest in land application of sludge as a disposal alternative. The USEPA (1983b) estimates that up to 40% of the sludge produced is applied to cropland. In Virginia, the application of sewage sludge to agricultural soils has increased from less than 200 ha to more than 8,900 ha between 1980 and 1985 (Rappaport et al., 1987). Land application of municipal sludge is economically more attractive, and, if properly managed, can be environmentally safer than other disposal alternatives, such as stream discharge, ocean dumping, landfilling, and incineration (Kelley et al., 1984; Environment Canada, 1984). Annual savings to Virginia municipalities due to land application of sludge is estimated at $12.5 million, with a fertilizer value to farmers of $2.5 million. Land-applied sewage sludge supplies essential nutrients for crop growth (N, P, and micronutrients), and may improve soil physical properties (Kelley et al., 1984; Rappaport et al., 1987).

In addition to supplying the soil with plant nutrients, land application of sewage sludge may affect soil chemical properties. Silviera and Sommers (1977) found soil pH to increase with sludge addition, while others (Epstein et al., 1976) found the opposite effect. Land application of sewage sludge has been observed to increase the cation exchange capacity of some soils (Epstein et al., 1976; Kladivko and Nelson, 1979b).

The USEPA (1983b) reported median organic carbon content for sewage sludge ranging from 27 to 32% of solids. Organic matter is known to improve soil physical properties. Observed changes in soil physical properties due to sludge additions include: decreases in bulk density

(Kladivko and Nelson, 1979b), increases in soil aggregate stability (Kladivko and Nelson, 1979a), increases in soil water-holding capacity (Kladivko and Nelson, 1979a; Gupta et al., 1977), increases in saturated hydraulic conductivity (Gupta et al., 1977), and increases in water infiltration (Kladivko and Nelson, 1979a).

Imprudent land application of sewage sludge can adversely affect the environment in any number of ways. Most of the N in sewage is present either in the organic form or as NH_4^+, while most of the P is present in inorganic forms. Transport of N or P in runoff can pollute surface waters. Kladivko and Nelson (1979a) found increasing in P and NH_4^+ in runoff with increasing sludge application to agricultural soils. Also, continued mineralization of organic matter ultimately produces NO_3^-, which can be leached to groundwater. Sewage is known to contain heavy metals in trace quantities, and continued land application of sludge can result in the buildup of such metals as cadmium (Cd), zinc (Zn), copper (Cu), nickel (Ni), cobalt (Co), manganese (Mn), arsenic (As), and lead (Pb). Accumulation of these elements in plants could be phytotoxic or could cause health problems in animals or humans that consume them (Kelley et al., 1984). The elements Cd, Cu, Mo, Ni, and Zn are classified as potential hazards in the land application of sludge (Council for Agricultural Science and Technology, 1976).

Although the amount of pathogens is reduced in stabilized sewage sludge, the end product is not entirely safe (Merillot, 1986). Most sludge-borne organisms do not survive in the soil for extended periods, as they are subject to desiccation and the germicidal effect of sunlight (Kelley et al., 1984). However, *Salmonella* species, which cause food poisoning, have been known to survive in soils from 5 to 968 days (Jones, 1986). This means *Salmonella* can contaminate vegetables or be transported to groundwater and surface waters. The World Health Organization (1981) considered *Salmonella* and the beef tape worm as the two pathogens posing hazards to humans in the land application of sewage sludge.

Sewage sludge has been known to contain harmful organics. The USEPA (1983b) reported median concentrations of polychlorinated aromatic hydrocarbons (PAHs) of 3.9 ppm in sludge. Wild et al. (1990) observed an increase followed by a steady decrease in the concentration of PAHs in soils subjected to long-term sludge application.

In the land application of sewage sludge, simulation models can be an important management tool in determining appropriate loading rates and timing of applications to optimize fertilizer value and avoid adverse environmental impacts. In the following sections, the results of simulations to investigate the possibility of using sludge as a fertilizer replacement, wholly or partly, are presented. Effects on crop yield and N leaching to groundwater of sewage sludge amounts and timing of applications are investigated.

7.3.1 Sewage Sludge Simulations

Simulations were done on land unit 8 to observe the long-term effects of municipal sewage applications on crop performance and N fluxes to groundwater. Twenty-six-year simulations were performed for conventionally tilled maize-wheat-soybean-fallow in a two-year rotation. All crops were conventionally tilled because of the necessity to incorporate sludge into the soil to reduce ammonia volatilization. Two sets of simulations were performed: the first to evaluate the effects of sludge amount on crop yield and N leaching; the second to investigate the effect of timing of applications.

The chemical composition of municipal sludge is highly variable, and is dependent on characteristics of the source wastewater as well as on the treatment processes to which it was subjected (USEPA, 1983b). In these simulations, median values reported by the USEPA (1983b) were used. Distributions of most hydrogeologic parameters are positively skewed with a zero lower bound. This makes their probability density functions non-normal. Frequently, such parameters are modeled as lognormal density functions. Howe (1990) found for lognormal parameter distributions, median values of parameters gave better predictions of N leaching concentrations than means. Therefore, median values of sludge composition parameters reported by the USEPA (1983b) for 191 sludge samples of various types from 15 states were used in the simulations. The median N content was 3.3%, and all N was assumed to be present in the organic form (the reported median organic N content was greater than 95% of total N). Median C-N ratios of sewage sludge have been reported to range from 9 to 19. A C-N ratio of 12 was used in the simulations.

7.3.1.1 Effects of Sewage Amount on Crop Performance and N Leaching. Three simulations were performed with varying amounts of sludge to evaluate the effects on crop performance and N leaching. The simulations were (1) 7500 kg ha^{-1} $year^{-1}$ sludge, i.e., 250 kg ha^{-1} of organic N (C-N ratio 12); (2) 3750 kg ha^{-1} $year^{-1}$ and 125 kg ha^{-1} $year^{-1}$ fertilizer N; and (3) zero sludge and 250 kg ha^{-1} $year^{-1}$ fertilizer N. Note that, in each simulation, the annual N input (mineral + organic) into the system was the same, at 250 kg ha^{-1}. In all cases, amendments were added to maize and wheat crops: for maize, inorganic N and sludge were applied at planting; for wheat, to reduce N leaching, sludge was applied 170 days after planting, 20% of the fertilizer was applied at planting and the remainder 170 days later.

Crop Water Budget and Yields: Table 47 shows mean annual crop water use, drainage, and runoff for the sewage sludge simulations. Differences between variables for the simulations are small.

Table 48 compares crop yield performances. Mean dry matter production for maize with no organic N was 0.1% more than that with 50% organic N, and 3.5% more than the 100% organic N treatment. Mean dry matter production for wheat supplied with no organic N was 0.2% more than for that supplied with 50% organic N, and 4.9% more than that supplied with 100% organic N. Mean maize grain yield with no organic N was 3% and 10% more than the 50% and 100% organic N treatments, respectively. Mean wheat grain yield for the zero sludge was 2% lower than the 50% organic treatment and 16% higher than the 100% organic N treatment. Total maize N uptake was lower for 100% sewage application by 7% and 14% for 50% and no organic N treatments, respectively. Total wheat N uptake was lower for 100% sewage application by 4% and 8% for 50% and no organic N treatments, respectively. Mean maize grain N content was lower for 100% sewage application by 7% and 12% for 50% and no sludge, respectively. Mean wheat grain N content was also lower for 100% sewage application by 5% and 15% for 50% and no sludge, respectively.

Nitrogen Balance: Table 49 shows means and CVs of annual sources and sinks of inorganic N for the sludge simulations. Note that all the mineral N input into soil systems for the 100% sewage simulation was through the mineralization of organic forms. Consequently, the amount of N supplied by mineralization was over 400% and 150% greater than for zero sludge and 50% sludge applications, respectively. There was 46 and 14 kg-N ha^{-1} $year^{-1}$ less mineral N input in the 100% sludge system than the no sludge and 50% sludge, respectively. On average, 295 kg ha^{-1} of organic N (250 kg ha^{-1} from sludge and 45 kg ha^{-1} from crop residue) is added to the soil system with 100% sludge application per year. On average, only 94% of the added organic N is being mineralized, with the remaining 6% being incorporated in the stable organic fraction. Over the long term, the stable organic N fraction was expected to reach a steady state, at which point N input and output would be equal. The results indicate that this was almost achieved.

Figure 46 plots N mineralization by rotation for the three systems against rainfall. The mineralization rate by rotation was fairly constant, with no apparent dependence on rainfall for sludge simulations.

The mean annual N removal by crop uptake, leaching, and denitrification was higher for fertilizer application than for sewage applications. These variables all exhibited higher variability as the amount of sludge applied increased; the CVs of the variables are shown in table 49. Mean annual N leached for the zero sludge simulation was 25% and 41% greater than the 50% and 100% sludge simulations, respectively. Figures 47a and 47b show N load and denitrification by rotation for the systems modeled. Mineral N applications demonstrated consistently higher removal rates via both mechanisms. Higher variability in leaching and denitrification rates between rotations resulted in a weak relationship with rainfall amounts. As discussed in section 6, drainage would be more closely related to these variables.

Soil N and Leaching Over a Rotation: Figure 48a shows monthly soil mineral N content over a two-year rotation for the simulations. The pattern of soil N was similar for the 50% and 100% sludge applications, but distinctly different for the zero sludge simulation, with a higher residual N content throughout. Soil mineral N rose sharply for months 2, 7, and 13 for the zero sludge, and months 2 and 13 for the others, with the steepest increase in the second month in response to fertilization of maize at planting. In months 7 and 12, 20% and 80% applications, respectively, of N fertilizer were added to wheat for the zero sludge simulation. Note the relative magnitude of these increases. Changes in soil mineral N content as a result of sludge additions were understandably less pronounced, and no sludge was added at wheat planting.

The periods of gradual N content increase due to continued mineralization and low N uptake were more pronounced for the 50% and 100% sludge treatments, which is not surprising since they have more readily mineralizable organic matter. The first period (months 4-7) corresponds to the fallow period between maize and wheat crops. The second period (months 15-21) covers soybean planting to extended fallow. During this period, there is reduced N uptake. Note the increase in the rate of soil N accumulation through mineralization from months 19-21 for the 50% and 100% sludge simulations following the soybean crop.

Figure 48b shows monthly N leaching for the systems modeled. The pattern of N leaching was similar for both 50% and 100% sludge systems, but different for the zero sludge system. Peak N leaching took place during January-April of the second year for all systems. However, this leaching period was more pronounced with nonzero sludge applications. With 100% sludge application, a total of 165 kg-N ha^{-1} was leached over the two years, of which 68% was leached from December to March of the second year; with 50% sludge, 57% of a total of 190 kg ha^{-1}. Over the corresponding period for the zero sludge simulation, 47% of a total of 272 kg-N ha^{-1} was leached.

7.3.1.2 Effects of Timing of Sludge Applications: The effects of early sludge application on crop yield and N leaching were evaluated by applying sludge at planting for wheat instead of 170 days later. Incidentally, this is a convenient, and probably routine, time to apply sludge, rather than later when the crop is established. Due to the volume of sludge that needs to be applied, and the requirement to have it incorporated in the soil to minimize volatilization and to bring it in intimate contact with the soil to facilitate mineralization, it may not be as practical to apply the sludge after the crop is established. The convenience of applying at planting has to be weighed against the potential increased N leaching that may take place from soil N accumulation due to organic N mineralization over this time period. No changes were made in the timing of sludge application to maize; sludge was already applied to maize at planting and, given the climatic conditions of winter, it may be impractical to apply sludge to the land significantly earlier.

Table 50 summarizes the result of a 26-year simulation with early application of sludge; results are compared to the 100% sludge treatment discussed in the previous section. Crop water budget is unaffected by the early application. All crop yield variables decreased—wheat more so than maize. More importantly, however, the amount of N leached increased by 7% with early application. Even though early application may be more convenient, there seem to be economic and environmental benefits from late application.

7.3.2 Summary of Sludge Simulations

Simulations were performed to evaluate the possibility of replacing fertilizer N with municipal sewage sludge. Sludge with a C-N ratio of 12 was applied at rates of 7,500 kg ha^{-1} $crop^{-1}$, and 3750 kg ha^{-1} $crop^{-1}$ plus 125 kg ha^{-1} $crop^{-1}$ fertilizer N, and the results were compared with a simulation using an equivalent amount of mineral fertilizer N (250 kg ha^{-1} $crop^{-1}$).

Mean yields were similar for the 50% sludge and zero sludge simulations, but a 10% and 16% reduction was observed with 100% sludge for maize and wheat, respectively. For comparable total N application rates, 41% and 25% less N was leached with 100% and 50% sludge application, respectively. A trade off thus is obtained between increasing yield and reduced N leaching. Also, higher sludge application rates may mitigate the yield discrepancy, but whether the N losses will increase proportionately was not investigated.

A demerit of 100% sludge application seems to be its inability to supply N demands during peak uptake. A 50% split between organic and inorganic N application appears to alleviate this problem, with the added incentive of a 25% reduction in the N load from the 100% commercial fertilizer simulation. Additional simulations would be useful in determining the optimal ratio of organic to fertilizer N that will give desired results, i.e., maximize yields and minimize N load.

Changes in soil mineral N content for the sludge applications were gradual over a rotation, with input of N coming from mineralization and output coming principally from crop uptake and leaching. For the nonzero fertilizer simulations, large changes in soil mineral N content occurred due to fertilizer applications and crop uptake during rapid uptake periods.

It is of interest to note that the median values of sludge NO_3^- and NH_4^+ concentrations used in this analysis were close to zero. However, it is not unusual to find sludge with mineral N contents upwards of 30% of the total N. If a sludge with a high mineral N content were applied, this would alleviate to some extent the N deficiency around peak crop productivity, resulting in higher crop yields.

Another alternative for increasing soil mineral N content at peak crop uptake periods is to make sludge applications early. Since mineralization is a relatively slow process, this would allow soil N content to build up. This might have practical limitations, however, since fields may be too wet in late winter or early spring to allow the passage of heavy equipment.

Application of high rates of sludge could accentuate pollution problems by building up soil mineral N contents during periods of slow uptake. This pool of N would be available for leaching during the winter months.

Over a typical rotation, 68% of the N leached with 100% sludge treatment and 58% for the 50% sludge treatment took place during January-April of the second year, as opposed to 47% for zero sludge treatment. It is apparent that the use of a cover crop during the extended fallow period is critical in any N leaching management for sludge applications, even more than for mineral N applications, as the principal source of N leached during this period is mineralization and not soil residual N left over from the previous crop. A cover crop during this period would serve to immobilize some of the mineral N made available by the continued high mineralization rate during the period.

A shortcoming of this study is that only the nutritional N value of sludge mineralization was accounted for. Other benefits to soil chemistry (e.g., pH, P, and other nutrient availability) and soil physical quality were not evaluated. Effects on soil physical properties would be difficult to model, as the mechanisms are not fully understood.

8 Epilogue

Concerns about the impact of agriculture on groundwater have fueled the desire to assess the long-term effects of agricultural practices on groundwater quality in Virginia. Given the complexity of agro-ecological systems, simulation models offer the only medium through which these concerns can be addressed in a reasonable period of time. Available N leaching models proved inadequate because they are one-dimensional and, over time, do not continuously simulate cropping systems. As such, research was undertaken to develop a deterministic model (VT-CROPS) to simulate N fate and transport in a soil-plant-atmosphere continuum to investigate long-term N leaching in the Northern Neck region of Virginia.

VT-CROPS simulates the growth of maize, wheat, soybean, and fallow periods in response to climatic stimuli. In the process, the model simulates soil water flow and N transport and the transformations that result. Model development consisted of model conceptualization, code development, model calibration, sensitivity analyses, model validation, and model evaluation. Code development included the translation of the conceptual model, code debugging, and verifying that the conceptual model received appropriate translation. Development proceeded from conceptualization through evaluation, but not in a unidirectional manner. As model inadequacies appeared, adjustments were made to the conceptual model, and the process was repeated. VT-CROPS incorporates or modifies portions from several previously developed models, namely VT-MAIZE, CERES-Wheat, and WGEN. Section 3 contains a detailed description of the modeling approach. Following development, the model was applied to the Northern Neck region to assess the impact of current agricultural practices on groundwater quality, and also to evaluate alternative practices.

This epilogue has two sections. The first focuses on the basic aspects of this research, i.e., summarizing overall model performance, high-lighting model weaknesses, and suggesting improvements. The second section examines the applied side of the research, i.e., comments on the state of water quality in the Northern Neck.

8.1 Model Performance and Research Needs

Available data were used to calibrate and validate the model as two independent exercises. Additionally, simulations were performed on a hypothetical soil type, and model performance was thoroughly investigated over the medium to long term. These exercises allow a summary of the model's performance and research needs.

8.1.1 Model Calibration and Validation

Credibility is probably the most important issue concerning a new model. A model will not gain wide acceptance, irrespective of how mechanistically sound, well-documented, and user-friendly it is, unless its credibility is established. Model credibility requires demonstration through thorough calibration and validation—herein lies the most pointed weakness of VT-CROPS. The unavailability of pertinent data prevented most of the needed work in this area. The following attempts to put this into perspective.

VT-CROPS predicts maize yields fairly accurately, with a tendency to greater error in dry years or on soil types with a low moisture-retention capacity. To improve the model's performance under conditions of moisture stress, N and water stress factors, and N and carbohydrate partitioning require more research. Predictions of yields for wheat were less accurate than for maize, partly due to the incompleteness of the data used in calibration and validation exercises. The use of complete wheat data sets would improve model predictions. The model does not account for crop lodging, which reduced wheat yields and N uptake on wheat data involving fertilizer application. If lodging poses a serious problem in wheat, incorporation of its effect on yield is recommended. Otherwise, wheat data that is free from lodging should be used in future validation exercises.

VT-CROPS predicts soil N content at the end of a crop growing season with good accuracy; however, N distribution with depth was predicted less accurately. The model's disregard for dispersive transport and spatially varying soil properties are probable reasons for this discrepancy. Even if VT-CROPS incorporated dispersive transport, estimation of dispersion coefficients on this scale would be subject to uncertainty. In any event, over the long term, the integral N content is a good indicator of N leaching potential.

Given the continuous time mode in which VT-CROPS simulates crops and fallow periods, residual effects are important. However, in the validation exercises, due to the lack of continuous data, this format was not adhered to; i.e., maize and wheat were validated independently. Future research requires pertinent data to validate the model in a continuous time framework.

The lack of data on N leaching and N transformation prevented these processes from being validated. To improve VT-CROPS' credibility as a nitrogen leaching model, it is important to accomplish this. To facilitate this, experiments in a relatively closed system would have to be conducted, which is often costly. A review of the literature may reveal available and applicable data. In addition to validating certain aspects of the model, these experiments in consort with the model also could contribute to the understanding of these mechanisms and their interactions.

To demonstrate its utility extensively, the model should be validated under a wide range of soil and climatic conditions. It should be borne in mind, however, that satisfying the model's validation weaknesses is an ideal scenario. Though technically feasible, a substantial cost may be involved if all options are to be exhausted, which may limit its economic feasibility.

8.1.2 Modeled System Needs

No model is ever complete—there are always process additions that could extend a model's scope, thereby increasing its utility. In this respect, VT-CROPS is no exception; thus, this section suggests a few salient processes that would result in an improved model.

The problem of lodging has already been discussed; hence, no further mention of it will be made here. If the model is to be used as a research tool that provides extensive evaluation of the land application of sludge, then the inclusion of a NH_3 volatilization routine would be useful. Ammonia volatilization results in significant gaseous N loss when sludge is surface applied. VT-CROPS models the effect of soil moisture on organic matter mineralization as a linear increase from low to high moisture contents; however, in reality, it goes through a maximum. This effect would be worthwhile to incorporate in the model. VT-CROPS simulates the presence of a water table under static conditions; however, it is not uncommon for water tables to fluctuate in a seasonal cyclical manner under field situations. If such water tables are shallow, they may affect crop growth, water movement, and N transport and transformation processes. Therefore, increasing model flexibility to handle fluctuating water tables would be advantageous. Model flexibility also could increase by added capability for handling uneven surfaces (i.e., ridges and furrows) brought about by tillage operations. This would preclude the use of finite difference as a numerical technique, and makes the finite element method particularly attractive.

8.2 Agriculture and Water Quality in Virginia

VT-CROPS was used to evaluate the long-term effects of agricultural practices on groundwater NO_3^--N concentration in the Northern Neck through a series of 26-year simulations. Therefore, a few comments on water quality and agriculture and research needs, as they relate to Virginia, would be germane.

It has been proven that reduced-tillage measures are effective in the reduction of soil erosion; however, their impact on N leaching is not clear. From the simulations conducted, it does not appear that reduced tillage impairs groundwater quality through increased N leaching, even though the drainage of soil water is enhanced. In fact, an interesting finding of this study is that drainage is not necessarily a surrogate measure of N leaching potential. Increased drainage between soil types did not always result in increased N leaching, as there are other mitigating processes, such as denitrification, mineralization, and root proliferation and subsequent N uptake, that are affected by increased water flux through a soil. Also, crop N uptake, for similar reasons, is not necessarily a good indicator of N leaching potential.

The popular use of 150 kg-N ha^{-1} $crop^{-1}$ for maize and wheat around the state was vindicated by simulations for a hypothetical soil type. In these simulations, maximum crop N-use efficiencies were obtained when 150-200 kg-N ha^{-1} $crop^{-1}$ was applied.

However, the practice of having a two-year crop rotation with an extensive fallow period at the end seems undesirable, since, over a typical rotation, more than 50% of N is lost during this period. Consequently, the elimination of the extended fallow period appears critical in any alternative N-leaching management scenario. A cover crop in this period would reduce N leaching by immobilizing soil mineral N and increasing water use.

It is estimated that 29% of the N fertilizer applied to the study area is being leached. The estimated impact on groundwater quality in the project area (cultivated and uncultivated areas) is an NO_3^--N concentration due to drainage of 5.1 mg l^{-1}, or a concentration to surface waters after dilution with runoff of 4.5 mg l^{-1}. Predicted mean drainage concentration agreed exactly with the mean observed concentration in the groundwater at Nomini Creek, a subwatershed within the study area. Mean drainage concentration from the cultivated areas is estimated at 9.9 mg l^{-1}, with local means for some land units as high as 21 mg l^{-1}. This indicates that, even with recommended management practices (i.e., no-till, conservative fertilizer amounts, timing of fertilizer application, crop rotation, etc.), maintaining leachate concentration below the drinking water limit may be a difficult proposition. It may be more meaningful to focus on groundwater concentration at distances downstream from cropped areas after mixing has taken place, rather than drainage concentration per se, in which case, higher drainage concentrations could be tolerated. Simulations with a groundwater transport model to optimize the N load that could be tolerated to achieve noncritical groundwater N concentrations at distances downstream would be useful.

It is clear that agricultural practices are affecting groundwater and surface water quality in the Northern Neck, although N concentrations in the Chesapeake Bay are below the permissible drinking water limit of 10 mg l^{-1}. Even though below drinking water standards, elevated N concentrations can upset the ecological balance by contributing to the bay's nutritional enrichment, which may effect algal blooms if phosphorus is a nonlimiting nutrient. Any expansion in agricultural activity using current technologies would further increase such problems. The hazard is not limited to surface water however, as a number of the cultivated units have estimates of N concentration in groundwater that are above the legal limit for drinking water. This poses a problem for rural families that use groundwater for domestic purposes. This hazard is directly related to how close drinking water wells are to these cultivated areas and the depth of the wells. Even though drainage concentration may be high, upstream and sufficiently far downstream of cultivated areas, groundwater concentration may be marginally affected, as downstream concentration will be attenuated due to dispersion and or decay in the groundwater. Also, high concentration is more likely to be a problem in shallow wells than in deeper ones. Therefore, there is a need to investigate management practices and technologies that could reduce the hazard of N contamination in these areas. Performing simulations for crop rotations without a period of extended fallow to evaluate the impact on groundwater quality would be a useful beginning. It also would be useful to simulate fertilizer application according to soil residual N; i.e., fertilize to bring soil N content to some desired level rather than adding a constant amount each time. This would be tantamount to fertilizing according to soil test results. Note that any reduction in the local hazard will effect reductions to the bay also.

Investigations were made as to the viability of using sewage sludge as a replacement for, or in consort with, mineral fertilizer. With sludge application, most of the N load to groundwater came from organic N mineralization during the period of extended fallow, and not from residual N following the soybean crop. Elimination of the period of extended fallow is, therefore, more critical for sewage application than it is for commercial N. For sludge application, approximately 70% of N leached during a typical rotation was lost over this period, as opposed to 47% for commercial N. Spring application of sludge to winter wheat gave superior results, i.e., higher crop yield and lower N load, than fall application. Sewage sludge was predicted to be environmentally safer than commercial fertilizers at comparable N application rates. The slow release of mineral forms makes sewage sludge less susceptible to leaching. However, this slow release is not advantageous during peak crop N uptake periods, and results in lower crop yields. Increased sludge load is not recommended since, with continued mineralization, this would be detrimental during periods of low crop N uptake. However, mixed applications of sewage sludge and commercial N fertilizer seems an attractive alternative, as comparable crop yields were obtained despite lower N loads to groundwater. The commercial N forms can supply the crop needs during critical periods, and sludge can supply N at a steady, low basal level. In this regard, additional simulations would be useful in determining the optimal combination of sludge and commercial N, and the timing of their application to maximize benefits. In addition, simulations on the application of sludge combined with the elimination of the extended fallow period from the cropping system also may prove useful. It should be borne in mind that yield predictions under sludge were, in all likelihood, underestimated, as other beneficial effects of sludge application on the soil, such as improved water and cation holding capacity and reduced bulk density, are not modeled.

References

Addiscott, T.M., and R.J. Wagenet. 1985. Concepts of Solute Leaching in Soils: A Review of Modeling Approaches. J. Soil Sci. 36: 411-424.

Alley, M.M., and P.C. Scharf. 1989. Research Progress Report, July 1, 1988 - June 30, 1989, On Optimizing Nitrogen Fertilization of Winter Wheat (*Triticum Aestivum L.*). Crop and Soil Env. Sci. Dept., VPI & SU, Blacksburg, Va.

Anderson, J.H. 1987. Agriculture and Natural Resources: The Broadening Horizon. In *Rural Groundwater Contamination*, F.M. D'Itri and L.G. Wolfson (eds.). Lewis Pub., Inc.

Bailey, G.W., and R.R. Swank, Jr. 1983. Modeling Agricultural Nonpoint Source Pollution: A Research Perspective. In *Agricultural Management and Water Quality*, F.W. Schallar and G.W. Bailey (eds.). Iowa State Univ. Press.

Baker, D.N., J.R. Lambert, and J.M McKinion. 1983. GOSSYM: A Simulator of Cotton Crop Growth and Yield. South Carolina Ag. Exp. Sta. Tech. Bull. 1089. Clemson Univ.

Barber, S.A. 1984. *Soil Nutrient Bioavailability, A Mechanistic Approach*. Wiley Interscience Pub.

Bear, J. 1972. *Dynamics of Fluids in Porous Media*. Am. Elsevier, N.Y.

Bear, J. 1987. *Modeling Groundwater Flow and Pollution. Theory and Application of Transport in Porous Media*. D. Reidel Pub. Co.

Bear, J., and A. Verruijt. 1987. *Modeling Groundwater Flow and Pollution*. D. Reidel Pub. Co.

Bigger, J.W., and D.R. Nielson. 1976. Spatial Variability of the Leaching Characteristics of a Field Soil. Water Resour. Res. 12:78-94.

Blackmer, A.M. 1984. Losses of Fertilizer N from Soil. In Proc. Iowa 38th Ann. Fert. and Ag. Chem. Dealers Conf. Iowa State Univ. Coop. Ext. Svc., CE-2081.

Bock, B.R., and G.W. Hergert. 1991. Fertilizer Nitrogen Management. In *Managing Nitrogen for Groundwater Quality and Farm Profitability*, R.F. Follett, D.R. Keeney, and R.M. Cruse (eds.). Soil Sci. Soc. Am., Inc., Madison Wisc.

Bowman, R.A., and D.D. Focht. 1974. The Influence of Glucose and Nitrate Concentration upon Denitrification Rates in Sandy Soils. Soil Biol. and Biochem. 6: 297301.

Bresler, E., H. Bielorai, and A. Laufer. 1979. Field Test of Solution Flow Models in a Heterogenous Irrigated Cropped Soil. Water Resour. Res. 15:645-652.

Brooks, R.H., and A.T. Corey. 1966. Properties of Porous Media Affecting Fluid Flow. J. Irr. Dr. Am. Soc. Civ. Eng. 92:61-88.

Brusseau, M.L. 1992. Rate-Limited Transfer and Transport of Organic Solutes in Porous Media That Contain Immobile Immiscible Organic Liquid. Water Resour. Res. 28:33-46.

Canter, L.W., R.C. Knox, and D.M. Fairchild. 1987. *Groundwater Quality Protection*. Lewis Pub., Inc.

Carsel, R.F., and R.S. Parrish. 1988. Developing Joint Probability Distributions of Soil-Water Retention Characteristics. Water Resour. Res. 24(5):755-769.

Carslaw, H.S., and J.C. Jaegar. 1959. *Conduction of Heat in Solids*. Oxford Sci. Pub.

Carson, J.S. 1986. Convincing Users of Model's Validity Is Challenging Aspect of Modeler's Job. Ind. Eng. J., 18:74-85.

Chichester, F.W., and S.J. Smith. 1978. Deposition of N-Labelled Fertilizer Nitrate Applied During Corn Culture in Field Lysimeters. J. Env. Qual. 7:227-233.

Claassen, N., and S.A. Barber. 1976. Simulation Model for Nutrient Uptake from Soil by a Growing Plant Root System. Agron. J. 68:961-966.

Coleman, G., and D.G. DeCoursey. 1976. Sensitivity and Model Variance Analysis Applied to Some Evaporation and Evapotranspiration Models. Water Resour. Res. 12:873879.

Conservation Tillage Information Center (CTIC). 1982-85. National Surveys Conservation Tillage Practices. CTIC, Ft. Wayne, Ind.

Cooke, R.A., and S. Mostaghimi. 1992. VTFIT: A Microcomputer Based Routine for Fitting Probability Distribution Functions to Data. Submitted to App. Eng. in Ag.

Corey, A.T. 1986. *Mechanics of Heterogenous Fluids in Porous Media*. Water Resour. Pub., Fort Collins, Col.

Council for Agricultural Science and Technology (CAST), 1976. Application of Sewage Sludge to Cropland: Appraisal of Potential Hazards of the Heavy Metals to Plants and Animals. EPA Report No. 430/9-76-013. Off. of Water Program Operations, USEPA, Washington, D.C.

Cox, W.J., and G.D. Jolliff. 1986. Growth and Yield of Sunflower and Soybeans Under Soil Water Deficits. Agron. J. 78:226-230.

Davis, J.C. 1986. *Statistics and Data Analysis in Geology*. John Wiley and Sons.

Dawdy, D.R., R.W. Lichty, and J.M. Bergmann. 1972. A Rainfall-Runoff Simulation Model for Estimation of Flood Peaks for Small Drainage Basins. U.S. Geological Survey Prof. Pap. 506-B.

De Smedt, F., and P.J. Wierenga. 1978. Approximate Analytical Solution for Solute Transport During Infiltration and Redistribution. Soil Sci. Soc. Am. J. 42:407-412.

Doorenbos, J., and A.H. Kassam. 1979. Yield Response to Water. FAO Irrig. Drain. Pap. #33.

Environment Canada. 1984. Manual of Land Application of Treated Municipal Wastewater and Sludge. Canadian Env. Protection Svc.

Epstein, E., J.M. Taylor, and R.L. Chaney. 1976. Effects of Sewage Sludge and Sludge Compost Applied to Soil on Some Soil Physical and Chemical Properties. J. Env. Qual. 5:422-26.

Fageria, N.K., V.C. Baligar, and C.A. Jones. 1991. *Growth and Mineral Nutrition of Field Crops*. Marcel Dekker, Inc.

Fletcher, D.A. 1991. A National Perspective. In *Managing Nitrogen for Groundwater Quality and Farm Profitability*, R.F. Follett, D.R. Keeney, and R.M. Cruse (eds.). Soil Sci. Soc. Am., Inc., Madison Wisc.

Focht, D.D., and W. Verstraete. 1977. Biochemical Ecology of Nitrification and Denitrification. Adv. Appl. Microbiol. 19:153-186.

Francis, J.D., B.L. Brown, W.F. Graham, O.W. Larson, III, J.L. McCall, and H.M. Vigorita. 1982. National Statistical Assessment of Rural Water Condition. Off. of Drinking Water, USEPA, Washington, D.C.

Free, G.R. 1970. Minimum Tillage for Corn Production. N.Y. (Cornell) Ag. Exp. Stn. Bull. 1030.

Frissel, M.J., and J.A. van Veen. 1981. Simulation Model for N Immobilization and Mineralization. In *Modeling Wastewater Renovation*, I.K. Iskander (ed.). Wiley Interscience Pub.

Gelhar, L.W., and C. Axness. 1983. Three Dimensional Stochastic Analysis of Macrodispersion in Aquifers. Water Resour. Res. 19:161-180.

Gelhar, L.W., A. Mantoglou, C. Welty, and K.R. Rehfeldt. 1985. A Review of Field Scale Solute Transport Processes in Saturated and Unsaturated Porous Media. EPRI, EA-4190, Res. Proj. 2485-5.

Gerwig, J.R., A.C. Caldwell, and L.L. Goodroad. 1979. Fertilizer Distribution Under Irrigation Between Soil Plant and Aquifer. J. Evi. Qual. 8: 281284.

Gilliam, J.W., and G.D. Hoyt. 1987. Effect of Conservation Tillage on Fate and Transport of Nitrogen. In *Effects of Conservation Tillage on Groundwater Quality*, T.J. Logan, J.M. Davidson, J.C. Baker, and M.R. Overcash (eds). Lewis Pub., Inc.

Glenn, S., and J.S. Angle. 1987. Atrazine and Simazine in Runoff from Conventional and No-till Corn Watersheds. Ag., Ecosys. and Env. 18:273-280.

Green, I.R.A., and D. Stephenson. 1986. Criteria for Comparison of Single Event Models. Hydrol. Sci. J. 31:395-411.

Groffman, P.M. 1985. Nitrification and Denitrification in Conventional and No-tillage Soils. Soil Sci. Soc. Am. J. 49:329-334.

Gupta, S.C., R.H. Dowdy, and W.E. Larson. 1977. Hydraulic and Thermal Properties of Sandy Soil as Influenced by Incorporation of Sewage Sludge. Soil Sci. Soc. Am. J. 41:601-605.

Haan, C.T. 1977. *Statistical Methods in Hydrology*. Iowa State Univ. Press.

Hallberg, G.R. 1987. Nitrates in Iowa Groundwater. In *Rural Groundwater Contamination*, F.M. D'Itri and L.G. Wolfson (eds.). Lewis Pub., Inc.

Hillel, D. 1971. *Soil and Water Physical Principles and Processes*. Academic Press.

Hillel, D. 1980. *Applications of Soil Physics*. Academic Press.

Howe, B. 1990. Stochastic Aspects of Nitrate Leaching from Agricultural Fields. In Model CASE90: Calibration and Reliability in Groundwater Modeling. Int'l Assoc. of Hydrol. Sci., Washington D.C., IAH Pub. #195.

IBSNAT. 1985. Draft Documentation of IBSNAT Crop Model Input and Output Files. Rev. 12/27/85.

IMSL. 1987. Stat/Math/Sfun/Libraries/Fortran Subroutines for Statistical Analysis.

James, L.D., and S.J. Burgess. 1982. Selection, Calibration and Testing of Hydrologic Models. In *Hydrologic Modeling of Small Watersheds*, C.T. Haan, H.P. Johnson, and D.L. Brakensiek (eds). Am. Soc. Ag. Eng., St. Joseph, Mich.

Jones, C.A., and J.R. Kiniry (eds.). 1986. CERES-Maize: A Simulation Model of Maize Growth and Development. Texas A&M Univ. Press, College Station, Tex.

Jones, P.W. 1986. Sewage Sludge as a Vector of Salmonellosis. In *Epidemiological Studies of Risks Associated with the Agricultural Use of Sewage Sludge: Knowledge and Needs*. Elsevier Appl. Sci. Pub., London and N.Y.

Jury, W.A. 1982. Simulation of Solute Transport Using a Transfer Function Model. Water Resour. Res. 18:363-368.

Jury, W.A., and K. Roth. 1990. *Transfer Functions of Solute Transport Through Soils. Theory and Applications*. Berkhauser, Basel.

Jury, W.A., W.R. Gardner, and W.H. Gardner. 1991. *Soil Physics*. John Wiley and Sons, Inc.

Kalurachchi, J.J., and J.C. Parker. 1990. Modeling Multicomponent Organic Chemical Transport in Three-Fluid-Phase Porous Media. J. Contam. Hydrol. 4:349-374.

Kanwar, R.S., J.L. Baker, and J.M. Laflen. 1985. Nitrate Movement Through the Soil Profile in Relation to Tillage System and Fertilization Application Method. Trans. ASAE 28:1802-1807.

Keeney, D.R. 1981. Soil N Chemistry and Biochemistry. In *Modeling Wastewater Renovation*, I.K. Iskander (ed.). Wiley Interscience Pub.

Keeney, D.R. 1983. Transformation and Transport of Nitrogen. In *Agricultural Management and Water Quality*, F.W. Schallar and G.W. Bailey (eds.). Iowa State Univ. Press.

Keeney, D.R., and R.F. Follett. 1991. Managing Nitrogen for Groundwater Quality and Farm Profitability: Overview and Introduction. In *Managing Nitrogen for Groundwater Quality and Farm Profitability*, R.F. Follett, D.R. Keeney, and R.M. Cruse (eds.). Soil Sci. Soc. Am., Inc., Madison, Wisc.

Kelley, W.D., D.C. Martens, R.B. Reneau Jr., and T.W. Simpson. 1984. Agricultural Use of Sewage Sludge: A Literature Review. Va. Water Resour. Res. Ctr, Bull. 143. VPI & SU, Blacksburg, Va.

Kitur, B.K., M.S. Smith, R.L. Blevins, and W.W. Frye. 1984. Fate of N-depleted Ammonium Nitrate Applied to No-Tillage and Conventional Tillage Corn. Agron. J. 76:240-242.

Kladivko, E.J., and D.W. Nelson. 1979a. Surface Runoff from Sludge-Amended Soils. J. Water Poll. Cont. Fed., 51:100-110.

Kladivko, E.J., and D.W. Nelson. 1979b. Changes in Soil Properties from Application of Anaerobic Sludge. J. Water Poll. Cont. Fed., 51:325-32.

Knisel, W.G. (ed). 1980. CREAMS: A Field Scale Model for Chemical Runoff and Erosion from Agricultural Management Systems. Conserv. Res. Rpt #26, U.S. Dept. of Ag., Washington D.C.

Kramer, P.J. 1983. *Water Relations of Plants*. Academic Press.

Law, A.M., and W.D. Kelton. 1991. *Simulation Modeling and Analysis*. McGraw-Hill, Inc.

Leggett, D.C., and I.K. Iskander. 1981. Evaluation of a Nitrification Model. In *Modeling Wastewater Renovation*, I.K. Iskander (ed.). Wiley Interscience Pub.

Lenhard, R.J., T.G. Johnson, and J.C. Parker. 1992. Experimental Observation of Nonaqueous Phase Liquid Subsurface Movement. Submitted to J. Contam. Hydrol.

Loague, K., and R.E. Green. 1991. Statistical and Graphical Methods for Evaluating Solute Transport Models: Overview and Application. J. Contam. Hydrol., 7:51-73.

Madison, R.J., and J.O. Brunett. 1985. Overview of Occurrence of Nitrate in Groundwater of the United States. USGS Water Supply Paper 2275. U.S. Gov. Print. Off., Washington, D.C.

Mannering J.V., D.L. Schertz, and B.A. Julian. 1987. Overview of Conservation Tillage. In *Effects of Conservation Tillage on Groundwater Quality*, T.J. Logan, J.M. Davidson, J.C. Baker, and M.R. Overcash (eds). Lewis Pub., Inc.

Matalas, N.C. 1967. Mathematical Analysis of Synthetic Hydrology. Water Resour. Res. 3(4):937-945.

Mehran, M., and K.K. Tanji. 1974. Computer Modeling of N Transformation in Soils. J. Env. Qual. 3:391-396.

Meisinger, J.J., and G.W. Randall. 1991. Estimating Nitrogen Budget for Soil-Crop System. In *Managing Nitrogen for Groundwater Quality and Farm Productivity*, R.F. Follett, D.R. Keeney, and R.M. Cruse (eds.). Soil Sci. Soc. Am., Inc., Madison Wisc.

Menelik, G. 1990. Leaching and Denitrification Losses of Nitrogen from Corn Fields as Influenced by Conventional and No-till Practices in Soils of the Chesapeake Bay Area. Ph.D. Dissertation. Crop and Soil Env. Sci. Dept., VPI & SU, Blacksburg, Va.

Mengel, K., and E.A. Kirby. 1979. *Principles of Plant Nutrition*. Int'l Potash Inst., Breve, Switzerland.

Merillot, M. 1986. Agricultural Use of Sewage: Consequences of Sanitary Hazards. In *Epidemiological Studies of Risks Associated with the Agricultural Use of Sewage Sludge: Knowledge and Needs*. Elsevier Appl. Sci. Pub., London and N.Y.

Mitchell, R.L., and W.J. Russell. 1971. Root Development and Rooting Patterns of Soybean Evaluated Under Field Conditions. Agron. J. 63:313-316.

Moltz, F.J. 1981. Simulation of Plant Water Uptake. In *Modeling Wastewater Renovation*, I.K. Iskander (ed.). Wiley Interscience Pub.

Moltz, F.J., and I. Remson. 1970. Extraction Term Models of Soil Moisture Use by Transpiring Plants. Water Resour. Res. 6:1346-1356.

Moschler, W.W., G.W. Shear, D.C. Martens, G.D. Jones, and R.R. Wilmouth. 1972. Comparative Yield and Fertilizer Efficiency of No-tillage and Conventionally Tilled Corn. Agron. J. 64:229-231.

Mostaghimi, S., U. Tim, P. McMillon, and K. Kives. 1990. Watershed/Water Quality Monitoring for BMP Effectiveness, Nomini Creek Watershed. Report n-51-9007, Ag. Eng. Dept., VPI & SU, Blacksburg, Va.

Mualem, Y. 1976. A New Model for Predicting the Hydraulic Conductivity of Unsaturated Porous Media. Water Resour. Res. 12:513-522.

National Research Council. 1989. *Alternate Agriculture*. Nat'l Academy Press, Washington, D.C.

Newkirk, K.W., J.C. Parker, T.B. Brumback, E.W. Carson, J.C. Baker, and, O. Balci. 1987a. User's Guide to VT-Maize, Version (1.0). Va. Water Resour. Res. Ctr, VPI & SU, Blacksburg, Va.

Newkirk, K.W., J.C. Parker, T.B. Brumback, E.W. Carson, J.C. Baker, and O. Balci. 1987b. Programmer's Guide to VT-Maize, Version (1.0). Va. Water Resour. Res. Ctr, VPI & SU, Blacksburg, Va.

Nimah, M.N., and R.J. Hanks. 1973. Model for Estimating Soil Water, Plant and Atmospheric Interrelations. 1. Description and Sensitivity. Soil Sci. Soc. Am. Proc. 37:522-527.

Novotony, V., and G. Chester. 1981. *Handbook of Nonpoint Pollution, Sources and Management*. van Nostrand Reinhold Co.

Nye, P.H., and F.H.C. Marriot. 1969. A Theoretical Study of the Distribution of Substances Around Roots Resulting from Simultaneous Diffusion and Mass Flow. Plant Soil 30:451-472.

Nye, P.H., and P.B. Tinker. 1977. *Solute Movement in the Soil-Root System*. Blackwell Sci. Pub., Oxford, England.

Rappaport, B.D., J.D. Scott, D.C. Martens, R.B. Reneau Jr, and T.W. Simpson. 1987. Availability and Distribution of Heavy Metals, Nitrogen, and Phosphorus from Sewage Sludge in the Plant-Soil-Water Continuum. Va. Water Resour. Res. Ctr, Bull. 154, VPI & SU, Blacksburg, Va.

Richardson, C.W. 1982. A Comparison of Three Distributions for the Generation of Daily Rainfall Amounts. In Statistical Analysis of Rainfall and Runoff. Proc. Int'l Symposium on Rainfall-Runoff Modeling, V.P. Singh (ed). Water Resour. Pub.

Richardson, C.W., and D.A. Wright. 1984. WGEN: A Model for Generating Daily Weather Variables. U.S. Dept. of Ag., Ag. Res. Svc., ARS-8.

Ritchie, J.T. 1972. Model for Predicting Evaporation from a Row Crop with Incomplete Cover. Water Resour. Res. 8:1204-1213.

Ritchie, J.T., and S. Otter. 1984. CERES-Wheat: A User-Oriented Wheat Yield Model. Preliminary documentation, AGRISTARS Pub. No. ym-u3-04442-jsc-18892.

Rolston, D.E., D.L. Hoffman, and D.W. Toy. 1978. Field Measurement of Denitrification: Flux of N_2 and N_2O. Soil Sci. Soc. Am. J. 42:813-819.

Romesburg, H.C. 1984. *Cluster Analysis for Researchers*. Lifetime Learning Pub.

Russo, D.W., A. Jury, and G.L. Butters. 1989. Numerical Analysis of Solute Transport During Transient Irrigation. 1. Effect of Hysteresis and Profile Heterogeneity. Water Resour. Res. 23:1257-1268.

Ryden, J.C. 1981. Gaseous N Losses. In *Modeling Wastewater Renovation*, I.K. Iskander (ed.). Wiley Interscience Pub.

Ryden, J.C., and L.J. Lund. 1980. Nature and Extent of Directly Measured Denitrification Loss from Some Vegetable Production Units. Soil Sci. Soc. Am. J. 44:505-511.

Ryden, J.C., J.K. Syers, and I.K. Iskander. 1981. Evaluation of a Simple Model for Predicting Phosphorus Removal by Soil During Land Treatment of Wastewater. In *Modeling Wastewater Renovation*, I.K. Iskander (ed.). Wiley Interscience Pub.

Schepers J.S., and A.R. Mosier. 1991. Accounting of N in Nonequilibrum Soil-Crop Systems. In *Managing Nitrogen for Groundwater Quality and Farm Productivity*, R.F. Follett, D.R. Keeney, and R.M. Cruse (eds.). Soil Sci. Soc. Am., Inc., Madison Wisc..

Seber, G.A.F. 1984. *Multivariate Observations*. John Wiley and Sons.

Seligman, N.G., and H. van Keulen. 1981. PAPRAN: A Simulation Model of Annual Pasture Production Limited by Rainfall and Nitrogen. In *Simulation of Nitrogen Behavior in Soil-Plant Systems*. M.J. Fissel and J.A. van Veen (eds.). Puedo, Wageningen, Netherlands.

Selim, H.M., and I.K. Iskander. 1981. A Model for Predicting N Behavior in Slow Infiltration Systems. In *Modeling Wastewater Renovation*, I.K. Iskander (ed.). Wiley Interscience Pub.

Shaffer, M.J. 1985. Simulation Model for Soil Erosion-Productivity Relationship. J. Env. Qual. 14:144-150.

Shaffer, M.J., A.D. Halvorson, and F.J. Pierce. 1991. Nitrate Leaching and Economic Analysis Package (NLEAP): Model Description and Application. In *Managing Nitrogen for Groundwater Quality and Farm Productivity*, R.F. Follett, D.R. Keeney, and R.M. Cruse (eds.). Soil Sci. Soc. Am., Inc., Madison, Wisc.

Shibles, R.M., I.C. Anderson, and A.H Gibson. 1975. Soybean. In *Crop Physiology, Some Case Histories*, L.T. Evans (ed). Cambridge Univ. Press.

Silviera, D.J., and L.E. Sommers. 1977. Extractability of Copper, Zinc, Cadmium and Lead in Soils Incubated with Sewage Sludge. J. Env. Qual. 9:47-52.

South Dakota Department of Water and National Resources. 1984. The Big Sioux Aquifer Water Quality Study. Pierre, S.D.

Stanford, G., O.L. Bennett, and J.F. Power. 1973. Conservation Tillage Practices and Nutrient Availability. In *Conservation Tillage*. Proc. Nat. Conserv. Tillage Conf. (28-30 March 1973, Des Moines, Iowa) Soil Cons. Soc. Am.

Tanji K.K., and S.K. Gupta. 1978. Computer Simulation for N in Irrigated Cropland. In *Nitrogen in the Environment, Volume 1*, D.R. Nielson and J.G. Mcdonald (eds). Academic Press.

The World Health Organization. 1981. *The Risk to Health of Microbes in Sewage Sludge Applied to Land.*

Thomann, R.V. 1982. Verification of Water Quality Models. J. Env. Eng. Div., ASCE., 108:923-941.

Thomas, G.W., R.L. Blevins, R.E. Phillips, and M.A. McMahan. 1973. Effect of a Killed Sod Mulch on Nitrate Movement and Corn Yield. Agron. J. 63:736-739.

Throckmorton, R.I. 1986. Tillage and Planting Equipment for Reduced Tillage. In *No-Tillage and Surface-Tillage Agriculture*. John Wiley and Sons.

Triplett, G.B., Jr., and J.V. Mannering. 1978. Crop Residue Management in Crop Rotation and Multiple Cropping System. In *Crop Residue Management System*, W.R. Oschwald (ed.). ASA Spec. Pub. No. 31, Madison, Wisc., 53711.

Tyler, D.D., and G.W. Thomas. 1979. Lysimeter Measurement of Nitrate and Chloride Losses from Conventional and No-tillage Corn. J. Env. Qual. 6:63-66.

USDA Office of Planning and Evaluation. 1975. Minimum Tillage: A preliminary Technology Assessment.

USDA Soil Conservation Service (SCS). 1972. National Engineering Handbook, Hydrology Sec. 4, Ch. 4-10.

USEPA. 1983a. Chesapeake Bay: A Framework for Action. EPA Region III Report.

USEPA. 1983b. Process Design Manual. Land Application of Municipal Sewage. Municipal Env. Res. Lab., Cincinnati Ohio.

USEPA. 1985. Nitrate/Nitrite Health Advisory (draft). Off. of Drinking Water, Washington, D.C.

Vachaud, G., M. Vauclin, and T.M. Addiscott. 1990. Solute Transport in the Unsaturated Zone. In Proc. Int'l Symposium on Water Quality Modeling of Agricultural Nonpoint Sources, Part 1. Ag. Res. Svc. ARS-81.

van Doren, Jr., D.M., and R.R. Allamoras. 1978. Effect of Residue Management Practices on the Soil Physical Environment, Microclimate and Plant Growth. In *Crop Residue Management System*, W.R. Oschwald (ed.). ASA Spec. Pub. No. 31, Madison, Wisc.

van Genuchten, M.T., J.M. Davidson, and P.J. Wierenga. 1974. An Evaluation of Kinetic and Equilibrium Equations for the Prediction of Pesticide Movement in Porous Media. Soil Sci. Soc. Am. J. 38:29-35.

van Genuchten, M.T. 1980. A Closed Form Equation for Predicting the Hydraulic Conductivity of Unsaturated Soils. Soil Sci. Soc. Am. J., 44:892-898.

Wagenet, R.J., and B.K. Rao. 1983. Description of N Movement in the Presence of Spatially Variable Soil Hydraulic Properties. Ag. Water Manag. 6:227-242.

Wagenet, R.J., and J.L. Hutson. 1987. LEAHM: Leaching Estimation and Chemistry Model. A Process Based Model of Water and Solute Movement, Transformation, Plant Uptake and Chemical Reactions in the Unsaturated Zone. Continuum Vol 2. Water Resour. Inst., Cornell Univ., Ithaca, N.Y.

Wagenet, R.J., M.J. Shaffer, and R.E. Green. 1990. Predictive Approaches for Leaching in the Unsaturated Zone. In Proc. International Symposium on Water Quality Modeling of Agricultural Non-Point Sources, Part 1. USDA Ag. Res. Svc., ARS-81.

Walpole, R.E., and R.H. Myers. 1989. *Probability and Statistics for Engineers and Scientists*. McMillan Pub. Co.

Wild, S.R., K.S. Waterhouse, S.P. McGrath, and K.C. Jones. 1990. Organic Contaminants in Agricultural Soils with Known History of Sewage Amendments: Polychlorinated Aromatic Hydrocarbons. Env. Sci. Tech. 24:1706-1709.

Williams, J.R., and K.G. Renard. 1985. Assessment of Soil Erosion and Crop Productivity with Process Model (EPIC). In *Soil Erosion and Crop Productivity*, R.F. Follett and B.A. Stewart (eds.). A.S.A. Pub.

Woolhiser, D.A., and D.L. Brakenside. 1982. Hydrologic Modeling of Small Watersheds. In *Hydrologic Modeling of Small Watersheds*, C.T. Haan, H.P. Johnson, and D.L. Brakensiek (eds). Am. Soc. Ag. Eng., St. Joseph, Mich.

Young, G.D., M.T. Tseng, and R.S. Taylor. 1971. Estuary Ware Temperature Sensitivity to Meteorological Conditions. Water Resour. Res. 7:11731181.

Tables

Table 1.
Crop and soil management practices used during calibration exercise.

Management Practice	Blacksburg	Nomini Creek	Brandon
Planting date (*Julian*)	114	115	301
Planting density (*plants* ha^{-1})	61,700	61,700	2.95×10^6
Sowing Depth (*cm*)	10.0	1.0	6.0
Amount of Straw (*kg* ha^{-1})	2,000	2,000	6,200
Depth of Straw	20	5	20
C – N Ratio of Straw	50	50	50
Tillage Management	Conventional	Minimum	Conventional
Variety	Delkel BXL71	Delkel BXL71	Coker 6815

Table 2.
Soil properties modeled at Blacksburg.

Depth of Layer (cm)	K_s $cm\ hr^{-1}$	α cm^{-1}	n –	ϕ –	OC $content$ %
25	250	0.02	1.098	0.50	3.35
40	300	0.008	1.098	0.56	0.89
55	207	0.008	1.098	0.60	0.39
70	1770	0.008	1.098	0.62	0.27
85	1000	0.008	1.098	0.61	0.27
100	1000	0.008	1.098	0.62	0.23
130	1000	0.019	1.32	0.60	0.23
160	1000	0.008	1.098	0.60	0.23
200	1000	0.019	1.32	0.61	0.23

Table 3.
Soil properties modeled at Nomini Creek.

Depth of Layer (cm)	K_s $cm\ hr^{-1}$	α cm^{-1}	n –	ϕ –	OC content %
25	716	0.075	1.158	0.48	3.35
40	396	0.075	1.158	0.45	0.89
55	588	0.059	1.158	0.44	0.39
70	814	0.059	1.158	0.46	0.27
85	518	0.075	1.158	0.49	0.27
100	951	0.124	1.158	0.51	0.23
130	1294	0.124	1.158	0.47	0.23
160	1300	0.145	1.158	0.50	0.23
200	1300	0.124	1.158	0.491	0.23

Table 4.
Soil properties modeled at Brandon Plantation.

Depth of Layer (cm)	K_s $cm\ hr^{-1}$	α cm^{-1}	n –	ϕ –	OC $content$ %
15	58	0.007	1.21	0.41	1.40
30	56	0.008	1.20	0.41	1.10
60	400	0.005	1.19	0.38	0.40
90	13	0.006	1.15	0.38	0.30
120	32	0.010	1.16	0.38	0.20

Table 5.
Model parameters fixed during calibration exercise.

Equation #	Parameter	Value	Comments
3.44	F_f	0.06	*Modifies fresh organic matter oxiidation rate in mineralization method-II.*
3.52a	Ω_n	0.03	*Threshold mineral N cell content ($mg.cm^{-3}$) for modifying fresh organic matter oxidation rate in method-II.*
–	MIN_{max}	0.05	*Maximum fraction of fresh organic matter that can be mineralized in a day with mineralization method-II*
3.55	k, n, KN	6.4,1.0, .65 5.0, .6, .85	*Constants for determining potential daily CHO production for maize and wheat respectively.*
3.61b	k_n	1.35	*Proportionality factor between N^1_{def} and N^2_{def}.*
3.62	k_θ	0.67	*Proportionality factor between θ^1_{def} and θ^2_{def}.*
3.63	f^A_m	0.25, 0.55	*Minimum fraction of CHO partitioned to the roots and stem in stage-I for maize and wheat, respectively.*
3.64	f^A_r	1.0, 0.6	*Minimum fraction of excess CHO after partition to the leaves, that goes to the roots for maize and wheat in stage-I.*

Table 5. (continued)

Equation #	Parameter	Value	Comments
3.63	f_m^2	0.25	*Minimum fraction of CHO partitioned to the roots and stem in stage-II for maize.*
3.64	f_r^2	1.0	*Minimum fraction of excess CHO after partition to the leaves, that goes to the roots for maize in stage-II.*
3.65a	k_l, k_3	0.15, 0.12	*Constant used in calculating CHO partitioned to wheat stem, in stage-II.*
3.66	k_1, k_2	0.70, 0.15	*Constant used in calculating fraction of CHO not partitioned to wheat roots in stage-II.*
3.65a	k_l, k_3	1.0, 0.0	*Constant used in calculating CHO partitioned to wheat stem in stage-III.*
3.66	k_1, k_2	0.75, 0.10	*Constant used in calculating fraction of CHO not partitioned to wheat roots in stage-III.*
3.68	k_4, k_5	0.14, 0.4	*Constant used in calculating CHO partitioned to ear and stem in maize stage-IV.*
–	f_{low}	0.06	*Minimum fraction of CHO that goes to the roots in maize for stage-IV.*

Table 5. (continued)

Equation #	Parameter	Value	Comments
3.65a	k_l, k_3	1.0, 0.0	*Constant used in calculating CHO partitioned to wheat stem in stage-IV.*
3.66	k_1, k_2	0.75, 0.10	*Constant used in calculating fraction of CHO not partitioned to wheat roots in stage-IV.*
3.69	f_r^5	0.1, 0.6	*Fraction of excess CHO that goes to root in maize and wheat after grain fill in stage-V.*
3.87	f_{up}		*Crop growth stage and nutritional status dependent factor for modifying N uptake rate.*
		20	*Stage-V and grain* $N < 1.6\%$ *(maize)*
		300	*Stage*$<$*V and plant* $N < 1.0\%$ *(maize*
		150	*Stage*$<$*V and plant* $N < 1.6\%$ *(maize)*
		0	*Plant* $N > 2.0\%$ *(maize)*
		0	*Plant* $N > 3.8$ *gm (maize)*
		20	*Stage-I (wheat)*
		200	*Stage=II and plant* $N < 1.0\%$ *(wheat)*
		20	*Stage>II and plant* $N < 1.0\%$ *(wheat)*

Table 6.
Predicted and observed variables at the end of model calibration.

Variable	Blacksburg		Nomini Creek		Brandon	
	meas.	pred.	meas.	pred.	meas.	pred.
Grain	3890	4359	2940	2343	4790	3686
Stover	9560	8637	6740	3874	–	–
Grain-N	53.0	55.0	46.0	35.0	68.0	59.4
Stover-N	84.0	84.5	63.0	62.5	–	–
Soil-N	182.3	96.4	175.3	211.6	59.0	55.3

Table 7.
Characteristics of hypothetical soil.

Depth (cm)	Sat. Conduct. (cm/hr)	Porosity (-)	Para. (1/cm)	Para. n (-)	Organic Carbon (%)	pH (-)
0-20	50	0.41	0.08	1.9	2.0	5.5
20-50	100	0.43	0.01	1.2	0.4	5.5
50-150	500	0.43	0.15	2.6	0.4	5.0

Table 8.
Sensitivity of maize yield state variables to forcing variables and input parameters.

Forcing Variables	Grain Yield	Stover Yield	Grain N	Stover N
Rainfall	0.16	-0.10	0.09	-0.15
Solar Radiation	-0.55	1.27	-0.42	1.20
Maximum Temperature	-0.39	-0.66	0.05	-0.70
Minimum Temperature	0.47	-0.22	0.54	-0.33
Input Parameters				
Sat. Conductivity	0.04	-0.10	0.06	-0.10
Retention Parameter n	0.04	0.02	0.39	-0.05
Retention Parameter alpha	-0.47	-0.04	-0.11	-0.05
Sat. Water Content	-0.03	-0.07	0.33	-0.10
Residual Water Content	0.05	0.08	0.01	0.10
Depth to Water Table	0.06	-0.03	0.26	-0.05
Humus Min. Rate	0.02	-0.11	0.21	-0.10
Fresh OM Min. Rate	0.19	-0.11	0.28	-0.10
Depth of Straw mixing	-0.06	-0.10	0.11	-0.10
Soil Albedo	0.08	-0.09	0.06	-0.08
Mean Annual Temp.	-0.49	-0.11	-0.06	-0.10
Temp. Amplitude	0.21	0.21	0.40	-0.08
Plant Density	-0.09	0.68	0.14	0.60
Depth of Sowing	-0.04	-1.53	0.11	-0.05

Table 9.
Sensitivity of wheat yield state variables to forcing variables and input parameters.

Forcing Variables	Grain Yield	Stover Yield	Grain N	Stover N
Rainfall	0.19	0.03	0.43	0.04
Solar Radiation	0.52	0.84	0.10	0.65
Maximum Temperature	0.81	0.54	1.51	0.54
Minimum Temperature	0.81	0.36	1.07	0.37
Input Parameters				
Sat. Conductivity	0.48	0.66	1.23	0.68
Retention Parameter n	0.64	0.70	1.45	0.70
Retention Parameter alpha	0.46	0.65	1.60	0.65
Sat. Water Content	0.66	0.29	0.95	0.30
Residual Water Content	0.36	0.32	0.57	0.33
Depth to Water Table	1.00	0.61	1.47	0.61
Humus Min. Rate	0.56	0.62	1.04	0.63
Fresh OM Min. Rate	0.32	0.29	0.59	0.30
Depth of Straw mixing	0.51	0.09	0.75	0.09
Soil Albedo	0.85	0.84	1.99	0.85
Mean Annual Temp.	0.47	0.26	0.94	0.26
Temp. Amplitude	0.30	0.06	0.57	0.06
Plant Density	0.92	1.22	1.88	1.22
Depth of Sowing	0.59	0.09	1.13	0.09

Table 10.
Sensitivity of soybean yield state variables to forcing variables and input parameters.

Forcing Variables	Grain Yield	Stover Yield	Grain N	Stover N
Rainfall	-0.04	-0.04	-0.04	-0.04
Solar Radiation	0.73	0.73	0.73	0.72
Maximum Temperature	0.46	0.46	0.46	0.46
Minimum Temperature	0.00	0.00	0.00	0.00
Input Parameters				
Sat. Conductivity	0.00	0.00	0.00	0.00
Retention Parameter n	0.50	0.50	0.50	0.50
Retention Parameter alpha	0.10	0.10	0.09	0.09
Sat. Water Content	0.05	0.05	0.04	0.04
Residual Water Content	-0.18	-0.18	-0.19	-0.20
Depth to Water Table	-0.18	-0.18	-0.21	-0.20
Humus Min. Rate	0.00	0.00	0.00	0.00
Fresh OM Min. Rate	0.00	0.00	0.00	0.00
Depth of Straw mixing	0.00	0.00	0.00	0.00
Soil Albedo	-0.01	-0.01	-0.01	-0.02
Mean Annual Temp.	0.00	0.00	0.00	0.00
Temp. Amplitude	0.00	0.00	0.00	0.00
Plant Density	0.00	0.00	0.00	0.00
Depth of Sowing	0.00	0.00	0.00	0.00

Table 11.
Sensitivity of water and N dynamics state variables to forcing variables and input parameters.

Forcing Variables	Drainage	Water Use	Runoff	N Leached	Mineralization	Denitrification
Rainfall	1.54	0.07	3.70	2.65	1.80	0.63
Solar Radiation	-0.61	0.68	-0.15	-1.56	0.25	-0.74
Maximum Temperature	-0.29	0.32	-0.19	-2.25	-0.79	-1.53
Minimum Temperature	-0.08	0.16	-0.11	-0.48	-0.12	-1.37
Input Parameters						
Sat. Conductivity	-0.08	0.07	-0.07	-0.81	0.75	-0.05
Retention Parameter n	0.19	-0.13	-0.43	-1.34	-0.53	-2.26
Retention Parameter alpha	0.30	0.46	-0.10	-0.44	0.29	0.58
Sat. Water Content	-0.40	0.46	-0.10	-0.64	0.29	0.58
Residual Water Content	0.24	-0.14	0.00	0.63	0.82	-0.26
Depth to Water Table	-0.06	0.11	0.00	-0.64	1.14	-0.05
Humus Min. Rate	-0.06	0.00	0.00	-0.75	0.56	0.00
Fresh OM Min. Rate	-0.07	0.00	-0.02	0.41	1.34	0.63
Depth of Straw mixing	-0.11	-0.05	0.03	0.10	0.73	0.26
Soil Albedo	0.13	-0.16	-0.05	-1.17	0.87	-0.11
Mean Annual Temp.	0.00	-0.07	0.00	0.27	0.18	0.00
Temp. Amplitude	-0.11	-0.05	0.03	0.33	0.47	0.53
Plant Density	-0.03	0.00	-0.03	-1.93	0.78	0.58
Depth of Sowing	0.01	-0.09	0.03	-0.34	0.56	0.16

Table 12.
Crop and cultural practices used in maize validation experiments.

Management Practice	Value Employed
Planting Date	124 (Julian)
Planting Density	61,700 (Plants/*ha*)
Sowing Depth	10 *cm* (Conventional) 1 *cm* (No-Till)
Variety	Delkal B XL71
Amount of Straw Incorporated	2,000 (*kg/ha*)
Depth of Straw Incorporated	20 *cm* (Conventional) Surface (No-Till)
Tillage Practice	Conventional, No-Till

Table 13.
Fertilizer management practices used in validation experiments.

Fertilizer Practice	Maize	Wheat
Amount of Fertilizer Applied	225 ,15 0, 75, 0 (*kg/ha*)	150, 0 (*kg/ha*)
Timing of Application	125 (Julian)	69 (Julian) *
Mode of Application	Broadcast	Broadcast
N-Source	Ammonium Nitrate	Urea
Depth of Application	0.0	0.0

* At Whitehorne, fertilizer was applied on day 75.

Table 14.
Model validation: maize grain and biomass yield, Blacksburg (conventional till).

Treatment (kg/ha)	Year					
	1986		1987		1988	
	Measured	Predicted	Measured	Predicted	Measured	Predicted
	Grain Yield (kg/ha)					
0	4910	4322	2730	4754		
75	5080	4984	2880	4962	5990	5869
150	5350	6308	3120	6210	7060	8222
225	4930	6357	3070	6864	7420	9065
	Biomass (kg/ha)					
0	10100	8185	8700	9940		
75	11100	9255	9900	10369	13100	10741
150	11500	11393	10400	12784	14800	14009
225	10900	11477	9450	13845	15800	15107

Table 15.
Model validation: maize grain and biomass yield, Blacksburg (minimum till).

Treatment (kg/ha)	Year					
	1986		1987		1988	
	Measured	Predicted	Measured	Predicted	Measured	Predicted
	Grain Yield (kg/ha)					
0	4700	5295	3420	4750	3560	4865
75	6270	5692	4670	5375	6000	5288
150	6390	6716	4470	5620	8010	6082
225	5660	6703	3960	4330	8040	6218
	Biomass (kg/ha)					
0	9580	9580	9380	10126	9370	9671
75	13700	10350	11500	11261	14600	9650
150	12900	11311	12700	11513	17200	11535
225	12600	11528	12100	9232	17900	11159

Table 16.
Model validation: maize grain and biomass N, Blacksburg (conventional till).

Treatment (kg/ha)	Year					
	1986		1987		1988	
	Measured	Predicted	Measured	Predicted	Measured	Predicted
	Grain N (kg/ha)					
0	81.0	37.4	38.0	64.2		
75	95.0	67.4	47.0	67.0	90.0	78.9
150	91.0	86.8	55.0	83.6	123.0	110.9
225	105.0	94.4	59.0	83.6	132.0	122.1
	Total N (kg/ha)					
0	109.0	63.6	60.0	119.8		
75	137.0	116.8	91.0	124.7	141.0	149.5
150	142.0	160.2	104.0	163.6	185.0	214.4
225	155.0	168.6	109.0	186.9	204.0	231.8

Table 17.
Model validation: maize grain and biomass N, Blacksburg (minimum till).

Treatment (kg/ha)	Year					
	1986		1987		1988	
	Measured	Predicted	Measured	Predicted	Measured	Predicted
	Grain N (kg/ha)					
0	72.0	47.7	40.0	49.1	45.0	65.5
75	105.0	79.0	74.0	72.5	83.0	70.9
150	128.0	91.1	81.0	75.8	137.0	88.7
225	111.0	93.5	76.0	57.7	150.0	99.1
	Total N (kg/ha)					
0	96.0	80.1	61.0	85.5	73.0	128.0
75	146.0	127.4	105.0	129.6	129.0	133.8
150	172.0	175.0	142.0	154.1	202.0	184.7
225	166.0	180.6	144.0	89.1	223.0	191.9

Table 18.
Model validation: maize grain and biomass yield, Nomini Creek (conventional till).

Treatment (kg/ha)	Year			
	1986		1988	
	Measured	Predicted	Measured	Predicted
	Grain Yield (kg/ha)			
0	2770	2273	1540	3494
75	2410	2806	1420	3713
150	2830	2742	1260	4220
225	2280	2753	700	5232
	Biomass (kg/ha)			
0	7370	3472	7570	9397
75	7060	3885	7950	9892
150	7720	3803	9220	10816
225	6640	3821	7160	14626

Table 19.
Model validation: maize grain and biomass yield, Nomini Creek (minimum till).

Treatment (kg/ha)	Year			
	1986		1988	
	Measured	Predicted	Measured	Predicted
	Grain Yield (kg/ha)			
0	2940	2343	1330	4384
75	3160	2804	1890	4757
150	4070	3046	1890	5780
225	3570	3146	1000	7231
	Biomass (kg/ha)			
0	6740	3874	7710	9723
75	6910	4406	10100	10543
150	8300	4600	11400	12085
225	7580	4597	8340	14626

Table 20.
Model validation: maize grain and biomass N, Nomini Creek (conventional till).

Treatment (kg/ha)	Year			
	1986		1988	
	Measured	Predicted	Measured	Predicted
	Grain N Uptake(kg/ha)			
0	63.0	33.2	26.0	7.1
75	50.0	57.6	28.0	49.0
150	65.0	57.6	26.0	55.9
225	49.0	60.0	16.0	69.3
	Total N Uptake (kg/ha)			
0	102.0	70.8	68.0	30.1
75	93.0	102.1	92.0	92.1
150	126.0	109.5	123.0	124.1
225	101.0	116.8	110.0	152.7

Table 21.
Model validation: maize grain and biomass N, Nomini Creek (minimum till).

Treatment (kg/ha)	Year			
	1986		1988	
	Measured	Predicted	Measured	Predicted
	Grain N Uptake(kg/ha)			
0	46.0	35.9	21.0	6.1
75	59.0	47.4	34.0	52.1
150	75.0	52.6	30.0	77.3
225	75.0	52.9	22.0	96.1
	Total N Uptake (kg/ha)			
0	63.0	62.5	57.0	26.3
75	82.0	77.8	96.0	94.6
150	110.0	87.7	117.0	140.7
225	110.0	86.2	125.0	208.9

Table 22.
Correlation coefficients for variables at sites.

Response variable	Blacksburg	Nomini Creek
Biomass	0.36	0.56
Biomass N	0.70	0.8
Grain Yield	0.55	-0.67
Grain N	0.67	0.03
Soil N	0.64	0.96

Table 23.
Crop and soil cultural practices used in wheat validation experiments.

Site	Planting Date (Julian)	Plant Population (Plants/ha)	Sowing Depth (cm)	Amount of Residue (kg/ha)	Depth of Residue Incorporation (cm)	Variety
Brandon	301	2.95×10^6	6	6200	20	Coker 6815
Montague	304	3.23×10^6	6	3500	20	Coker 6815
Randolph	286	3.02×10^6	6	3300	10	Coker 6815
VCIA	287	$3.55 \mathrm{X} 10^6$	6	3200	10	Coker 6815
Walker	313	3.83×10^6	6	2800	10	Coker 6815
Whitehorne	284	3.72×10^6	6	800	20	Coker 6815

Table 24.
Model validation: wheat grain and N content (no N added).

Local	Soil Classification	Grain (kg/ha) Measured	Grain (kg/ha) Predicted	Grain N (kg/ha) Measured	Grain N (kg/ha) Predicted
Brandon	Ultic Hapludalf				
Montague	Typic Hapludult	4,450	5,621	N/A	113.6
Randolph	Typic Hapuldult	1,481	2,235	N/A	40.9
V.C.I.A.	Aquic Hapludult	2,412	3,397	34.2	69.9
Walker	Typic Hapuldult	2,525	4,000	28.6	81.4
Whitehorne	Aquic Hapludult	N/A	3,949	N/A	68.7

Table 25.
Model validation: wheat grain and N content (150 kg-N/ha added).

Local	Soil Classification	Grain (kg/ha) Measured	Grain (kg/ha) Predicted	Grain N (kg/ha) Measured	Grain N (kg/ha) Predicted
Brandon	Ultic Hapludalf	3,853	3,883	84.0	101.1
Montague	Typic Hapludult	4,389	5,630	N/A	156.8
Randolph	Typic Hapuldult	4,121	3,902	N/A	101.8
VCIA	Aquic Hapludult	5,200	5,370	34.2	127.6
Walker	Typic Hapuldult	4,300	5,154	28.6	134.5
Whitehorne	Aquic Hapludult	N/A	5,589	N/A	112.9

Table 26.
Summary of regression analysis.

Response Variable	Slope	Intercept	Correlation Coefficient	Model Std. Error (kg/ha)	Coefficient of Variation (%)
Biomass	0.53* (0.13)	5349.8* (1329)	0.56	2902.9	28
Biomass N	0.64* (0.09)	38.9* (12.1)	0.76	1930	49
Grain Yield	0.69 (0.14)	517.1 (796.0)	0.55	32.8	33
Grain N	1.03 (0.17)	1.48 (12.0)	0.72	24.5	48
Soil N	0.87 (0.08)	27.6 (20.13)	0.83	65.5	62

$*$ Criterion not satisfied at $\alpha = 0.05$

() Standard error of estimate

Table 27.
Summary of K-S test analysis.

Response Variable	n	K-S Stat.	p Value
Biomass	38	0.63	$p < 0.85$
Biomass N	38	0.63	$p < 0.85$
Grain Yield	38	0.78	$0.85 < p < 0.9$
Grain	38	0.65	$p < 0.85$
Soil N	49	0.80	$0.85 < p < 0.90$
Composite	201	0.57	$p < 0.05$

Table 28.
Summary of paired-t confidence analysis.

Response Variable	n	$\bar{Z}(n)$	$S^2_{\bar{Z}(n)}$	$\bar{Z}_{lower}$	$\bar{Z}_{upper}$
Biomass	38	820.4	193,832.0	-80.1	1,720.6
Grain Yield*	38	-1,190.8	257.0	-1,710.1	-671.5
Total N Uptake	38	-6.6	25.7	-16.8	3.7
Grain Nitrogen	38	2.5	18.4	-6.2	11.2
Soil N Content	49	1.8	1.70	-0.8	4.4

* Confidence interval does not contain zero at $\alpha = 0.05$.

Table 29.
Crop and soil management practices simulated.

Management Practices	Maize	Wheat
Planting Date	131 (Julian)	288 (Julian)
Planting Density	60,000 (plants/ha)	3,000,000 (plants/ha)
Sowing Depth	10 cm (Conventional 1 cm (Minimum)	5 cm
Variety	Delkal B XL71	Moris Huntsman
Depth of Straw Mixing	20 cm (Conventional) Top cell (Minimum)	Top cell (Minimum)
Tillage Practice	Conventional, Minmum	Minimum Till

Table 30.
Fertilizer management practices modeled.

Fertilizer Practice	Maize	Wheat
Amount of Fertilizer	150 (kg/ha)	150 (kg/ha)
Timing of Application	100% at Planting	20% at Planting 80% 180 Days Later
Mode of Application	Broadcast	Broadcast
N-Source	Ammonium Nitrate	Urea
Depth of Application	Surface	Surface

Table 31.
Summary of model long-term N input and output variables for management systems simulated.

N Input & Output Variable	Management 1		Management 2	
	Mean (kg/ha/rotation)	Coefficient of Variation (%)	Mean (kg/ha/rotation)	Coefficient of Variation (%)
Fertilizer	300.0	0.0	300.0	0.0
Mineralization	114.6	18.7	111.8	17.8
N Input	414.6	5.2	411.8	4.9
Denitrification	21.4	15.7	21.6	18.2
Crop Uptake	300.0	4.8	299.3	5.6
N Load	84.2	26.3	85.9	26.8
N output	407.6	7.1	408.9	6.5

Table 32.
Water inflow and outflow into the soil system for a 26-year period.

Rotation		Mgmt-1	Mgmt-2
		(mm/yr)	
1	Mean Annual Evapotranspiration	500.1	488.5
	Mean Annual Drainage	529.1	558.6
	Mean Annual Runoff	44.8	26.4
	Total	1074.0	1,073.5
	Mean Annual Rainfall	1,083.0	1,083.0
2	Mean Annual Evapotranspiration	491.0	497.3
	Mean Annual Drainage	551.0	571.5
	Mean Annual Runoff	47.7	32.9
	Total	1,099.7	1,101.7
	Mean Annual Rainfall	1,108.0	1,108.0
3	Mean Annual Evapotranspiration	476.5	469.9
	Mean Annual Drainage	519.9	540.2
	Mean Annual Runoff	59.7	42.2
	Total	1,056.1	1,052.3
	Mean Annual Rainfall	1,058.0	1,058.0
4	Mean Annual Evapotranspiration	502.3	503.7
	Mean Annual Drainage	608.5	629.3
	Mean Annual Runoff	89.2	69.9
	Total	1,200.0	1,200.9
	Mean Annual Rainfall	1,171.5	1,171.5
5	Mean Annual Evapotranspiration	456.5	455.9
	Mean Annual Drainage	445.5	466.1
	Mean Annual Runoff	50.5	30.8
	Total	952.5	952.8
	Mean Annual Rainfall	975.5	975.5
6	Mean Annual Evapotranspiration	502.3	505.7
	Mean Annual Drainage	518.8	543.1
	Mean Annual Runoff	1,07.9	79.4
	Total	1,129.0	1,128.2
	Mean Annual Rainfall	1,129.0	1,129.0
7	Mean Annual Evapotranspiration	514.0	513.7
	Mean Annual Drainage	369.7	387.0
	Mean Annual Runoff	43.2	27.1
	Total	926.9	927.8
	Mean Annual Rainfall	899.0	899.0
8	Mean Annual Evapotranspiration	480.4	476.3
	Mean Annual Drainage	338.3	363.9
	Mean Annual Runoff	68.3	46.2
	Total	887.0	886.4
	Mean Annual Rainfall	885.5	885.5
9	Mean Annual Evapotranspiration	462.1	495.6
	Mean Annual Drainage	628.3	646.7
	Mean Annual Runoff	80.7	47.8
	Total	1,191.1	1,190.1
	Mean Annual Rainfall	1,260.5	1,260.5
10	Mean Annual Evapotranspiration	437.4	434.7
	Mean Annual Drainage	454.2	463.1
	Mean Annual Runoff	41.4	32.8
	Total	933.0	930.6
	Mean Annual Rainfall	314.5	914.5
11	Mean Annual Evapotranspiration	477.6	478.5
	Mean Annual Drainage	520.6	545.1
	Mean Annual Runoff	68.0	45.6
	Total	1,066.2	1,069.2
	Mean Annual Rainfall	1,091.5	1,091.5
12	Mean Annual Evapotranspiration	532.3	535.0
	Mean Annual Drainage	524.1	550.1
	Mean Annual Runoff	75.0	45.6
	Total	1,131.4	1,130.6
	Mean Annual Rainfall	1,087.0	1,087.0
13	Mean Annual Evapotranspiration	510.1	509.2
	Mean Annual Drainage	424.7	445.7
	Mean Annual Runoff	54.5	33.3
	Total	989.3	998.2
	Mean Annual Rainfall	948.5	948.5

Table 33.
Simulated long-term (26 years) maize yield, N uptake, and partitioning for 150 kg-N/ha.

Rotation #		Mgmt-1	Mgmt-2		Mgmt-1	Mgmt-2
		(kg/ha)				
1	Grain [1]	6,231	6,902	Grain-N	93.3	91.4
	Stover	5,290	5,621	Stover-N	52.4	54.3
	Roots	2,733	2,444	Root-N	27.3	23.4
	Biomass	11,457	12,960	Total-N	174.4	172.3
2	Grain	5,766	5,782	Grain-N	92.3	92.8
	Stover	4,015	4,015	Stover-N	39.9	40.0
	Roots	1,601	1,603	Root-N	15.6	15.6
	Biomass	10,451	10,465	Total-N	148.1	148.7
3	Grain	5,627	5,331	Grain-N	82.2	93.0
	Stover	5,677	4,242	Stover-N	50.1	31.7
	Roots	1,694	1,459	Root-N	16.8	15.0
	Biomass	12,025	10,369	Total-N	149.3	140.0
4	Grain	6,616	6,460	Grain-N	89.2	88.0
	Stover	6,357	6,276	Stover-N	59.1	61.9
	Roots	2,577	2,279	Root-N	25.8	22.7
	Biomass	13,495	13,265	Total-N	174.7	173.1
5	Grain	5,352	5,383	Grain-N	92.2	96.3
	Stover	3,618	4,002	Stover-N	33.7	32.5
	Roots	1,477	1,594	Root-N	14.7	16.0
	Biomass	9,499	9,795	Total-N	140.9	145.2
6	Grain	6,002	6,247	Grain-N	101.3	103.1
	Stover	3,979	4,183	Stover-N	40.3	41.5
	Roots	1,367	1,400	Root-N	19.4	14.0
	Biomass	10,373	10,869	Total-N	161.0	159.7
7	Grain	6,272	6,783	Grain-N	102.6	112.0
	Stover	4,581	4,359	Stover-N	46.2	43.9
	Roots	1,695	1,610	Root-N	16.9	16.1
	Biomass	11,497	11,670	Total-N	166.1	172.3
8	Grain	6,825	7,002	Grain-N	108.9	110.7
	Stover	5,358	5,006	Stover-N	53.0	49.3
	Roots	1,955	1,741	Root-N	19.5	17.4
	Biomass	12,864	12,625	Total-N	182.2	178.0
9	Grain	5,365	5,864	Grain-N	84.6	78.9
	Stover	4,839	5,446	Stover-N	45.6	54.0
	Roots	1,472	1,720	Root-N	14.7	17.0
	Biomass	10,765	11,832	Total-N	145.5	150.5
10	Grain	5,519	4,801	Grain-N	73.3	83.6
	Stover	4,971	3,803	Stover-N	42.5	29.1
	Roots	1,843	1,489	Root-N	18.3	14.8
	Biomass	10,964	9,239	Total-N	134.9	127.2
11	Grain	5,694	5,886	Grain-N	95.8	102.8
	Stover	3,209	3,107	Stover-N	39.3	39.6
	Roots	1,287	1,431	Root-N	15.9	18.7
	Biomass	9,343	9,381	Total-N	152.4	162.7
12	Grain	5,709	6,023	Grain-N	94.5	93.4
	Stover	4,576	4,838	Stover-N	45.1	48.4
	Roots	1,889	1,833	Root-N	18.7	18.3
	Biomass	11,060	11,542	Total-N	158.8	160.4
13	Grain	5,707	5,807	Grain-N	96.4	100.4
	Stover	3,496	3,519	Stover-N	36.7	36.8
	Roots	1,115	1,084	Root-N	11.3	11.1
	Biomass	9,536	9,612	Total-N	148.2	149.4

[1] Grain yield reported at 13.5% moisture.

Table 34.
Simulated long-term (26 years) wheat yield, N uptake, and partitioning for 150 kg-N/ha.

Rotation #		Mgmt-1	Mgmt-2		Mgmt-1	Mgmt-2
		(kg/ha)				
1	Grain [1]	4,774	3,066	Grain-N	84.5	67.9
	Stover	3,078	5,098	Stover-N	26.6	44.1
	Roots	2,940	2,654	Root-N	29.4	25.5
	Biomass	7,852	8,165	Total-N	140.5	137.5
2	Grain	3,341	3,447	Grain-N	68.0	70.6
	Stover	5,310	5,312	Stover-N	45.9	45.9
	Roots	2,480	2,485	Root-N	23.1	23.2
	Biomass	8,656	8,758	Total-N	137.0	139.7
3	Grain	3,276	3,238	Grain-N	72.2	73.9
	Stover	5,383	5,327	Stover-N	46.6	46.1
	Roots	2,315	2,162	Root-N	22.0	20.4
	Biomass	8,659	8,566	Total-N	140.7	140.4
4	Grain	3,188	3,068	Grain-N	87.4	83.5
	Stover	4,962	4,804	Stover-N	42.9	41.6
	Roots	1,762	1,609	Root-N	16.2	15.3
	Biomass	8,150	7,871	Total-N	146.5	140.4
5	Grain	3,294	2,888	Grain-N	79.4	85.0
	Stover	4,922	4,887	Stover-N	42.6	42.3
	Roots	2,105	1,965	Root-N	19.4	19.2
	Biomass	8,216	7,774	Total-N	141.4	146.5
6	Grain	3,466	3,290	Grain-N	66.9	70.8
	Stover	5,377	5,120	Stover-N	46.4	44.5
	Roots	2,545	2,248	Root-N	23.1	20.3
	Biomass	8,843	8,436	Total-N	136.4	135.6
7	Grain	3,664	3,559	Grain-N	76.2	79.4
	Stover	5,429	5,467	Stover-N	47.0	47.3
	Roots	2,406	2,184	Root-N	22.1	19.9
	Biomass	9,093	9,027	Total-N	145.3	146.6
8	Grain	4,718	5,425	Grain-N	101.1	89.5
	Stover	2,963	3,118	Stover-N	25.6	27.0
	Roots	2,661	2,541	Root-N	26.6	25.4
	Biomass	8,682	8,543	Total-N	153.3	141.9
9	Grain	3,357	3,300	Grain-N	84.2	82.1
	Stover	5,121	5,105	Stover-N	44.3	44.2
	Roots	1,529	1,529	Root-N	14.0	13.9
	Biomass	8,478	8,405	Total-N	142.5	140.2
10	Grain	3,164	3,123	Grain-N	57.2	57.2
	Stover	5,465	5,420	Stover-N	47.3	46.8
	Roots	3,367	3,381	Root-N	34.6	31.5
	Biomass	8,465	8,543	Total-N	139.1	135.5
11	Grain	3,494	2,881	Grain-N	88.5	82.5
	Stover	5,012	5,125	Stover-N	43.4	44.3
	Roots	1,858	1,609	Root-N	17.0	74.7
	Biomass	8,507	8,006	Total-N	148.8	141.5
12	Grain	3,780	3,795	Grain-N	78.1	78.4
	Stover	6,299	6031	Stover-N	51.3	52.2
	Roots	2,465	2,328	Root-N	22.3	21.1
	Biomass	9,714	9,826	Total-N	151.8	151.7
13	Grain	3,744	3,667	Grain-N	49.3	64.7
	Stover	5,763	5,584	Stover-N	49.7	48.2
	Roots	3,041	2,684	Root-N	27.8	26.1
	Biomass	9,505	9,251	Total-N	146.8	139.0

[1] Grain yield reported at 13.5% moisture.

Table 35.
Simulated long-term (26 years) soybean yield, N uptake, and partitioning.

Rotation #		Mgmt-1	Mgmt-2		Mgmt-1	Mgmt-2
		(kg/ha)				
1	Grain[1]	2,604	2,615	Grain-N	143.9	144.5
	Stover	3,183	3,196	Stover-N	24.4	24.5
	Roots	900	903	Root-N	7.7	7.7
	Biomass	5,787	5,811	Symbiotic-N	152.0	171.9
2	Grain	2,573	2,571	Grain-N	142.0	142.1
	Stover	3,144	3,142	Stover-N	24.0	24.0
	Roots	889	888	Root-N	7.6	7.6
	Biomass	5,717	5,714	Symbiotic-N	165.4	164.6
3	Grain	2,911	2,921	Grain-N	160.9	161.4
	Stover	3,559	3,570	Stover-N	27.2	27.3
	Roots	1,006	1,009	Root-N	8.6	8.6
	Biomass	6,470	6,491	Symbiotic-N	189.5	189.9
4	Grain	2,771	2,771	Grain-N	153.1	153.1
	Stover	3,386	3,387	Stover-N	23.9	25.9
	Roots	957	957	Root-N	8.1	8.1
	Biomass	6,157	6,158	Symbiotic-N	179.1	178.9
5	Grain	3,006	3,009	Grain-N	166.1	166.3
	Stover	3,674	3,678	Stover-N	28.1	28.1
	Roots	1,038	1,040	Root-N	8.8	8.8
	Biomass	6,680	6,687	Symbiotic-N	194.05	193.0
6	Grain	2,803	2,820	Grain-N	154.8	155.8
	Stover	3,425	3,447	Stover-N	26.2	26.4
	Roots	968	974	Root-N	8.2	8.3
	Biomass	6,228	6,267	Symbiotic-N	179.6	180.5
7	Grain	2,995	3,002	Grain-N	165.5	165.9
	Stover	3,662	3,669	Stover-N	28.0	28.1
	Roots	1,035	1,037	Root-N	8.8	8.8
	Biomass	6,657	6,671	Symbiotic-N	191.1	192.1
8	Grain	2,899	3,003	Grain-N	160.2	165.9
	Stover	3,543	3,670	Stover-N	27.1	28.1
	Roots	1,002	1,037	Root-N	8.5	8.8
	Biomass	6,442	6,673	Symbiotic-N	184.4	189.9
9	Grain	2,821	2,826	Grain-N	155.9	156.2
	Stover	3,448	3,455	Stover-N	26.4	26.4
	Roots	975	976	Root-N	8.3	8.3
	Biomass	6,269	6,281	Symbiotic-N	181.1	179.4
10	Grain	2,749	2,756	Grain-N	151.9	152.3
	Stover	3,359	3,369	Stover-N	25.7	25.8
	Roots	950	952	Root-N	8.1	8.1
	Biomass	6,108	6,125	Symbiotic-N	175.3	175.5
11	Grain	2,887	2,887	Grain-N	159.5	159.5
	Stover	3,529	3,529	Stover-N	27.0	27.0
	Roots	997	997	Root-N	8.5	8.3
	Biomass	6,416	6,416	Symbiotic-N	186.3	186.3
12	Grain	2,887	2,894	Grain-N	159.5	159.9
	Stover	3529	3,537	Stover-N	27.0	27.1
	Roots	997	1,000	Root-N	8.3	8.5
	Biomass	6,416	6,431	Symbiotic-N	186.5	186.1
13	Grain	2,683	2,683	Grain-N	148.3	148.2
	Stover	3,280	3,279	Stover-N	25.1	25.1
	Roots	927	927	Root-N	7.9	7.9
	Biomass	5,963	5,962	Symbiotic-N	171.4	170.0

[1] Grain yield reported at 13.5% moisture.

Table 36.
Correlation coefficients of soil N and hydrologic variables with N load over short and long term.

Variable	Correlation Coefficient (%)	
	Short-Term	Long-Term
Residual N	15.0	-
Rainfall	15.0	55.0
Water Use	44.0	5.0
Drainage	58.0	53.0

Table 37.
Eigenvalues of the covariance matrix,
their incremental and cumulative variances.

Vector	*Eigenvalue*	*Marginal Variance (%)*	*Cumulative Variance (%)*
1	2.80	31.1	31.1
2	1.46	16.2	47.3
3	1.16	12.9	60.2
4	1.06	11.7	71.9
5	0.83	9.3	81.2
6	0.61	6.7	87.9
7	0.49	5.5	93.4
8	0.34	3.8	97.2
9	0.25	2.8	100.0

Table 38.
Summary of cluster analysis methods used in grouping soils.

Similarity Measure	*Aglomerative Method*	*Principal Component Analysis*	*Cophenetic Correlation*
Sum of Absolute Difference	Maximum Distance	yes	0.70
Maximum Difference	Maximum Distance	yes	0.54
Absolute Cosine	Ward's Method	yes	0.30
Mahalanobis Distance	Maximum Distance	no	0.66

Table 39.
Properties of soil series used in analysis.

Land Unit	Series	# of Horizons	pH	Bulk Density (gm/mL)	Water Hold. Capacity (cm/cm)	Permea-bility (cm/hr)	Depth to WT (m)	OM Content (%)	Hydrologic Group	Slope (%)
1	Bojac	3	5.5	1.4	0.08	4.0	1.52	1.25	2	1
1	Kempville	4	5.0	1.4	0.14	2.0	1.98	1.25	2	4
2	Congree	3	5.8	1.4	0.17	1.3	1.37	1.00	3	3
2	Emporia	4	5.0	1.4	0.13	0.3	0.30	10.80	3	1
2	Metapek	3	4.4	1.4	0.18	1.1	0.53	3.25	3	1
2	Sassafras	5	5.4	1.4	0.12	1.3	1.22	1.75	3	7.5
2	Teototum	3	4.1	1.3	0.15	1.3	0.61	1.25	3	3
3	Lakeland	4	6.1	1.5	0.05	13.0	2.13	1.00	2	3
3	Nansemon	4	4.8	1.4	0.09	4.0	0.61	1.50	3	2
3	Savannah	3	5.0	1.6	0.13	0.4	0.30	1.75	3	1
4	Augusta	3	5.3	1.4	0.14	1.3	0.38	2.00	3	9
4	Orthello	5	4.5	1.4	0.16	0.4	0.30	9.40	4	5
4	Roanoke	3	5.2	1.4	0.13	0.2	0.30	2.00	4	5
5	Marr	3	5.0	1.5	0.13	1.3	1.68	1.75	1	1
5	Turbeville	2	5.5	1.4	0.15	1.3	1.68	1.25	3	3
5	Wickham	3	5.5	1.4	0.13	4.2	1.68	2.25	1	4
6	Beltville	4	4.8	1.4	0.16	0.2	0.46	1.20	1	4
6	Caroline	2	5.0	1.4	0.11	4.0	1.68	1.00	3	1
6	Craven	3	5.0	1.4	0.15	0.1	1.14	2.30	2	6
6	Pooler	3	5.0	1.4	0.12	0.2	0.38	2.50	4	4
7	Bourne	4	5.0	1.4	0.13	0.2	0.30	1.00	2	1
7	Dogue	3	5.0	1.5	0.15	0.4	0.91	1.20	3	3
7	Woodstow	5	4.8	1.4	0.15	1.3	0.53	2.20	3	5
8	Catpoint	3	5.5	1.4	0.12	13.0	1.37	1.00	1	3
8	Matapeake	4	6.2	1.4	0.18	1.1	2.44	1.70	2	5
8	State	3	5.0	1.4	0.12	1.3	1.52	1.50	2	3
9	Bertie	4	4.6	1.4	0.14	1.3	0.46	1.50	3	3
9	Cartecay	3	5.5	1.4	0.11	4.1	0.46	1.00	3	5
9	Rumpford	3	4.6	1.3	0.10	4.0	1.98	1.25	1	6
10	Altavista	3	5.5	1.4	0.15	1.3	0.91	2.00	3	5
10	Aura	3	5.1	1.4	0.12	1.3	1.83	2.00	2	3
10	Luka	3	5.0	1.4	0.13	1.3	0.91	2.00	3	2
10	Pamunky	3	6.5	1.5	0.12	1.3	1.07	1.00	2	1
10	Suffolk	4	5.0	1.5	0.23	1.3	1.98	1.25	2	3

Table 40.
Properties of land units simulated.

Land Unit	USDA Soil Classification	Depth (cm)	Texture	Saturated Conduct. (cm/hr)	Sat. MC	Resid. MC	Alpha (1/cm)	n	pH	Bulk Density (gm/cc)	Organic Carbon (%)	Depth to WT (cm)	Slope (%)	Hydrologic Group
I	Typic Hapludult	0-25	SL	106.00	0.41	0.065	0.075	1.89	5.0	1.56				
		25-125	SCL	31.40	0.43	0.089	0.01	1.23	5.0	1.51	0.73	>150	4	B
		125-200	SC	2.88	0.38	0.100	0.027	1.23	5.0	1.74				
II	Typic Hapludult	0-25	SL	106.00	0.41	0.065	0.075	1.89	5.5	1.56				
	Aquic Hapludult	25-75	SCL	31.40	0.43	0.089	0.01	1.23	5.0	1.51	1.01	120	6	C
		75-200	CL	6.24	0.41	0.095	0.019	1.31	5.0	1.51				
III	Aquic Hapludult	0-25	SL	106.00	0.41	0.065	0.075	1.89	5.0	1.56				
	Typic Fragiudult	25-60	CL	6.24	0.41	0.095	0.019	1.31	5.5	1.56	0.87	60	2	C
	Typic Quartzisamments	60-150	SL	106.00	0.41	0.065	0.075	1.89	5.5	1.56				
IV	Typic Ochraquult	0-15	SL	106.00	0.45	0.065	0.02	1.41	4.1	1.46				
	Aeric Ochraquult	15-80	CL	6.24	0.41	0.095	0.019	1.31	4.4	1.56	4.06	30	2	D
		80-150	LS	350.20	0.41	0.057	0.124	2.28	4.8	1.56				
V	Typic Hapludult	0-30	SL	106.00	0.41	0.065	0.075	1.89	5.0	1.56				
	Typic Paleudult	30-80	CL	6.24	0.41	0.089	0.019	1.31	5.0	1.56	1.00	>150	2	B
		80-150	SCL	31.40	0.43	0.095	0.01	1.23	5.0	1.51				
VI	Typic Paleudult	0-25	SL	106.00	0.41	0.065	0.075	1.89	5.0	1.59				
	Typic Fragiudult	25-125	CL	6.24	0.41	0.095	0.019	1.31	5.0	1.56	1.16	120	1	A
	Aquic Hapludult	125-200	CL	6.24	0.41	0.095	0.019	1.31	5.0	1.56				
	Aeric Ochraquult													
	Aquic Hapludult	25-90	SCL	31.40	0.43	0.089	0.01	1.23	5.0	1.51	1.16	60	2	C
		90-150	SCL	31.40	0.43	0.089	0.01	1.23	4.5	1.51				
VIII	Typic Hapludult	0-25	SL	106.00	0.41	0.065	0.075	1.89	5.5	1.56				
	Ultic Udipsamments	25-90	LS	350.20	0.41	0.057	0.124	2.28	5.5	1.56	0.80	>150	4	B
		90-200	S	713.00	0.43	0.045	0.145	2.68	5.0	1.51				
IX	Aquic Hapludult	0-40	LS	350.20	0.41	0.057	0.124	2.28	4.0	1.56				
	Typic Hapludult	40-75	SL	106.00	0.41	0.065	0.075	1.89	5.0	1.56	0.87	150	6	A
	Aquic Udifluvent	75-200	S	713.00	0.43	0.045	0.145	2.68	4.5	1.51				
X	Ultic Hapludult	0-25	SL	106.00	0.41	0.065	0.075	1.89	5.0	1.56				
	Typic Hapludult	25-75	SL	106.00	0.41	0.065	0.075	1.89	5.0	1.56	0.75	>150	3	B
	Aquic Udifluvent	75-170	CL	6.24	0.41	0.095	0.019	1.31	5.0	1.56				

Table 41.
Average crop performance for land units (kg/ha).

(kg\ha)

Land Unit	Maize Yield		Wheat Yield		Maize N Uptake		Wheat N Uptake	
	Mgmt 1	*Mgmt 2*	*Mgmt 1*	*Mgmt 2*	*Mgmt 1*	*Mgmt 2*	*Mgmt 1*	*Mgmt 2*
1	5899	5840	3488	3319	139	136	151	154
2	5826	5853	3555	3592	137	137	158	156
3	5601	5471	3366	3442	133	131	151	152
4	5016	5106	3136	3013	118	118	151	151
5	5931	5907	3503	3480	139	138	153	154
6	5814	5748	3612	3616	136	135	158	158
7	5507	5543	3401	3435	132	134	156	152
8	6000	5940	3732	3740	139	139	158	156
9	5285	5325	3172	3163	116	118	148	148
10	5769	5846	3536	3542	136	134	157	154
Mean	**5664.8**	**5657.9**	**3450.1**	**3434.2**	**132.5**	**132.0**	**154.1**	**153.5**
CV	**5.3**	**4.7**	**5.1**	**6.0**	**6.1**	**5.5**	**2.3**	**1.8**

Table 42.
Mean and coefficient of variation of runoff, water use, and drainage for land units and management practices.

Land Unit	Soil Runoff				Crop Water Use				Soil Drainage			
	Management 1		Management 2		Management 1		Management 2		Management 1		Management 2	
	Mean (mm/rot)	CV (%)	Mean (mm/rot)	CV (%)	Mean (mm/rot)	CV (%)	Mean (mm/rot)	CV (%)	Mean (mm/rot)	CV (%)	Mean (mm/rot)	CV (%)
1	248.5	21.9	204.1	21.9	1104.2	3.7	1105.8	3.4	742.9	23.4	784.8	22.6
2	344.7	20.5	275.5	22.5	1089.4	3.1	1092.4	2.6	661.8	21.9	728.1	21.5
3	251.8	22.9	228.1	23.8	1025.2	3.7	1025.1	3.4	823.9	18.5	848.1	18.4
4	362.7	19.0	249.8	24.0	930.0	7.1	940.2	7.0	810.4	15.5	910.2	14.7
5	255.9	23.1	204.3	24.9	1112.8	3.8	1108.8	3.6	721.2	23.9	776.8	23.8
6	61.5	35.5	47.8	40.1	1089.5	3.8	1083.9	3.3	944.8	21.3	963.6	20.9
7	295.8	23.3	270.6	24.0	1047.5	3.0	1045.2	3.0	755.2	20.3	782.5	20.4
8	126.7	29.9	84.0	34.4	1015.5	5.5	1013.6	5.3	957.9	16.6	1002.0	16.7
9	16.2	51.5	9.5	66.5	839.2	7.5	837.7	7.5	1231.8	15.1	1240.2	15.2
10	172.7	24.8	127.5	29.3	1087.6	3.3	1084.2	3.3	834.1	22.3	881.9	21.8

Table 43.
Mean and coefficient of variation of mineralization, denitrification, and N load for land units and management practices.

Land Unit	Mineralization				Denitrification				N Leached			
	Management 1		Management 2		Management 1		Management 2		Management 1		Management 2	
	Mean (kg/rot)	CV (%)	Mean (kg/rot)	CV (%)	Mean (kg/rot)	CV (%)	Mean (kg/rot)	CV (%)	Mean (kg/rot)	CV (%)	Mean (kg/rot)	CV (%)
1	213.2	10.4	214.2	11.0	89.2	20.2	89.4	17.7	120.0	40.6	121.1	37.1
2	138.1	17.3	137.6	15.8	35.4	18.4	34.9	18.3	88.8	26.7	92.0	24.9
3	105.5	25.5	108.5	25.2	14.5	19.1	14.8	16.9	86.3	25.9	88.5	27.4
4	121.4	19.1	122.4	16.2	11.3	12.7	10.8	15.5	127.2	15.7	130.5	16.9
5	166.8	11.0	168.1	10.6	49.1	16.0	50.5	14.3	114.3	11.0	116.5	9.2
6	142.5	15.5	142.5	15.1	31.8	19.8	32.7	18.4	90.8	23.2	92.3	24.8
7	107.8	31.3	101.2	31.4	16.3	21.2	16.3	20.9	91.7	27.9	95.4	28.4
8	106.3	20.9	105.2	21.2	20.2	11.2	20.5	12.5	98.9	23.3	101.3	26.3
9	57.2	50.0	58.8	47.5	13.8	27.0	13.0	22.2	66.4	25.7	66.1	30.4
10	151.0	12.6	151.5	13.0	43.9	14.8	44.5	14.8	90.6	12.1	93.1	12.6

Table 44.
Estimated water use and drainage from uncropped area.

Rotation	*Rainfall (mm)*	*Water Use (mm)*	*Drainage (mm)*
1	2166	1304.5	861.1
2	2216	1317.2	900.4
3	2096	1287.9	808.4
4	2343	1334.7	1000.8
5	1951	1260.4	690.4
6	2258	1323.9	934.2
7	1798	1218.0	579.4
8	1771	1204.4	566.2
9	2521	1361.5	1159.8
10	1829	1219.3	608.7
11	2183	1311.2	872.2
12	2174	1309.6	864.0
13	1897	1240.6	656.5
Average	**2092.5**	**1284.1**	**807.9**

Table 45.

Summary of estimated cultivated acreage, annual average runoff, N loads, and drainage concentrations for land units over 26 years.

Land Unit	*Cultivated Area (ha)*	*Runoff Volume ($10^6 m^3$)*	*Drainage Volume ($10^6 m^3$)*	*N-Load ($10^6 kg$)*	*Concentration of Drainage (mg/L)*
1	13081	31.3	98.3	1.58	16.1
2	39917	132.1	269.5	3.57	13.2
3	3975	9.8	32.9	0.34	10.5
4	1523	5.2	12.6	0.19	15.4
5	3431	8.4	25.1	0.39	15.7
6	1833	1.1	17.4	0.17	9.6
7	4972	14.5	37.8	0.46	21.1
8	5608	6.6	54.2	0.56	10.3
9	337981	5.0	416.7	2.24	5.4
10	14671	24.0	123.8	1.33	10.8
Total	122794	238.0	1088.3	10.83	9.9
Annual Avg.		119.0	544.2	5.42	9.9

Table 46.
Long-term average N load, runoff, drainage, and concentration of drainage to groundwater and bay.

Land Use	*Area (10^6 ha)*	*Drainage (10^6 m)*	*Runoff (10^6 m)*	*N Load (10^6 kg)*	*Concentration to Groundwater (mg/L)*	*Concentration to Bay (mg/L)*
Cropped	122794	544.0	117.0	5.4	5.1	4.5
Noncropped	129206	521.9	0.0	0.0		

Table 47.
Mean annual crop water budget for sludge simulations.

Variable	*100% Sludge (mm)*	*50% Sludge (mm)*	*0% Sludge (mm)*
Water Use	508.7	509.0	509.0
Drainage	477.7	477.5	478.4
Runoff	63.1	63.1	63.0

Table 48.
Mean crop and N uptake for sludge simulations.

Variable	Maize (kg/ha)			Wheat (kg/ha)		
	100% Sludge	50% Sludge	0% Sludge	100% Sludge	50% Sludge	0% Sludge
Biomass	11151	11527	11544	9748	10189	10212
Grain	6403	6808	7021	4863	5911	5789
N-Uptake	152	165	177	172	179	187
Grain N	108	115	123	100	112	118

Table 49.
Mean annual N input and output for sludge simulations.

	Variable	100% Sewage		50% Sewage		0% Sewage	
		Mean (kg/ha)	CV (%)	Mean (kg/ha)	CV (%)	Mean (kg/ha)	CV (%)
Input	Fertilizer	0	0	125	0	250	0
	Mineralization	272	15.1	179	21.4	68	18.6
	Total	272	15.1	304	12.6	318	6.5
Output	Crop Uptake	184	10	197	7.2	210	8.6
	Leaching	86	33.6	97	27.4	121	18.3
	Denitrification	15	21	16	16.7	18	15.3
	Total	285	13.8	310	11.2	349	7.8

Table 50.
Effects of sludge application timing on crop performance and N leaching.

Model Variable	*Mean Response*	*Percentage Change*
Wheat Yield (kg/ha)	4535	-7
Wheat N Uptake (kg/ha)	154	-11
Maize Yield (kg/ha)	6246	-2
Maize N Uptake (kg/ha)	146	-4
Water Use (mm)	510	0
Drainage (mm)	479	0
Runoff (mm)	63	0
N Load (kg/ha)	92	+7

Figures

Figure 1.
General flow of model logic.

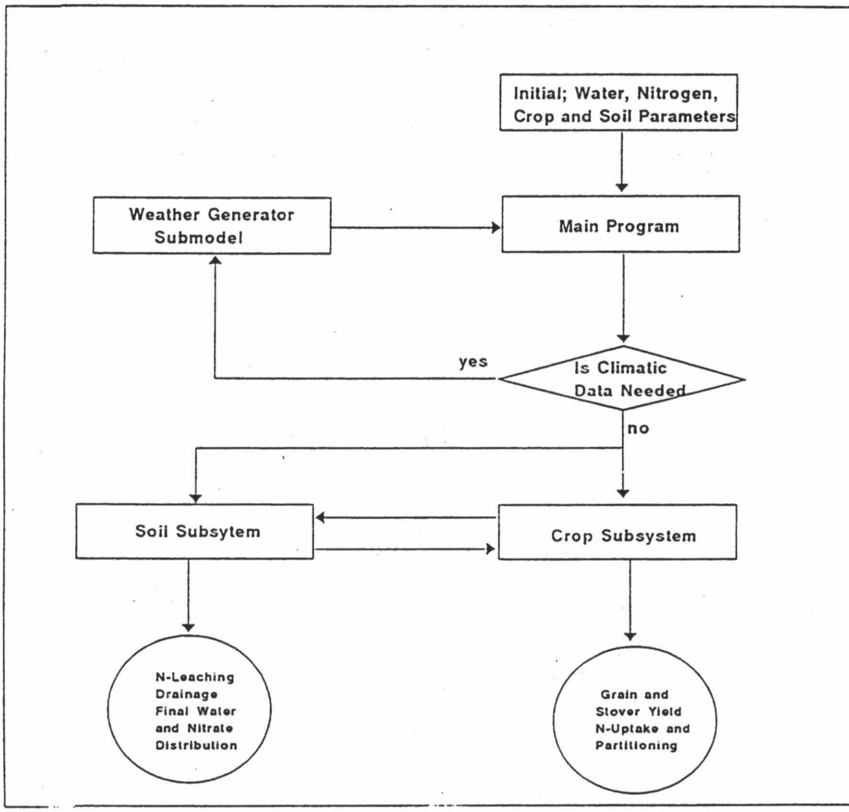

Figure 2.
Detail subroutine flow of model VT-CROPS.

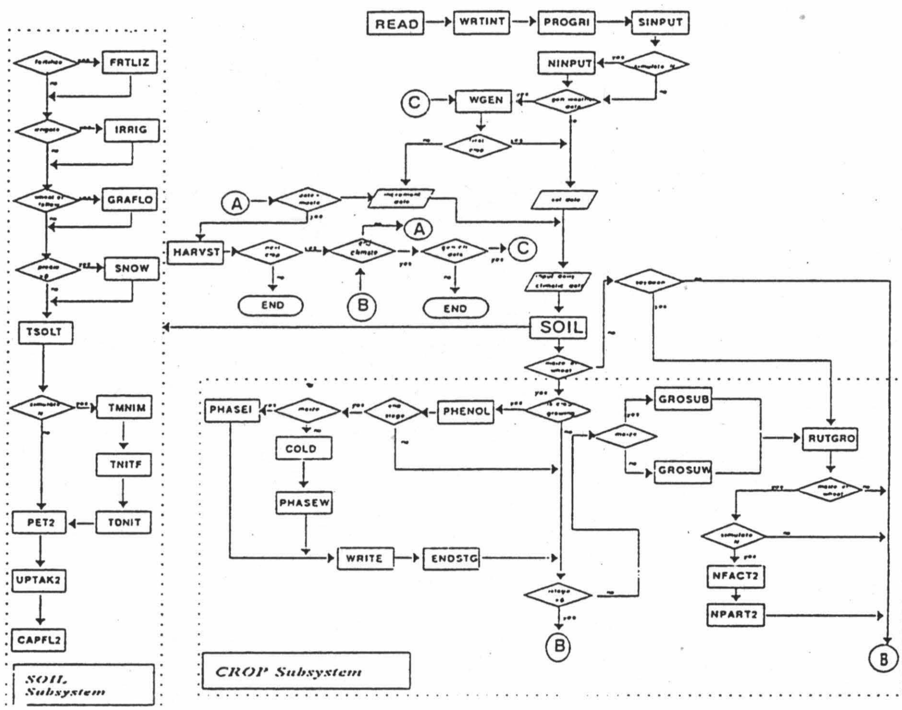

Figure 3.
Two-dimensional inter-row between two plants showing model conceptualization and domain discritization (Newkirk et al., 1987a).

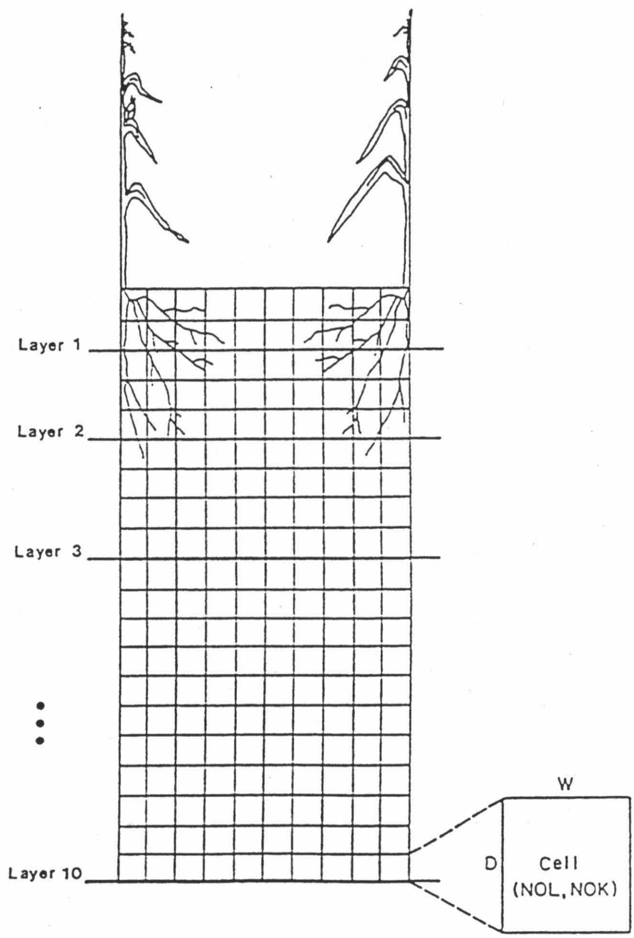

Figure 4.
Two-dimensional conceptualization of multilayered soil profile.

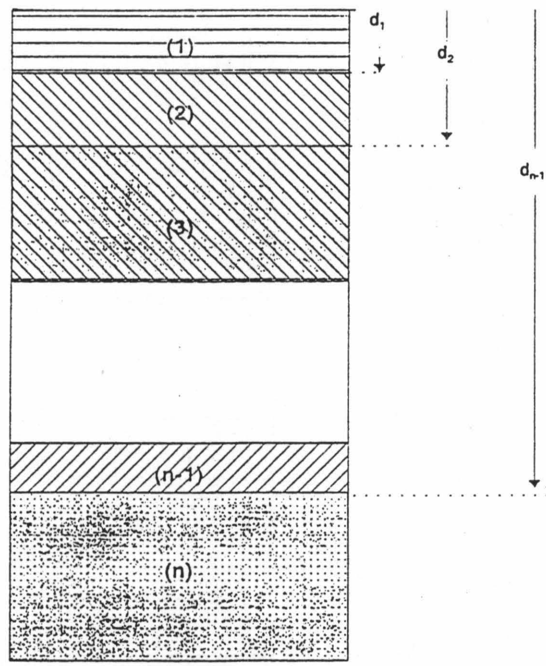

$h_i = h_{i+1}$ $\quad z_i = d_i \geq 0 \quad i = 1,2....n-1$

Figure 5.
Block diagram of the soil subsystem.

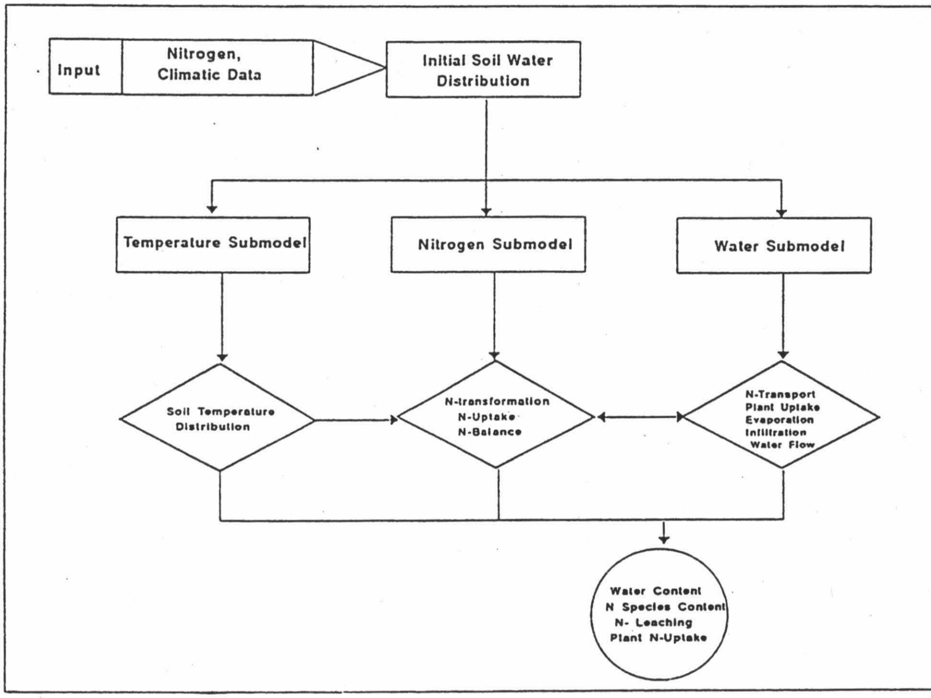

Figure 6.
Nitrogen transformation and transport processes considered by VT-CROPS.

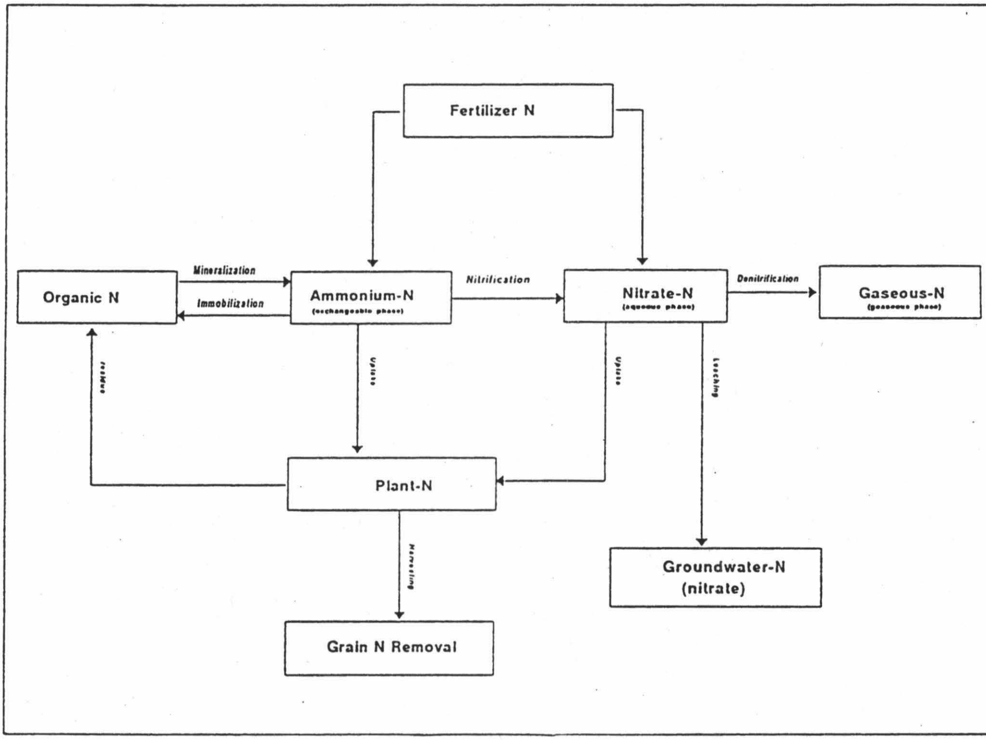

Figure 7.
Measured and predicted soil mineral N content distribution at the end of model calibration for maize at Blacksburg (A) and Nomini Creek (B), and wheat at Brandon Plantation (C).

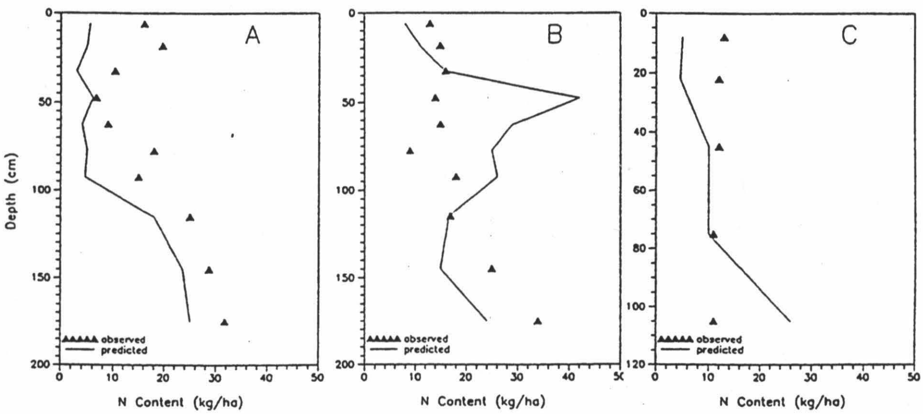

Figure 8.
Measured and predicted soil inorganic N distributions for maize at the end of the growing season for (A) 75 kg-N/ha conventional till, (B) 75 kg-N/ha minimum till, (C) 150 kg-N/ha conventional till, and (d) 150 kg-N/ha minimum till (Nomini Creek, 1986).

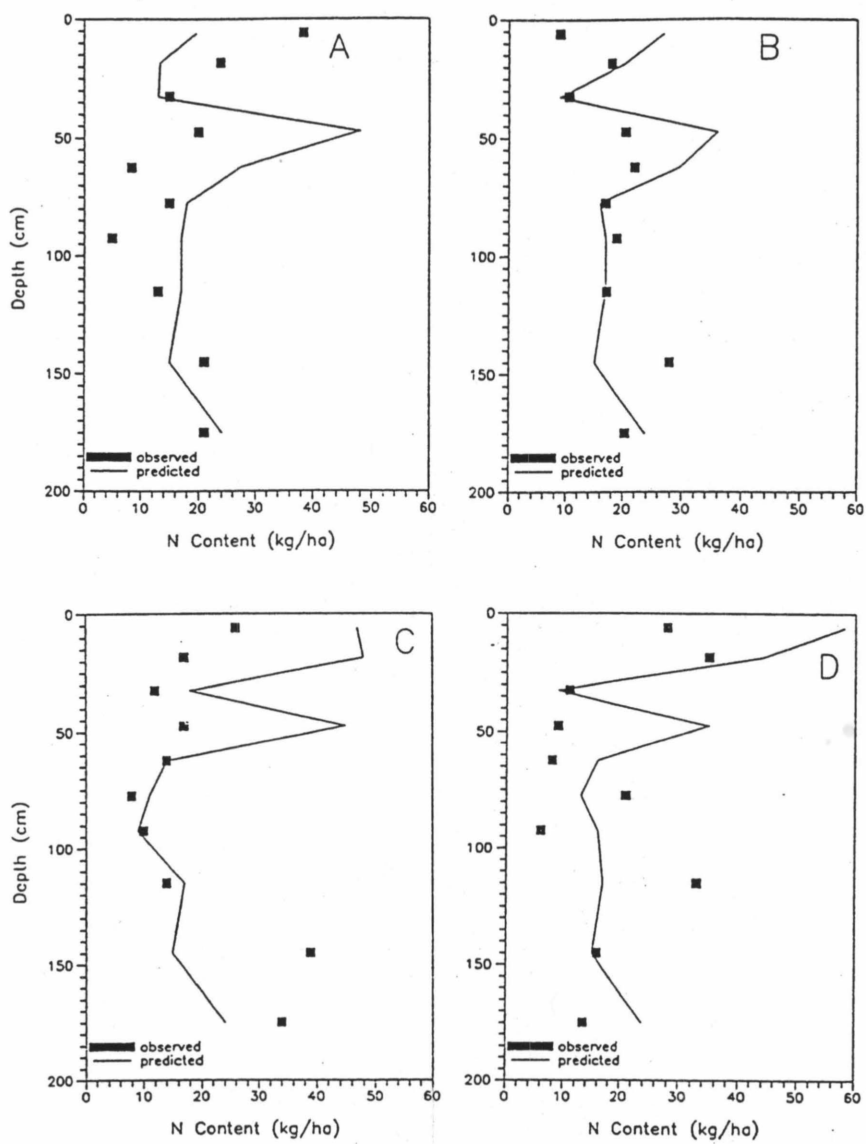

Figure 9.
Measured and predicted soil inorganic N distributions for maize at the end of the growing season for (A) 75 kg-N/ha conventional till, (B) 75 kg-N/ha minimum till, (C) 150 kg-N/ha conventional till, and (D) 150 kg-N/ha minimum till (Blacksburg, 1988).

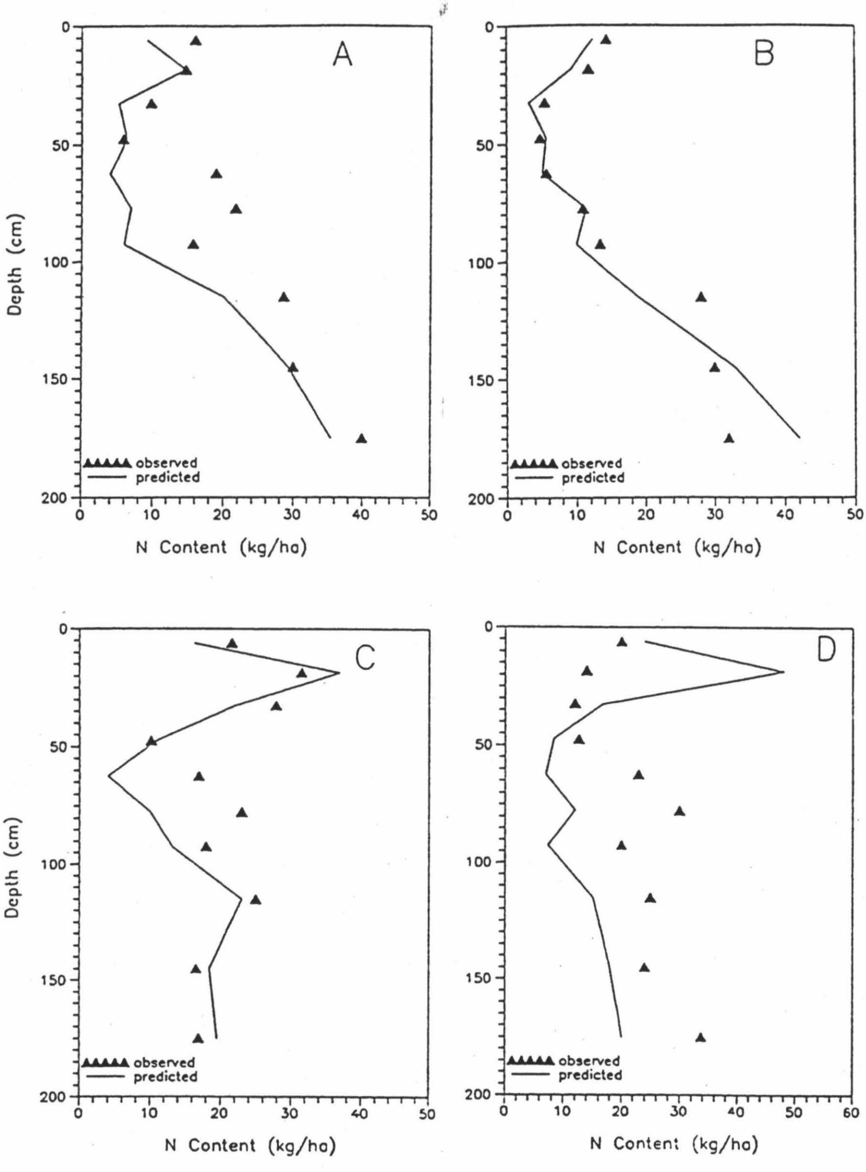

Figure 10.
Measured and predicted total soil inorganic N for maize at the end of the growing season for (A) minimum till and (B) conventional till (Nomini Creek, 1986).

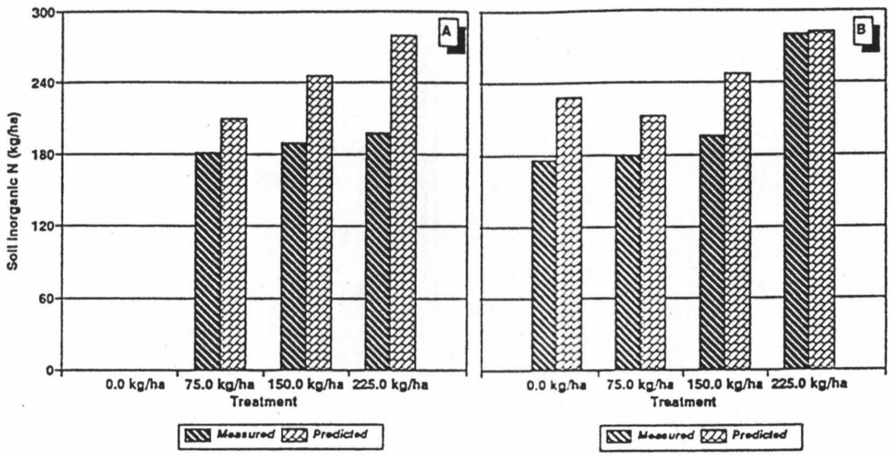

Figure 11.
Measured and predicted total soil inorganic N for maize at the end of the growing season for (A) minimum till and (B) conventional till (Nomini Creek, 1988).

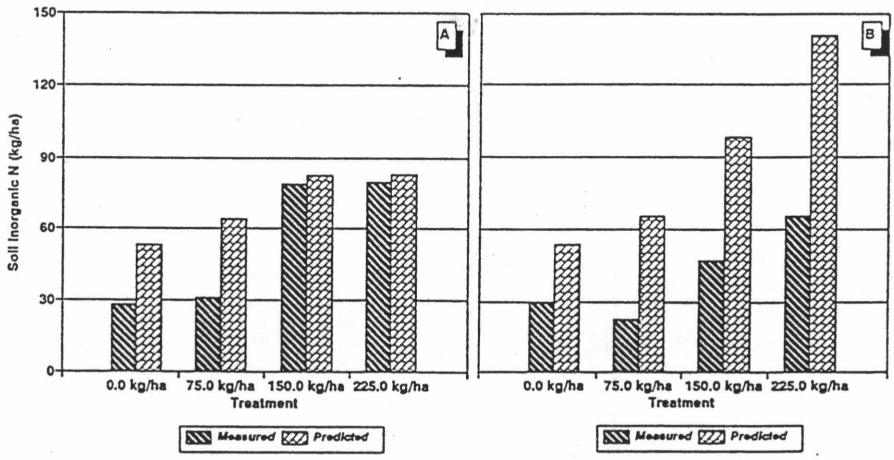

Figure 12.
Measured and predicted total soil inorganic N for maize at the end of the growing season for (A) minimum till and (B) conventional till (Blacksburg, 1986).

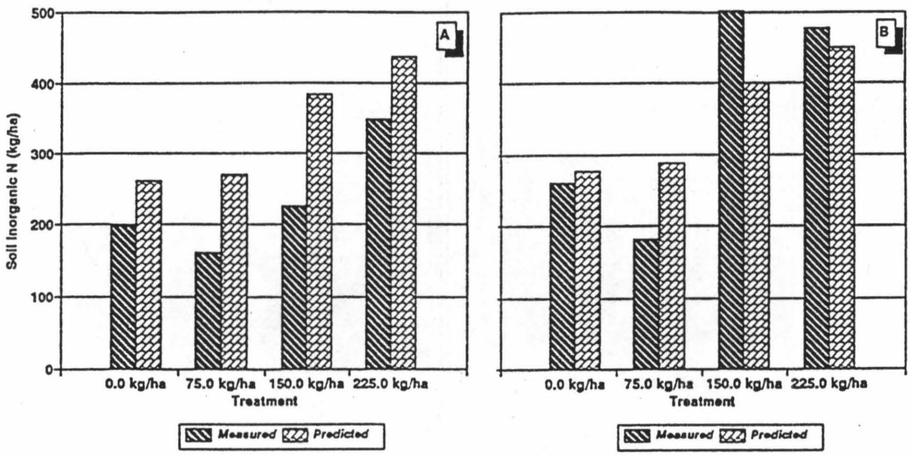

Figure 13.
Measured and predicted total soil inorganic N for maize at the end of the growing season for (A) minimum till and (B) conventional till (Blacksburg, 1987).

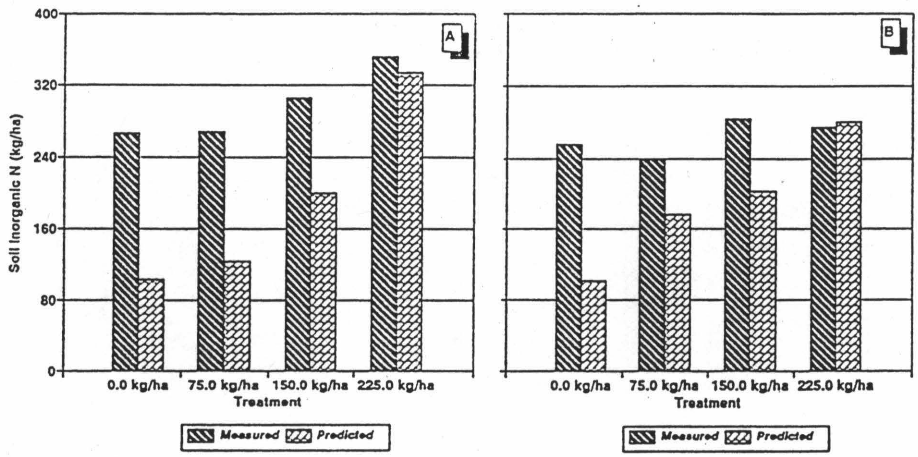

Figure 14.
Measured and predicted total soil inorganic N for maize at the end of the growing season for (A) minimum till and (B) conventional till (Blacksburg, 1988).

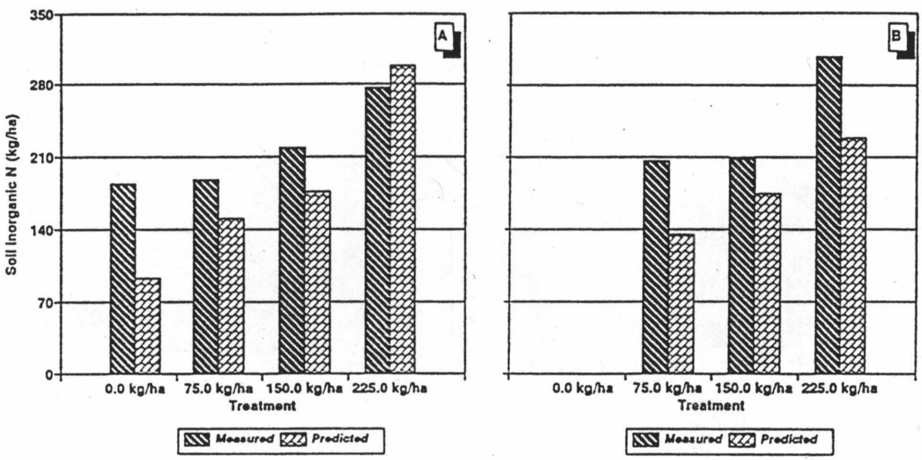

Figure 15.
Measured and predicted soil inorganic N distributions for wheat at the end of the growing season for (A) zero N at Randolf, (B) 150 kg-N/ha at Randolf, (C) zero N at VCIA, and (D) 150 kg-N/ha at VCIA (1988-89).

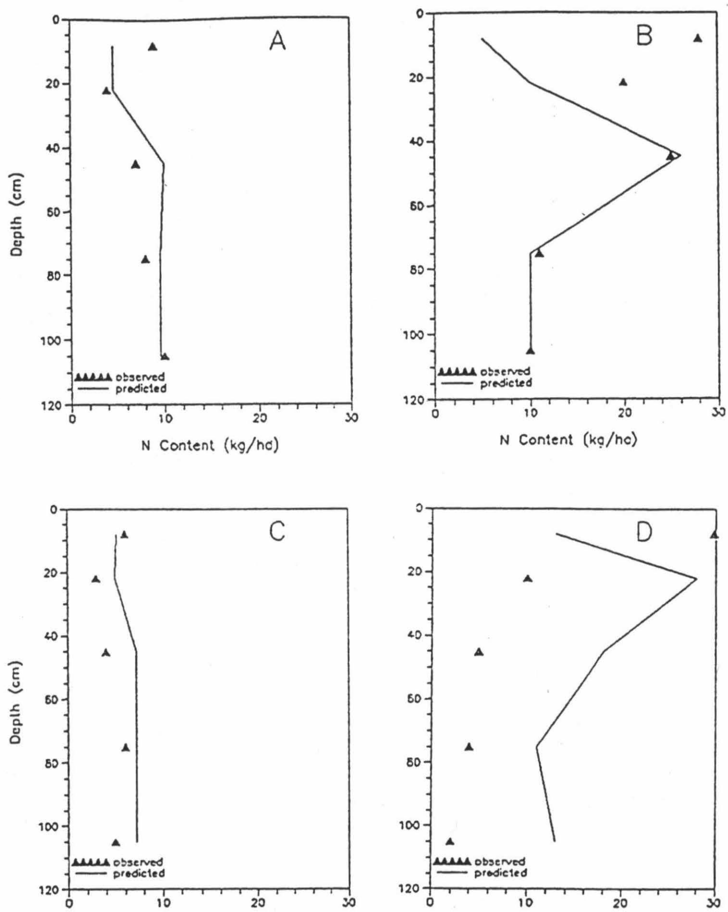

Figure 16.
Measured and predicted total soil inorganic N late in the wheat growing season for (A) no fertilizer added (B) 150 kg-N/ha (1988-89).

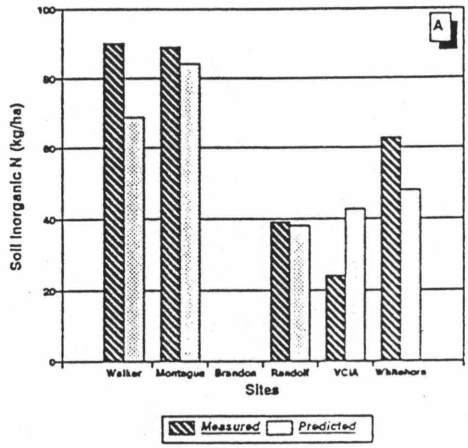

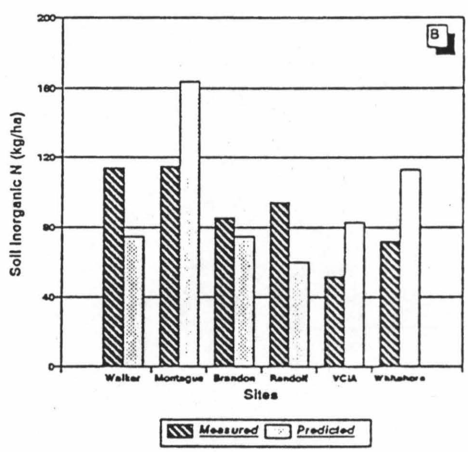

Figure 17.
Regression of measured against predicted (A) biomass and (B) biomass N.

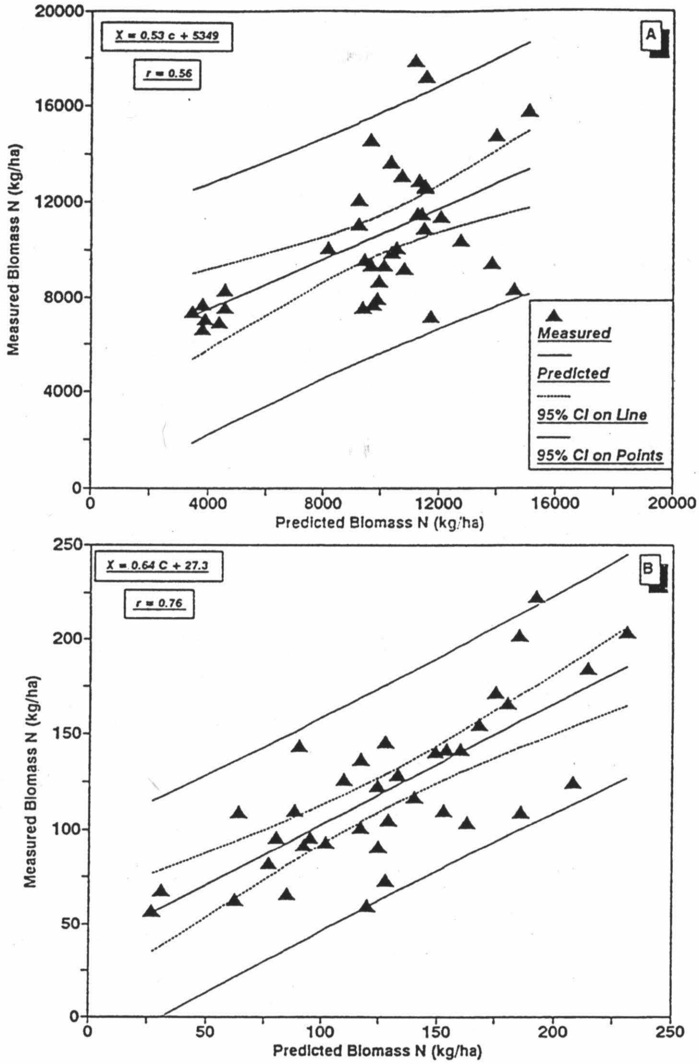

Figure 18.
Regression of measured against predicted (A) grain and (B) grain N.

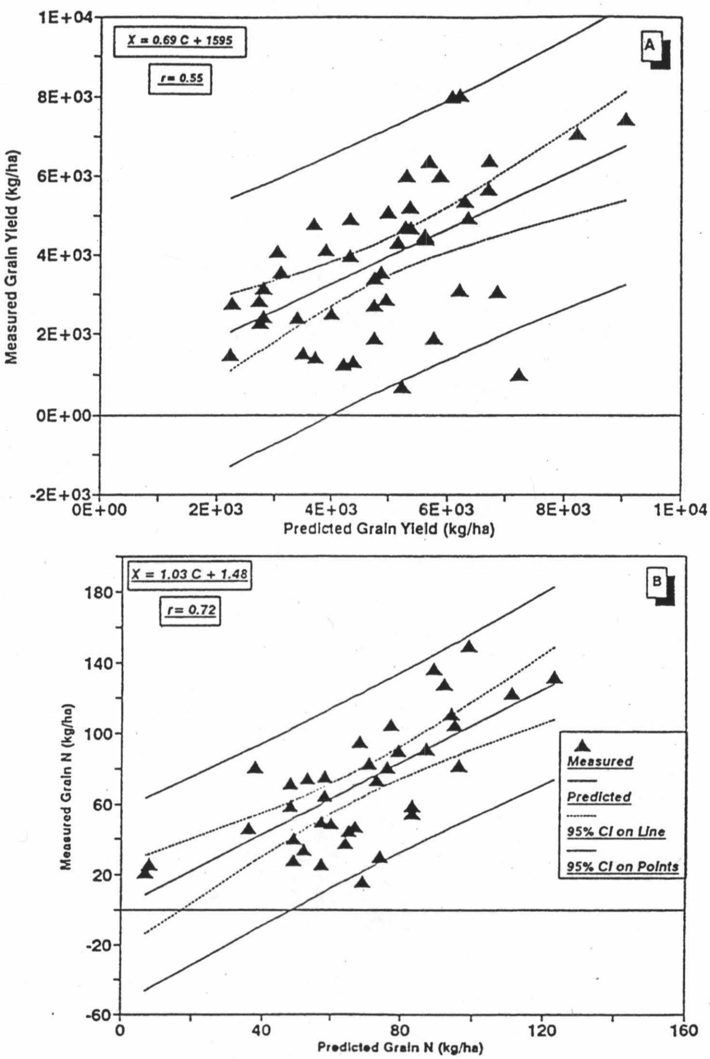

Figure 19.
Regression of measured against predicted soil mineral N.

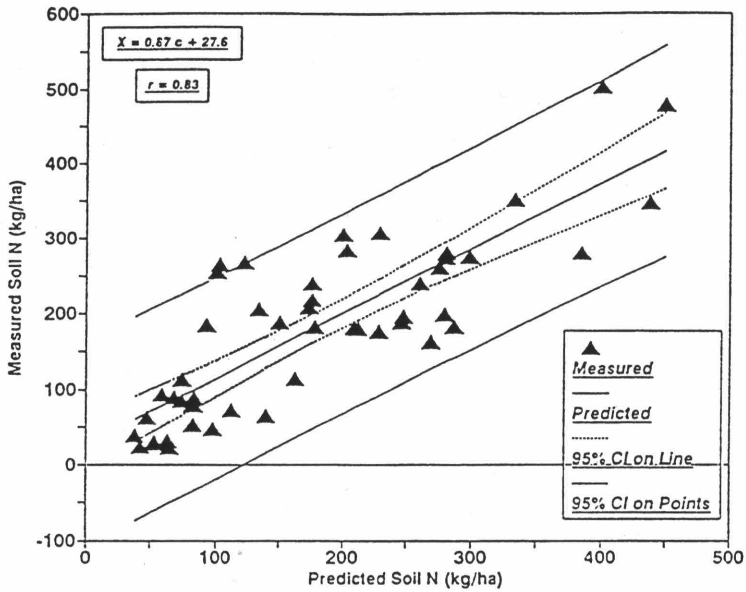

Figure 20.
Plot of composite standardized residuals against normalized model predictions.

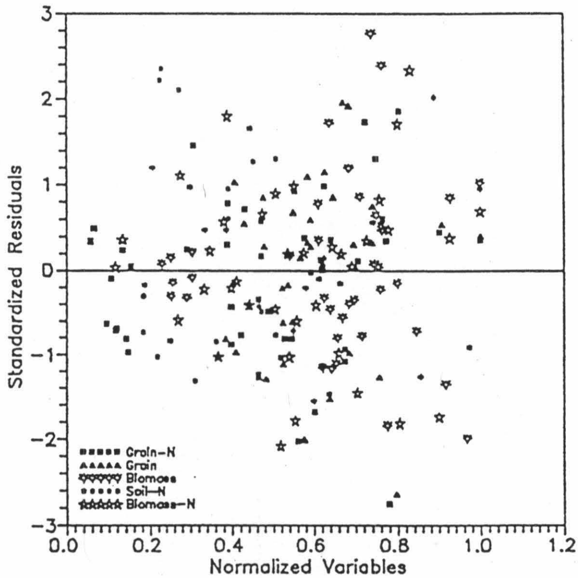

Figure 21.
Frequency plots of standardized residuals: (A) relative frequency histogram and fitted gaussian (normal) probability density function, and (B) fitted cumulative frequency curves.

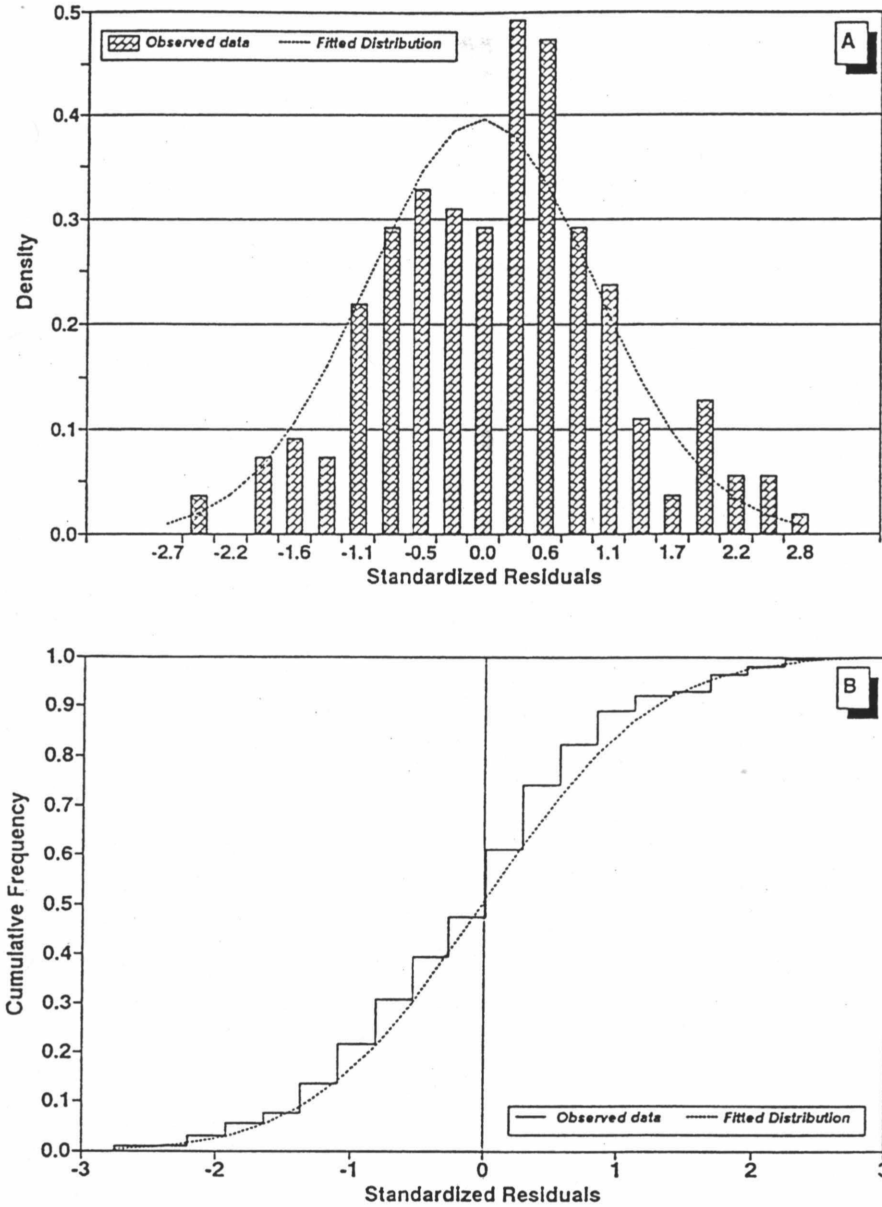

Figure 22.
Average daily maximum and minimum temperatures (A) and average daily solar radiation and annual temperature (B), generated by climatic submodel over 25 years.

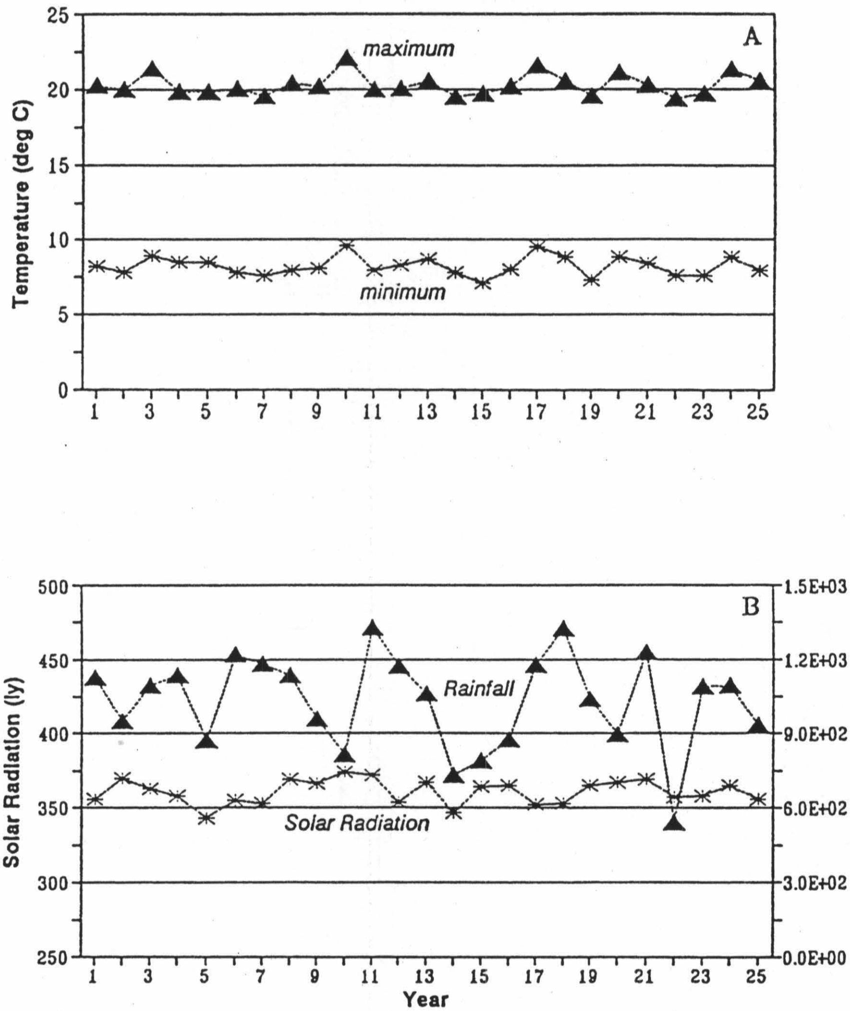

Figure 23.
Distribution of mineralized N and humus, and fresh organic and soil mineral N contents over two years, resulting from the incorporation of 15 tons/ha of low C-N ratio organic material, with no residue incorporation.

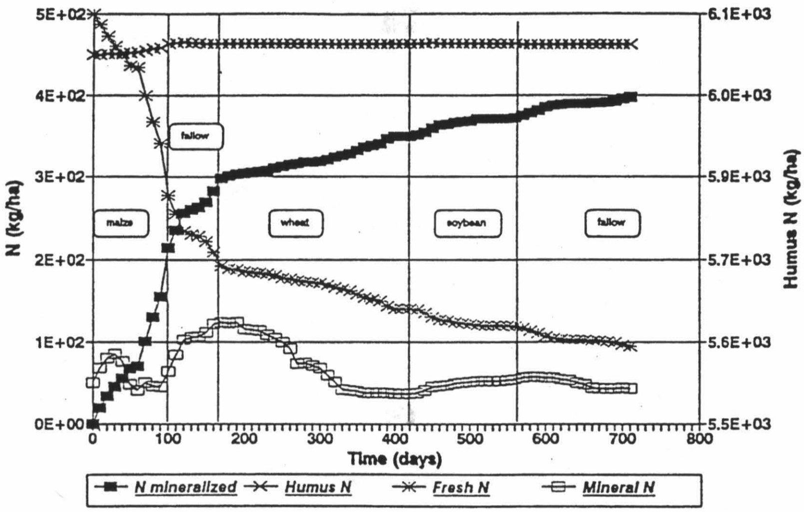

Figure 24.
Distribution of mineralized N and humus, and fresh organic and soil mineral N contents over two years, resulting from the incorporation of 15 tons/ha of low C-N ratio organic material, with residue incorporation.

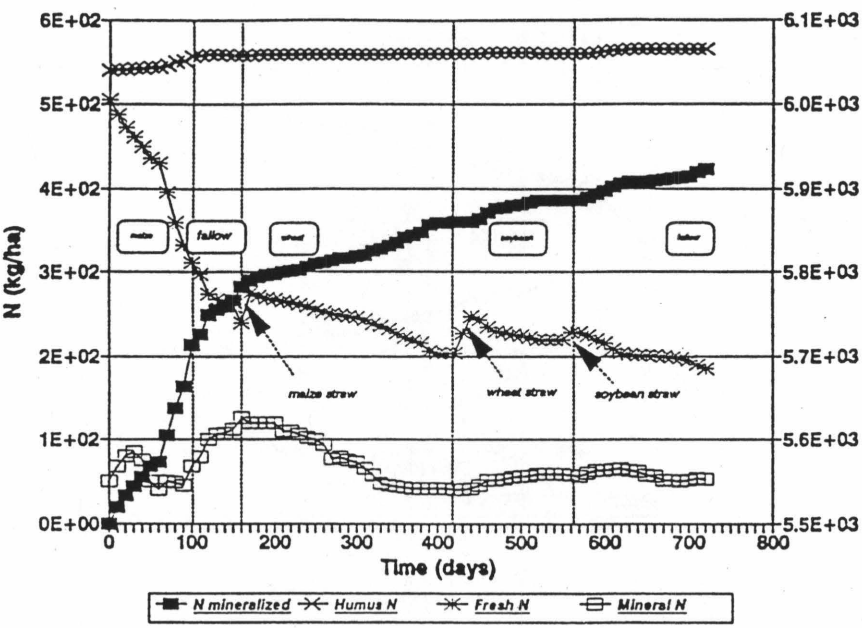

Figure 25.
Distribution of fresh organic N and C-N ratio resulting from the incorporation of 15 tons/ha of low C-N ratio organic material, with residue incorporation.

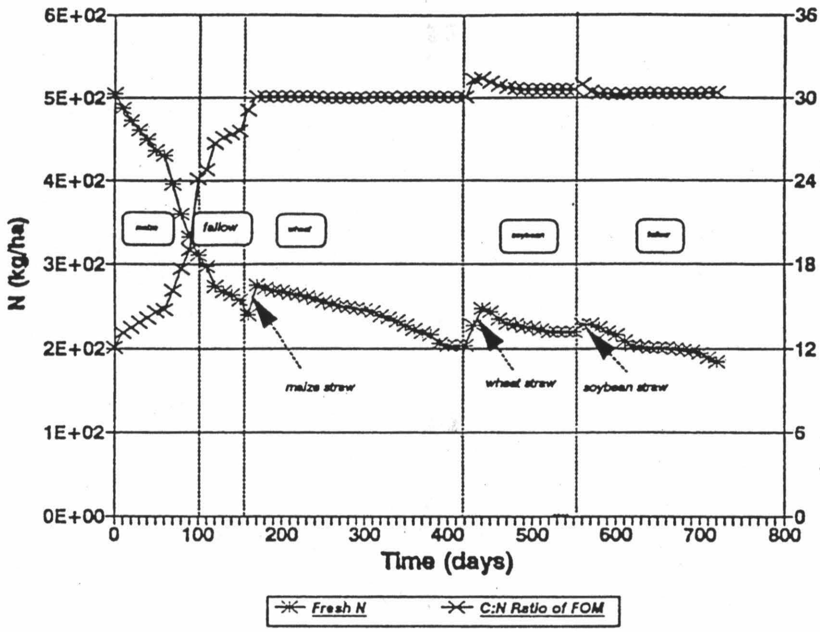

Figure 26.
Distribution of mineralized N and humus, and fresh organic and soil mineral N contents over two years, resulting from two incorporations (15 tons/ha initially, followed by 7.5 tons/ha at peak wheat N uptake) of low C-N ratio organic material, with residue incorporation.

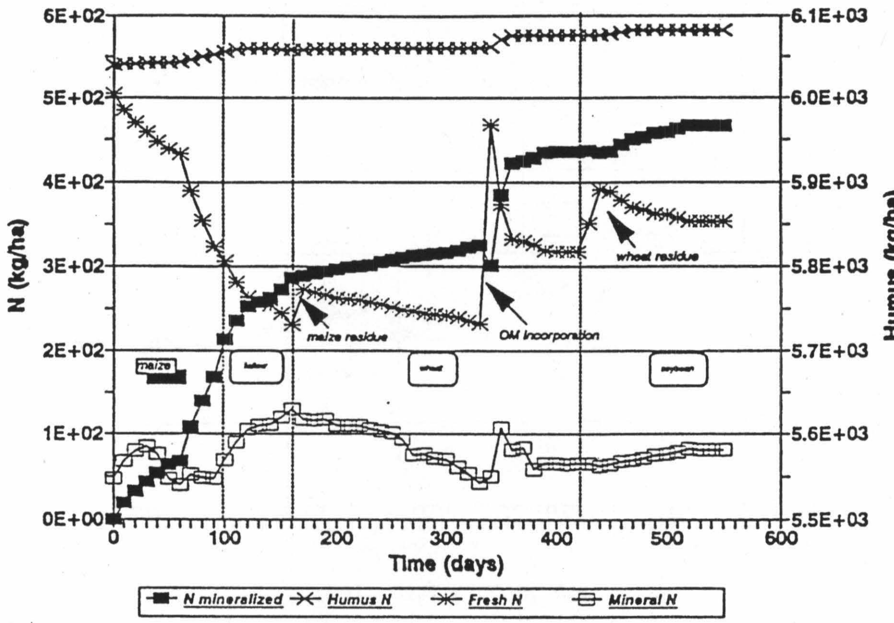

Figure 27.
Distribution of mineralized N and humus, and fresh organic and soil mineral n contents over two years, resulting from the incorporation of 15 tons/ha of high ratio organic material (C-N ratio 50), into soil with initially low mineral N content (A) and initially high mineral N content (B).

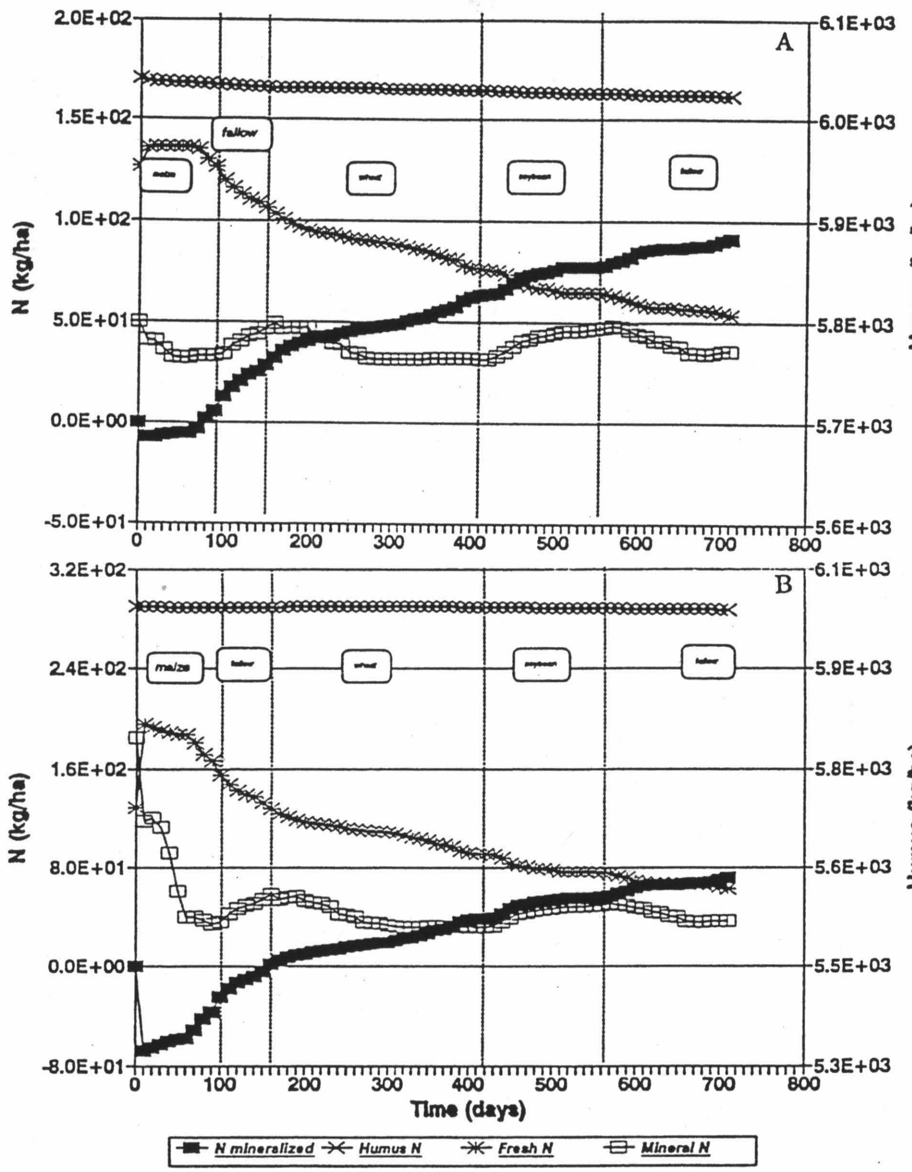

Figure 28.
Distribution of fresh organic n and C-N ratio resulting from the incorporation of 15 tons/ha of high C-N ratio organic material in soil initially high in mineral N.

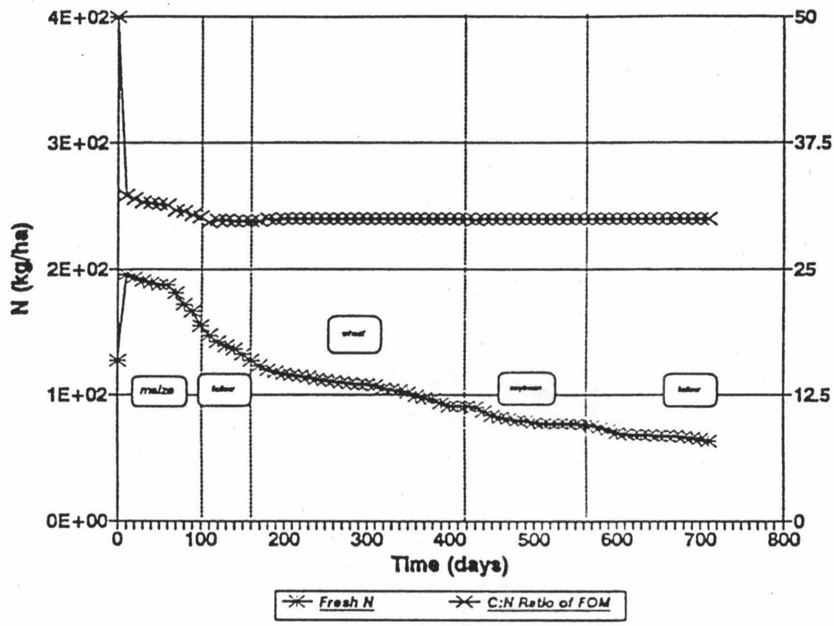

Figure 29.
Soil inorganic N profile during the first six months (A) and the second six months (B) of the third year of a 26-year simulation for management 1.

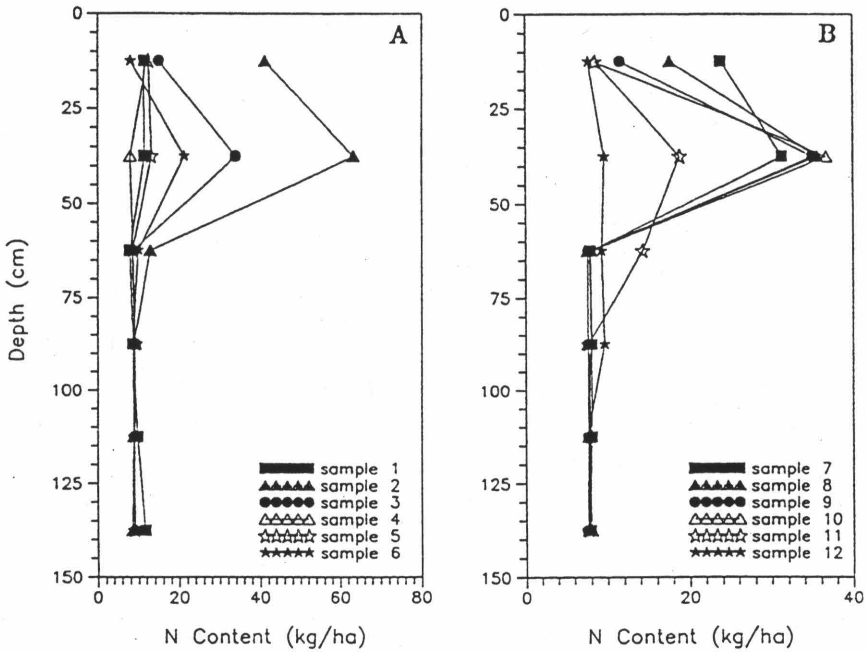

Figure 30.
Organic N mineralization (A) and mineral N denitrification (B) by rotation over a 26-year simulation for both management systems.

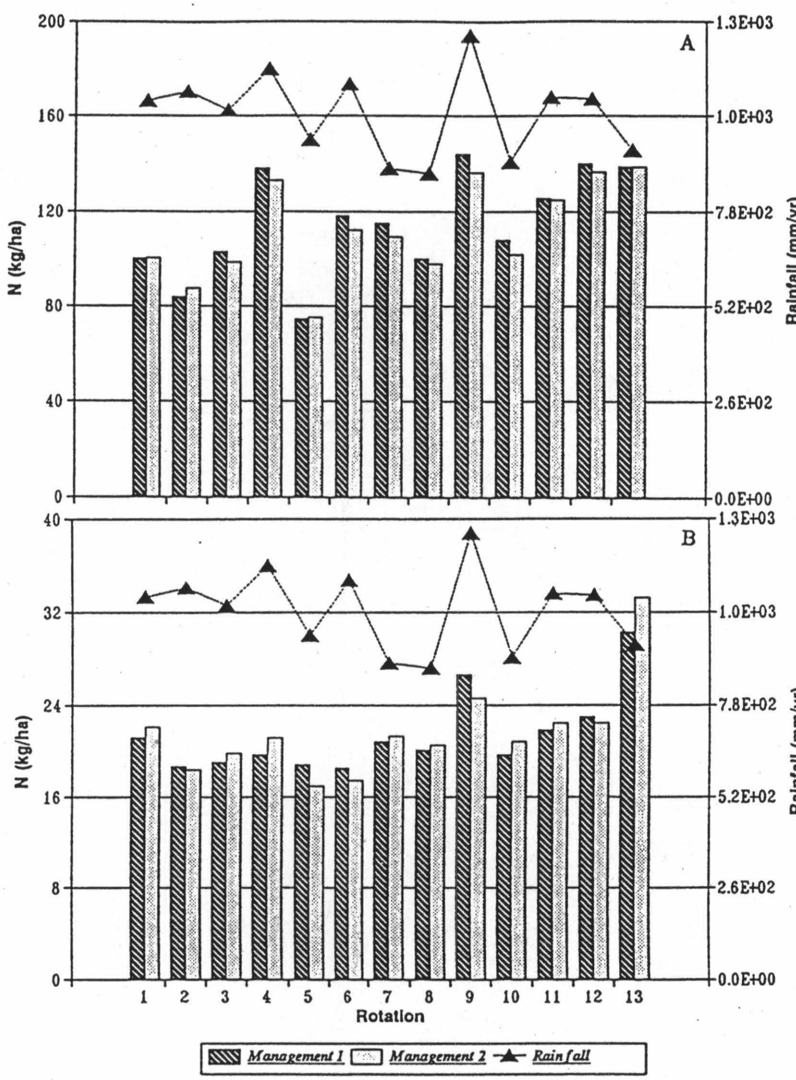

Figure 31.
Nitrogen uptake (A) and N leached (B) by rotation over a 26-year simulation for both management systems.

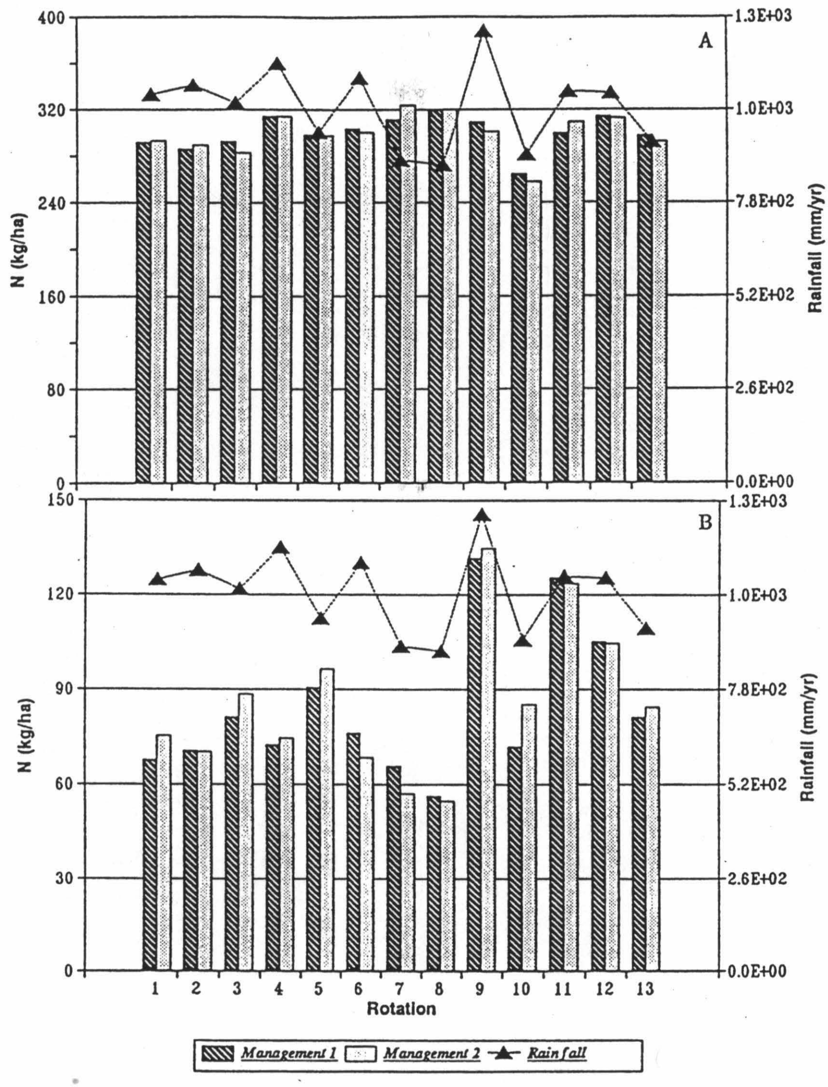

Figure 32.
Mineral N input and output totals and mass balance errors over a 26-year simulation for management 1 (A) and management 2 (B).

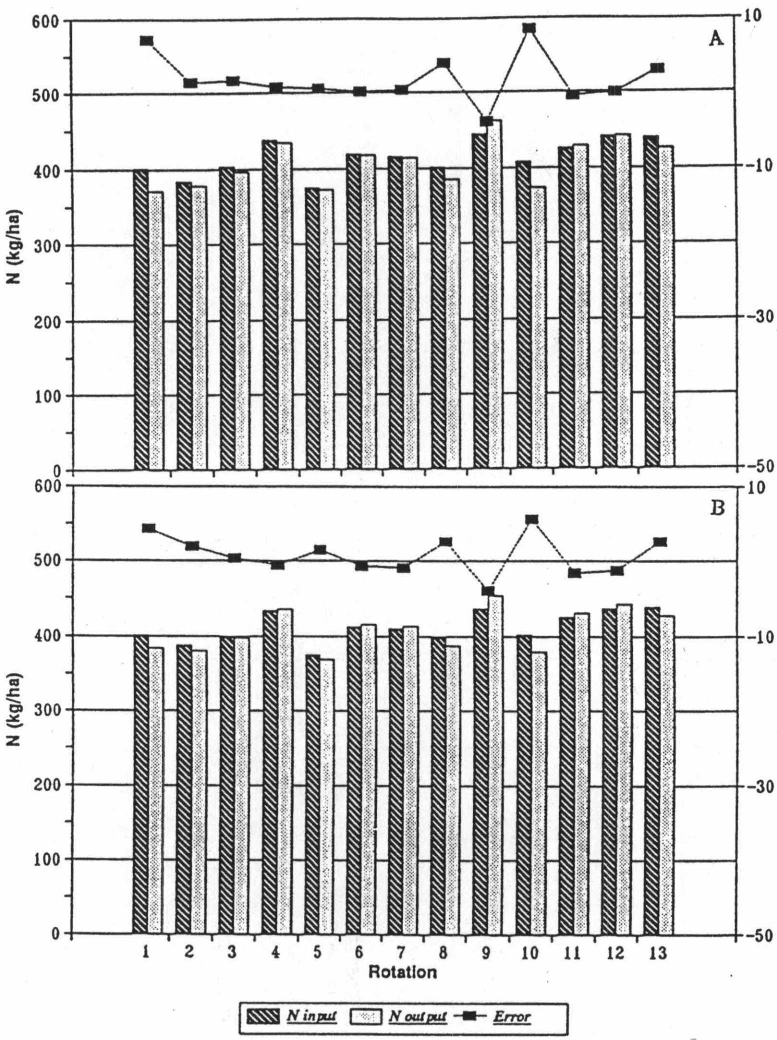

Figure 33.
Typical potential evapotranspiration (Pot Et), transpiration (Transp), soil evaporation (evap), and evapotranspiration (ET) curves over the growing season for maize (A), wheat (B), and soybean (C).

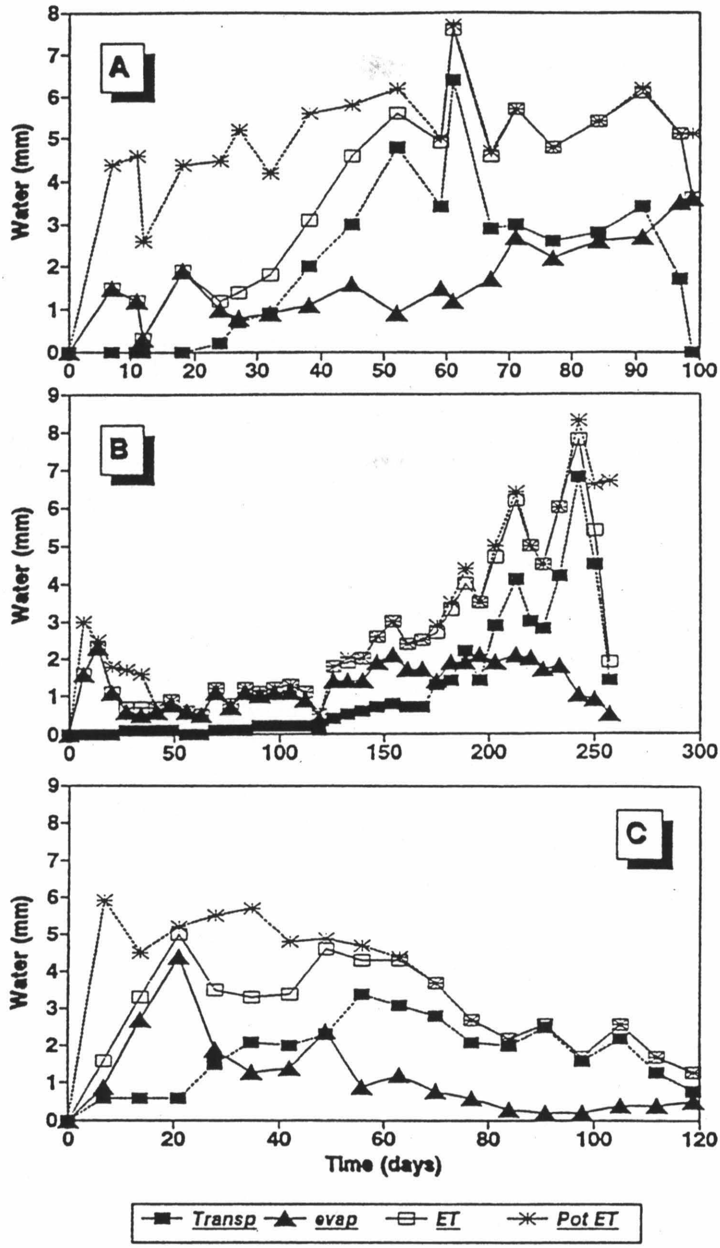

Figure 34.
Crop water budget for the second rotation of management 1 over a 26-year simulation.

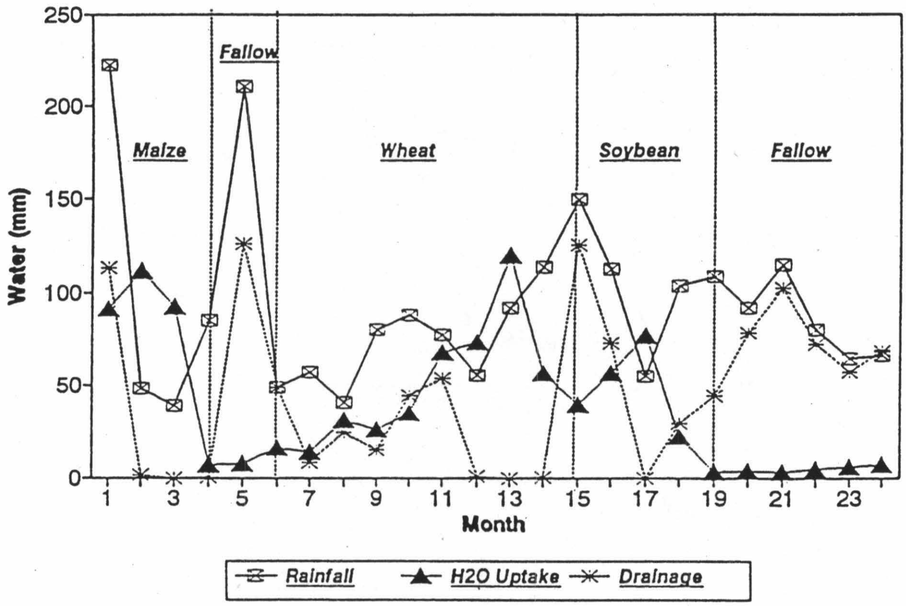

Figure 35.
Hydrologic budget over a 26-year simulation
for management 1 (A) and management 2 (B).

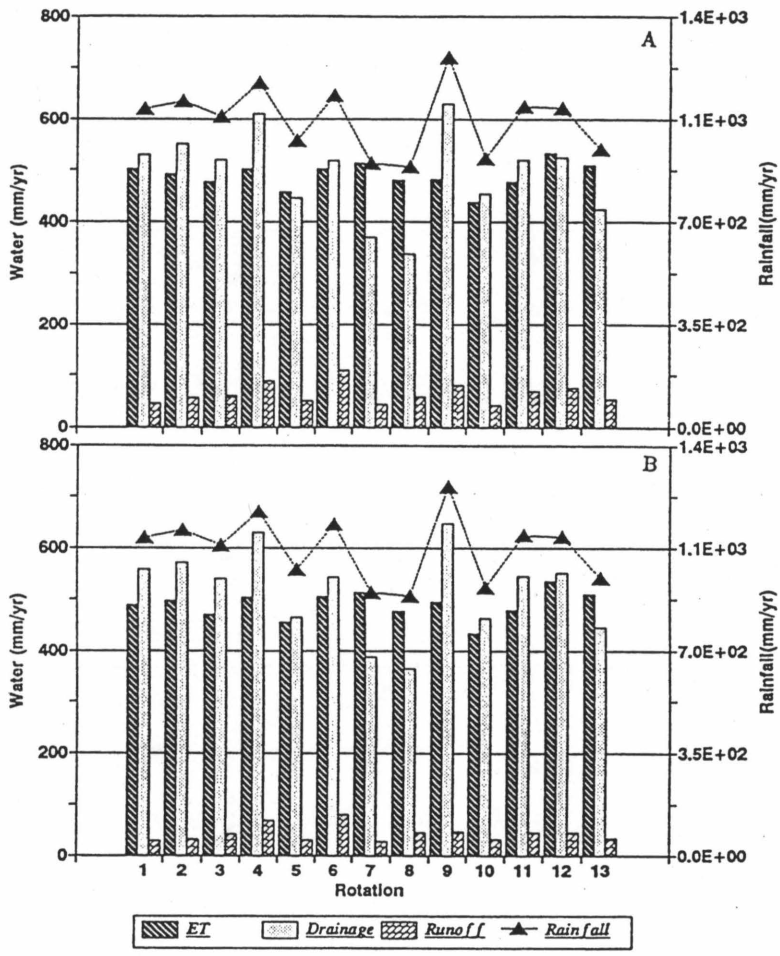

Figure 36.
Monthly soil N content and load over a two-year rotation for 150 kg-N/ha applied to both maize and wheat under management 1 (A) and management 2 (B).

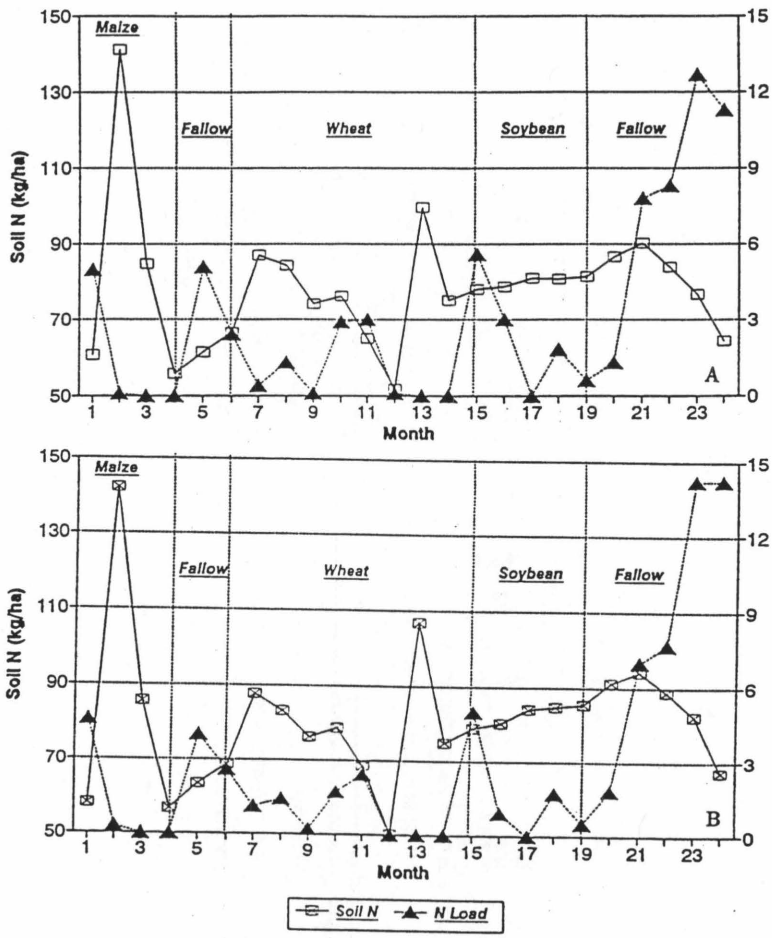

Figure 37.
Relationship between N load, rainfall, and water use (A) or drainage (B) over a two-year rotation for 150 kg-N/ha applied to both maize and wheat under management 1.

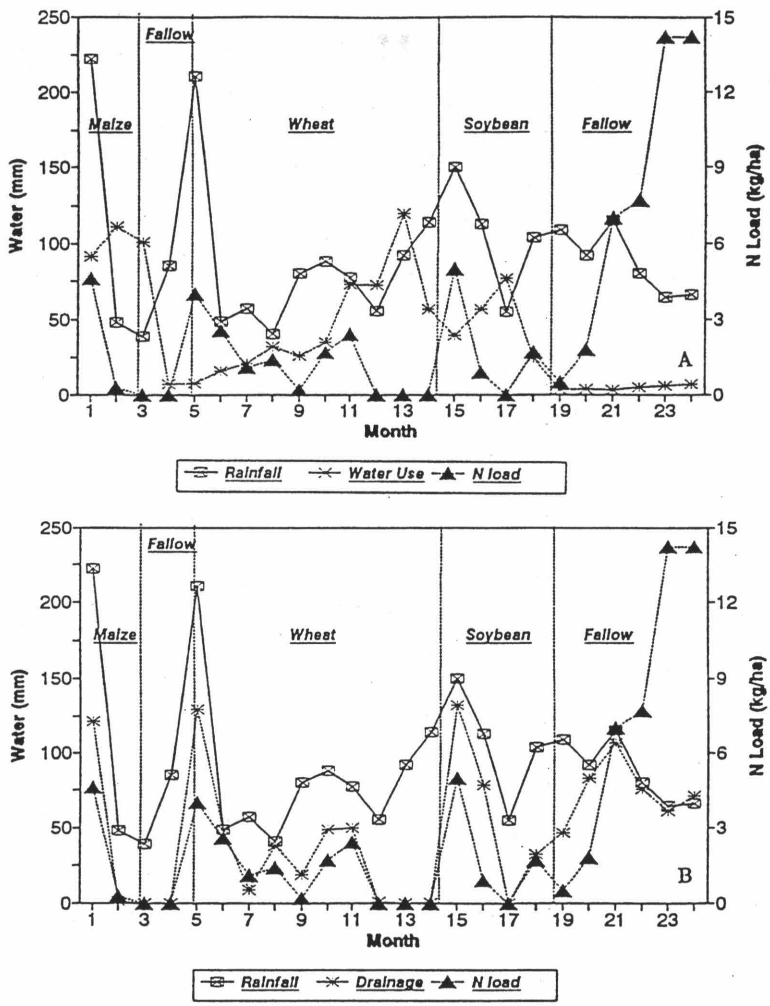

Figure 38.
Summarized N load by four monthly intervals over a two-year rotation for the management systems simulated.

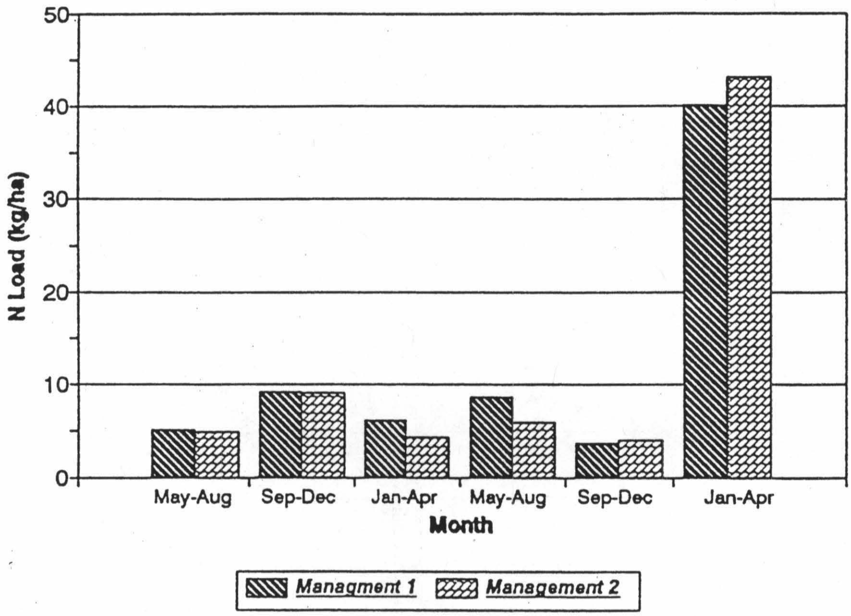

Figure 39.
Relationships between long-term N loads and drainage (A) or water use (B) over a 26-year simulation with 150 kg-N/ha applied per crop of maize and wheat for both management systems.

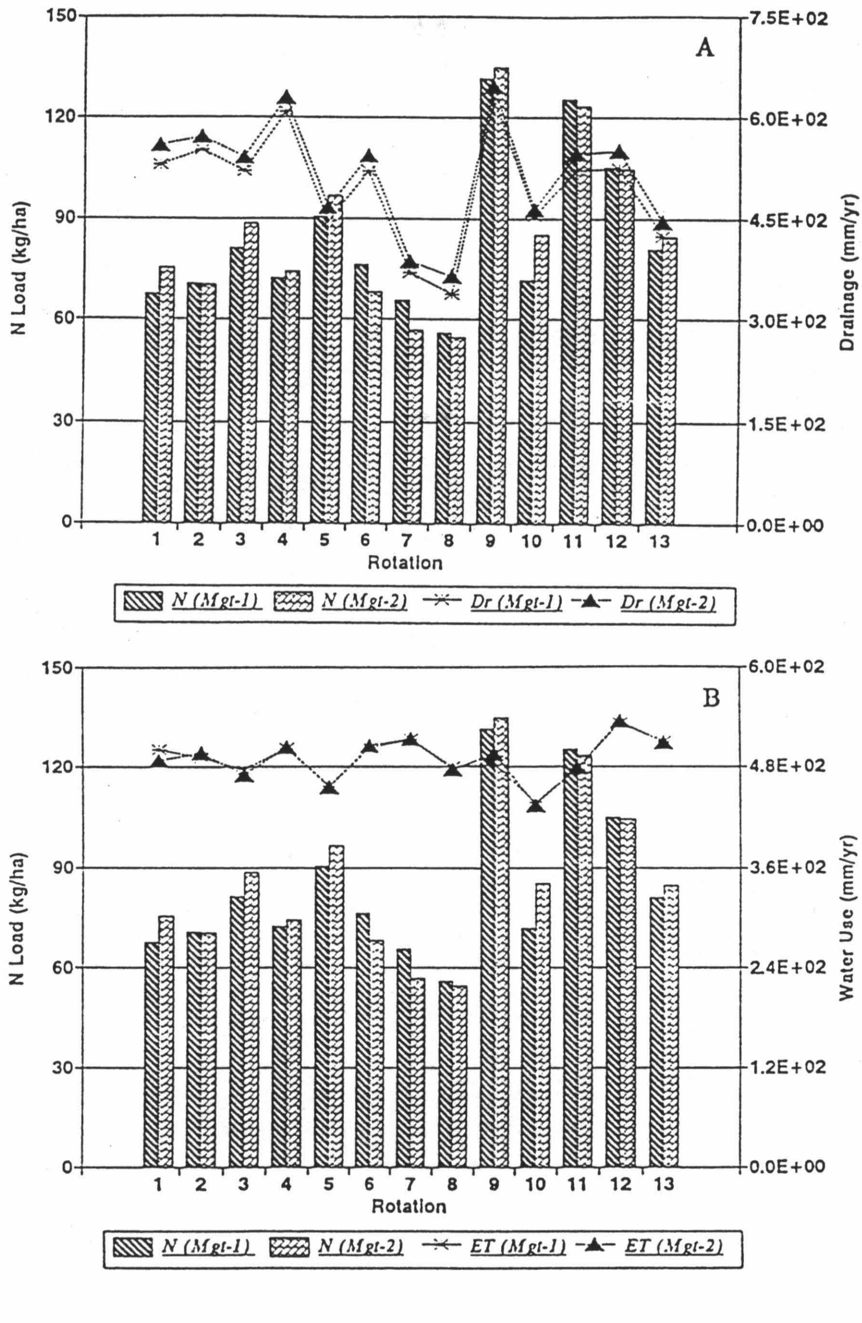

Figure 40.
Sensitivity of maize yields (A) and N uptake (B) to
varying fertilizer amounts under two management scenarios.

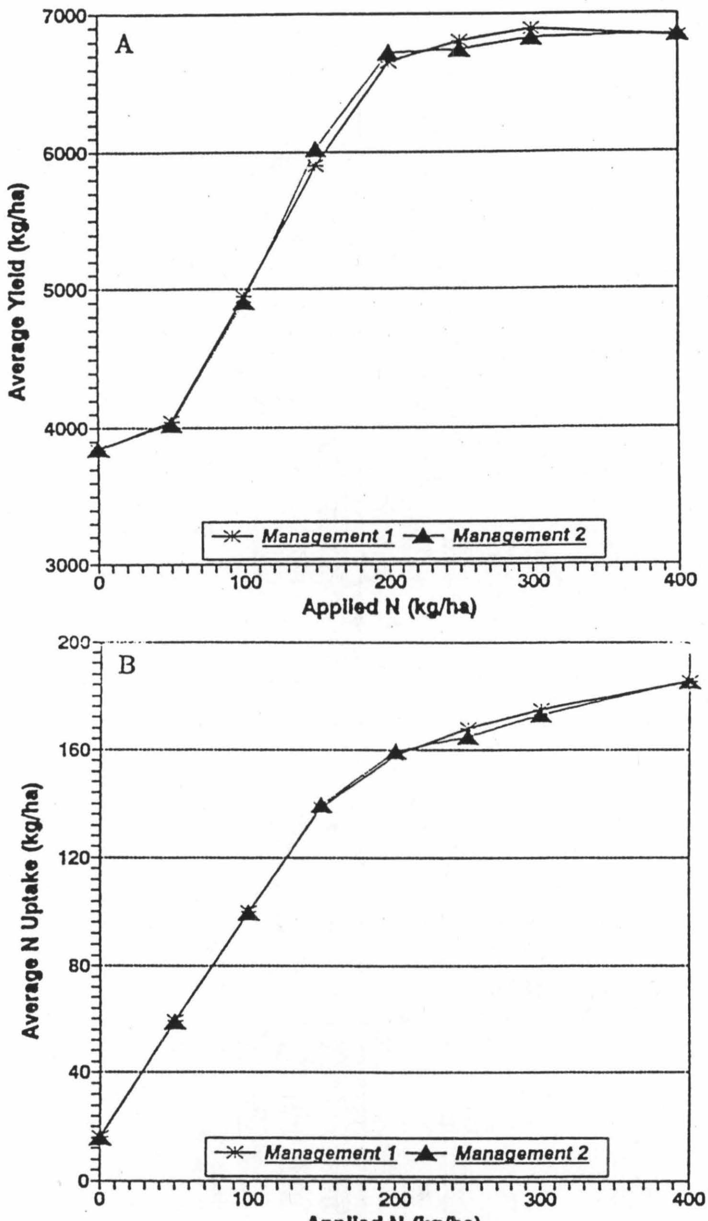

Figure 41.
Sensitivity of wheat yields (A) and N uptake (B) to varying fertilizer amounts under two management scenarios.

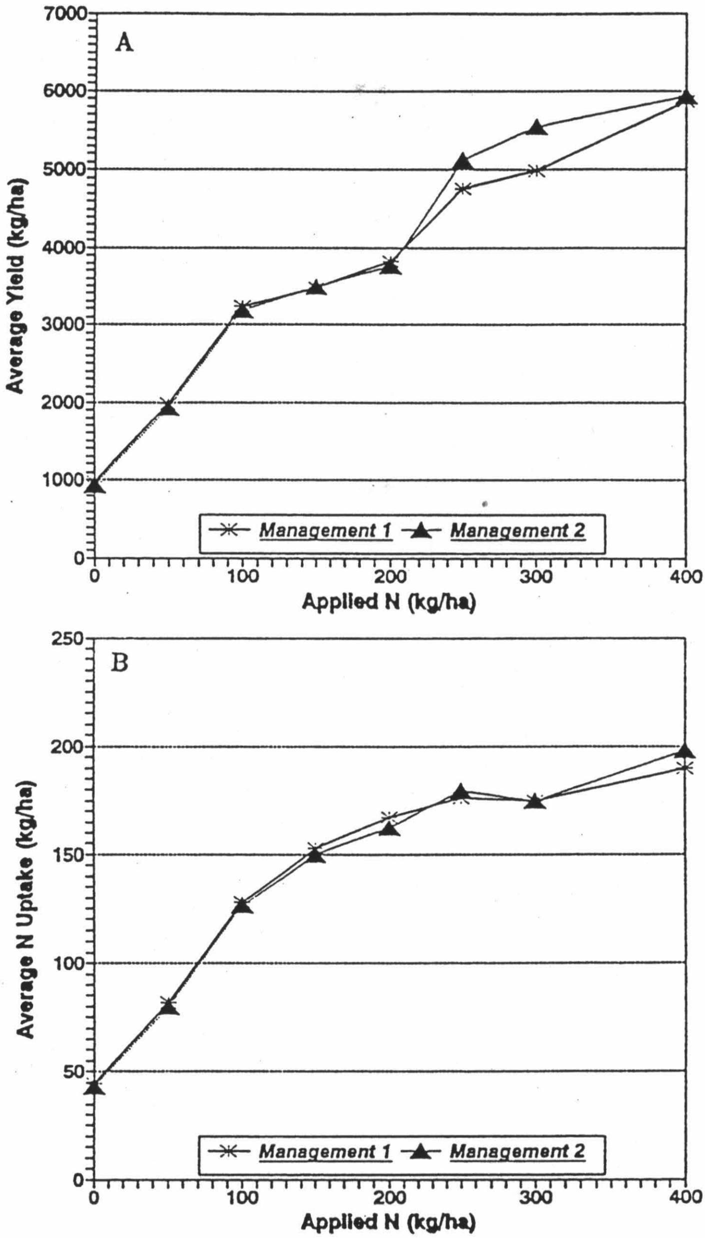

Figure 42.
Average annual soil runoff (A) and crop water use (B) to varying fertilizer amounts under two management scenarios.

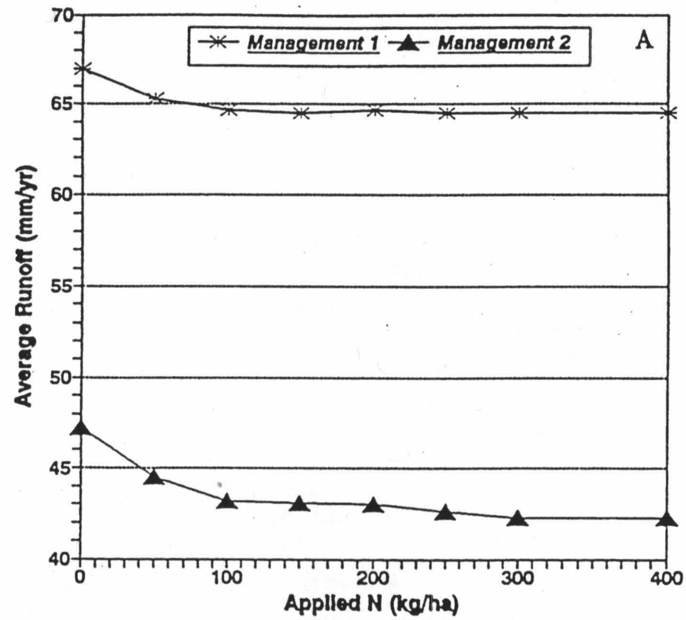

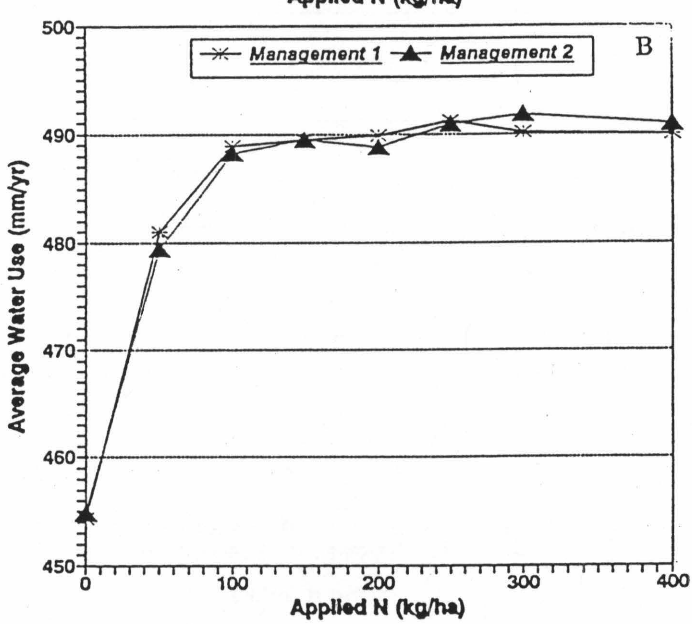

Figure 43.
Average annual drainage to varying fertilizer amounts under two management scenarios.

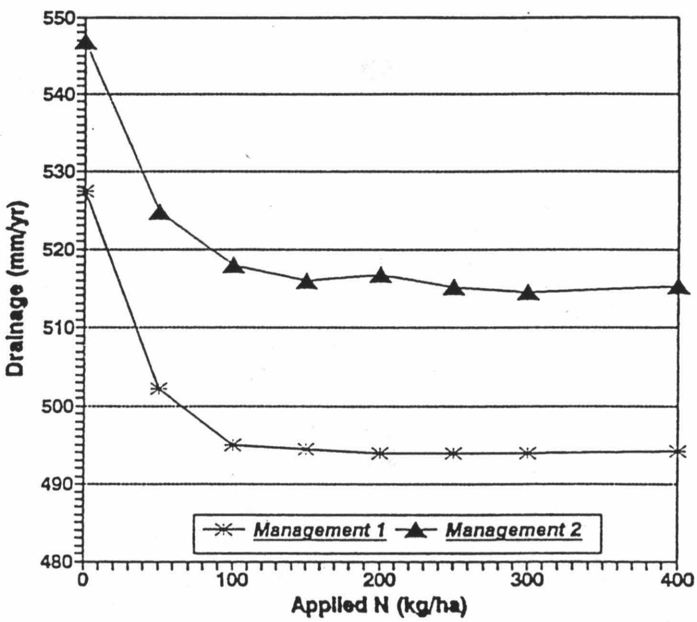

Figure 44.
Average annual N leached (A) and N leached as a percentage of N applied (B) under two management scenarios.

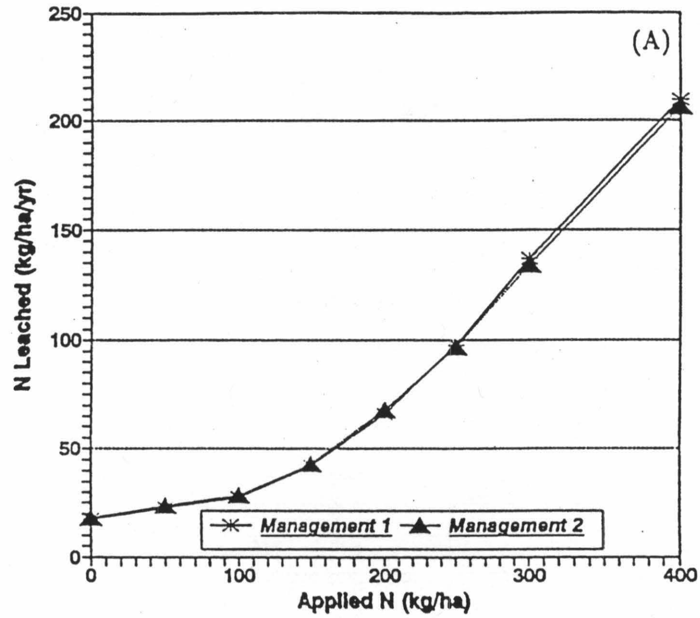

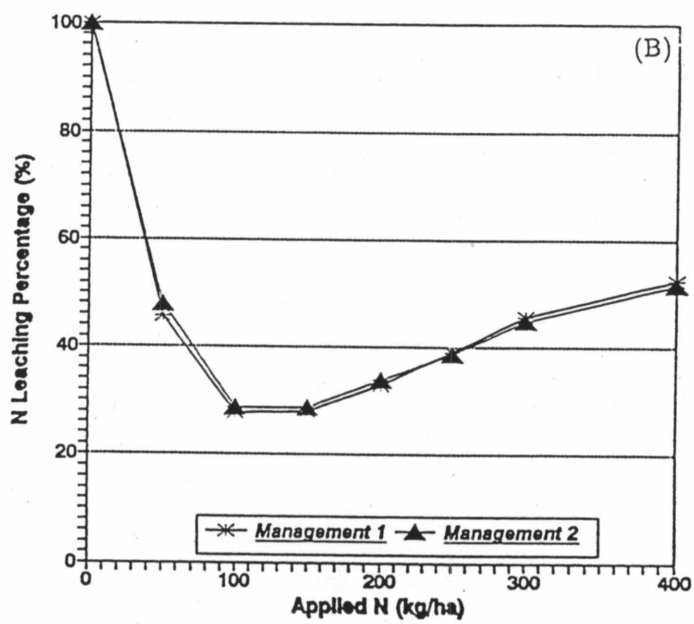

Figure 45.
Mean N leaching percentage for land units over 13 rotations for the management systems simulated.

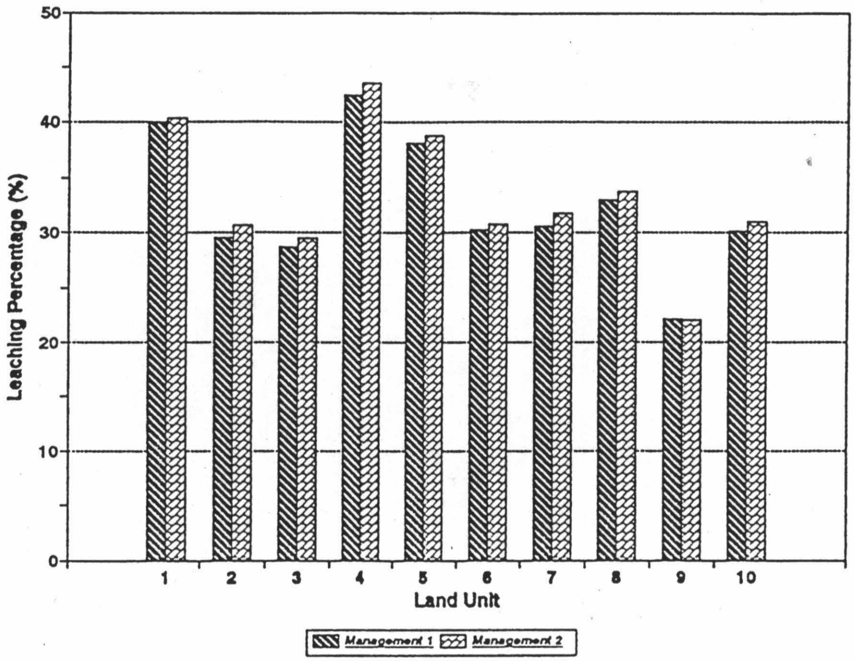

Figure 46.
Mineralization (A) and N uptake (B) over 13 rotations
for sludge simulations.

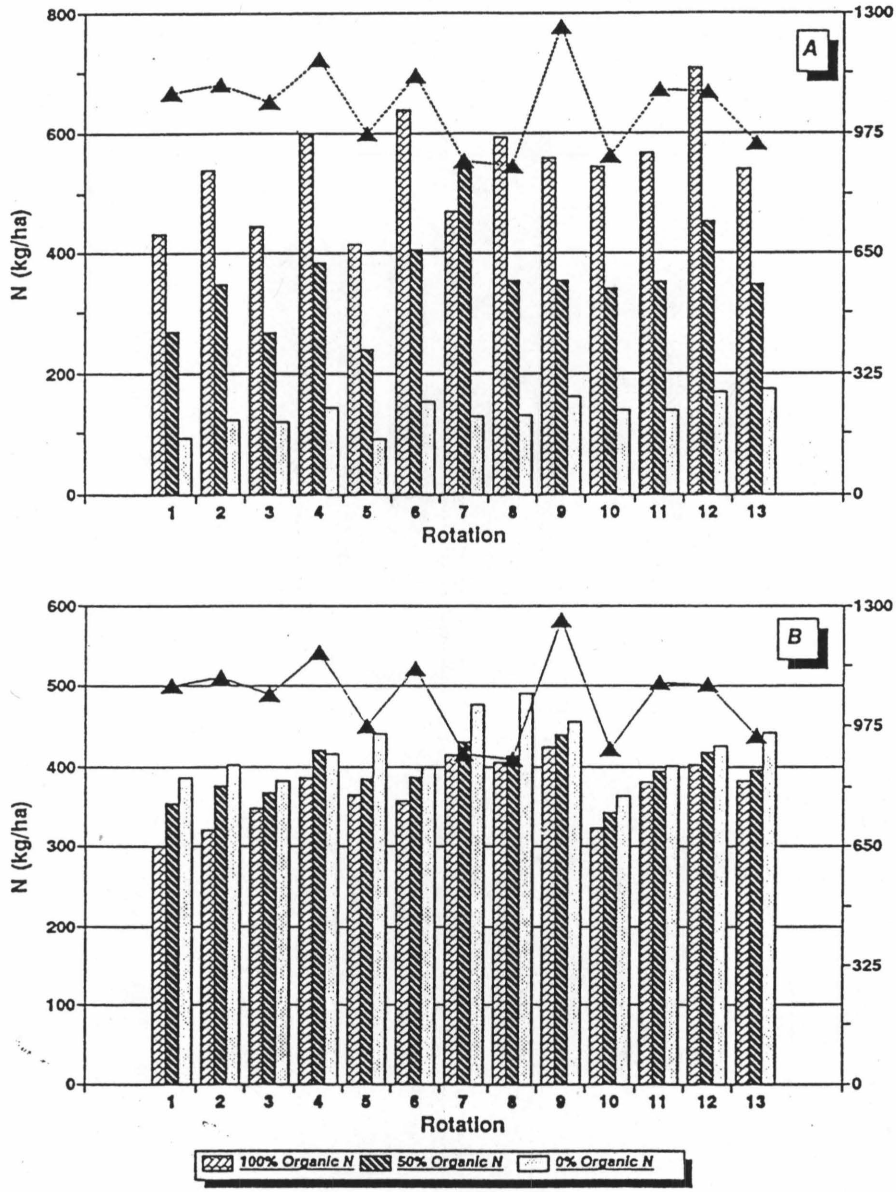

Figure 47.
Nitrogen load (A) and denitrification (B) over 13 rotations for sludge simulations.

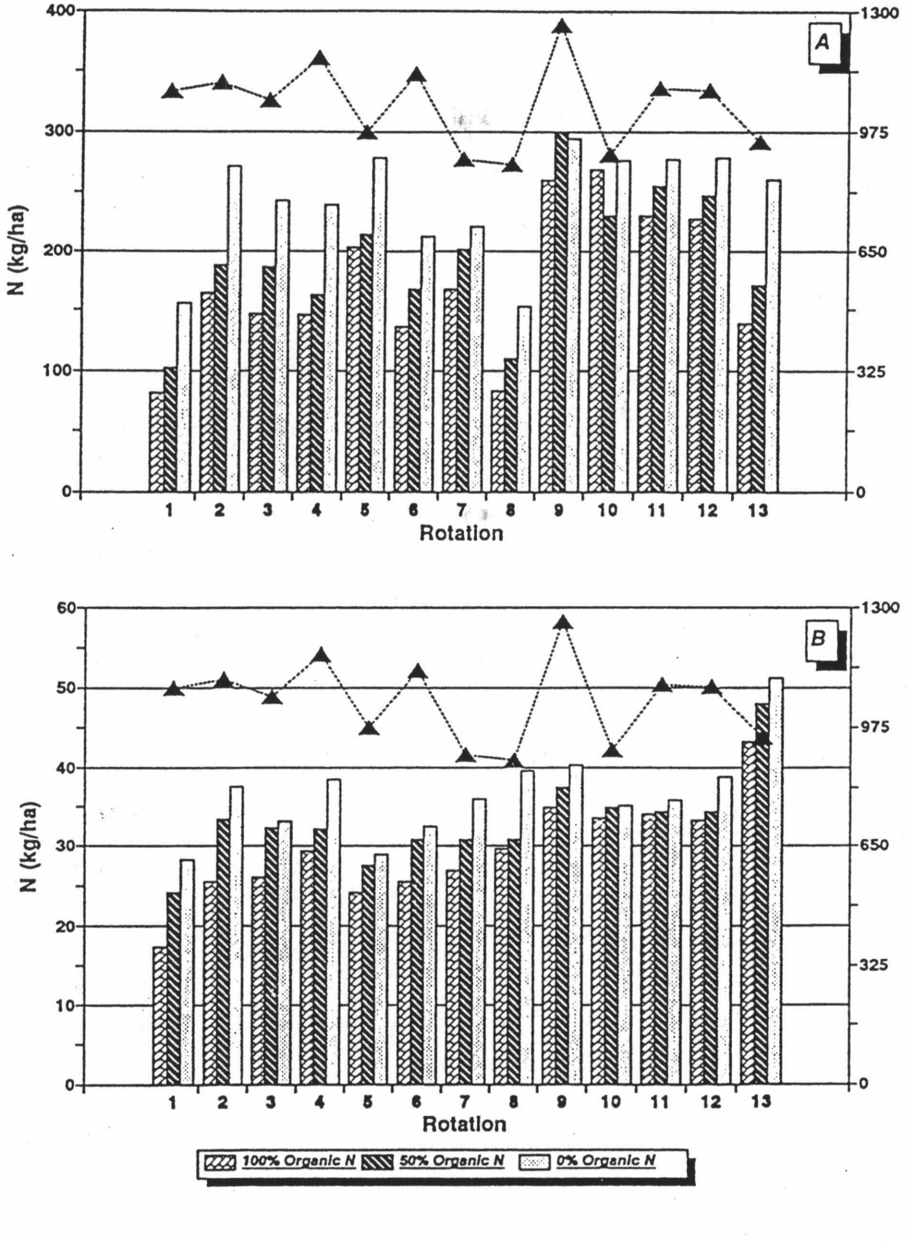

Figure 48.
Monthly soil N content (A) and N leaching (B) over a typical rotation for sludge simulations.

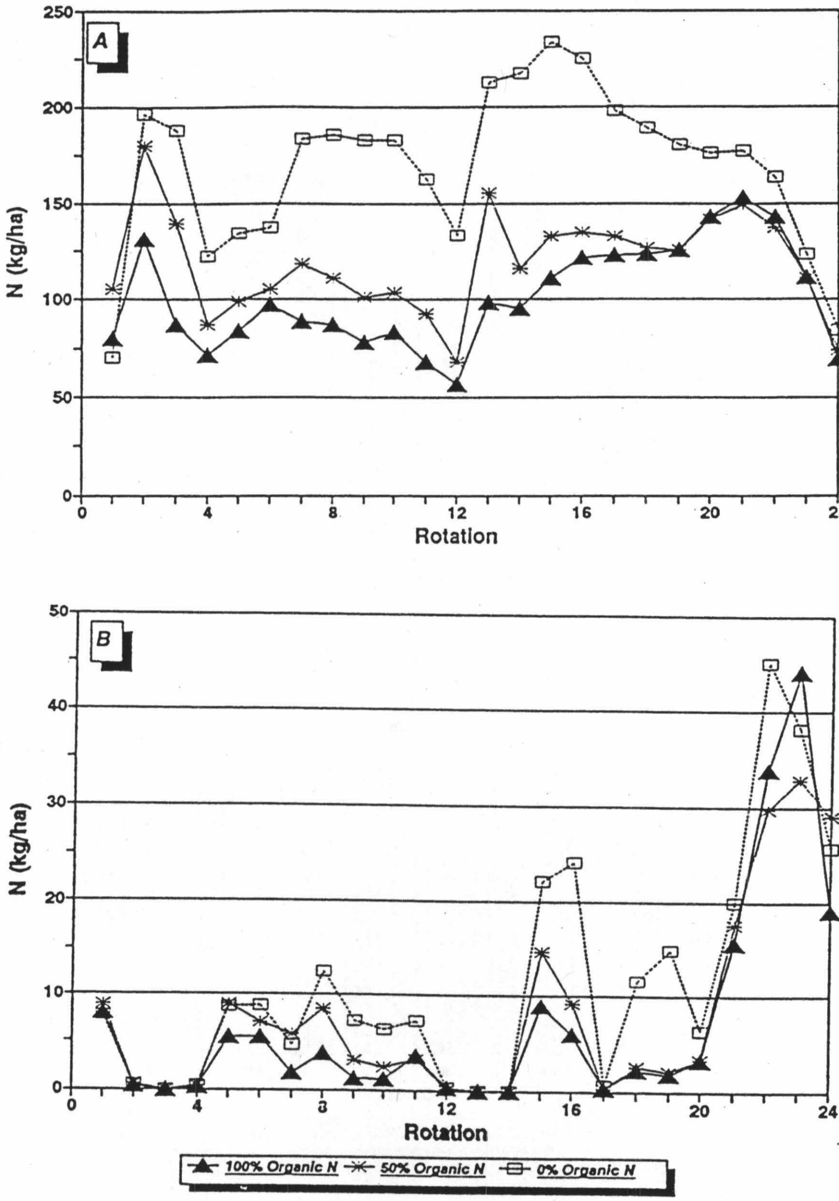

Appendix A: Program Execution and Data File Description

VT-CROPS consists of five FORTRAN files with filenames ONE, TWO, THREE, FOUR, and GENW. Input data are given in 15 input files; results are written in 5 output files. Program execution control under VM-CMS (IBM mainframe) is performed by an EXEC file. The EXEC file performs compilation to generate executable codes (TEXT files), define input/output units, and initiate program execution. A minimum of 7 cylinders of disk space and virtual storage of 1,536 K are required for execution under VM-CMS.

Detailed descriptions of input files are provided here. Examples of input and output files are provided in Appendix B.

File 1: Run Specification File A (Unit 57)

Line #	Variable	Format	Description
1	MXROT	I2	Maximum number of crop rotations to be simulated.
1	IROT	I1	Index for cropping sequence to be simulated. =1 maize-wheat-soybean-fallow =2 continuous maize-fallow =3 maize or wheat validation run
1	KRSV1	I1	Climatic data option. =1 synthetic climatic data =2 climatic data read from input file
1	KYEAR	I2	year to start simulation.

File 2: Run Specification File B (Unit 21)

Line #	Variable	Format	Description
1	KINST	A2	User selected identifier for matching variable INST.
1	KSTAT	A2	Identifier for matching variable STAT.
1	KSID	A2	Identifier for matching variable SITID.
1	KEXPT	I2	Identifier for matching variable EXPT.
1	KTRT	I2	Identifier for matching variable TRT.
1	KYR	I3	Identifier for matching variable IYR.
1	ISWB	I2	Soil water approach index 0 = soil water non-limiting >0 = soil water limiting
1	INIT	I2	Soil nitrogen approach index 0 = nitrogen non-limiting >0 = nitrogen limiting
1	KOUT	I3	Output increment for results.
1	TITLE	A60	Title of simulation experiment.

File 3: Crop Management File (Unit 18)

If IROT = 2 or 3, line one is entered once; if IROT = 1, line one is repeated for wheat and line 3 is entered for soybean. Note that NOL x D is equal to the soil depth (SOLDEP) in file 22. If IROT = 1, NOK x W for maize should be twice that for wheat.

Line #	Variable	Format	Description
1	INST	A2	Identifier for matching KINST
1	SITID	A2	Identifier for matching KSID
1	EXPT	I2	Identifier for matching KEXPT
1	TRT	I2	Identifier for matching KTRT
1	ISOW	I4	Crop sowing date (julian day)
1	ISIM	I4	Simulation starting day (julian day)
1	PLANTS	F6.2	Plant population (plants/sq m)
1	SDEPTH	F5.1	Sowing depth (cm)
1	NOL	I3	Number of rows in matrix
1	NOK	I3	Number of columns in matrix
1	D	F4.1	Depth of each cell in matrix (cm)
1	W	F4.1	Width of each cell in matrix (cm)
1	LAT	F7.2	Latitude of site (degrees)

1	IIRR	I2	Irrigation switch 0 = no irrigation 1 = irrigation schedule supplied 99 = program applies water as needed to root zone
1	KFERT	I2	Nitrogen Fertilization switch 0 = no fertilizer applied 1 = fertilization schedule supplied
1	KVARTY	I3	Variety to be selected from Genetics input file (FT19)
1	NOTIL	I2	Index for tillage practice 0 = minimum till 1 = conventional till
1	STDEP	F6.0	Depth of straw incorporation (cm)
3	INST	A2	Identifier for matching KINST
3	SITID	A2	Identifier for matching KSID
3	EXPT	I2	Identifier for matching KEXPT
3	TRT	I2	Identifier for matching KTRT
3	SDEPTH	F5.1	Sowing depth
3	NOTIL	I2	Index for tillage practice 0 = minimum tillage 1 = conventional tillage

File 4: Weather Data File (Unit 11)

Needed if KRSVI = 1; line occurs once for each day in data file.

Line #	Variable	Format	Description
1	INST (I)	A2	Identifier for matching KINST
1	STAT (I)	A2	Identifier for matching KSTAT
1	MON (I)	I2	Month of year
1	DAY (I)	I2	Day of month
1	IYR (I)	I5	Identifier for matching KYR
1	JUL (I)	I4	Calendar day of year
1	SOLRAD (I)	F7.0	Daily solar radiation (langley/day)
1	XTMAX (I)	F6.1	Daily maximum temperature (C)
1	XTMIN (I)	F6.1	Daily minimum temperature (C)
1	XRAIN (I)	F6.1	Daily rainfall (mm)

File 5: Soil and Site Characteristics File A (Unit 13)

Line #	Variable	Format	Description
1	INST	A2	Identifier for matching KINST
1	SITID	A2	Identifier for matching KSID
1	SALB	F10.2	Soil Albedo
1	U	F7.2	Upper limit of stage-1 drying
1	SWCON	F7.2	
1	CN2	F14.2	Average surface runoff curve number
1	TAV	F6.1	Annual average ambient temperature
1	AMP	F6.1	Annual amplitude in mean monthly temperature
1	DMOD	F5.1	Fraction for reducing average mineralization rate
1	RWUMX	F5.1	
2	SITE	A10	Name of experimental site
2	PEDON	A12	Soil Series name
3	TAXON	A70	Soil family taxonomic classification

File 6: Soil and Site Characteristics File B (Unit 22)

Line #	Variable	Format	Description
1	INST	A2	Identifier for matching KINST
1	SITID	A2	Identifier for matching KSID
1	EXPT	I2	Identifier for matching KEXPT
1	TRT	I2	Identifier for matching KTRT
1	ITER	I4	Number of daily iterations to be performed within each daily time step
1	LYRSOL	I4	Number of soil profile horizons
1	CRTH2O	F6.2	Critical soil moisture content of root zone below which irrigation water is to be applied when irrigation is to be calculated by the program
1	CNF	F4.0	Fallow Runoff Curve Number
1	IWP	I2	Bottom Boundary switch 0 = unit gradient >0 = water table

File 7: Soil Properties File (Unit 23)

1 = 1,LYRSOL

Line #	Variable	Format	Description
1	INST	A2	Identifier for matching KINST
1	SITID	A2	Identifier of matching KSID
1	EXPT	I2	Identifier of matching KEXPT
1	TRT	I2	Identifier of matching KTRT
1	SATK (I)	E10.3	Saturated hydraulic conductivity (cm/day)
1	ALPHA (I)	F9.4	van Genuchten (1980) soil constant (cm^{-1})
1	VN (I)	F9.4	van Genuchten (1980) soil constant
1	SOLDEP (I)	F7.2	Depth to bottom of soil profile layer (cm)
1	THETAS (I)	F5.2	Saturated volumetric soil moisture content (cm^3/cm^3)
1	THETAR (I)	F5.2	Residual volumetric soil moisture content (cm^3/cm^3)
1	BD (I)	F5.2	Bulk density (g/cm^3)

File 8: Initial Soil Conditions File (Unit 25)

1 = 1,LYRSOL

Line	Variable	Format	Description
1	INST	A2	Identifier for matching KINST
1	SITID	A2	Identifier of matching KSID
1	EXPT	I2	Identifier of matching KEXPT
1	TRT	I2	Identifier of matching KTRT
1	VH2OI (I)	F10.3	Initial volumetric soil moisture content (cm^3/cm^3)
1	NH4 (I)	F5.1	Initial ammonium concentration (g elemental N/Mg soil)
1	NO3 (I)	F5.1	Initial nitrate concentration (g elemental N/Mg soil)
1	PH (I)	F5.1	Initial soil pH
1	OC (I)	F5.1	Initial percent organic carbon (%)

File 9: Irrigation Scheduling File (Unit 16)

Need only if IIRR $\neq$ 0; I = 1, number of irrigations

Line #	Variable	Format	Description
1	INST	A2	Identifier for matching KINST
1	SITID	A2	Identifier of matching KSID
1	EXPT	I2	Identifier of matching KEXPT
1	TRT	I2	Identifier of matching KTRT
1	JDAY (I)	I4	Day of irrigation application (calendar day)
1	AIRR (I)	F4.0	Amount of irrigation water applied (mm)

File 10: Nitrogen Dynamics File (Unit 14)

Line #	Variable	Format	Description
1	INST	A2	Identifier for matching KINST
1	SITID	A2	Identifier of matching KSID
1	EXPT	I2	Identifier of matching KEXPT
1	TRT	I2	Identifier of matching KTRT
1	STRAW	F6.0	Amount of straw residue incorporated into surface (kg/ha)
1	SCN	F6.0	Carbon nitrogen ratio of incorporated straw (g carbon/g nitrogen)
1	ROOT	F6.0	Weight of roots left from previous crop (kg/ha)
1	RCN	F6.0	Carbon nitrogen ratio of roots left from previous crop (g carbon/g nitrogen)
1	MINMET	I3	Indicator for choice of mineralization method 1=Method 1 (PAPRAN) 2=Method 2 (VTCROPS)
1	DMOD1	F5.2	Factor for adjusting humus mineralization rate
1	DMOD2	F5.2	Factor for adjusting fresh organic matter mineralization rate-method 2

1	MINZ	I3	Indicator variable 1=incorporation of sludge or other organic material
2	NMDAT	I5	Date to incorporate sludge for maize crop
2	NOMDAT	I5	Date to incorporate sludge for wheat crop
2	OMMZ	F6.2	Mass of sludge for maize (kg/ha)
2	SCNMZ	F6.2	C-N ratio of sludge for maize crop
2	OMWT	F6.2	Mass of sludge for wheat (kg/ha)
2	SCNMZ	F6.2	C-N ratio of sludge for wheat crop

File 11: Nitrogen Fertilizer Scheduling File (Unit 24)

I = 1, number of fertilizer applications

Line #	Variable	Format	Description
1	INST	A2	Identifier for matching KINST
1	SITID	A2	Identifier of matching KSID
1	EXPT	I2	Identifier of matching KEXPT
1	TRT	I2	Identifier of matching KTRT
1	JFDAY (I)	I4	Day of fertilizer application (calendar day)
1	AFERT (I)	F6.1	Amount of nitrogen fertilizer applied (kg/ha)
1	DFERT (I)	F6.1	Depth of fertilizer incorporation (cm)
1	IFTYPE (I)	I3	Type of fertilizer applied 1 = urea 2 = ammonium nitrate 3 = anhydrous ammonia 4 = ammonium nitrate of lime 5 = other nitrate salts
1	BAND (I)	F6.1	Distance from plant band of fertilizer is applied (cm)
1	JK1	I3	Indicator variable, when not equal to the crop number being simulated stops data file from being read

File 12: Maize Genetic Specifications Data Base File (Unit 19)

Needed if maize is being simulated; line one occurs once for each variety in the data base.

Line #	Variable	Format	Description
1	IVARTY (I)	I4	Data base identifier for matching with user selected variety KVARTY
1	VARTY (I)	1X,A16	Variety name
1	P1 (I)	F6.2	Growing degree days at base temperature 8 C accumulated through growth stage 1
1	P2 (I)	F5.3	Photoperiod sensitivity coefficient
1	P5 (I)	F6.1	Growing degree days at base temp-ature 8 C accumulated through growth stages 4, 5, and 6
1	G2 (I)	F6.1	Maximum kernal number (kernal/plant)
1	G3 (I)	F6.2	Potential maximum kernal growth rate (mg/(kernal day))

File 13: Wheat Genetic Specifications Data Base File (Unit 37)

Needed if maize is being simulated; line one occurs once for each variety in the data base.

Line #	Variable	Format	Description
1	IVARTY (I)	I4	Data base identifier for matching with user selected variety KVARTY
1	VARTY (I)	A16	Variety name
1	P1V (I)	F6.2	Wheat Genetic constant
1	P10 (I)	F5.3	Wheat Genetic constant
1	P5 (I)	F6.1	Wheat Genetic constant
1	G2 (I)	F6.1	Wheat Genetic constant
1	G3 (I)	F6.2	Wheat Genetic constant
1	G4 (I)	F6.2	Wheat Genetic constant
1	G5 (I)	F6.2	Wheat Genetic constant

File 14: Validation Data File (Unit 30)

File optional; used only for maize validation runs.

Line #	Variable	Format	Description
1	INST	A2	Identifier for matching KINST
1	SITID	A2	Identifier of matching KSID
1	EXPT	I2	Identifier of matching KEXPT
1	TRT	I2	Identifier of matching KTRT
1	XYIELD	F6.0	Measured yield at 15 percent moisture (Kg/ha)
1	XGRWT	F6.4	Measured average grain weight (g/kernal)
1	XGPSM	F5.0	Measured average grains per square meter (grains/sq m)
1	XGPE	F4.0	Measured average grains per ear (grains/ear)
1	XLAI	F5.2	Measured final LAI (sq m/sq m)
1	XBIOM	F6.2	Measured final biomass (kg/ha)
1	XSTRAW	F7.1	Measured final stover weight (kg/ha)
1	ISLKJD	I4	Measured silking date (calendar day)
1	MATJD	I4	Measured maturity date (calendar day)

1	GRPCTN	F6.2	Measured grain nitrogen percent (%)
1	XTOTNP	F6.2	Measured total N uptake (kg/ha)
1	XAPTNP	F6.2	
1	XGNUP	F6.2	Observe given N (g/plant)

File 15: Validation Data File (Unit 40)

File optional; used only for wheat validation runs.

Line #	Variable	Format	Description
1	INST	A2	Identifier for matching KINST
1	SITID	A2	Identifier of matching KSID
1	EXPT	I2	Identifier of matching KEXPT
1	TRT	I2	Identifier of matching KTRT
1	XYIELD	F6.0	Measured yield at 15 percent moisture (Kg/ha)
1	XGRWT	F6.4	Measured average grain weight (g/kernal)
1	XGPSM	F5.0	Measured average grains per square meter (grains/sq m)
1	XGPE	F4.0	Measured average grains per ear (grains/ear)
1	XLAI	F5.2	Measured final LAI (sq m/sq m)
1	XBIOM	F6.2	Measured final biomass (kg/ha)
1	XSTRAW	F7.1	Measured final stover weight (kg/ha)
1	ISLKJD	I4	Measured silking date (calendar day)
1	MATJD	I4	Measured maturity date

			(calendar day)
1	GRPCTN	F6.2	Measured grain nitrogen percent (%)
1	XTOTNP	F6.2	Measured total N uptake (kg/ha)
1	XAPTNP	F6.2	
1	XGNUP	F6.2	Observe given N (g/plant)

File 16: Climatic Parameter File (Unit 5)

Needed when KRSV1 = 0; line 1 is repeated once for each month of the year, i.e., I=1,12.

Line #	Variable	Format	Description
1	IYR	A3	Number of years to generate climatic data
2	SHAPE(I)	F6.4	Monthly rainfall shape parameter
2	SCALE(I)	F6.4	Monthly rainfall scale parameter
2	PWW	F6.4	Probability of a wet day following a wet day
2	PWD	F6.4	Probability of a wet day following a dry day
3	TXMD	F6.2	Average daily maximum temperature on a dry day
3	ATXD	F6.2	Amplitude of daily maximum temperature on a dry day
3	CVTXD	F6.3	Average coefficient of variation (CV) of maximum temperature on dry day
3	ACTXD	F7.3	Amplitude of CV of maximum temperature on a dry day
4	TXMW	F6.2	Average daily maximum temperature on a wet day
4	ATXW	F6.2	Amplitude of daily maximum

			temperature on a wet day
4	CVTXW	F6.3	Average coefficient of variation (CV) of maximum temperature on dry day
4	ACTXW	F7.3	Amplitude of CV of maximum temperature on a wet day
5	TMNMD	F6.2	Average daily minimum temperature on a dry day
5	ATMND	F6.2	Amplitude of daily minimum temperature on a dry day
5	CVTMND	F6.3	Average coefficient of variation (CV) of minimum temperature on dry day
5	ACTMND	F7.3	Amplitude of CV of minimum temperature on a dry day
6	TMNMW	F6.2	Average daily minimum temperature on a wet day
6	ATMNW	F6.2	Amplitude of daily minimum temperature on a wet day
6	CVTMNW	F6.3	Average coefficient of variation of minimum temperature on dry day
6	ACTMNW	F7.3	Amplitude of CV of minimum temperature on a wet day
7	RMD	F6.2	Average daily solar radiation on a dry day

7	ARD	F6.3	Amplitude of daily solar radiation on a dry day
7	CVRD	F6.3	Average coefficient of variation of daily solar radiation on dry day
7	ACVRD	F7.3	Amplitude of CV of daily solar radiation on a dry day
8	RMW	F6.2	Average daily solar radiation on a wet day
8	ARW	F6.3	Amplitude of daily solar radiation on a wet day
8	CVRW	F6.3	Average coefficient of variation of daily solar radiation on wet day
8	ACVRW	F7.3	Amplitude of CV of daily solar radiation on a wet day

Appendix B:
Measured and Predicted Soil Nitrogen Distribution from Validation Analyses

Table B1.
Blacksburg - soil nutrient content,
October 1986 (measured vs. predicted).

Depth (cm)	Treatment 0 kg N/ha			
	Conventional Till (kg/ha)		No-Till (kg/ha)	
	Measured	Predicted	Measured	Predicted
6	25.61	4.54	35.46	4.64
18.5	27.30	5.64	17.41	4.32
32.5	11.15	13.18	5.13	10.99
47.5	13.25	63.74	4.04	55.73
62.5	54.16	51.82	22.13	49.12
77.5	22.02	44.75	14.67	42.55
92.5	14.02	31.86	6.41	32.99
115.0	22.91	18.26	23.25	18.44
145.0	27.17	19.54	23.75	18.99
175.0	40.70	23.00	41.86	23.68
Total	258.29	276.4	239.65	261.41

Table B2.
Blacksburg - soil nitrogen content,
October 1986 (measured vs. predicted).

Depth (cm)	Treatment 75 kg N/ha			
	Conventional Till (kg/ha)		No-Till (kg/ha)	
	Measured	Predicted	Measured	Predicted
6	24.03	7.09	30.63	5.60
18.5	36.28	17.69	14.59	11.85
32.5	15.87	16.08	6.69	15.01
47.5	20.64	78.00	8.06	77.83
62.5	17.49	58.42	8.94	61.72
77.5	9.20	41.25	9.54	38.62
92.5	9.81	16.05	9.23	16.34
115.0	17.42	15.14	27.37	13.39
145.0	16.85	17.23	26.08	18.99
175.0	31.90	20.11	22.67	20.12
Total	199.49	287.1	163.8	279.47

Table B3.
Blacksburg - soil nitrogen content,
October 1986 (measured vs. predicted).

Depth (cm)	Treatment 150 kg N/ha			
	Conventional Till (kg/ha)		No-Till (kg/ha)	
	Measured	Predicted	Measured	Predicted
6	43.65	8.65	30.90	11.43
18.5	56.06	29.54	19.40	32.38
32.5	95.84	19.17	12.61	43.26
47.5	75.72	67.0	20.80	58.13
62.5	20.91	47.82	19.26	25.98
77.5	22.55	35.09	12.32	30.60
92.5	13.38	18.28	12.18	13.63
115.0	32.08	48.33	26.46	47.91
145.0	86.62	55.75	39.37	58.07
175.0	53.26	65.48	34.69	64.31
Total	500.07	395.1	227.99	385.7

Table B4.
Blacksburg - soil nitrogen content,
October 1986 (measured vs. predicted).

Depth (cm)	Treatment 225 kg N/ha			
	Conventional Till (kg/ha)		No-Till (kg/ha)	
	Measured	Predicted	Measured	Predicted
6	36.15	18.22	37.70	16.19
18.5	95.98	70.99	31.70	53.0
32.5	51.60	37.56	37.48	69.56
47.5	65.10	112.73	53.57	99.93
62.5	42.03	54.72	28.98	39.67
77.5	33.64	22.44	25.44	23.55
92.5	18.02	12.47	20.57	20.48
115.0	53.84	38.99	33.65	39.12
145.0	30.75	42.63	39.96	43.07
175.0	28.53	34.04	38.23	34.20
Total	455.64	444.8	347.28	438.77

Table B5.
Blacksburg - soil nitrogen content, October 1987 (measured vs. predicted).

Depth (cm)	Treatment 0 kg N/ha			
	Conventional Till (kg/ha)		No-Till (kg/ha)	
	Measured	Predicted	Measured	Predicted
6	25.65	10.51	35.76	15.63
18.5	21.64	6.02	20.82	10.09
32.5	10.47	4.55	10.33	3.51
47.5	10.59	7.63	8.43	5.34
62.5	19.00	3.78	14.77	3.66
77.5	34.04	3.69	26.59	3.12
92.5	26.81	3.69	22.62	3.51
115.0	28.31	9.54	34.51	8.01
145.0	29.36	27.02	33.14	22.51
175.0	51.60	25.19	61.73	26.95
Total	257.47	101.61	268.7	102.33

Table B6.
Blacksburg - soil nitrogen content, October 1987 (measured vs. predicted).

Depth (cm)	Treatment 75 kg N/ha			
	Conventional Till (kg/ha)		No-Till (kg/ha)	
	Measured	Predicted	Measured	Predicted
6	21.24	60.08	35.54	30.98
18.5	29.02	4.83	33.11	3.20
32.5	24.49	4.88	16.99	2.94
47.5	10.76	7.68	19.46	5.40
62.5	13.08	3.84	14.54	4.02
77.5	8.65	3.63	11.56	3.66
92.5	14.06	3.81	16.37	3.93
115.0	30.14	11.92	36.18	10.67
145.0	32.34	30.76	36.62	23.14
175.0	54.25	44.34	47.55	34.26
Total	238.03	175.77	267.92	122.2

Table B7.
Blacksburg - soil nitrogen content,
October 1987 (measured vs. predicted).

Depth (cm)	Treatment 150 kg N/ha			
	Conventional Till (kg/ha)		No-Till (kg/ha)	
	Measured	Predicted	Measured	Predicted
6	35.26	91.64	26.94	112.11
18.5	39.05	4.82	33.17	6.33
32.5	15.73	4.63	21.36	4.64
47.5	11.55	5.48	24.10	5.52
62.5	26.04	3.69	34.11	3.75
77.5	26.16	3.93	31.24	3.42
92.5	16.70	3.78	21.97	3.78
115.0	41.53	11.43	33.57	9.37
145.0	31.79	30.82	31.33	19.63
175.0	37.86	42.21	42.72	28.54
Total	281.67	202.43	300.51	197.09

Table B8.
Blacksburg - soil nitrogen content, October 1987 (measured vs. predicted).

Depth (cm)	Treatment 225 kg N/ha			
	Conventional Till (kg/ha)		No-Till (kg/ha)	
	Measured	Predicted	Measured	Predicted
6	34.38	173.26	52.17	201.91
18.5	36.32	11.52	41.79	9.92
32.5	29.63	5.82	33.83	4.65
47.5	18.09	8.00	27.60	14.47
62.5	24.43	3.69	25.89	15.22
77.5	32.24	3.93	33.28	11.18
92.5	15.48	3.98	21.87	7.14
115.0	23.79	18.73	30.80	13.92
145.0	24.87	26.00	31.58	24.78
175.0	33.93	25.57	52.05	31.23
Total	273.16	280.5	350.86	334.42

Table B9.
Blacksburg - soil nitrogen content, October 1988 (measured vs. predicted).

Depth (cm)	Treatment 0 kg N/ha			
	Conventional Till (kg/ha)		No-Till (kg/ha)	
	Measured	Predicted	Measured	Predicted
6	16.10	4.32	30.62	5.02
18.5	19.65	4.84	15.20	4.96
32.5	10.36	3.10	8.73	3.17
47.5	6.76	5.75	8.63	5.78
62.5	9.97	4.24	7.27	4.02
77.5	18.34	5.00	15.21	3.50
92.5	15.07	4.64	16.42	3.44
115.0	25.66	17.96	34.15	10.20
145.0	28.68	22.20	23.62	17.39
175.0	31.70	24.31	23.80	35.3
Total	182.29	96.36	183.65	92.78

Table B10.
Blacksburg - soil nitrogen content,
October 1988 (measured vs. predicted).

Depth (cm)	Treatment 75 kg N/ha			
	Conventional Till (kg/ha)		No-Till (kg/ha)	
	Measured	Predicted	Measured	Predicted
6	16.92	9.21	14.39	12.33
18.5	14.74	14.77	11.83	9.26
32.5	9.81	5.20	5.48	3.15
47.5	5.94	5.35	4.79	5.67
62.5	19.68	3.90	5.67	5.09
77.5	21.68	6.54	10.97	11.42
92.5	15.88	5.49	13.41	9.54
115.0	28.56	19.55	27.96	18.88
145.0	30.44	29.31	29.67	32.96
175.0	40.50	35.41	32.07	42.48
Total	204.15	134.79	156.24	150.78

Table B11.
Blacksburg - soil nitrogen content, October 1988 (measured vs. predicted).

Depth (cm)	Treatment 150 kg N/ha			
	Conventional Till (kg/ha)		No-Till (kg/ha)	
	Measured	Predicted	Measured	Predicted
6	21.57	16.27	19.69	24.02
18.5	31.47	36.88	14.12	48.34
32.5	27.85	21.80	12.02	16.73
47.5	10.17	11.02	12.63	8.37
62.5	17.55	3.88	23.06	6.68
77.5	23.06	10.02	30.23	12.06
92.5	17.99	13.16	20.02	7.41
115.0	24.95	22.93	25.26	14.76
145.0	16.59	18.49	24.30	17.94
175.0	16.95	19.51	33.74	19.96
Total	208.15	173.96	215.07	176.27

Table B12.
Blacksburg - soil nitrogen content,
October 1988 (measured vs. predicted).

Depth (cm)	Treatment 225 kg N/ha			
	Conventional Till (kg/ha)		No-Till (kg/ha)	
	Measured	Predicted	Measured	Predicted
6	29.23	22.40	30.39	31.46
18.5	35.25	66.41	26.61	74.34
32.5	36.98	37.87	22.91	37.91
47.5	35.97	11.71	14.55	29.74
62.5	41.49	9.67	31.85	13.27
77.5	35.32	20.13	27.34	18.38
92.5	20.91	11.32	16.97	13.69
115.0	27.35	18.84	30.94	20.12
145.0	18.62	16.10	31.35	29.80
175.0	23.78	13.43	41.95	30.13
Total	304.90	227.88	274.86	298.84

Table B13.
Westmoreland - soil nitrogen content, October 1986 (measured vs. predicted).

Depth (cm)	Treatment 0 kg N/ha			
	Conventional Till (kg/ha)		No-Till (kg/ha)	
	Measured	Predicted	Measured	Predicted
6	24.36	5.03	13.97	7.36
18.5	28.74	9.00	15.05	10.80
32.5	16.91	14.72	15.85	15.60
47.5	7.19	44.01	13.37	42.36
62.5	12.41	29.10	14.16	29.59
77.5	17.21	25.46	8.35	25.05
92.5	12.43	24.90	18.27	25.93
115.0	19.81	16.89	16.92	16.59
145.0	14.67	14.97	25.12	14.52
175.0	21.85	43.96	34.23	23.84
Total	175.58	228.13	175.29	211.64

Table B14.
Westmoreland - soil nitrogen content, October 1986 (measured vs. predicted).

Depth (cm)	Treatment 75 kg N/ha			
	Conventional Till (kg/ha)		No-Till (kg/ha)	
	Measured	Predicted	Measured	Predicted
6	38.40	19.52	8.32	26.93
18.5	23.84	13.30	18.14	20.37
32.5	15.16	12.90	10.64	9.00
47.5	19.59	48.12	20.48	36.23
62.5	8.42	27.21	21.59	29.48
77.5	14.49	18.08	16.78	15.98
92.5	5.23	17.58	19.35	16.39
115.0	13.10	16.89	17.19	16.59
145.0	21.33	14.61	28.44	14.52
175.0	20.59	23.96	20.38	23.84
Total	180.15	212.16	181.31	209.43

Table B15.
Westmoreland - soil nitrogen content, October 1986 (measured vs. predicted).

Depth (cm)	Treatment 150 kg N/ha			
	Conventional Till (kg/ha)		No-Till (kg/ha)	
	Measured	Predicted	Measured	Predicted
6	25.92	47.61	27.31	58.46
18.5	17.33	47.72	34.44	43.87
32.5	12.13	17.88	10.73	8.32
47.5	16.30	45.74	8.69	35.82
62.5	14.40	13.98	7.90	16.14
77.5	7.53	10.70	20.78	12.35
92.5	9.81	8.42	5.42	16.40
115.0	14.20	16.89	33.95	16.59
145.0	39.02	14.61	16.22	14.52
175.0	34.02	23.96	23.40	23.84
Total	190.66	247.51	188.84	246.3

Table B16.
Westmoreland - soil nitrogen content, October 1986 (measured vs. predicted).

Depth (cm)	Treatment 225 kg N/ha			
	Conventional Till (kg/ha)		No-Till (kg/ha)	
	Measured	Predicted	Measured	Predicted
6	14.69	75.66	18.49	93.86
18.5	27.21	69.36	33.50	80.76
32.5	23.14	8.83	13.74	9.46
47.5	28.59	22.46	15.27	17.18
62.5	18.65	21.54	16.46	19.97
77.5	24.22	14.39	5.60	10.53
92.5	8.06	13.92	19.13	10.67
115.0	52.08	16.89	17.16	9.22
145.0	26.38	14.61	15.55	14.52
175.0	35.16	23.96	42.33	13.92
Total	258.18	281.62	197.23	280.09

Table B17.
Westmoreland - soil nitrogen content, October 1988 (measured vs. predicted).

Depth (cm)	Treatment 0 kg N/ha			
	Conventional Till (kg/ha)		No-Till (kg/ha)	
	Measured	Predicted	Measured	Predicted
6	8.15	5.21	5.47	5.02
18.5	6.08	3.97	4.94	4.12
32.5	2.55	2.90	2.73	2.82
47.5	0.82	5.48	2.67	5.16
62.5	1.32	3.78	1.91	3.84
77.5	0.47	3.76	2.02	3.69
92.5	0.64	3.70	1.26	3.81
115.0	1.84	7.51	2.22	7.38
145.0	1.82	7.51	2.96	7.44
175.0	5.58	10.01	1.46	9.92
Total	29.27	53.83	27.64	53.2

Table B18.
Westmoreland - soil nitrogen content, October 1988 (measured vs. predicted).

Depth (cm)	Treatment 75 kg N/ha			
	Conventional Till (kg/ha)		No-Till (kg/ha)	
	Measured	Predicted	Measured	Predicted
6	3.85	10.75	1.27	9.93
18.5	3.61	7.58	2.59	6.74
32.5	2.13	4.32	1.39	2.82
47.5	1.21	6.13	0.32	5.41
62.5	0.74	4.24	0.89	3.92
77.5	0.51	3.74	0.88	3.71
92.5	0.82	3.69	0.83	4.26
115.0	0.87	7.51	0.68	9.27
145.0	0.56	7.51	0.81	8.00
175.0	3.50	10.01	9.82	9.96
Total	17.8	65.48	19.48	64.02

Table B19.
Westmoreland - soil nitrogen content,
October 1988 (measured vs. predicted).

Depth (cm)	Treatment 150 kg N/ha			
	Conventional Till (kg/ha)		No-Till (kg/ha)	
	Measured	Predicted	Measured	Predicted
6	5.64	18.09	26.63	21.84
18.5	5.26	27.52	15.04	13.01
32.5	3.53	9.51	5.89	5.72
47.5	1.98	6.14	2.96	5.67
62.5	1.18	4.08	2.50	3.91
77.5	1.43	3.76	1.98	3.70
92.5	2.10	3.70	1.80	4.00
115.0	3.38	7.89	2.66	7.39
145.0	1.70	7.51	1.66	7.45
175.0	20.12	10.01	17.92	9.93
Total	47.32	98.21	79.04	82.62

Table B20.
Westmoreland - soil nitrogen content, October 1988 (measured vs. predicted).

Depth (cm)	Treatment 225 kg N/ha			
	Conventional Till (kg/ha)		No-Till (kg/ha)	
	Measured	Predicted	Measured	Predicted
6	15.64	31.63	13.24	21.30
18.5	17.90	46.16	13.31	13.97
32.5	12.57	19.65	14.85	5.35
47.5	3.17	6.58	7.53	5.75
62.5	1.54	3.99	3.03	4.17
77.5	1.96	3.77	2.00	3.68
92.5	.65	3.69	2.09	3.81
115.0	1.12	7.51	3.00	7.38
145.0	1.46	7.51	4.46	7.44
175.0	9.50	10.01	16.16	9.92
Total	65.51	140.42	79.67	82.77

Table B21.
Montogue - soil nitrogen content,
April 1989 (measured vs. predicted).

Depth (cm)	0 kg N/ha (kg/ha)		150 kg N/ha (kg/ha)	
	Measured	Predicted	Measured	Predicted
8	19.0	4.41	39.0	20.5
22	9.0	4.41	10.0	39.9
45	15.0	10.00	15.0	16.89
75	12.0	24.8	16.0	35.3
105	34.0	40.4	35.0	50.6
Total	89.0	83.9	115.0	163.2

Table B22.
Brandon - soil nitrogen content,
April 1989 (measured vs. predicted).

Depth (cm)	0 kg N/ha (kg/ha)		150 kg N/ha (kg/ha)	
	Measured	Predicted	Measured	Predicted
8	13.0	4.5	23.0	13.66
22	12.0	4.5	18.0	10.16
45	12.0	9.8	16.0	10.29
75	11.0	10.0	14.0	10.70
105	11.0	26.6	14.0	29.80
Total	59.0	55.3	85.0	74.7

Table B23.
Randolph - soil nitrogen content, April 1989 (measured vs. predicted).

Depth (cm)	0 kg N/ha (kg/ha)		150 kg N/ha (kg/ha)	
	Measured	Predicted	Measured	Predicted
8	9.0	4.56	28.0	4.7
22	4.0	4.56	20.0	9.74
45	7.0	9.66	25.0	26.0
75	8.0	9.6	11.0	9.7
105	10.0	9.6	10.0	9.8
Total	37.0	38.1	94.0	59.8

Table B24.
VCIA - soil nitrogen content,
April 1989 (measured vs. predicted).

Depth (cm)	0 kg N/ha (kg/ha)		150 kg N/ha (kg/ha)	
	Measured	Predicted	Measured	Predicted
8	6.0	5.1	31.0	12.94
22	3.0	5.04	10.0	27.7
45	4.0	7.2	5.0	17.8
75	6.0	7.2	4.0	11.0
105	5.0	7.2	2.0	12.9
Total	24.0	42.6	52.0	82.5

Table B25.
Whitehorn - soil nitrogen content,
April 1989 (measured vs. predicted).

Depth (cm)	0 kg N/ha (kg/ha)		150 kg N/ha (kg/ha)	
	Measured	Predicted	Measured	Predicted
8	25.0	4.14	37.0	5.68
22	19.0	4.15	20.0	9.6
45	9.0	9.36	7.0	21.4
75	6.0	9.42	4.0	20.05
105	3.0	19.99	4.0	55.4
Total	62.0	47.06	72.0	112.13

**Table B26.
Walker - soil nitrogen content,
April 1989 (measured vs. predicted).**

Depth (cm)	0 kg N/ha (kg/ha)		150 kg N/ha (kg/ha)	
	Measured	Predicted	Measured	Predicted
8	21.0	6.6	32.0	5.91
22	8.0	5.8	9.0	5.5
45	18.0	10.9	23.0	19.1
75	22.0	24.8	25.0	22.1
105	27.0	20.76	25.0	22.3
Total	96.0	68.9	114.0	74.7

Appendix C: Summary of Water and Nitrogen Dynamics for the Land Units

Table C1:
Summary of water and nitrogen dynamics for land unit 1.

Rotation	Rainfall (mm)	Water Use (mm)		Drainage ge (mm)		Runoff f (mm)		N Load (kg/ha)		Minz. (kg/ha)		Denit. (kg/ha)	
		Mgmt 1	Mgmt 2	Mgmt 1	Mgmt 2	Mgmt 1	Mgmt 2	Mgmt 1	Mgmt 2	Mgmt 1	Mgmt 2	Mgmt 1	Mgmt 2
1	2166	1153	1120	685	773	220	184	77	85	224	231	57	63
2	2216	1089	1073	880	925	246	197	130	131	215	214	84	81
3	2096	1086	1083	814	845	229	188	119	118	210	211	89	87
4	2343	1078	1097	978	995	350	307	133	130	231	236	87	92
5	1951	1086	1088	619	668	213	162	74	79	171	170	83	84
6	2258	1141	1133	767	819	337	292	137	146	205	205	94	93
7	1798	1107	1126	579	596	175	139	86	76	199	194	92	90
8	1771	1122	1135	434	456	224	181	64	82	196	190	82	89
9	2521	1054	1059	1035	1093	288	232	249	243	246	246	105	102
10	1829	1199	1191	494	521	182	161	92	93	188	198	63	60
11	2183	1037	1038	822	872	280	229	177	160	202	200	102	98
12	2174	1116	1130	864	887	292	232	136	143	234	241	88	98
13	1897	1087	1102	687	752	194	149	86	88	250	249	133	125
Average	2092.5	1104.2	1105.8	742.9	784.8	248.5	204.1	120.0	121.1	213.2	214.2	89.2	89.4
CV	10.5	3.7	3.4	23.4	22.6	21.9	24.6	40.6	37.1	10.4	11.0	20.2	17.7

Table C2.
Summary of water and nitrogen dynamics for land unit 2.

Rotation	Rainfall (mm)	Water Use (mm)		Drainage ge (mm)		Runoff f (mm)		N Load (kg/ha)		Minz. (kg/ha)		Denit. (kg/ha)	
		Mgmt 1	Mgmt 2	Mgmt 1	Mgmt 2	Mgmt 1	Mgmt 2	Mgmt 1	Mgmt 2	Mgmt 1	Mgmt 2	Mgmt 1	Mgmt 2
1	2166	1149	1113	655	762	302	239	56	61	105	111	24	26
2	2216	1077	1071	776	856	347	264	76	75	128	127	31	29
3	2096	1076	1078	724	778	318	260	101	91	127	129	37	32
4	2343	1078	1083	865	935	455	388	91	90	161	158	40	39
5	1951	1062	1073	545	614	299	222	93	103	102	102	36	35
6	2258	1125	1131	673	741	460	383	80	90	136	133	34	34
7	1798	1115	1121	491	535	253	199	75	86	128	128	31	33
8	1771	1065	1095	402	438	307	242	68	75	129	126	33	31
9	2521	1051	1066	896	979	434	336	155	152	186	174	44	42
10	1829	1134	1121	470	522	254	215	74	73	124	128	27	28
11	2183	1029	1031	733	813	378	306	112	125	138	136	38	39
12	2174	1118	1129	747	807	398	317	83	88	160	166	35	35
13	1897	1083	1089	626	685	276	211	90	87	171	171	50	51
Average	2092.5	1089.4	1092.4	661.8	728.1	344.7	275.5	88.8	92.0	138.1	137.6	35.4	34.9
CV	10.5	3.1	2.6	21.9	21.5	20.5	22.5	26.7	24.9	17.3	15.8	18.6	18.3

Table C3.
Summary of water and nitrogen dynamics for land unit 3.

Rotation	Rainfall (mm)	Water Use (mm)		Drainage ge (mm)		Runoff f (mm)		N Load (kg/ha)		Minz. (kg/ha)		Denit. (kg/ha)	
		Mgmt 1	Mgmt 2	Mgmt 1	Mgmt 2	Mgmt 1	Mgmt 2	Mgmt 1	Mgmt 2	Mgmt 1	Mgmt 2	Mgmt 1	Mgmt 2
1	2166	1067	1030	890	946	207	189	53	52	62	68	11	11
2	2216	994	1028	965	964	246	214	79	71	79	85	16	15
3	2096	1015	1016	871	890	227	205	80	83	89	87	12	13
4	2343	1040	1034	1032	1062	331	308	105	107	132	133	16	17
5	1951	972	976	722	738	214	190	73	75	62	62	12	13
6	2258	1057	1069	833	850	368	342	74	94	115	119	9	13
7	1798	1083	1080	594	616	179	161	79	79	102	104	13	12
8	1771	1013	1014	528	550	236	214	50	42	91	95	14	14
9	2521	1017	1011	1055	1093	310	276	130	127	147	154	18	20
10	1829	961	962	718	730	181	169	86	95	104	107	15	16
11	2183	987	987	884	909	272	247	120	125	120	124	18	18
12	2174	1075	1069	884	919	301	271	97	97	136	143	17	17
13	1897	1047	1050	735	758	202	179	96	103	133	130	17	14
Average	2092.5	1025.2	1025.1	823.9	848.1	251.8	228.1	86.3	88.5	105.5	108.5	14.5	14.8
CV	10.5	3.7	3.4	18.5	18.4	22.9	23.8	25.9	27.4	25.5	25.2	19.1	16.9

Table C4.
Summary of water and nitrogen dynamics for land unit 4.

Rotation	Rainfall (mm)	Water Use (mm)		Drainage ge (mm)		Runoff f (mm)		N Load (kg/ha)		Minz. (kg/ha)		Denit. (kg/ha)	
		Mgmt 1	Mgmt 2	Mgmt 1	Mgmt 2	Mgmt 1	Mgmt 2	Mgmt 1	Mgmt 2	Mgmt 1	Mgmt 2	Mgmt 1	Mgmt 2
1	2166	950	923	903	1034	316	207	131	124	123	129	11	10
2	2216	923	940	925	1040	354	223	117	141	95	96	9	8
3	2096	878	885	906	985	425	238	136	135	118	117	10	11
4	2343	1006	1012	965	1057	437	337	128	137	141	142	11	12
5	1951	870	863	751	847	313	199	105	113	63	75	10	8
6	2258	975	979	795	891	488	389	113	114	136	133	10	10
7	1798	980	977	612	700	268	183	106	109	104	114	12	11
8	1771	888	881	563	670	327	229	95	90	119	120	10	11
9	2521	955	955	993	1126	435	299	170	181	148	147	13	14
10	1829	801	801	788	858	271	205	145	148	127	128	12	10
11	2183	847	951	827	932	366	252	139	136	114	123	14	13
12	2174	1031	1043	804	916	420	293	120	119	139	118	13	12
13	1897	986	1012	703	777	295	194	149	150	151	152	12	10
Average	2092.5	930.0	940.2	810.4	910.2	362.7	249.8	127.2	130.5	121.4	122.6	11.3	10.8
CV	10.5	7.1	7.0	15.5	14.7	19.0	24.0	15.7	16.9	19.1	16.2	12.7	15.5

Table C5.
Summary of water and nitrogen dynamics for land unit 5.

Rotation	Rainfall (mm)	Water Use (mm)		Drainage ge (mm)		Runoff f (mm)		N Load (kg/ha)		Minz. (kg/ha)		Denit. (kg/ha)	
		Mgmt 1	Mgmt 2	Mgmt 1	Mgmt 2	Mgmt 1	Mgmt 2	Mgmt 1	Mgmt 2	Mgmt 1	Mgmt 2	Mgmt 1	Mgmt 2
1	2166	1163	1107	677	759	204	174	84	90	153	160	37	42
2	2216	1090	1084	866	933	252	191	109	107	164	164	49	51
3	2096	1096	1093	785	836	230	183	112	117	162	161	50	51
4	2343	1093	1083	950	1015	351	301	122	120	190	191	55	54
5	1951	1082	1082	594	653	229	167	109	107	135	133	47	48
6	2258	1132	1142	754	813	372	307	124	122	162	161	48	49
7	1798	1127	1135	540	573	182	142	113	114	161	158	44	46
8	1771	1126	1126	419	465	231	184	99	111	150	156	41	44
9	2521	1074	1067	1002	1091	302	225	127	127	198	199	49	49
10	1829	1212	1207	462	484	185	164	112	122	157	165	43	44
11	2183	1041	1049	813	861	285	231	133	131	157	159	56	58
12	2174	1134	1142	822	880	300	235	115	116	187	187	49	50
13	1897	1096	1097	691	735	204	152	127	130	193	191	70	71
Average	2092.5	1112.8	1108.8	721.2	776.8	255.9	204.3	114.3	116.5	166.8	168.1	49.1	50.5
CV	10.5	3.8	3.6	23.9	23.8	23.1	24.9	11.0	9.2	11.0	10.6	16.0	14.3

Table C6.
Summary of water and nitrogen dynamics for land unit 6.

Rotation	Rainfall (mm)	Water Use (mm)		Drainage ge (mm)		Runoff f (mm)		N Load (kg/ha)		Minz. (kg/ha)		Denit. (kg/ha)	
		Mgmt 1	Mgmt 2	Mgmt 1	Mgmt 2	Mgmt 1	Mgmt 2	Mgmt 1	Mgmt 2	Mgmt 1	Mgmt 2	Mgmt 1	Mgmt 2
1	2166	1149	1103	939	995	45	36	62	65	118	122	26	27
2	2216	1060	1061	1073	1087	56	41	78	77	132	130	26	26
3	2096	1071	1073	993	1002	47	38	102	103	134	133	31	34
4	2343	1075	1060	1225	1244	103	91	87	82	161	160	35	36
5	1951	1048	1052	810	826	46	32	98	101	109	109	29	32
6	2258	1121	1119	1038	1050	98	81	89	91	140	139	34	31
7	1798	1105	1102	718	724	36	29	89	89	133	135	29	32
8	1771	1106	1097	592	621	72	55	80	81	132	132	30	30
9	2521	1038	1043	1268	1287	74	51	139	145	183	183	36	38
10	1829	1171	1166	652	663	35	30	56	56	124	127	22	24
11	2183	1025	1029	1036	1053	79	60	121	128	140	138	33	34
12	2174	1115	1107	1081	1100	67	50	92	92	169	170	33	32
13	1897	1080	1079	857	876	41	28	88	90	177	175	49	49
Average	2092.5	1089.5	1083.9	944.8	963.7	61.5	47.8	90.8	92.3	142.5	142.5	31.8	32.7
CV	10.5	3.8	3.3	21.3	20.9	35.5	40.1	23.2	24.8	15.5	15.1	19.8	18.4

Table C7.
Summary of water and nitrogen dynamics for land unit 7.

Rotation	Rainfall (mm)	Water Use (mm)		Drainage ge (mm)		Runoff f (mm)		N Load (kg/ha)		Minz. (kg/ha)		Denit. (kg/ha)	
		Mgmt 1	Mgmt 2	Mgmt 1	Mgmt 2	Mgmt 1	Mgmt 2	Mgmt 1	Mgmt 2	Mgmt 1	Mgmt 2	Mgmt 1	Mgmt 2
1	2166	1077	1045	814	859	246	226	59	53	61	66	11	10
2	2216	1038	1032	870	913	298	266	90	83	90	91	16	15
3	2096	1027	1027	809	830	271	248	100	101	95	93	15	14
4	2343	1032	1033	976	1006	395	368	111	111	133	133	18	18
5	1951	1014	1017	637	655	258	232	72	74	61	63	14	14
6	2258	1070	1071	762	789	424	398	79	95	110	110	14	16
7	1798	1078	1084	563	581	214	194	82	91	102	106	17	17
8	1771	1063	1057	461	490	252	229	53	57	85	86	16	17
9	2521	1013	1010	993	1030	376	340	141	147	161	60	21	19
10	1829	1082	1087	579	588	199	188	65	73	68	69	10	11
11	2183	985	985	837	862	320	293	126	137	136	136	20	19
12	2174	1094	1091	815	848	351	319	113	116	151	151	18	19
13	1897	1044	1049	701	722	242	217	101	102	149	151	22	23
Average	2092.5	1047.5	1045.2	755.2	782.5	295.8	270.6	91.7	95.4	107.8	101.2	16.3	16.3
CV	10.5	3.0	3.0	20.3	20.4	23.3	24.0	27.9	28.4	31.3	31.4	21.2	20.9

Table C8.
Summary of water and nitrogen dynamics for land unit 8.

Rotation	Rainfall (mm)	Water Use (mm)		Drainage ge (mm)		Runoff f (mm)		N Load (kg/ha)		Minz. (kg/ha)		Denit. (kg/ha)	
		Mgmt 1	Mgmt 2	Mgmt 1	Mgmt 2	Mgmt 1	Mgmt 2	Mgmt 1	Mgmt 2	Mgmt 1	Mgmt 2	Mgmt 1	Mgmt 2
1	2166	1042	1006	1048	1111	87	57	61	57	67	64	15	15
2	2216	996	997	1087	1139	114	66	104	102	85	85	20	20
3	2096	979	982	1017	1034	118	82	104	100	98	94	19	18
4	2343	1050	1048	1181	1225	170	130	101	107	128	121	21	22
5	1951	940	942	868	909	97	57	106	116	67	67	18	19
6	2258	1049	1052	991	1051	215	153	84	73	112	112	18	18
7	1798	1078	1077	696	728	84	52	93	89	103	103	20	20
8	1771	987	992	652	694	134	90	48	59	110	104	21	23
9	2521	1023	1020	1194	1259	163	100	133	153	134	134	24	25
10	1829	904	900	888	908	79	63	118	127	109	108	21	22
11	2183	986	993	1011	1050	130	87	127	126	102	110	23	23
12	2174	1120	1109	989	1058	148	90	113	116	135	137	22	21
13	1897	1048	1059	831	860	108	65	94	92	132	130	20	20
Average	2092.5	1015.5	1013.6	957.9	1002.0	126.7	84.0	98.9	101.3	106.3	105.3	20.2	20.5
CV	10.5	5.5	5.3	16.6	16.7	29.9	34.4	23.3	26.3	20.9	21.2	11.2	12.4

Table C9.
Summary of water and nitrogen dynamics for land unit 9.

Rotation	Rainfall (mm)	Water Use (mm)		Drainage ge (mm)		Runoff f (mm)		N Load (kg/ha)		Minz. (kg/ha)		Denit. (kg/ha)	
		Mgmt 1	Mgmt 2	Mgmt 1	Mgmt 2	Mgmt 1	Mgmt 2	Mgmt 1	Mgmt 2	Mgmt 1	Mgmt 2	Mgmt 1	Mgmt 2
1	2166	866	838	1301	1334	11	6	52	35	15	19	16	14
2	2216	841	842	1355	1358	11	6	38	40	15	17	11	11
3	2096	785	790	1311	1313	14	8	70	69	23	26	11	11
4	2343	706	701	1467	1480	31	23	47	50	44	45	12	11
5	1951	804	803	1099	1104	6	2	63	64	29	30	9	9
6	2258	873	876	1356	1366	28	16	62	61	60	60	12	12
7	1798	903	904	948	951	7	3	56	48	60	63	12	11
8	1771	847	845	902	914	29	19	49	53	65	66	11	11
9	2521	826	826	1537	1543	21	13	91	93	84	85	16	17
10	1829	755	760	1091	1092	11	6	82	82	80	80	17	13
11	2183	848	848	1280	1288	19	11	92	103	75	79	15	14
12	2174	941	944	1303	1308	14	7	77	76	87	88	14	15
13	1897	915	913	1064	1071	8	3	84	85	106	106	24	20
Average	2092.5	839.2	837.7	1231.8	1240.2	16.2	9.5	66.4	66.1	57.2	58.8	13.8	13.0
CV	10.5	7.5	7.5	15.1	15.2	51.5	66.5	25.7	30.4	50.0	47.5	27.0	22.2

Table C10.
Summary of water and nitrogen dynamics for land unit 10.

Rotation	Rainfall (mm)	Water Use (mm)		Drainage ge (mm)		Runoff f (mm)		N Load (kg/ha)		Minz. (kg/ha)		Denit. (kg/ha)	
		Mgmt 1	Mgmt 2	Mgmt 1	Mgmt 2	Mgmt 1	Mgmt 2	Mgmt 1	Mgmt 2	Mgmt 1	Mgmt 2	Mgmt 1	Mgmt 2
1	2166	1116	1078	871	937	144	103	74	76	130	131	35	37
2	2216	1066	1068	972	1039	161	107	85	86	148	145	46	43
3	2096	1074	1073	875	910	149	116	93	91	142	142	43	43
4	2343	1064	1063	1104	1143	236	193	91	93	177	178	48	52
5	1951	1057	1062	714	750	141	93	89	99	118	119	41	43
6	2258	1101	1107	882	934	259	210	87	89	143	144	40	42
7	1798	1099	1099	637	662	119	87	80	79	145	145	40	39
8	1771	1097	1099	497	552	179	131	84	88	138	137	37	38
9	2521	1051	1046	1121	1184	205	144	108	115	181	186	49	47
10	1829	1179	1177	548	581	126	103	90	84	148	151	37	37
11	2183	1031	1028	910	956	198	144	117	118	143	141	49	50
12	2174	1117	1113	939	1000	198	141	84	96	172	173	46	46
13	1897	1087	1082	773	817	124	86	96	96	178	177	60	61
Average	2092.5	1087.6	1084.2	834.1	881.9	172.2	127.5	90.6	93.1	151.0	151.5	43.9	44.5
CV	10.5	3.3	3.3	22.3	21.8	24.8	29.3	12.1	12.7	12.6	13.0	14.8	14.8

The Virginia Water Resources Research Center is a federal-state organization established at Virginia Polytechnic Institute and State University in 1965 under provisions of the federal Water Resources Research Act of 1964.

Under law, the Center's activities are to:

- consult with the General Assembly, governmental agencies, water user groups, private industry, and other potential users of research;
- establish and administer research agreements with all universities in Virginia;
- facilitate and stimulate research that concerns policy issues facing the General Assembly, supports water resource agencies, and provides organizations with tools to increase effectiveness of water management;
- disseminate new information and facilitate application of new technology;
- serve as a liaison between Virginia and federal research funding agencies as an advocate for Virginia's water research needs; and
- encourage the development of academic programs in water resources management in conjunction with the State Council on Higher Education.

The Water Center is a member of the National Institutes for Water Resources. More information on programs and activities may be obtained by writing or telephoning the Water Center.

Virginia Tech is an Equal Opportunity/Affirmative Action employer; for more information, contact the EO/AA office.

Printed on Recycled Paper

Virginia Water Resources Research Center
Virginia Polytechnic Institute and State University
617 North Main Street
Blacksburg, Virginia 24060-3397
Phone (703)231-5624